Pacific
Northwest
NATIONAL LABORATORY

Deep Vadose Zone Treatability Test of Uranium Reactive Gas Sequestration for the Hanford Central Plateau: Final Report

September 2018

MJ Truex
JE Szecsody
CE Strickland
DA St. John
MM Snyder
CT Resch
MD Miller
Z Wang

SA Saslow
ME Bowden
SR Baum
II Leavy
BN Gartman
RE Clayton
WL Garcia
EC Gillispie

U.S. DEPARTMENT OF
ENERGY

DISCLAIMER

This report was prepared as an account of work sponsored by an agency of the United States Government. Neither the United States Government nor any agency thereof, nor Battelle Memorial Institute, nor any of their employees, makes **any warranty, express or implied, or assumes any legal liability or responsibility for the accuracy, completeness, or usefulness of any information, apparatus, product, or process disclosed, or represents that its use would not infringe privately owned rights**. Reference herein to any specific commercial product, process, or service by trade name, trademark, manufacturer, or otherwise does not necessarily constitute or imply its endorsement, recommendation, or favoring by the United States Government or any agency thereof, or Battelle Memorial Institute. The views and opinions of authors expressed herein do not necessarily state or reflect those of the United States Government or any agency thereof.

PACIFIC NORTHWEST NATIONAL LABORATORY
operated by
BATTELLE
for the
UNITED STATES DEPARTMENT OF ENERGY
under Contract DE-AC05-76RL01830

This document was printed on recycled paper.
(8/2010)

Deep Vadose Zone Treatability Test of Uranium Reactive Gas Sequestration for the Hanford Central Plateau: Final Report

MJ Truex   SA Saslow
JE Szecsody   ME Bowden
CE Strickland   SR Baum
DA St. John[1]   II Leavy
MM Snyder   BN Gartman
CT Resch   RE Clayton
MD Miller   WL Garcia
Z Wang   EC Gillispie

September 2018

Pacific Northwest National Laboratory
Richland, Washington 99352

[1]CH2M Hill Plateau Remediation Company

Summary

Over decades of operation, the U.S. Department of Energy (DOE) and its predecessors have released nearly 2 trillion L (450 billion gal.) of liquid into the vadose zone at the Hanford Site. Much of this liquid waste discharge into the vadose zone occurred in the Central Plateau, a 200 km^2 (75 mi^2) area that includes approximately 800 waste sites. Some of the inorganic and radionuclide contaminants in the deep vadose zone at the Hanford Site are at depths where direct exposure pathways (human health or ecological) are not of concern, but the contamination may need to be remediated to protect groundwater. The Tri-Party Agencies (DOE, the U.S. Environmental Protection Agency, and the Washington State Department of Ecology) established Milestone M-015-50, which directed DOE to submit a treatability test plan for remediation of technetium-99 (Tc-99) and uranium in the deep vadose zone. These contaminants are mobile in the subsurface environment and have been detected at high concentrations deep in the vadose zone, and, at some locations, have reached groundwater. Testing of technologies to remediate Tc-99 and uranium will also provide information relevant to remediating other contaminants in the vadose zone. The uranium reactive gas sequestration (URGS) test described herein was conducted as an element of the deep vadose zone treatability test plan published to meet Milestone M-015-50. The URGS technology was tested as a potential remedy to decrease the mobility of uranium in the vadose zone as a mechanism to protect groundwater. Information about URGS obtained from this test is intended for use in subsequent feasibility studies for Hanford Central Plateau waste sites with uranium contamination in the deep vadose zone.

Prior to developing the URGS field test plan, technology development efforts were applied to identify an appropriate reactive-gas technology to decrease the mobility of uranium in the vadose zone. Based on these laboratory results, pH manipulation with ammonia gas was selected as the most promising reactive-gas approach to decrease the mobility of uranium. Additional laboratory efforts were applied to describe the treatment process and obtain information for scaling to field application. The field test plan for URGS by ammonia treatment identified the 216-U-8 site for the field test. The 216-U-8 crib was selected for the URGS test because (1) historical characterization data indicated that the site contained a significant inventory of uranium that was likely to be in a mobile form, (2) the uranium concentration/distribution was favorable for a test, (3) the test could be conducted with shallow wells, (4) there were minimal logistical issues, and (5) suitable site characterization data were available. The field test plan specified the parallel application of (1) laboratory tests with field-site sediments to evaluate URGS effectiveness and (2) installation, operation, and assessment of a field injection of ammonia. Laboratory testing requires about 1 year from when samples are available, so a parallel effort was selected to reduce the overall duration of the treatability testing.

The URGS technology is based on a series of geochemical reactions that occur when ammonia vapor is injected into uranium-contaminated vadose zone sediments. Injected ammonia vapor partitions into the moisture in the sediment and increases the pore-water pH from initially around pH 8 to about pH 11.5. Dissolution of sediment phases is induced by the high pH, followed by a re-precipitation process that is intended to create uranium precipitates or coatings that render uranium less mobile than before treatment. Prior development testing with ammonia-treated sediments from other Hanford waste sites showed promising results, with uranium mobile phases reduced by an average of 68% and immobile phases increased by an average of 71%. Soil column leaching tests were conducted by flowing simulated pore water through untreated and ammonia-treated sediments and measuring the amount of uranium that eluted from the sediments. These tests showed a uranium leaching reduction of greater than 80% following

ammonia treatment. However, the initial testing was limited by two factors. First, only a few sediment types could be tested with the soil column leaching method because a sufficient quantity of material was only available for a few sediment types. Second, samples were available only for limited types of waste disposal chemistries that did not include acidic disposal because sampling of this type of waste site was not being conducted as part of Hanford Site characterization efforts at the time of the technology development efforts.

The field component of the treatability test was targeted at the 216-U-8 crib within the 200-WA-1 operable unit on the Central Plateau. This crib received acidic process condensate from the 221-U and 224-U buildings, along with drainage from the 291-U stack. While the waste was passed through a lime tank prior to discharge, the pH was not specifically managed. This type of waste is similar to the acidic waste disposal at about 60% of the high-inventory uranium disposal sites in the Hanford Central Plateau. Characterization of the 216-U-8 crib region indicated uranium and other contaminants discharged to the crib spread laterally in the vadose zone soils surrounding the crib. Uranium contamination present south of the crib at a relatively shallow depth of approximately 10.6 to 15 m (35 to 50 ft) below ground surface was targeted for the field test.

Field site efforts included installation of the injection well and monitoring borehole network. During drilling, samples were collected for use in laboratory testing, as specified in the field test plan. Site work also included design, construction, and functional testing of the ammonia injection and field test monitoring systems. Thus, information about the design and construction process and requirements for application of the URGS technology was gathered as part of the test.

For the field test site, laboratory tests with site sediments were conducted concurrently with the field test design and construction to evaluate effectiveness of laboratory-scale ammonia treatment. In these tests, almost all ammonia-treated samples showed a higher total mass of uranium leached for the same number of pore-volume flushes than was leached for the corresponding untreated sample. Thus, the laboratory results for field-site sediments demonstrated that there were interferences that affect the ammonia treatment. Hypothesized interference factors included the type of uranium phases present, the presence of co-contaminant interferences, or sediment/co-contaminant properties that lead to the need for higher ammonia doses for the treatment to be effective. The reason for the site-specific interferences was evaluated to assess applicability of the technology to other sites. Results suggest that areas below acidic waste discharge sites (such as the location of the 216-U-8 field test site), where sediment carbonate is depleted and where the uranium distribution in the soil is concentrated in small hot spots, would not be suitable for use of URGS ammonia treatment. Because the ammonia treatment process was found to be sensitive to these conditions, there may be other geochemical conditions that interfere with ammonia treatment effectiveness. For this reason, the field test was not conducted and the treatability test report includes the recommendations described below.

The URGS treatability test demonstrated that interactions of the ammonia treatment chemistry and site-specific geochemistry are important to the effectiveness of the treatment for decreasing uranium mobility. Thus, while laboratory experiments during technology development suggested that the technology was robust with broad applicability, the treatability test effort demonstrated that the technology has limitations with respect to effectiveness. These limitations must be considered when evaluating potential use of the technology at other waste sites. If treatment effectiveness at another waste site were verified, the field design and laboratory testing conducted for the URGS treatability testing and the gas-injection experience from another gas-phase field test conducted as an element of the deep vadose zone treatability test plan

published to meet Milestone M-015-50 provide a basis for design of ammonia injection at prospective sites. Injection effectiveness is related to the subsurface properties, and site-specific ammonia injection trials may also be necessary prior to full implementation at another site.

Treatability test information suggests that applicability at acidic discharge sites may be poor at locations in the subsurface where the waste chemistry impacted the sediments, as observed in the shallow vadose zone below the 216-U-8 test site. However, effective URGS treatment may be possible at neutral or basic discharge sites or deeper in the vadose zone below sites if subsurface geochemistry has not been significantly affected by the waste discharge chemistry. If the URGS technology is determined to be potentially applicable at a site in the future, site-specific laboratory testing would be necessary to confirm treatment effectiveness. As an overall recommendation for the URGS technology, a future feasibility study would first need to consider the waste discharge, associated subsurface geochemistry, and uranium mobility at a site. For sites where uranium mobility is determined to be a risk to groundwater, the URGS ammonia treatment can be evaluated using the technical information for the ammonia treatment process in this report. URGS treatment may be applicable if (1) site information suggests that ammonia treatment has the potential to reduce uranium mobility, (2) production of nitrate from the ammonia injection is within an acceptable range, and (3) ammonia injection appears to be feasible based on injection design calculations. For sites meeting these criteria, this report recommends that a site-specific evaluation of ammonia treatment effectiveness be conducted using sediments from the zone targeted for treatment. These tests would include sequential extraction and soil column leaching tests for untreated and ammonia-treated sediments to quantify the change in uranium mobility. This testing would require about 1 year from the time of sediment sample receipt to the reporting of laboratory testing results. For sites with positive results, where the decrease in uranium mobility will meet groundwater protection needs, an ammonia injection design can be implemented using a phased approach, if the URGS ammonia treatment technology is included in the remedial alternative selected in the Record of Decision.

This treatability test report compiles the technology information gained from the laboratory testing during technology development, the laboratory tests for ammonia-treatment effectiveness using field-site sediments, and a laboratory study assessing geochemical interferences at 216-U-8 that may affect ammonia treatment performance. In addition, this treatability test report describes the field injection and monitoring equipment design and associated design calculations. Collectively, this information will enable evaluation of this technology for applicability at other sites. This report documents closeout of the URGS treatability test as an element of the deep vadose zone treatability test plan published to meet Milestone M-015-50 for the Hanford Central Plateau. The treatability test effort accomplished the goal of providing sufficient data on the URGS ammonia treatment process for its consideration in a future feasibility study.

Acronyms and Abbreviations

ALARA	as low as reasonably achievable
ARAR	applicable or relevant and appropriate requirement
bgs	below ground surface
CCU	Cold Creek Unit
CERCLA	*Comprehensive Environmental Response, Compensation, and Liability Act of 1980*
CHPRC	CH2M Hill Plateau Remediation Company
C_R	count ratio
DOE	U.S. Department of Energy
DQO	data quality objective
EC	electrical conductivity
ERDF	Environmental Restoration Disposal Facility
ERT	electrical resistivity tomography
EXAFS	extended X-ray absorption fine structure
FTP	field test plan
FY	fiscal year
GC-MS	gas chromatography mass spectrometry
GPR	ground-penetrating radar
IC	ion chromatography
ICP-MS	inductively couple plasma mass spectrometry
ICP-OES	inductively coupled plasma optical emission spectrometry
IDF	Integrated Disposal Facility
IR	infrared absorption
KPA	kinetic phosphorescence analysis
LHeT	liquid helium temperature
LIFS	laser induced fluorescence spectroscopy
ND	not detected
OU	operable unit
PNNL	Pacific Northwest National Laboratory
PSD	particle size distribution
PSQ	principal study question
SAP	sampling and analysis plan
sed	sediment
SGLS	spectral-gamma logging system
SIM	Soil Inventory Model
TC	total carbon

TIC	total inorganic carbon
TOC	total organic carbon
TPA	Tri-Party Agreement
UNH	uranyl nitrate hexahydrate
URGS	uranium reactive gas sequestration
XANES	X-ray absorption near edge structure
XRD	X-ray diffraction
XRF	X-ray fluorescence

Contents

Figures

Tables

1.0   Introduction

Although the depth of some inorganic and radionuclide contamination in the vadose zone at the U.S. Department of Energy (DOE) Hanford Site is beyond the point where direct exposure pathways are relevant, remediation may still be required to protect groundwater (DOE 2008). However, remediation options for contamination deep in the vadose zone are limited by the physical and hydrogeologic properties of the vadose zone (Dresel et al. 2011). In response to the Tri-Party Agreement Milestone M-015-50, the *Deep Vadose Zone Treatability Test Plan for the Hanford Central Plateau* (DOE 2008) was issued in March 2008. This overall plan is for a treatability test program to evaluate potential deep vadose zone remedies for groundwater protection at the Hanford Site. As part of this program, evaluation of a uranium reactive gas sequestration (URGS) technology was planned (DOE 2015a,b) and test activities were implemented.

Some reactive gases can induce geochemical changes in sediments, and these changes can render contaminants, such as uranium, less mobile. A range of potential amendments was tested in the laboratory, as described by Szecsody et al. (2010a). The amendments targeted oxidation-reduction reactions, pH manipulation, and phosphate addition to induce precipitation reactions that could make contaminants less mobile. Based on these laboratory results, pH manipulation with ammonia gas was selected as the most promising reactive-gas approach to decrease the mobility of uranium. Additional laboratory efforts were applied to describe the treatment process and obtain information for scaling to field application (Szecsody et al. 2010a,b, 2012; Zhong et al. 2015; Truex et al. 2014). Thus, ammonia treatment was selected for treatability testing as the URGS technology.

The URGS technology is based on a series of geochemical reactions that occur when ammonia vapor is injected into uranium-contaminated vadose zone sediments. Injected ammonia vapor partitions into the moisture in the sediment and increases the pore water pH from initially around pH 8 to about pH 11.5. Dissolution of sediment phases is induced by the high pH, followed by a re-precipitation process that is intended to create uranium precipitates or coatings that render uranium less mobile than before treatment.

The field component of the treatability test was planned for execution in the 200-WA-1 operable unit (OU) adjacent to the 216-U-8 crib (DOE 2015a,b). The field test was not completed because of the poor treatment effectiveness observed in the laboratory for field-site sediments. Field-site laboratory results and interpretation of the site-specific interferences related to the poor observed effectiveness are presented in this report. In addition, the report includes information gained in the treatability test effort about technology effectiveness, implementability, and cost factors. The report is organized following the guidelines for reporting of *Comprehensive Environmental Response, Compensation, and Liability Act of 1980* (CERCLA) treatability tests (EPA 1992). This introductory section includes a description of the technology (Section 1.1) and information about the uranium waste sites at the Hanford Central Plateau (Section 1.2). Section 2.0 provides the conclusions and recommendations for the study. The test approach is described in Section 3.0, followed by a presentation of the detailed results in Section 4.0. Quality assurance and the cost and schedule for the project are presented in Sections 5.0 and 6.0, respectively.

1.1 Technology Description

The treatment technology being tested is geochemical manipulation via ammonia injection. Previous laboratory evaluation of gas-phase technologies focused on immobilization of uranium (Szecsody et al. 2010a) and recommended pursuing ammonia injection because it was best suited for field implementation and was effective at reducing uranium mobility. Additional study of the ammonia gas treatment process and large-scale application has also been conducted (Szecsody et al. 2010b, 2012; Zhong et al. 2015; Truex et al. 2014).

The URGS technology is based on a series of geochemical reactions that occur when ammonia vapor is injected into uranium-contaminated vadose zone sediments. As conceptually depicted in Figure 1.1, when ammonia gas flows into vadose zone sediments, a large portion of the injected ammonia vapor partitions into the moisture in the sediment. A 5 vol% ammonia vapor produces an equilibrium pore-water concentration of about 3 M ammonia. Self-dissociation of ammonia at this concentration results in an increase in the pore water pH from initially around pH 8 to about pH 11.5. Ion exchange and mineral dissolution (including silicate dissolution) is caused by the caustic pH. With high total dissolved solids, precipitates start to form, especially as the pH is buffered back toward neutral. The precipitates may incorporate uranium (e.g., uranium silicates) and include aluminosilicates and other precipitates. The goal of the dissolution and re-precipitation process is to create uranium precipitates or coatings that render uranium less mobile than before treatment. Decreasing the fraction of uranium contamination that is mobile reduces its potential to contaminate groundwater.

Field implementation of the ammonia treatment technology involves injection of an ammonia gas mixture into a subsurface target zone. The ammonia partitions into the pore water and approaches a pore-water concentration dependent on the concentration of ammonia in the gas phase and the Henry's law coefficient for ammonia. Because partitioning is very rapid and volatility is low, a sharp dissolution front is observed with near-equilibrium ammonia gas and liquid concentrations behind the front and low concentrations elsewhere (Figure 1.2); thus, the physical properties of ammonia are favorable for controlled injection.

Ammonia treatment results in uranium surface phases being coated with or incorporated into aluminosilicates. In this process, uranium is not chemically reduced, so the oxidation state of the uranium does not affect treatment effectiveness, and the sequestration process is not readily reversible in an oxic vadose zone. Under post-treatment circum-neutral pH conditions, precipitates formed during ammonia treatment have low solubility and would dissolve slowly over long periods as part of natural weathering processes. Transport of uranium that is bound or coated by precipitates will be limited, thereby reducing the migration of uranium to the groundwater.
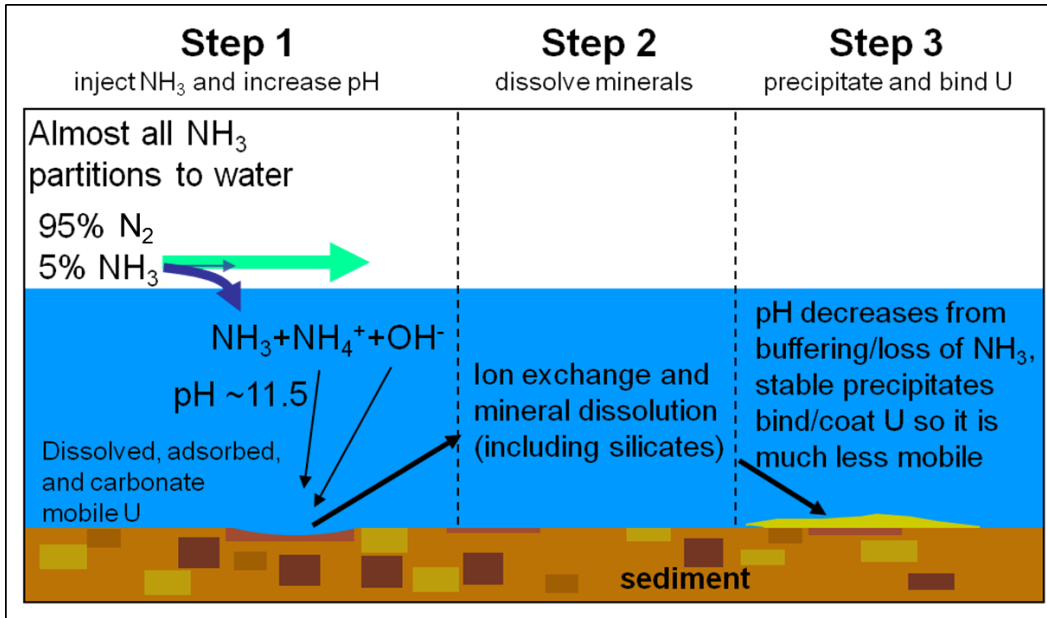
Figure 1.1. Conceptual Depiction of Ammonia Treatment Mechanism
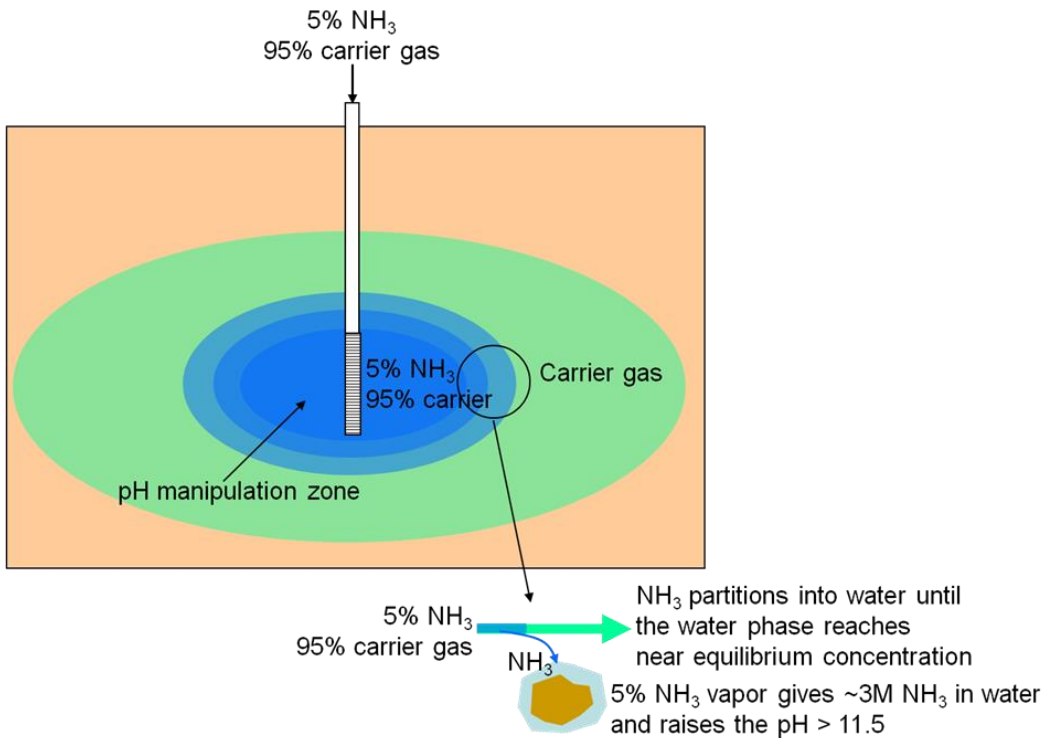
Figure 1.2. Conceptual Depiction of Ammonia Distribution in the Subsurface from an Injection Well

During the ammonia treatment process, the increase in pore-water pH releases ions into solution where they will be in a mobile state until the pH returns to neutral, causing precipitation reactions. In most unsaturated vadose zone conditions, movement of pore water is very slow, and a decrease in pH will occur before any significant movement. In other words, the reaction processes are rapid compared to potential contaminant transport.

The long-term fate of ammonia added to the subsurface to induce uranium treatment, as described in laboratory testing (Truex et al. 2014), is (1) volatilization and upward ammonia gas migration in the vadose zone, (2) microbial conversion of ammonia to nitrate in the pore water, and/or (3) ammonium sorption or incorporation into aluminosilicate precipitates. To examine the relative importance of the second and third processes, sediment dosed with 5%, 0.5%, or 0.05% ammonia gas was incubated for varying lengths of time in closed containers so that volatilization of ammonia was not possible. Sacrificial treatments were analyzed for ammonia, nitrate, and nitrite concentrations. In all treatments, minimal increases in nitrate or nitrite were observed over 3 months of incubation time. Total microbial populations were also measured before ammonia dosing and during incubation. With exposure to a 5% ammonia gas concentration, representative of the treatment zone concentration, microbial populations starting at about 1×10^7 cells/mL declined to nondetectable levels. Microbial populations exposed to 0.05% and 0.5% ammonia gas concentrations declined by orders of magnitude. The microbial populations exposed to 0.05% ammonia gas concentrations recovered quickly on exposure to air, whereas populations exposed to higher concentrations showed minimal recovery. These results suggest that the nitrification pathway is insignificant during ammonia injection because microbial populations are significantly reduced.

The potential for injected ammonia to generate nitrate over time was investigated for the field test application and for different conceptual scenarios of full-scale application. The field test target was treatment of 700 m^3 of the vadose zone by injection of about 3000 kg of ammonia. If all of this ammonia was converted to nitrate (through ammonia oxidation by bacteria), it would theoretically produce about 11,000 kg of nitrate and this mole-per mole conversion to nitrate may be the ultimate fate of the injected ammonia. However, laboratory data show that the aqueous ammonia concentration decreases by two orders of magnitude (3 M to about 0.03 M) during the buffering and precipitation reactions that occur over a duration of about a month after ammonia injection (Figure 1.3). Thus, the vast majority of added ammonia is included in precipitates or sorbed to zeolites that are created during the precipitation processes. After a month, the observed nitrate concentration was only about 0.1 mM (6 mg/L), which is much lower than the theoretical 3 M (180,000 mg/L) that would have occurred if all of the ammonia were to be converted to nitrate. If the ammonia concentration 1 month after treatment (~0.03 M) were all converted to nitrate, 110 kg of nitrate would be produced from the injection of 3000 kg of ammonia. These data do not directly show the fate of ammonia over long periods, but if most of the ammonia is associated with precipitates, it may not be converted to nitrate. The association of ammonia with sediments and its low volatility will also limit the volatilization pathway, but volatilization will be a slow and steady process that disperses ammonia away from where it was injected at low concentrations.
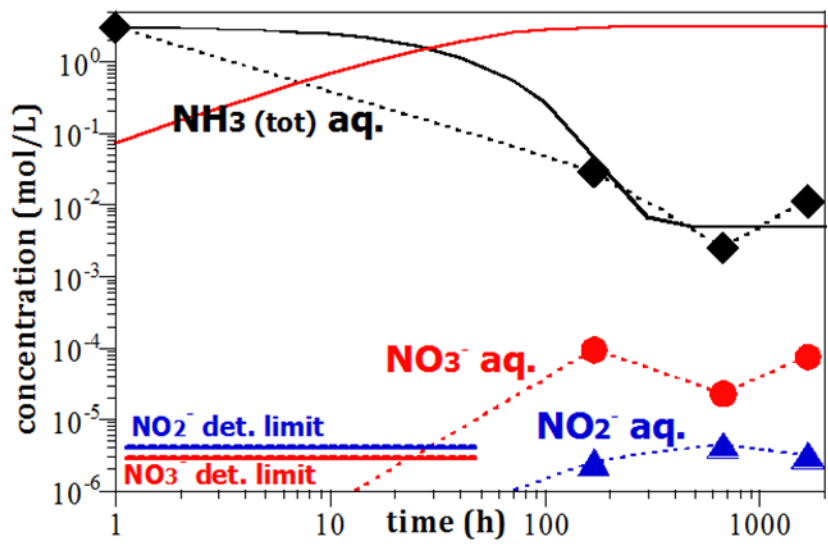
Figure 1.3. Changes in Ammonia, Nitrate, and Nitrite over Time after Sediment Exposure to 5 vol%
Ammonia. Note that the y axis is on a log scale. For reference, the red line is the theoretical
concentration from full conversion of ammonia to nitrate. For reference, the black line is a
modeled ammonia decrease over time based on the data (black diamonds with connecting
black dashed line) Observed nitrate and nitrate are shown with connecting dashed lines.
(Truex et al. 2014).

Tables 1.1 through 1.3 show estimates for test-zone properties and quantities of amendments to apply the
ammonia treatment for uranium. Table 1.1 is from the field test plan (DOE 2015a), describing the
quantities estimated for the current field testing effort. (Note: An indication of the gallons of ammonia
required and the estimated mass of nitrate produced were added and are not in the table in the field test
plan.) This same estimation approach was then applied to selected scenarios to develop estimates for
amendment quantities. The sizes of the treatment zones used in the scenarios (other than the current field
test) are rough estimates to examine a range of different targets and may be under- or over-estimates for a
specific example site. For scaling purposes, several different injection radii and flow rates were
estimated, depending on the scenario. The estimated radii ranged from 10 to 20 m and the estimated flow
rates were 100 or 200 scfm. The injection radius and injection flow rates have not been confirmed by
testing yet. All scenarios are for a target treatment thickness of about 6 m.

Table 1.1. Estimate for the 216-U-8 Field Test Design

Parameter	Value
Water Content (g H_2O/g total dry sed)	0.04
Porosity	0.2
Particle Density (g/mL)	2.5625
Dry Bulk Density (g/mL)	2.05
Water Volume Fraction (mL H_2O/mL dry sed)	0.082
Gas Volume Fraction (mL/mL)	0.118
Equilibrium NH_3 Concentration (M)	3.192
Calculated Equilibrium pH	11.88
Target Screen Interval (m)	3.1
Target Radius of Injection (m)	6
Target Treatment Volume (m^3) (cylinder + 40% of a sphere)	713
Total NH_3 Mass (kg)	3,170
Total NH_3 Volume (gal)	1,370
NH_3 Mass/Pore Volume (kg)	3.00
Pore Volumes Needed	1,100
Total Gas Volume Needed (NH_3 + carrier) (m^3)	92,000
Gas Flow Rate (ft^3/min)	100
Time for NH_3 Delivery (d)	23
Potential NO_3 Generated (kg)	**109**

Table 1.2. Estimate for Treating the Cold Creek Unit under the U-8 Crib (20×80 m)

Parameter	Value
Water Content (g H_2O/g total dry sed)	0.1
Porosity	0.3
Particle Density (g/mL)	2.5625
Dry Bulk Density (g/mL)	1.794
Water Volume Fraction (mL H_2O/mL dry sed)	0.179
Gas Volume Fraction (mL/mL)	0.121
Equilibrium NH_3 Concentration (M)	3.192
Calculated Equilibrium pH	11.88
Target Screen Interval (m)	3.1
Target Radius of Injection (m)	10
Number of Injection Wells	4
Target Treatment Volume (m^3) (cylinder + 40% of a sphere)	11,000
Total NH_3 Mass (kg)	107,000
Total NH_3 Volume (gal)	46,000
NH_3 Mass/Pore Volume (kg)	47
Pore Volumes Needed	2,300
Total Gas Volume Needed (NH_3 + carrier) (m^3)	3,052,000
Gas Flow Rate per Well (ft^3/min)	100
Total Gas Flow Rate (ft^3/min)	400
Time for NH_3 Delivery (d)	187
Potential NO_3 Generated (kg)	**3,670**

Table 1.3. Estimate for Treating the Ringold Formation under the U1/U2 Cribs (80×80 m)

Parameter	Value
Water Content (g H_2O/g total dry sed)	0.04
Porosity	0.2
Particle Density (g/mL)	2.5625
Dry Bulk Density (g/mL)	2.05
Water Volume Fraction (mL $H2O$/mL dry sed)	0.082
Gas Volume Fraction (mL/mL)	0.118
Equilibrium NH_3 Concentration (M)	3.192
Calculated Equilibrium pH	11.88
Target Screen Interval (m)	3.1
Target Radius of Injection (m)	20
Number of Injection Wells	4
Target Treatment Volume (m^3) (cylinder + 40% of a sphere)	69,000
Total NH_3 Mass (kg)	307,000
Total NH_3 Volume (gal)	133,000
NH_3 Mass/Pore Volume (kg)	291
Pore Volumes Needed	1,100
Total Gas Volume Needed (NH_3 + carrier) (m^3)	8,956,000
Gas Flow Rate per Well (ft^3/min)	200
Total Gas Flow Rate (ft^3/min)	800
Time for NH_3 Delivery (d)	275
Potential NO_3 Generated (kg)	**10,500**

1.2   Uranium Waste Sites at the Hanford Central Plateau

Vadose zone contamination at the Hanford Site results from past uranium and plutonium extraction activities and the intended or unintended release of 202,703 kg of uranium to the ground surface (Corbin et al. 2005). A compilation of the major uranium discharges at Hanford (Simpson et al. 2006) showed that 81% of the uranium inventory is in 10 sites and 9.7% in the next 10 sites. Types of uranium discharge to the natural surface or subsurface were (1) cold start and fuel rod dissolution wastes, (2) uranium nitrate hexahydrate waste with poorly defined pH, (3) high acid discharge waste, and (4) waste with high base and inorganic complexants (CO_3 and PO_4). As the uranium-laden waste infiltrates, the acidic and alkaline components dissolve some minerals (but eventually the pH is neutralized) and uranium precipitates primarily in carbonates and phosphates (acidic wastes) and silicates (alkaline wastes) in the vadose zone. Uranium is present in vadose zone sediment at medium to high concentrations as carbonates (liebigite and rutherfordine), co-precipitated with carbonates, and hydrous silicates (uranophane [$Ca(UO_2)_2(SiO_3OH)_2 \cdot 5H_2O$] and Na-boltwoodite [$Na(UO_2)(SiO_4) \cdot 1.5H_2O$] (Zachara et al. 2007; Um et al. 2009a). Uranium is also present in more mobile aqueous and adsorbed phases.

A survey of Hanford Central Plateau waste sites that had a substantial uranium inventory was conducted as part of site selection activities for the treatability test. Additional information about site selection and a map of the sites considered are included in Appendix A. Table 1.4 summarizes the waste stream, disposal site features, and characterization data available (not including data from recent 200-DV-1 OU or treatability test efforts). Of the 11 high-uranium-inventory sites listed in the table (not including the uranium solids disposed at the A-19 crib), 6 had acidic discharges (including the 216-U-8 crib selected for the field test) and 5 were neutral to basic discharges (similar to the site samples used for the ammonia technology development testing).

Table 1.4. Description of Selected Uranium Waste Discharge Sites for the Hanford Central Plateau

Site	Description
216-A-19 Crib	Waste Stream(s): The site received PUREX startup waste during November and December 1955. Although several references state it also received condenser cooling water from the 241-A-431 building via the 216-A-34 ditch, drawings do not show the 216-A-34 ditch connecting to the 216-A-19 crib. While the U inventory (~43 metric tons) is the largest discharged to any Hanford liquid disposal waste site, all but 31 kg U is estimated to have been discharged as solids (Soil Inventory Model [SIM]). Cumulative discharge inventory summary (SIM) is: • U: 43,444 kg (depleted) • Na: 27, 671 kg • Fe: 18,345 kg • NO_3: 10,919 kg • CO_3: 5102 kg • SO_4: 4604 kg • Cs-137: 0 Description: The crib is a $7.6 \times 7.6 \times 4.6$ m deep ($25 \times 25 \times 15$ ft deep) excavation with no liquid dispersion structure. Characterization: The only characterization data is from the C3245 borehole drilled through the crib in April 2003. Borehole logging indicates uranium at 20 to 80 pCi/g located from 3.0 to 9.4 m (10 to 31 ft) below ground surface (bgs). Maximum Cs-137 activity level observed was 560 pCi/g at 2.4 m (8 ft) bgs. Sediment sampling showed 51 pCi/g U-238 (max) at 4.4 m (14.5 ft) bgs.
216-U-1&2 Cribs	Waste Stream(s): The cribs received overflow from the 241-U-361 settling tank, which received cell drainage from the 5 to 6 tanks in 221-U and waste from the 224-U building until the uranium recovery process operations shut down in 1957. From July 1957 through May 1967, the 216-U-1&2 cribs received waste from the 224-U facility and equipment decontamination waste and reclamation waste from the 221-U canyon. The waste was low in salt and neutral to basic, except for the highly acidic discharge late in its history. Cumulative discharge inventory summary (SIM) is: • U: 3955 kg • C-137: 1.8 Ci • Na: 8467 kg • K: 127,476 kg • NO_3: 1,669,917 kg • CO_3: 6536 kg • PO_4: 6633 kg • SO_4: 171,222 kg Description: The cribs include two wooden liquid dispersion structures in adjacent excavations $27.1 \times 8.5 \times 4.9$ m deep ($89 \times 28 \times 16$ ft deep) that operated in series. Characterization Data: Characterization borehole 299-W19-96 (A9797) was drilled through the 216-U-1 crib in 1995. The highest zone of contamination was found at a depth of 6 to 12 m (20 to 40 ft). Maximum contamination levels in this zone included 2,400,000 pCi/g Sr-90, 1,430,000 pCi/g Cs-137, and 438 pCi/g Pu- 239/240.

Site	Description
	Three additional characterization boreholes (299-W19-95, 299-W19-96, and 299-W19-97) were drilled near the 216-U-1&2 cribs in 1995. Borehole sediment samples and surface soil samples were collected and analyzed. Uranium-contaminated perched water was observed in the Cold Creek Unit (CCU).
	Shallow push holes surround the crib at various distances. Isopleth maps of uranium and Cs-137 contamination indicate significant lateral contamination spread.
	There are thought to be two zones of uranium concentration: one that is shallow and another in the deeper Cold Creek silt and carbonate layer.
	Unusual Occurrence 85-17: Unusual Occurrence 85-17 reports groundwater samples taken in January 1985 from wells 299-W19-03 and 299-W19-11, indicating 60,000 and 85,000 pCi/L of uranium, respectively. Previous routine samples averaged less than 500 pCi/L. Investigation revealed that liquid waste from the 216-U-16 crib, located south of the 216-U-1&2 cribs, had migrated north along a subsurface caliche layer. Existing groundwater monitoring wells around the 216-U-1&2 cribs provided a pathway for the contamination to reach the groundwater.
216-U-8	Waste Stream(s): The cribs received acidic process condensate from the 221-U and 224-U buildings, along with drainage from the 291-U stack via an underground vitrified clay pipeline.
	The waste was acidic. Discharge inventory summary (SIM) is: • U: 25,512 kg • Tc-99: 2.7 Ci • C-137: 0.05 Ci • Am-241: 4.7 Ci • Na: 7482 kg • K: 3,624,455 kg • Ca: 5852 kg • NO_3: 4,556,685 kg • PO_4: 79,023 kg • F: 7295 kg • Cl: 8192 kg
	Description: The site consists of three wood timber liquid dispersion structures set in series within a $48.8 \times 15.2 \times 9.7$ m deep ($160 \times 50 \times 32$ ft deep) excavation. Each structure is $4.9 \times 4.9 \times 3.0$ m deep ($16 \times 16 \times 10$ ft). The structures were filled with 1.3 cm (0.5 in.) crushed stone. There is roughly 2070 m^3 (73,000 ft^3) of gravel fill in the cribs.
	Characterization: During the 1995 Limited Field Investigation, a borehole (299-W19-94) was drilled though the crib to a depth of 60.6 m (199 ft) and abandoned following characterization. Gamma logging detected U-238 (831 pCi/g at 11.4 m [37.5 ft] bgs and 150 pCi/g at 56.4 m [185 ft] bgs) in the borehole. Soil samples showed high concentrations of Cs-137 and Sr-90 near the underground vitrified clay pipeline.
	Isopleth maps of uranium, Tc-99, and Cs-137 contamination obtained from boreholes drilled to approximately 45 ft deep during 2005 indicate significant lateral spread of contamination.
216-U-12 Crib	Waste Stream(s): From April 1960 to May 1967, the site received 291-U-1 stack drainage, 241-WR vault waste, and 224-U process condensate via the C-5 tank. Contaminated water from the 241-WR vault was discharged to the crib in October 1965, which included 3.14 kg (6.9 lb) of thorium. From May 1967 to September 1972, the site received the above wastes (excluding the 241-WR vault waste) and occasional waste via the C-7 tank in the 224-U

Site	Description
	building. From September 1972 to November 1981, the site was inactive. From November 1981 to January 1987, the site received acidic process condensate (typical pH range was 0.5 to 1.5) from the 224-U building. The crib also received miscellaneous storm drain wastes from the 224-U building. Between April 1960 and September 1972, 6.7E+5 kg nitrate was released to the crib from the uranium tri-oxide process. The waste was acidic. Cumulative discharge inventory summary (SIM) is: • U: 6458 kg • Tc-99: 0.7 Ci • Cs-137: 69.6 Ci • Am-241: 1.4 Ci • Na: 3921 kg • K: 1,834,294 kg • Ca: 2965 kg • NO_3: 2,279,820 kg • PO_4: 40,049 kg • F: 3707 kg • Cl: 8192 kg Description: The 216-U-12 crib includes a below-grade, 30 cm (12 in.) diameter vitrified clay pipe running horizontally for the length of the crib within a $30.5 \times 3.0 \times 4.6$ m deep ($100 \times 10 \times 15$ ft deep) excavation that was filled with 264 m^3 gravel. Characterization: Limited characterization data are available from a 1994 borehole placed adjacent to the crib footprint, which showed no contaminants above background. Spectral gamma borehole logging of a borehole through the crib to 53 m (175 ft) bgs indicates Cs-137 from 5 to 18 m (16 to 59 ft) (maximum activity of 16,100 pCi/g at 7 m [23 ft]) and U-238 from 5 to 24 m (17 to 80 ft) (maximum activity of 500 pCi/g at 23 m [76 ft] bgs). Isopleth maps of uranium and Cs-137 contamination obtained from boreholes drilled to approximately 40 to 50 ft deep during 2005 indicate significant lateral contamination spread.
216-B-12	Waste Stream(s): The crib originally received 221-U and 224-U condensate waste transported from 200 West Area via the cross-site transfer line (line V219). Later, the crib received condensate waste from the 221-B Plant. From November 1952 to December 1957, the site received the process condensate waste from the tributyl phosphate uranium recovery processes at the 221-U and 224-U buildings as well as B Plant condensate. From December 1957 to May 1967, the site was inactive. From May 1967 to November 1967, the site received construction waste from the 221-B building. After November 1967, the site received process condensate from the 221-B building. The waste was low in salt and neutral-to-basic. Cumulative discharge inventory summary (SIM) is: • U: 15,112 kg • Na: 14,051 kg • Ca: 8147 kg • K: 2,286,683 kg • NO_3: 2,860,615 kg • CO_3: 11,676 kg • PO_4: 50,066 kg • F: 4743 kg • Sr-90: 120 Ci

Site	Description
	• Tc-99: 1.6 Ci • Cs-137: 326 Ci Description: The unit consists of a series of three cascading, $4.9 \times 4.9 \times 3.0$ m ($16 \times 16 \times 10$ ft) high wooden boxes in a $48.8 \times 15.2 \times 9.1$ m deep ($160 \times 50 \times 30$ ft deep) excavation. A 1.3 cm (0.5 in.) rock backfill lies in the bottom 3.7 m (12 ft) of the excavation and beneath each box is approximately 1.2 m (4 ft) of this rock. The site contains 2900 m^3 (3800 yd^3) of 1.3 cm (0.5 in.) gravel. Characterization: Wells 299-E28-9, 299-E28-16, 299-E28-65, and 299-E28-66 monitor this unit. Characterization borehole C3246, drilled into the crib in June 2003, was drilled to a depth of 308 ft. Geophysical logging found Cs-137, U-238, and Eu-154. The maximum concentration of Cs-137, 121,000 pCi/g, was found at 35 ft bgs. Approximately 10 pCi/g of U-238 was observed at 36.0 to 36.6 m (118 to 120 ft) bgs. Logging of 299-E28-16 (A6794), located approximately 9.1 m (30 ft) south of the crib, showed ~100 pCi/g of U-238 at 47 m (155 ft) bgs. This hole also indicated ~100,000 pCi/g of Cs-137 at 30.5 m (100 ft) bgs, which may have masked the presence of U-238. Logging of 299-E28-65 (A6816), located in the crib, showed greater than 10,000 pCi/g of Cs-137 from the bottom of the crib to 21 m (70 ft) bgs, with a maximum of approximately 250,000 pCi/g at a depth corresponding to the bottom of the crib.
241-BX-102 overfill event (UPR-200-E-5)	Waste Stream(s): In 1951, this tank was receiving the "metal waste" stream from the bismuth phosphate plutonium separation process at B Plant. On March 20, 1951, a cascade outlet became plugged, resulting in the BX-102 tank overfilling. The bismuth phosphate process released approximately 348,000 L (91,600 gal) of metal waste containing approximately 10.1 metric tons of uranium. Description: Contamination migrated beyond the 241-BX/BY fence, to the northeast and under the road north of the B Farm with increasing depth to the northeast. Some of this waste is contained in the saturated sediments that are perched on the Cold Creek fine-grained interval and is, over time, slowly leaking through and contributing to the groundwater plumes. A groundwater uranium plume that originates beneath the perched zone has flowed to the northwest under the BY tank farm and cribs. Characterization: There is excellent characterization information available for various depths and locations of holes. Shallow push holes within the tank farm surround the release point. There are several deep boreholes next to the tank and eastward to the point of the projected release to groundwater. The depth of the uranium in the vadose zone increases from the source location to the northeast. Contamination near the CCU is thought to represent the most severe vadose zone threat to groundwater from uranium on the Hanford Site. Well 299-E33-45 (C3269), located west of the BX-102 tank but inside the tank farm fence, revealed silt bands in the upper 51.8 m (170 ft) that exhibit uranium, sodium, nitrate, and Tc-99 contamination. Soil pH is elevated from 22.8 to 51.8 m (75 to 170 ft). U-238 was present between 21.9 and 60.3 m (72 and 198 ft) with a peak value of 240 pCi/g at 41.5 m (136 ft). Tc-99 was noted from 36.6 to 70.1 m (120 to 230 ft) with a maximum of about 30 pCi/g (water extraction) at 51.8 m (170 ft).

Site	Description
	Borehole 299-E33-343, located at the northwest corner of the B tank farm, shows the uranium contamination has migrated deeper within the vadose zone, and appears to be near the perched water zone in the CCU. Boreholes 299-E33-18 (A4844) and 299-E33-345, located approximately 38 m (125 ft) east of 299-E33-343, also revealed high uranium contents in the CCU. Recent wells 299-E33-350 and 299-E33-351 had no vadose zone contamination above the perched water. Well 299-E33-360 also had no vadose zone contamination above the perched water zone, indicating the uranium had moved into this deep zone laterally from near the leaking tank. However, the uranium concentrations within the saturated perched water interval are consistent with other existing perched water concentrations.
BC Cribs and Trenches	Waste Stream(s): The BC cribs and trenches were active in 1956-1957. They received waste produced by the bismuth phosphate separations process that was reprocessed at 221-U to recover the uranium from the waste. After the uranium was removed, the Cs-137 and Sr-90 contents of the effluent were reduced by precipitation with nickel ferrocyanide. A total of 6 cribs and 16 unlined trenches received scavenged tank waste from the uranium recovery process. Trenches 216-B-53A, 216-B-53B, 216-B-54, and 216-B-58 received laboratory and Plutonium Recycle Test Reactor waste from the 300 Area. The scavenged tank waste was high in salt and neutral-to-basic. Cumulative discharge inventory summary (SIM) to the 216-B-17 crib (example) is: - U: 104 kg - Na: 279,059 kg - Ca: 503 kg - K: 1984 kg NO_3: 561,917 kg NO_2: 18,709 kg CO_3: 19,658 kg PO_4: 20,064 kg SO_4: 37,363 kg - F: 6111 kg - Cl: 9944 kg - Sr-90: 82.9 Ci - Tc-99: 9.8 Ci - Cs-137: 119.7 Ci Description: The 216-B-17 crib is constructed of a single wood/concrete block/steel plate liquid dispersion structure measuring $3 \times 3 \times 0.9$ m ($10 \times 10 \times 3$ ft) high that is set below grade on a 1.5 m (5 ft) thick bed of 3-inch gravel. The 216-B-26 trench is an unlined trench 154 m (500 ft) long, 3 m (10 ft) wide, and 2.4 m (8 ft) deep. Earthen dams divide the trench into three sections. Characterization: In 2005, characterization borehole C4191 was drilled through the 216-B-26 trench to groundwater. Two regions of contamination were found: a near-surface region of Cs-137 and Sr-90 associated with the bottom of the trench and a deeper region of Tc-99 and nitrate from 27.4 to 41.1 m (90 to 135 ft) bgs. Maximum near-surface contamination concentrations observed were Cs-137: 529,000 pCi/g, Sr-90: 974,000 pCi/g, Am-241: 41 pCi/g, Pu: 195 pCi/g. Spectral-gamma logging system (SGLS) logging of boreholes installed to support a subsequent excavation-focused treatability test revealed a highly contaminated region (~1 ft thick) at a depth of approximately 3.3 to 3.6 m (11 to 12 ft) with Cs-137 concentrations exceeding 1E+06 pCi/g.

Site	Description
	In 2008, borehole C5923 was drilled to groundwater near the 216-B-17 crib. No near-surface contamination was observed because it was intentionally located outside the footprint of the crib. Peaks of Tc-99 contamination were observed at approximately 15.2, 27.4, 38.1, and 68.6 m (50, 90, 125, and 225 ft) bgs, indicating significant lateral spread, as well as deep mobile contamination. Maximum mobile U contamination observed was ~40 µg/L at approximately 21.3 m (70 ft) bgs.
216-A-3, and -9 Cribs	**216-A-3 Crib** Waste Stream(s): Until November 1967, the site received wastes from the silica-gel regeneration in the 203-A building, the uranyl nitrate hexahydrate (UNH) storage pit drainage, and the liquid waste from the 203-A pump house. After November 1967, the site received UNH storage pit drainage, liquid drainage, liquid waste from the 203-A building enclosure sumps, and the heating coil condensate from the P1 through P4 UNH tanks. Between 1967 and 1970, the site discontinued receiving discharge from silica-gel regeneration wastes. The waste included uranium, Cs-137, Sr-90 and Ru-106. The site was taken out of service in April 1981. Description: The unit contains a 10 cm (4 in.) diameter Schedule 10 perforated 304 stainless steel pipe placed horizontally 2.4 m (8 ft) below grade and two 6.1 m (20 ft) lengths of this pipe placed perpendicularly to the first pipe, forming an H pattern in a $6.1 \times 6.1 \times 4.9$ m deep ($20 \times 20 \times 16$ ft deep) excavation. The site has approximately 2.4 m (8 ft) of gravel fill with a volume of 280 m^3 (10,000 ft^3) and has been backfilled. **216-A-9 Crib** Waste Stream(s): Until February 1958, the site received acid fractionator condensate and condenser cooling water from the 202-A building. In February 1958, the crib was judged to have reached its capacity and was taken out of service. In April 1966, the crib was approved for disposal of liquid N Reactor decontamination waste, which continued to October 1966. From October 1966 to August 1969, the site was inactive. In August 1969, the site again received acid fractionator condensate from the 202-A building. The waste was acidic. Description: The site contains a 25 cm (10 in.) diameter Schedule 30 steel perforated pipe, placed horizontally, 2.7 m (9 ft) below grade in a $420 \times 20 \times 13$ ft deep excavation. The site has 1840 m^3 (65,000 ft^3) of gravel fill and has been backfilled. Characterization: Groundwater wells 299-E24-3, E24-4, E24-5, and E24-63 monitor this unit. The data indicate that no breakthrough to groundwater has occurred at this site.
216-A-4 Crib	Waste Stream(s): The site received the laboratory cell drainage from the 202-A building. (The site was reported to have also received 291-A-1 stack drainage.) The 216-A-4 crib also received waste solution from the 216-A-2 waste collection tank, the U cell U-3 and U-4 laboratory waste receiver tanks (located in the acid storage vault), the dissolver off-gas scrubbers, and the 241-A-151 diversion box catch tank. The waste was low in salt and neutral-to-basic. Cumulative discharge inventory summary (SIM) is: • U: 5388 kg • K: 75,974 kg • NO$_3$: 95,373 kg • PO$_4$: 1691 kg • Cs-137: 4.9 Ci

Site	Description
	Description: Excavation was $20 \times 20 \times 26$ ft deep. Two 6.1 m (20 ft) lengths of 15 cm (6 in.) perforated vitrified clay pipe form a horizontal cross pattern and are located 5.5 m (18 ft) below grade. The excavation has 2.4 m (8 ft) of coarse rock fill with a volume of 280 m^3 (10,000 ft^3) and has been backfilled. Characterization: Characterization borehole C4560 was drilled into the crib in 2004. Drilling was suspended due to an unexpected extremely high zone of radiological contamination encountered. Dose rates of 2.2 R at 6.7 m (22 ft) and 2.4 R at 7.0 m (23 ft) were observed. Borehole C5301 (299-E24-23), drilled in late 2006/early 2007, was placed south of the southwest corner of the crib and drilled 109.7 m (360 ft) deep. Cs-137 was the only manmade isotope detected.
216-S-1&2	Waste Stream(s): This unit was used as a subsurface liquid distribution system that received cell drainage and process condensate from the REDOX facility. The waste had a pH of 2.1. The waste was discharged to the cribs in batches, with each batch being approximately 19,000 L (4940 gal.), and an average of 10 batches discharged each day. When the crib was abandoned, it had received approximately 750,000 Ci of mixed fission products. The site received cell drainage from the D-1 receiver tank and process condensate from the D-2 receiver tank in the 202-S building. The waste was acidic. Cumulative discharge inventory summary (SIM) is: • U: 2220 kg • Na: 9778 kg • NO$_3$: 210,879 kg • Sr-90: 959 Ci • Tc-99: 2.6 Ci • Cs-137: 827 Ci Description: The excavation includes two open-bottomed crib boxes, each measuring 3.7×3.7 m (12 ft $\times$ 12 ft), made of timber, and placed in a 3.0 m (10 ft) thick gravel bed in a $27.4 \times 12.2 \times 10.4$ m deep ($90 \times 40 \times 34$ ft deep) excavation. The cribs are connected in series where overflow from the crib box S1 flows into crib box S2 via an underground pipe. Characterization: Core samples from wells drilled in 1956 determined that Cs-137 was contained in the upper strata beneath the cribs, but that Sr-90 had reached groundwater. Core samples from five additional wells drilled near the 216-S-1&2 cribs in 1966 indicated that 90% of the Cs-137 and less than 10% of the Sr-90 was contained in the soil between 4.8 m (16 ft) and 10 m (33 ft) below the cribs. Geophysical logging performed in 1984 indicated that Cs-137 concentrations were highest just below the bottom of the crib and decreased rapidly with depth. There has been little change in the gamma activity profiles since 1958.
216-S-7	Waste Stream(s): From January 12, 1956, to April 12, 1959, the unit received REDOX cell drainage from the D-1 receiver tank, process condensate from the D-2 receiver tank, and condensate from the H-6 condenser in the 202-S building. A buildup of beta activity in this crib prompted the rerouting of H-6 waste material to the underground waste storage tanks. The crib continued to receive waste from D-1 and D-2 vessels until July 1965. The waste was acidic. Cumulative discharge inventory summary (SIM) is: • U: 3411 kg • Na: 11,760 kg • NO$_3$: 432,149 • Sr-90: 1471 Ci

Site	Description
	- Tc-99: 2.5 Ci - Cs-137: 979 Ci - Pu-239/240: 83.7 Ci Description: The unit consists of two wooden structures measuring 4.9 m (16.1 ft) square and 1.6 m (5.2 ft) high. The structures are set 15.2 m (50 ft) apart, center to center, in a 30.5 × 15.2 × 6.7 m deep (100 × 50 × 22 ft deep) excavation. The structures were set in gravel and covered with backfill. The two structures are connected in parallel by a pipe, allowing the flow to be equally distributed to both cribs. Characterization: Characterization borehole C4557 was installed in late 2004 and completed in early 2005. Geophysical logging indicated maximum Cs-137 of two million pCi/g at 7.8 m (25 ft) bgs. No other manmade radionuclides were detected. SGLS characterization of 299-W22-33, located in the crib footprint, indicated 300 pCi/g of Cs-137 at 8.4 m (27.5 ft). No other manmade radionuclides were detected.

2.0 Conclusions and Recommendations

This section provides conclusions and recommendations for the URGS ammonia treatment technology based on the completed treatability test elements and assessment of implications for consideration of the technology for remediation implementation.

2.1 Overall Conclusions

URGS is intended to protect groundwater by decreasing the mobility of uranium contamination in the vadose zone. To achieve this objective, the amendments need to be distributed to contact the targeted treatment zone and the technology needs to induce a robust geochemical change that decreases uranium mobility. The treatability test was designed to evaluate the technology through a combination of laboratory testing and a field test at the 216-U-8 site.

The laboratory testing for ammonia technology development conducted prior to initiating efforts at the field test site demonstrated the treatment process and provided information needed to scale the treatment for field applications (Szecsody et al. 2010a,b, 2012; Zhong et al. 2015; Truex et al. 2014). A variety of vadose zone, low-water-content sediments were treated with ammonia to evaluate the treatment. Injection of ammonia in the gas-phase created high dissolved-phase ammonia concentrations that followed equilibrium partitioning behavior. The injection led to an increase in pH from 8.0 to about 11.5 when the injected gas phase was 5 vol% ammonia. The increase in pore water pH resulted in a large increase in pore water cations and anions from mineral-phase dissolution. Minerals showing the greatest dissolution included montmorillonite, muscovite, and kaolinite. Pore-water ion concentrations then decreased with time. Geochemical simulations based on initial pore-water ion concentrations indicated that quartz, chrysotile, calcite, diaspore, hematite, and Na-boltwoodite (a hydrous uranium silicate) should precipitate (Szecsody et al. 2010b).

During laboratory testing for ammonia technology development conducted prior to initiating efforts at the field test site, several types of analyses were conducted to evaluate changes in uranium mobility after ammonia treatment (Szecsody et al. 2010a,b, 2012; Zhong et al. 2015). These studies used approaches similar to those described in Section 3.0. Of these, the most important for evaluating ammonia treatment effectiveness were sequential extractions and soil column leaching tests. Sequential extractions were applied to assess how the distribution of uranium among aqueous and sediment-associated phases changed during treatment. For sequential extractions, the sediment was first contacted with simulated groundwater and then the groundwater was removed and analyzed for uranium. This same approach was then sequentially applied with an ion exchange solution, a weak acetic acid, a strong acetic acid, and finally strong acid (see Section 3.0 for details). Sequential extractions for pre- and post-treatment sediments samples were compared to quantify the effect of the ammonia treatment. Soil column leaching tests were also conducted for some sediments when sufficient sediment was available to quantify the amount of uranium that eluted from a sediment when exposed to flowing simulated groundwater. The sediment was placed in a small soil column and simulated groundwater was pumped through the column at a relatively slow rate for about 100 pore volumes. Effluent samples were analyzed for uranium with comparison of tests for pre- and post-treatment sediments.

Results of the technology development laboratory tests prior to the field test showed good ammonia treatment performance. Laboratory testing of the ammonia treatment was conducted for a range of

sediments and associated uranium precipitate phases and sediment samples that were available from the Hanford Site at the time of the technology development efforts. Sediments were primarily from beneath tank farms and from other sites with neutral-to-basic waste discharge conditions. Over 80% of the sequential extraction tests showed good mobility reduction (125 tests on 18 sediments), with mobile phases reduced by an average of 68% and immobile phases increased by an average of 71%. The soil column results showed over 80% less uranium leaching due to ammonia treatment (tests on three sediments). Other tests also showed good results. However, testing was limited by two factors. First, only a few sediment types could be tested with the soil column leaching method because a sufficient quantity of material was only available for a few sediment types. Second, samples were available only for limited types of waste disposal chemistries that did not include acidic disposal and associated neutralization processes because sampling of this type of waste site was not scheduled to include the technology development effort needs.

Initial activities at the field test site included characterization of site sediments, laboratory dosing and effectiveness testing of site sediments, and construction of the injection and monitoring system. Laboratory effectiveness testing with field-site sediments from the 216-U-8 crib included sediment characterization, sequential extraction analysis, and soil column leach testing of pre- and post-treated sediments (Section 3.0). Acidic waste had been discharged at the URGS field site (the waste was passed through a lime tank prior to discharge, but the pH was not specifically managed), in contrast to the sites providing sediment for previous laboratory tests. Sequential extraction results for field test site sediment samples showed a decrease in uranium mobility after ammonia treatment for 17 of 18 samples based on reductions observed in mobile uranium phases. These results suggested that uranium mobility was decreased by treatment. However, for many of the sediment samples, there was not a corresponding increase in the immobile (harsh acid extraction) phases.

In soil column leaching tests with field test site sediment, almost all ammonia-treated samples showed a higher total mass of uranium leached for the same number of pore-volume flushes than was leached for the corresponding untreated sample. For some samples, part of this difference may be due to differing starting uranium concentrations between the untreated and treated subsamples. However, looking across all of the data, this variability does not explain the consistently greater leaching of uranium from ammonia-treated sediments. The soil column leaching results were inconsistent with sequential extraction results for mobile uranium phases with respect to total mass leached and the initial uranium concentrations in the column effluent. Most ammonia-treated samples showed a high uranium concentration eluted from the soil column in the first few pore volumes when only the mobile phase of the uranium should elute from the column.

Ammonia treatment at the field test site, as indicated by the sequential extraction results, should have significantly reduced the highly mobile phases and the initial eluted uranium concentrations should have been low. Based on previous technology development testing, the ammonia treatment process requires at least 2 to 4 months incubation time to work. However, reaction times used in the current study with the field test samples are consistent with these previous studies (all greater than 2 months) and treatment effectiveness was the same for all of the tested reaction times. Thus, observed ammonia treatment results are not due to the reaction time that was used in the test.

The laboratory results with field test sediments demonstrated that there were interferences that affect the ammonia treatment. These interference factors may be caused by the types of uranium phases present, the presence of co-contaminant interferences, or sediment/co-contaminant properties that lead to the need for

higher ammonia doses for the treatment to be effective. The reason for the site-specific interferences was evaluated to assess applicability of the technology to other sites. Results with the field test sediments suggest that areas below acidic waste discharge sites (such as the location of the 216-U-8 field test site), where sediment carbonate is depleted and where the microscopic uranium distribution on soil particles is concentrated in localized deposits rather than more uniformly precipitated at the soil surface, would not be suitable for use of URGS ammonia treatment. Because the ammonia treatment process was found to be sensitive to these conditions, there may be other geochemical conditions that may interfere with ammonia treatment effectiveness. For this reason, the treatability test report includes the recommendations for site-specific testing, as described in Section 2.2.

Because the field test was not conducted because of the observed poor treatment effectiveness in the laboratory for field-site sediments, the conclusions and recommendations focus on information gained in the treatability test effort for technology effectiveness, implementability, and cost factors. This information was derived from the laboratory testing during technology development, laboratory testing for the field test site, and from the field test design and construction activities.

The treatability test report compiles the technology information gained from the laboratory testing during technology development, the laboratory testing using field-site samples, and a laboratory study assessing geochemical interferences that affect ammonia treatment performance. In addition, the treatability test report describes the field injection and monitoring equipment design and associated design calculations. Collectively, this information will assist in evaluating this technology for applicability at other sites. Information suggests that applicability at acidic discharge sites may be poor at locations in the subsurface where the waste chemistry impacted the sediments as observed in the shallow vadose zone below the 216-U-8 test site. However, effective URGS treatment may be possible at neutral or basic discharge sites or deeper in the vadose zone below sites if subsurface geochemistry has not been significantly affected by the waste discharge chemistry However, if the URGS technology is determined to be potentially applicable at a site in the future, site-specific laboratory testing would be necessary to confirm treatment effectiveness prior to field-scale implementation. The field design and laboratory testing conducted for the URGS treatability testing and gas-injection experience from the Hanford desiccation field test (Truex et al. 2018), conducted as part of the *Deep Vadose Zone Treatability Test Plan for the Hanford Central Plateau* (DOE 2008), provide a basis for design of ammonia injection at prospective sites. There are also two anticipated uses of ammonia injection outside Hanford that may also provide relevant information. One of these tests is for a U.S. Department of Defense research application evaluating injection of ammonia to increase the rate of alkaline hydrolysis of organic contaminants (Reactive Gas Process for In Situ Treatment of 1,2,3-Trichloropropane in Vadose Zone Soils, ER-201632, https://www.serdp-estcp.org/Program-Areas/Environmental-Restoration/Contaminated-Groundwater/Persistent-Contamination/ER-201632). For another test, ammonia will be injected to provide an electrical conductivity increase in the water within subsurface fractures so that electrical resistivity tomography (ERT) can be used to identify the location of the fractures (Pacific Northwest National Laboratory [PNNL] project number 68073). Injection effectiveness is related to the subsurface soil properties (e.g., soil moisture content and gas permeability) and potential short-circuit pathways (e.g., pipelines), and site-specific ammonia injection trials may also be necessary prior to full implementation at another site.

The URGS test demonstrated that interactions of the ammonia treatment chemistry and site geochemistry are important to the effectiveness of the treatment for decreasing uranium mobility. This report documents closeout of the URGS treatability test as part of the *Deep Vadose Zone Treatability Test Plan for the Hanford Central Plateau* (DOE 2008) effort. The treatability test effort accomplished the goal of

providing sufficient data for the URGS ammonia treatment process for its consideration in a future feasibility study.

2.1.1   Effectiveness Considerations

The URGS ammonia treatment technology is based on dissolving aluminosilicates, a ubiquitous component of Hanford Site sediments, to create conditions for precipitation of low-solubility uranium silicates and re-precipitation of aluminosilicates. These processes are expected to decrease uranium mobility because low-solubility materials such as uranium silicates are created. While this basic geochemical process is robust, laboratory results using samples from the field test site demonstrated that the process may not decrease uranium mobility. In essence, if the geochemical manipulation of silicate dissolution and precipitation does not adequately enable uranium silicate precipitation, or re-precipitated aluminosilicates do not coat uranium, then uranium mobility will not be reduced. Further, if these interactions do not occur and the dissolution/re-precipitation process causes uranium to be present in higher-solubility forms than pretreatment conditions, then uranium mobility may be increased by the ammonia treatment. This latter situation appears to occur for the field test site conditions. Thus, site-specific information is needed to determine whether the geochemical manipulation induced by ammonia treatment will decrease uranium mobility.

Laboratory tests were conducted to evaluate potential causes of the poor ammonia treatment effectiveness observed with laboratory dosing of ammonia to field site sediments. Site sediment characterization tests showed low sediment carbonate (e.g., calcite) concentrations, low concentrations of uranium associated with the alkaline sediment extraction analysis used to identify carbonate-associated uranium, and microscopic uranium distribution on the soil particles concentrated in localized deposits rather than more uniformly precipitated at the soil surface. Low amounts of carbonate and carbonate-associated uranium can affect the uranium compound dissolution that is induced by ammonia treatment, the uranium complexation in the pore water during ammonia treatment, and the pH neutralization process that occurs after ammonia injection is terminated. Having microscopic uranium concentrated in localized deposits rather than more uniformly precipitated at the soil surface can affect the uranium compound dissolution that is induced by ammonia treatment. Post-ammonia-treatment surface analysis also showed localized microscopic uranium deposits, suggesting poor dissolution during ammonia treatment and likely poor coating by aluminosilicates. Collectively, these conditions, and potentially others, hindered ammonia treatment effectiveness in laboratory tests of samples from the field test site.

Other factors were investigated, but no evidence was found that these other factors affected ammonia treatment. For instance, the field test site did not have high organic carbon or phosphate concentrations that might indicate presence of tributyl phosphate or other uranium complexing agents. Similarly, tests for the other hypotheses listed in Section 3.2.1.3 did not identify a factor related to poor ammonia treatment performance. However, those potential concerns (e.g., presence of organic carbon) could affect the treatment process at other sites. In summary, interference testing identified specific concerns at acidic waste discharge sites where the discharge has altered the sediment carbonate concentrations and caused uranium to be deposited in sparse hot spots in the sediment. The overall treatability test results, including these interference tests, lead to a recommendation that site-specific effectiveness testing is needed for evaluation of this technology prior to selection for application at another site because URGS ammonia treatment effectiveness can be impacted by site-specific geochemical factors.

The URGS technology uses ammonia vapor to alter the subsurface pH and induce the targeted geochemical reactions. To achieve the necessary pH change (from an initial value of about pH 8 to a treatment value of about pH 11.5), a large quantity of ammonia must be added. The treatment results in a 3 M ammonia concentration in the vadose zone moisture. The long-term fate of this ammonia is primarily incorporation into precipitates and biological conversion of ammonia to nitrate. Thus, the treatment adds nitrate "in exchange" for reducing the uranium mobility. Because nitrate is also a contaminant of concern, the mass of nitrate added during treatment must be considered as part of evaluating the suitability of the technology for a site. Section 1.1 provides estimates of nitrate mass for conceptual ammonia treatment scenarios. The largest of these scenarios is treatment of uranium for a 80×80 m target (69,000 m^3), with an estimated 10,500 kg of nitrate produced from the added ammonia.

2.1.2   Implementability and Cost Considerations

The URGS technology requires injection of a sufficient mass of gas-phase ammonia into the targeted area of the vadose zone to raise the pore water concentration of ammonia to about 3 M. As shown in Section 1.1, the mass of ammonia estimated for the field test and for potential Hanford applications ranged from 3000 kg (1300 gal of liquid ammonia) to over 300,000 kg (130,000 gal of liquid ammonia). Thus, a substantial amount of ammonia must be handled for injection operations. Large-scale ammonia handling is conducted for other industries (e.g., anhydrous ammonia refrigeration, use of anhydrous ammonia as agricultural fertilizer) and equipment for ammonia is available with ammonia-compatible materials. However, care must be taken in the design to ensure ammonia compatibility, and equipment is typically not off-the-shelf (implying higher costs and longer lead times). There are also construction codes that must be followed because of ammonia's properties and the handling of pressurized systems (liquid ammonia at 20 °C is pressurized at about 114 psig [https://webbook.nist.gov/]). The field-test design described in Section 4.0 includes information about equipment requirements, although a less complicated ammonia delivery system using a single stock tank could be used for a remediation application in place of the multiple-tank design prepared for the field test. Ammonia injection in the gas phase at a low percentage concentration (i.e., 5 vol%) must use anhydrous gas because of ammonia's affinity for water. Thus, a dry liquid nitrogen carrier gas was specified for the field test and would likely be needed for remediation applications. Estimated volumes for the carrier gas range from 85,000 to 8,500,000 m^3 (gas-phase). Thus, large quantities of liquid nitrogen are needed and the injection system must be made compatible with handling of the cryogenic liquid nitrogen and the potential for oxygen depletion in enclosed spaces unless a large unit for creating dry air is used.

Use of ammonia also requires health and safety equipment and planning. The field test design (Section 4.0) is indicative of the type of ammonia monitoring that would be required for health and safety for a remediation application. This health and safety monitoring included an ammonia sensor in the areas that leaks were likely to occur (e.g., piping joints, connection points, and valves), in the ammonia storage and injection equipment enclosure, on the pressure relief off-gas stack, and surface monitoring across the area above the vadose zone injection target. Ammonia sensors are readily available, but they are typically applied in an industrial setting, not at a field site where sensor application can be more problematic because of the environmental conditions in the field versus the controlled environment in an industrial facility. Because odor and hazard thresholds for ammonia are low, sensors for ambient health and safety monitoring were operated at the low end of their range for the planned field test, with an alarm threshold imposed at 12 ppmv. Experience at the field test site showed ammonia sensor drift and sporadic readings not associated with ammonia (because no ammonia was present at the test site). These issues are

problematic because false positive readings require a response and may affect work both for the remediation operation and for any adjacent unrelated operations. Emergency planning is substantial due to the hazard and flammability concerns with ammonia. Releases into the atmosphere are of specific concern due to the rapid movement outside of areas controlled by the remediation operation. Field test planning included interactions with the fire department and nearby facilities, such as the 200 West pump-and-treat facility, where a release would have had broad implications for personnel safety and facility operations. Because of the low odor threshold for ammonia, concerns may also arise if staff smell ammonia odors below the alarm threshold and respond with a stop work and emergency notification. Thus, future implementation for remediation will need to consider the project risks and health and safety aspects related to use of a hazardous gas.

2.1.3   Technology Resources

Detailed descriptions of the URGS technology development effort are available in the following reports and articles.

Reports

- DOE. 2015a. *Field Test Plan for the Uranium Sequestration Pilot Test*. DOE/RL-2010-87, U.S. Department of Energy Richland Operations Office, Richland, Washington.

- DOE. 2015b. *Sampling and Analysis Plan for the Uranium Sequestration Pilot Test*. DOE/RL-2010-88, U.S. Department of Energy Richland Operations Office, Richland, Washington.

- Truex MJ, JE Szecsody, L Zhong, JN Thomle, and TC Johnson. 2014. *Scale-Up Information for Gas-Phase Ammonia Treatment of Uranium in the Vadose Zone at the Hanford Site Central Plateau*. PNNL-23699, Pacific Northwest National Laboratory, Richland, Washington.

- Szecsody JE, MJ Truex, L Zhong, MD Williams, and CT Resch. 2010a. *Remediation of Uranium in the Hanford Vadose Zone Using Gas-Transported Reactants: Laboratory-Scale Experiments*. PNNL-18879, Pacific Northwest National Laboratory, Richland, Washington.

- Szecsody JE, MJ Truex, L Zhong, NP Qafoku, MD Williams, JP McKinley, CT Resch, JL Phillips, D Faurie, and J Bargar. 2010b. *Remediation of Uranium in the Hanford Vadose Zone Using Ammonia Gas: FY10 Laboratory-Scale Experiments*. PNNL-20004, Pacific Northwest National Laboratory, Richland, Washington.

Articles

- Zhong L, JE Szecsody, MJ Truex, and MD Williams. 2015. "Ammonia Gas Transport and Reactions in Unsaturated Sediments: Implications for Use as an Amendment to Immobilize Inorganic Contaminants." *Journal of Hazardous Materials* 289:118–129. doi:10.1016/j.jhazmat.2015.02.025

- Szecsody JE, MJ Truex, L Zhong, TC Johnson, NP Qafoku, MD Williams, JW Greenwood, EL Wallin, JD Bargar, and DK Faurie. 2012. "Geochemical and Geophysical Changes During NH3 Gas Treatment of Vadose Zone Sediments for Uranium Remediation." *Vadose Zone J.* 11(4). doi:10.2136/vzj2011.0158

- Emerson HP, S Di Pietro, Y Katsenovich, and J Szecsody. 2018. "Potential for U sequestration with select minerals and sediments via base treatment." *J. Environmental Management* 223:108-114.

- Katsenovich YP, C Cardona, J Szecsody, LE Lagos, and W Tang. 2018. "Assessment of calcium addition on the removal of U(VI) in the alkaline conditions created by NH$_3$ gas." *Applied Geochemistry* 92:94-103.

- Emerson HP, S Di Pietro, Y Katsenovich, and J Szecsody. 2017. "Effects of ammonium on uranium partitioning and kaolinite mineral dissolution." *J. Environmental Radioactivity* 167:150-159.

- Katsenovich YP, C Cardona, R Lapierre, J Szecsody, and LE Lagos. 2016. "The effect of Si and Al concentrations on the removal of U(VI) in the alkaline conditions created by NH3 gas." *Applied Geochemistry* 73:109-117.

2.2   Recommendations

Using the information collected from technology development and treatability test efforts, recommendations were developed with respect to URGS applicability (Section 2.2.1), lessons learned for the URGS and other reactive gas technologies (Section 2.2.2), and additional efforts that could be applied to refine the knowledge of URGS effectiveness, implementability, and limitations (Section 2.2.3).

As an overall recommendation for the URGS technology, a future feasibility study would first need to consider the waste discharge, associated subsurface geochemistry, and uranium mobility at a site. For sites where uranium mobility is determined to be a risk to groundwater, the URGS ammonia treatment can be evaluated using the technical information for the ammonia treatment process in this report and may be applicable if (1) site information suggests that ammonia treatment has the potential to reduce uranium mobility, (2) production of nitrate from the ammonia injection is within an acceptable range, and (3) ammonia injection appears to be feasible based on injection design calculations. For sites meeting these criteria, this report recommends that a site-specific evaluation of ammonia treatment effectiveness be conducted using sediments from the zone targeted for treatment. These tests would include sequential extraction and soil column leaching tests for untreated and ammonia-treated sediments to quantify the change in uranium mobility. This testing would require about 1 year from the time of sediment sample receipt to the reporting of laboratory results. For sites with positive results, where the decrease in uranium mobility will meet groundwater protection needs, an ammonia injection design can be implemented using a phased approach, if the URGS ammonia treatment technology is included in the remedial alternative selected in the Record of Decision.

2.2.1   URGS Applicability

From Section 1.2, of the 11 major uranium disposal sites in the Hanford Central Plateau (not including the uranium solids disposed at the A-19 crib), 6 were acidic-waste disposal sites where the ammonia technology may not be applicable because they may have the low sediment carbonate concentrations and microscopic uranium concentrated in localized deposits rather than more uniformly precipitated at the soil surface that were likely causes of poor ammonia treatment effectiveness at the field test site. For deeper ammonia treatment applications at acidic waste sites, the subsurface conditions may be appropriate for use of the technology, but site-specific evaluation would be needed. Of the 11 major sites, 5 were neutral-to-alkaline waste disposal and are more similar to the conditions tested during technology development. These 5 neutral-to-alkaline sites would potentially be more suitable for application of URGS, although site-specific testing for treatment effectiveness is recommended, with this testing to

include use of soil-column leaching tests to evaluate the change in uranium mobility induced by ammonia treatment.

Uranium disposal sites in the Hanford Central Plateau have a wide range of disposed inventory and disposal chemistry. As shown by 200-DV-1 OU characterization (Truex et al. 2017; Szecsody et al. 2017; Demirkanli et al. 2018), uranium in the tested sediments was dominantly in sediment-associated phases that limit uranium mobility. Thus, as a first step, remedial investigation of uranium mobility at sites is important to determine whether remediation to decrease uranium mobility is warranted. This determination for Hanford Central Plateau sites will occur as part of future remedial investigations and associated baseline risk assessments.

As a preliminary estimate, Eslinger et al. (2006) used the System Assessment Capability (a simplified assessment of contaminant transport) and the Soil Inventory Model available at the time of their work to evaluate which sites in the Hanford Central Plateau may be expected to affect groundwater with uranium concentrations above the drinking water standard. Sites in the U tank farm, REDOX cribs and trenches, TY cribs, PUREX cribs and trenches, U cribs, and B-Complex tank farms were identified as having a potential for uranium impact to groundwater. This information was later interpreted by Truex and Carroll (2013) as a preliminary estimate of uranium waste sites of concern, adding to the sites identified in Eslinger et al. (2006) based on observed uranium concentrations in groundwater beneath some waste sites. The bulleted list below shows this preliminary list of uranium waste sites of concern, indicating where information is known about the waste discharge pH (acidic [A]; basic or neutral [B/N]) and whether near-term (<100 year) or long-term (>100 to 1000+ years) arrival of uranium in the groundwater is expected. Additional sites considered for the URGS treatability test, but not identified in the preliminary estimates (Truex and Carroll 2013), are also shown below (denoted with an "*"). Determination of baseline risk for uranium will be finalized in the remedial investigation reports for vadose zone OUs. The intent of the list below is to provide an estimate of potential waste sites where remediation of uranium in the vadose zone may be required. This list shows a relatively small number of sites compared to the total number for which uranium was included in the waste stream or leak. Of these sites, based on the site-selection activities for the URGS treatability test (Appendix A), the 241-BX-102 and 216-B-12 sites are two high-uranium inventory sites for which ammonia treatment may be effective based on similarity to the sediment conditions used for laboratory test during technology development activities and based on the site properties relative implementation of the treatment process.

- 241-BX-102 tank (near term) [B/N]
- 216-B-12 (near term) [B/N]
- 216-A-4 (near term) [B/N]
- 216-U-10 (near term) [B/N]
- U tank farm (241-U-104) (long term) [B/N]
- 216-T-26 (long term) [B/N]
- 216-A-3* [B/N]
- 216-U-1/2 (near term) [A]
- 216-U-12 (long term) [A]
- 216-S-7 (long term) [A]

- 216-U-8* [A]

- 216-A-9* [A]

- 216-S-1&2* [A]

Because of the poor effectiveness observed in the laboratory for the samples from the treatability test site (216-U-8), applicability at these (or other) sites would need to confirmed based on site-specific evaluations, including laboratory testing on site sediments. Of the above sites, the 241-BX-102 site was included in pre-field-test laboratory evaluations and showed good treatment effectiveness. The 241-BX-102 site, however, is related to the B-Complex perched water contamination and ammonia treatment would only be applicable, if needed, for treatment of contaminated zones with relatively low moisture content, not perched water.

Surface infrastructure, contaminant depth, and contaminated sediment properties would also need to be considered with respect to implementability and cost when considering URGS applicability.

- Surface infrastructure and other administrative limitations (e.g., tank farm operations) add to the cost and difficulty of any in situ treatment.

- Contaminant depth is not a direct issue, but does affect cost (e.g., well costs) and may be of concern related to production of nitrate due to ammonia injection. Adding nitrate closer to the water table would create higher groundwater concentrations than the same amount of nitrate added higher in the vadose zone.

- Sediment properties are important for several reasons related to ammonia injection (in addition to geochemical considerations for treatment effectiveness).

  – Heterogeneity in sediment properties within the target treatment zone will affect injected gas distribution, with gases following the highest permeability pathways. Laboratory tests have shown that ammonia diffusion and partitioning behavior will help distribute ammonia into lower-permeability zones adjacent to the high-permeability pathways. However, significant heterogeneities can't be overcome by these processes.

  – Moisture content is important because it is directly proportional to the mass of ammonia required per volume of treatment zone that must be added to reach the targeted pore-water concentrations for effective treatment. Compared to a lower moisture content, a higher moisture content results in longer ammonia injection time and higher mass – both increasing the cost of treatment. Higher injected ammonia mass at the higher moisture content also results in a higher mass of nitrate produced within the treatment zone (although at the same concentration as for low moisture content).

  – Lower permeability zones will also potentially limit the gas injection rate or require higher pressures to achieve the same injection rate as for higher permeability zones. Longer injection times increase costs and higher pressure operations may lead to increased costs or safety concerns.

2.2.1.1   URGS Evaluation Needs

For full-scale URGS, the following site-specific information would be needed to evaluate effectiveness and any limitations for use of ammonia treatment.

- The uranium contaminant concentration and mobility prior to treatment must be determined to evaluate uranium fate and transport and the targeted reduction in mobility that would meet groundwater protection goals.

- The uranium distribution in sediment layers and sediment layer physical properties are needed to assess the ability to deliver sufficient ammonia gas for treatment.

- The sediment moisture content distribution and geochemical conditions (including sediment carbonate concentration) are needed to determine the ammonia treatment design and assess site-specific interferences for ammonia treatment effectiveness.

- Laboratory ammonia dosing and evaluation of the effectiveness in decreasing uranium mobility using soil column leaching methods are needed to determine whether ammonia treatment is applicable for a site. This testing would require up to 1 year of laboratory work because the dosing component needs about 4 months of reaction time and the soil column testing requires about 3 to 4 months to complete.

2.2.1.2   URGS Implementability Requirements and Limitations

To estimate URGS design, an equilibrium partitioning approach can be assumed for the ammonia loading into the targeted treatment area of the vadose zone. A mass balance type calculation can be used to estimate the ammonia loading needed for a targeted region of sediment at a specified water content and ammonia gas concentration (Truex et al. 2014; Zhong et al. 2015). Additionally, ammonia dissociation can be computed based on thermodynamic information so that the pH of the pore water can also be estimated. The tables in Section 1.1 show the results of these calculations for the field test site and for conceptual future applications on the Hanford Central Plateau. While these estimates do not account for all of the phenomena that can occur, they capture the dominant phenomena. Laboratory testing has confirmed that these estimates are close to what is observed at the laboratory scale.

The ammonia treatment design calculations provide a basis for estimating the ammonia injection and other equipment requirements under ideal conditions and include assumptions based on laboratory experience and professional judgment. Thus, some safety factors may need to be assumed for use of these calculations for a feasibility study. For instance, the example calculations in Section 1.1 assume that with anisotropy in the subsurface, the injected gas flow is expected to be more horizontal than vertical. In this case, the volume impacted by ammonia can be approximated as a cylinder with the target radius and height of the injection well screen (i.e., a radius of 6 m [20 ft] and a height of the injection well of 3.1 m [10 ft] for the test site) to represent the horizontal core of the injection zone. To account for some movement vertically (upward and downward), 40% of the volume of a sphere with the selected radius is added to the cylindrical volume in these calculations to account for expected vertical movement from the injection well. Gas advection, partitioning, and diffusion processes control the distribution of ammonia during injection. Partitioning causes a sharp concentration front in the ammonia gas phase. This front then moves slowly compared to the carrier gas advection. The slow advective movement of ammonia in the gas phase and the high-concentration gradient provide a large driving force and relatively long period for gas-phase diffusion processes to occur. Intermediate-scale laboratory tests show ammonia distribution into small-scale, low-permeability zones adjacent to and embedded in high-permeability zones (Szecsody et al. 2010b). The gas-phase diffusion rate was shown to be significant with respect to distributing ammonia to lower-permeability zones (Truex et al. 2014; Zhong et al. 2015). The relatively slow advective movement, rapid partitioning process, and contribution of diffusion are expected to

improve the uniformity of ammonia distribution during injection and improve the chances that use of an injection-only design will effectively distribute ammonia to the targeted treatment zone.

Recommended monitoring includes use of ERT to verify ammonia distribution to the subsurface target zone (as indicated by the increase in bulk conductivity when ammonia partitions into the pore water) and injection flow, pressure, and concentration monitoring. Spacing of ERT electrodes would be modified to be appropriate for the size and depth of the treatment application. The field test design provides a reasonable template for the type of monitoring needed (Sections 3.0 and 4.0). However, use of subsurface temperature monitoring would not be necessary for a remedy implementation.

The recommended aboveground equipment is the same as shown in the field test design except that a single bulk ammonia tank and appropriate sizing for the target application should be considered to significantly reduce ammonia delivery equipment and control system complexity, and daily manual handling of ammonia cylinders. A multiple small volume container approach was chosen during this test to address site specific emergency planning hazardous material volume limitations for individual containers. This approach resulted in design of a more complicated manifold, equipment and control system, in addition to requiring daily handling of ammonia containers. While the field test design was for treatability test purposes, similar equipment is needed for implementation because of the need for careful control of gas mixing and injection and handling of the ammonia and liquid nitrogen stocks.

The injection operating period is expected to be as estimated in the tables shown in Section 1.1. Higher injection flow rates than listed in this table are not recommended because of the need to have a controlled injection, dissolution, and diffusion processes that are important for distribution of the ammonia. Operational concerns and limitations are described in the Implementability and Cost Considerations section (Section 2.1.2) and the Lessons Learned section (Section 2.2.2).

2.2.2   Lessons Learned

Several lessons learned were derived from the treatability test effort and are applicable to conducting other treatability tests for reactive-gas technologies and for full-scale consideration of ammonia treatment. Laboratory testing, test design, field system design, and field system functional testing contributed to the lessons learned.

Laboratory testing included a variety of methods to evaluate treatment effectiveness and support scale-up to the field. Laboratory methods were based on those described in the literature and applied for similar purposes and for uranium characterization activities. Because of the reasonable correlation observed between sequential extraction results and soil column leaching across multiple related laboratory investigations, good correlation for these methods for assessing uranium mobility changes after ammonia treatment was expected. In addition, good correlation was observed in initial tests of ammonia treatment that were conducted during technology development efforts (Szecsody et al. 2012; Zhong et al. 2015) using sediments from other waste sites at Hanford, although there were a limited number of soil column tests conducted. However, poor correlation was observed in the laboratory between sequential extraction results and soil column leaching using samples from the field test site. Because these correlations were not tested prior to initiating field test design and construction efforts, problems with treatment effectiveness at the test site were not discovered until after the field test system was fully constructed. While it is, therefore, necessary to conduct soil column leaching as part of evaluating the effectiveness of

2.11

ammonia treatment for a specific site, these soil column tests for ammonia-treated sediments require about a year from receipt of samples to produce leaching data.

It is difficult to evaluate all possible interferences for treatment effectiveness in laboratory testing. Thus, technology development focused on understanding the primary mechanism of treatment and evaluated effectiveness for a moderate number of field-contaminated sediments. This information demonstrated that ammonia treatment should be effective and was based on a treatment mechanism that should be applicable at most sites (i.e., dissolution and precipitation of aluminosilicates). While this approach provides suitable technology information, consideration of in situ reaction-based technologies like ammonia treatment should consider site-specific conditions and, in many cases, would need a site-specific laboratory test to verify treatment effectiveness prior to being selected or implemented.

The treatability test design in the field test plan (FTP, DOE 2015a) and sampling and analysis plan (SAP, DOE 2015b) included all of the necessary testing and evaluation related to treatment effectiveness. However, the test schedule included parallel efforts of laboratory testing for ammonia treatment effectiveness and field testing. As demonstrated in the laboratory using samples from the field test site, interferences were present that resulted in poor treatment effectiveness. Because the ammonia treatment is sensitive to interferences, future scheduled testing or activities should include demonstration of effectiveness in the laboratory or by verification of likely effectiveness through diagnostic characterization prior to embarking on field activities.

Ammonia is used for industrial processes, thus, equipment and ammonia are available that are suitable for use in a remediation effort, but are not specifically designed for a remediation effort. Companies specifically experienced in ammonia system design and handling should be partnered with to take advantage of their experience. When applying a reactive gas for remediation, it should be recognized that there are equipment requirements and design codes applicable to ammonia that increase the cost and rigor needed in design and for system construction and acceptance testing. More frequent instrument calibrations due to the hazardous nature of ammonia should also be considered. There are also health and safety considerations, specifically emergency preparedness hazardous material volume limitations. that need to be incorporated into the design and operational procedures that add cost and time to the design, construction, and acceptance testing process. Section 2.2.1 provides additional field equipment information.

Health and safety monitoring for ammonia as part of the field test design included both process and area ammonia sensor deployment. Ammonia area sensors proved to be problematic for monitoring and providing alarms at the low ammonia health and safety thresholds that were established (12 ppmv). This alarm point was chosen to reduce the time it takes to recognize an exposure risk and initiate protective actions. However, this low ammonia level is difficult to detect and is well below the level used by commercial sites. Because the sensors demonstrated drift and sent false-positive alarms, management of ammonia injection operations would have been difficult. Ammonia sensor testing in the laboratory did not reproduce the same type of drift and false alarms observed in the field. Additional evaluation indicated that field problems may have been related to the interface of the sensors and the data logging system. False positives would unnecessarily exercise emergency response and have project and economic impacts outside the ammonia injection project. Thus, all reactive gas technologies will need to consider the project and economic risk of using a hazardous material that has the potential to be readily transported long distances (e.g., well outside the control boundaries of the injection site).

2.2.3　Technology Uncertainties

Existing information from this treatability test may be sufficient to evaluate URGS ammonia treatment applicability alone or in combination with site-specific information. This information is likely suitable to support the technology screening portion of a feasibility study. Because of the uncertainty in technology effectiveness, it is likely that most sites where URGS is considered beyond the screening portion of a feasibility study would need to have site-specific testing to evaluate effectiveness for the targeted treatment zone.

Additional information may help address uncertainties for technology screening or for evaluation of a remediation alternative that includes URGS. Efforts to address uncertainty include an expanded knowledge of interferences that cause poor effectiveness and an improved knowledge of implementation design and performance (e.g., ammonia injection). The following sections describe potential additional efforts to address these uncertainties.

2.2.3.1　Understanding of Interferences and Effectiveness Limitations

Only minimal remedial investigation activities for the Hanford Central Plateau 200-WA-1 and 200-EA-1 OUs have been conducted, such that limited sediment samples are available to assess uranium mobility and ammonia treatment effectiveness across the multiple uranium waste disposal conditions at the Hanford Central Plateau. At the time of this report, 200-DV-1 OU remedial investigation is underway. Available sediments from 200-DV-1 OU characterization activities included collection of samples from some locations previously investigated as part of technology development (e.g., associated with waste similar to the 241-BX-102 samples used in URGS technology development). The observed uranium concentrations and mobility in sediments characterized during the 200-DV-1 OU effort were low in almost all of these samples (Szecsody et al. 2017; Truex et al. 2017; Demirkanli et al. 2018). Sediment samples for acidic waste disposal sites will not become available until new boreholes are installed and samples are collected at waste sites for 200-WA-1 OU characterization efforts. Thus, near-term laboratory studies to assess interferences and treatment effectiveness at sites other than the 216-U-8 field test site and the sites used in technology development are not possible before additional remedial investigation begins.

Based on current data reported herein, URGS ammonia treatment effectiveness is expected to be site-specific, affected by the waste disposal chemistry and resulting geochemical conditions in the zone targeted for treatment. Because of this site-specific performance, technology effectiveness and identification of interferences are best addressed as the remedial investigation proceeds. A stepwise approach to this evaluation is recommended as described above in the introduction to Section 2.2.

2.2.3.2　URGS Implementation Needs

The implementation of URGS can be estimated using the information in this report, including the field test design information and the design calculations provided. Laboratory scale-up data are available (Truex et al. 2014; Zhong et al. 2015) that can be used to assess the viability of ammonia injection for candidate sites. The field design provides important information on equipment needed to inject and monitor ammonia for both operational and health and safety needs. Design calculations show the quantities of ammonia needed and provide an estimate of the potential mass of nitrate produced from

injection of ammonia (e.g., Section 1.1). This information can be used to produce a sufficient conceptual design for a feasibility study evaluation of the URGS ammonia treatment technology. If the URGS technology is promising for a site, additional implementation detail may be needed.

As a continuation of the phased technology evaluation approach recommended in Section 2.2, site-specific assessment of ammonia injection would be a final step in the evaluation to collect more detailed implementation information for a specific site. For sites with positive effectiveness results using the steps in Section 2.2, where the decrease in uranium mobility will meet groundwater protection needs, an ammonia injection design could be tested within a phased implementation approach, if the URGS ammonia treatment technology is selected as part of the most promising remedial alternative.

3.0 Approach

This section presents the approach for the treatability test. The field test component was not completed because of the observed poor treatment effectiveness in the laboratory for field-site sediments. However, this section documents the treatability test design and methods and the laboratory components of the treatability testing. This information may be relevant for future treatability studies or for evaluating implementation of reactive gas technologies.

3.1 Objectives

Test objectives were developed and presented in the FTP (DOE 2015a). These objectives are summarized in the bulleted items below and guided the test design efforts. However, the objectives were not fully achieved because the test was not completed due to the effectiveness issues revealed in the laboratory testing with field-site sediments.

- Determine the design parameters for applying uranium sequestration via ammonia injection to the study area. This includes determining the operational parameters such as reactant flow rates and properties (e.g., gas composition) and identifying the target areas to achieve acceptable reduction of mobile uranium.

- Demonstrate field-scale treatment for targeted areas within the vadose zone by quantifying the following:

  - Reduction of uranium mobility in the field test treatment zone compared to the reduction of uranium mobility observed in laboratory-induced treatment of site sediments with a goal of decreasing the mobile uranium fraction in the sediment by half. Extent is determined by a decrease in the amount of uranium that can be extracted using a sequential application of groundwater, an ion exchange solution, and a mild acetic acid solution as the extracting solutions.

  - Stability of sequestered uranium in terms of dissolution rate of uranium into the pore water.

- Demonstrate the ability to deploy operational equipment and instrumentation necessary to implement the treatment process on a large scale.

- Collect data to support consideration of uranium sequestration via ammonia injection as a remedy in the feasibility study process. Although the objectives of the treatability test are focused on uranium sequestration, impacts to expected co-contaminants (Tc-99, Sr-90, and Cs-137) will also be quantified.

3.2 Laboratory Evaluation for the Field Test Site

Laboratory evaluation for field site characterization and for ammonia treatment effectiveness for both laboratory- and field-dosed sediments was included in the FTP and SAP (DOE 2015a,b). Methods for site characterization and laboratory-dosed ammonia treatment assessment are summarized below and described in more detail in the FTP and SAP (DOE 2015a,b). Methods for field-dosed ammonia treatment effectiveness are not included because these activities were not conducted. After poor ammonia treatment was observed in the laboratory, additional laboratory testing was also conducted to evaluate the

potential site-specific interferences related to the poor effectiveness. The hypotheses and methods for interference testing are also included below.

3.2.1 Site Characterization and Laboratory-Dosed Ammonia Treatment Effectiveness

Site characterization was conducted using samples collected from six boreholes installed at the field test site as part of the ammonia injection and monitoring system. Four of the boreholes were sampled to characterize the vadose zone soils. The characterization data were used to (1) validate the test site selection, (2) obtain baseline information for site characterization, (3) determine the effectiveness of ammonia on uranium present at the site, and (4) select a target treatment zone. The boreholes were drilled in a manner to retain the representativeness of vadose zone soil samples. Borehole locations are conceptually shown on Figure 3.1 in relation to the 216-U-8 crib, with the NAD83, *North American Datum of 1983*, coordinates provided in Table 3.1. Laboratory analyses for site characterization and laboratory-dosed ammonia treatment effectiveness applied to samples collected from the first borehole drilled at the site (C9520) were conducted using the approach shown in Table 3.2 (additional information available in the SAP, DOE 2015b).

- Borehole C9520 was drilled to a depth of approximately 24.3 m (80 ft) bgs. Soil samples were collected continuously, starting at approximately 9.1 m (30 ft) bgs. Sampling was performed using a 10.2 cm (4 in.) diameter, 0.76 m (2.5 ft) long split-spoon sampler equipped with four separate nonconductive plastic liners that were each 15.2 cm (6 in.) long. Liners were sealed and shipped to the laboratory for analysis. The borehole was geophysically logged using downhole neutron, spectral gamma, total gamma, and temperature technology. This borehole was installed in fiscal year (FY) 2015.

- Samples were analyzed from borehole C9520. The data from borehole C9520 showed that uranium concentrations and mobile uranium content at the study site were suitable for the treatability test, so the remainder of the site boreholes were then drilled. Boreholes C9515, C9518, and C9519 (injection well) were drilled, sampled, and logged using the same approach as described for borehole C9520. These boreholes were installed in FY17.

- Boreholes C9515, C9518, C9519, C9517, and C9583 were also installed in FY17, but no laboratory analyses were conducted. These boreholes were logged as described for borehole C9520.
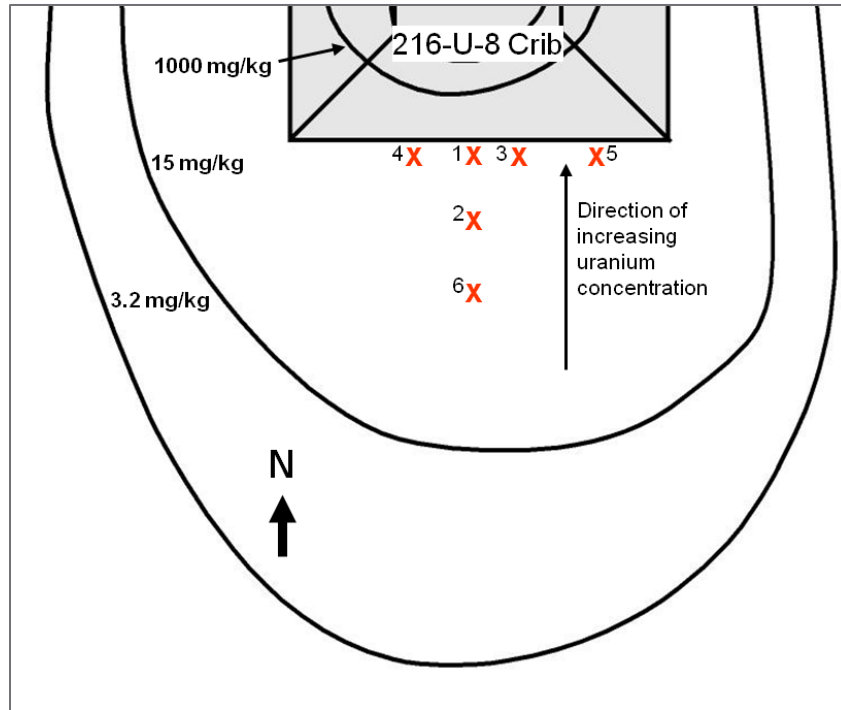
Note: Uranium concentration data is from D&D-27783, *200-UW-1 Field Summary Report for Fiscal Years 2004 and 2005*. Contours are the estimated uranium sediment concentrations from previous characterization in the upper 25 m (82 ft) of the vadose zone (not to scale).

Figure 3.1. Location of Boreholes (DOE 2015a)

Table 3.1. Borehole Location Coordinates (State Plane Coordinate System – Washington South, NAD83)

Location	Borehole/Well Identification	Northing (m)	Easting (m)
1 (Injection)	C9519/299-W22-121	134662.99	567618.98
2	C9515/299-W22-117	134659.96	567619.03
3	C9518/299-W22-120	134662.99	567621.01
4	C9520/299-W22-122	134663	567615.93
5	C9517/299-W22-119	134662.99	567624.05
6	C9583/299-W22-124	134657.00	567619.00

NAD83, *North America Datum of 1983*.

Table 3.2. Sample Design for Borehole C9520 (adapted from DOE 2015b)

	Sample Depth		Approximately 9.1 to 24.3 m (30 to 80 ft) bgs
	Total Depth		Approximately 24.3 m (80 ft) bgs
Media	Sample Type[a]	Sample Location	Analytes
Soil	All split-spoon liners	Continuous	Lithology description
			Core photographs
			Air permeability screening
			Gamma scan
	Obtain sample material from intact split-spoon liners in positions A, B, or C. Hold split-spoon liner D in reserve for additional sampling, if needed.	Select five intervals for characterization. Select sample intervals (split-spoon liners A, B, or C) based on a combination of downhole neutron and spectral gamma geophysical measurements. Hold split-spoon liner D in reserve. For each interval, use one liner for sequential extraction, and use adjacent liners for other physical/ chemical analyses.	Uranium using sequential chemical extraction (<4 mm grain-size fractions), assayed for uranium, technetium, cesium, and strontium
			Gamma energy analysis
			Total uranium (microwave acid (?) digestion)
			Deionized water extraction (<4 mm grain-size fractions)
			pH
			Electrical conductivity
			Cations (calcium, sodium, aluminum, silicon, magnesium, iron, potassium, barium, uranium, technetium, strontium, and cesium)
			Anions (NO_3^-, NO_2^-, SO_4^{2-}, chloride, and bromide)
			Carbonate (by total inorganic carbon)
			Total alpha/beta
			Acid (8 M HNO_3) extraction (<4 mm grain-size fractions)
			Cations (calcium, sodium, aluminum, silicon, magnesium, iron, potassium, barium, uranium, technetium, strontium, and cesium)
			Total alpha/beta
			Moisture content
			Grain size (laboratory analysis)
			Soil resistivity
	Select an intact split-spoon liner from the five separate previously characterized intervals.	In the laboratory, expose sample material from the five split-spoon liners selected for sequential extraction to ammonia treatment. After ammonia treatment, conduct analyses.	Uranium using sequential extraction (<4 mm grain-size fractions), assayed for uranium, technetium, cesium, and strontium
			Uranium leaching in the soil column with both untreated and treated sediments for these samples (<4 mm grain-size fractions), assayed for uranium, technetium, cesium, and strontium in effluent
			pH analysis
			Electrical conductivity

Note: Depths are approximate; field conditions need to be considered for actual collection depth.

(a) Does not include samples for quality assurance/quality control.

Because of the phased drilling approach and change from use of C9520 as the injection well to the use of C9519 as the injection well, the approach for boreholes C9515, C9518, and C9519 was modified in Tri-Party Agreement (TPA) Change Notices to the FTP and SAP (TPA-CN-0764 and TPA-CN-0766). The specific SAP analyses to be applied for boreholes C9515, C9518, and C9519 were determined in a meeting of the CH2M Hill Plateau Remediation Company and PNNL project team. In this meeting, the existing data from the URGS site boreholes were reviewed and discussed with respect to selecting the

next set of laboratory tests to be conducted. Selection of a focused set of analyses and samples is consistent with the TPA Change Notice, recognizing that the project team can adjust sample numbers and analyses based on the previous results from the C9520 borehole (for which the full suite of SAP analyses was conducted). At the time of the meeting, uranium sequential extraction analyses (including U, Tc-99, Cs, and Sr) for untreated samples had been completed for boreholes C9515, C9518, and C9519.

The laboratory effort for boreholes C9515, C9518, and C9519 and completion of C9520 analyses included:

1. Saving untreated samples and ammonia dosing of sufficient samples for subsequent sequential extraction and leaching tests were conducted for

    a. C9519 depths 42.3, 46.5, 48.5, 51.9, and 54.7 ft bgs

    b. C9515 depth 47.2, 48.7, and 52.8 ft bgs

    c. C9518 depth 47.4, 48.9, and 52.9 ft bgs

2. Sediment characterization analyses listed in Table 3.3 (a subset of SAP analyses based on C9520 results) for

    a. C9519 depths 42.3, 46.5, 48.5, 51.9, and 54.7 ft bgs

    b. C9515 depths 47.2 and 48.7 ft bgs

    c. C9518 depths 47.4 and 48.9 ft bgs

3. Soil column leaching tests for untreated and ammonia-dosed samples (dosed as part of previous lab work) from borehole C9520 with

    a. 4-month dosed samples (remainder air) for depths 42.9 and 47.2 ft bgs

    b. 1-year dosed samples for depths 42.9 and 47.2 ft bgs

    c. Untreated samples for depths 42.9 and 47.2 ft bgs

Table 3.3. Sediment Characterization Analyses Conducted for Boreholes C9515, C9518, and C9519

Amended Analysis List
Lithology description
Core photographs
Deionized WE (<4 mm grain-size fractions)
pH
Electrical conductivity
Cations (calcium, sodium, aluminum, silicon, magnesium, iron, potassium, barium, uranium, technetium, strontium, and cesium)
Anions (NO_3, NO_2, SO_4, chloride, and bromide)
Carbonate (by total inorganic carbon)
Acid (8 M HNO_3) extraction (<4 mm grain-size fractions)
Cations (calcium, sodium, aluminum, silicon, magnesium, iron, potassium, barium, uranium, technetium, strontium, and cesium)
Moisture content
Grain size

Laboratory methods for constituent and physical characterization of the site sediments are specified in the SAP (DOE 2015b). However, of particular importance are the methods for (1) sequential extraction and soil column leaching that are used to assess pre- and post-treatment uranium mobility and (2) the investigation of site-specific interferences for ammonia treatment effectiveness that were applied after soil column testing with laboratory-dosed sediments showed poor effectiveness. These methods are summarized below. The SAP contains additional information for the sequential extraction and soil column test methods.

3.2.1.1   Sequential Extractions

As described in the FTP (DOE 2015a) and by laboratory reports (Szecsody et al. 2010a,b), sequential extractions are a baseline measurement used to evaluate uranium mobility. The sequential extraction approach described in Szecsody et al. (2010b) was applied with the extraction solutions listed below, where the oxalate extraction from Szecsody et al. (2010b) was not applied because it did not provide significant value for interpreting the effectiveness of ammonia treatment. An additional separate extraction was also included to provide a better comparison to methods used for evaluating sorbed uranium by others (e.g., Zachara et al. 2007). The sequential extraction solutions are as follows (Szecsody et al. 2010b):

- Synthetic groundwater (1 hour)

- 0.5 M magnesium nitrate solution for ion exchange (1 hour)

- pH 5 sodium-acetate (1 hour)

- pH 2.3 acetic acid (1 week)

- 8 M nitric acid at 95 °C (2 hours)

In addition, the following extraction was conducted on a separate subsample:

- Carbonate solution (0.0144 M $NaHCO_3$, 0.0028 M Na_2CO_3) for ion exchange (1000 hours) (Zachara et al. 2007)

3.2.1.2   Soil Column Tests

Sequential extractions evaluate uranium mobility based on an interpretation of how the extraction relates to uranium transfer into the pore water. Saturated soil column leaching tests provide a measure of uranium mobility based on contact with water over time. Soil column leaching tests were conducted on a subset of the samples analyzed by sequential extraction, ensuring that the samples have been held for a suitable length of time for ammonia sequestration. These tests provide uranium mobility information that can be analyzed both in terms of a comparison to the sequential extractions and as an estimate of uranium transport parameters. While these experiments are conducted under saturated conditions, the kinetic parameters can be translated to unsaturated flow conditions. Leaching tests were performed on untreated and laboratory-treated samples collected during field site borehole installation.

A laboratory test instruction was used to guide the soil column tests. In summary, sediment from the samples selected for leaching tests was emptied and sieved to remove particles greater than 4 mm (0.16 in.). Sieved material was packed into soil columns. High-performance liquid chromatography

pumps were used to inject simulated groundwater upward through the column with a residence time of about 4 to 10 hours. Effluent was collected using a fraction collector, and selected time interval samples were analyzed for uranium. At selected times, flow was stopped for a period from sixteen to hundreds of hours to allow kinetically controlled processes and reactions to reach equilibrium. The difference in uranium concentrations before and after the stop-flow events was used to evaluate the presence of kinetically controlled uranium release from the sediment.

3.2.1.3   Site-Specific Interference Study

The purpose of this work was to evaluate potential site-specific interferences to the ammonia treatment process for vadose zone sediments from the 216-U-8 field test site for the URGS test. This work is related to the effort described by the SAP (DOE 2015b), but focuses on specific issues identified for the laboratory ammonia treatment portion of these tests. Tests were conducted using 216-U-8 site sediments and sediments that had previously shown good uranium mobility decreases after ammonia treatment. Table 3.4 summarizes the hypotheses, data collected, and assessment approach for the experiments.

Table 3.4. Interference Testing Approach

Hypothesis	Data Collected	Anticipated Assessment
Hypothesis 1: The waste chemistry at the 216-U-8 site caused uranium distribution in a way that includes U surface phases different from other previously tested sites or U contained in microfractures, and when ammonia treatment (high pH) is applied, U does not re-precipitate as silicates or get coated by alumino-silicates.	For untreated and NH_3-treated sediments: • Whole sediment X-ray diffraction (XRD) • Clay fraction XRD • X-ray absorption near edge structure/extended X-ray absorption fine structure (XANES/EXAFS) • Laser induced fluorescence spectroscopy (LIFS) • Total inorganic carbon (TIC) • Total organic carbon (TOC) • Sediment radiography • Alkaline U extraction	U surface phases (Na-boltwoodite, U in carbonates, aqueous/adsorbed U-carbonates) present in previous sediments that showed good treatment will be compared to phases are present at 216-U-8 (untreated and treated). Radiography and electron microprobe analyses will evaluate U distribution as discrete high U precipitates and the potential for U in microfractures, both of which may be less amenable to NH_3 treatment than distributed U surface phases. The assessment also considered carbonate content because low-CO_3 water results in different U-precipitates, which are more mobile upon NH_3 treatment. Waste chemistry for the previously tested sites and the 216-U-8 site will be considered in conjunction with the laboratory results to help interpret differences between previous sites and the 216-U-8 site.

Hypothesis	Data Collected	Anticipated Assessment
Hypothesis 2: Constituents present in the 216-U-8 sediment complex with uranium during the NH_3 treatment process such that uranium does not associate with silicates and precipitates as a high-solubility precipitate instead.	For untreated and 5% NH_3-treated sediments, during 20 pore volume leach, aqueous samples for: • U, Th, P, Si, Al, Ca, Mg, Fe, Mn, Na, K • Anions (including CO_3) • TOC • U complexes Sediment extractions: • Organic extractions • Phosphate	Lack of aqueous (and solid phase) carbonate has previously been shown to result in less effective NH_3 treatment of U in sediments. Pore-water chemistry may have components that create precipitates that are released with carbonate-rich synthetic groundwater. For instance, high Na-NO_3 results in weak Na-carbonate complexes, which decreases formation of U-carbonates and U solubility until artificial groundwater is introduced. An organic or organo-PO_4 (e.g., tri-butyl phosphate) may complex with U, preventing the formation of U-silicates. Waste constituents such as Th may cause different precipitates to form, which may relate to Hypothesis 1.
Hypothesis 3: Dissolution of silicates at the pH induced by 5% NH_3 treatment (~pH 11.5) is not sufficient to create uranium-silicate precipitates or enough silicate precipitates to coat uranium surface phases – thus, a higher pH (~pH 12.2) may be needed to induce treatment.	For 100% NH_3-treated sediments, during 20 pore volume leach, aqueous samples for: • U, P, Si, Al, Ca, Mg, Fe, Mn, Na, K • Anions (including CO_3) • TOC • Sequential U extractions	The pore-water chemistry just after ammonia treatment will be evaluated to assess anticipated uranium precipitates formed and by comparing the U, Si, Al, Ca, Mg, Fe, Mn, Na, K, P concentrations to the concentrations in sediments where ammonia treatment was successful.

Additional detail for the data collected to support each hypothesis is discussed below.

Hypothesis 1:

Solid phase characterization included the following:

1.1. Whole sediment XRD for major minerals: 216-U-8 sediment C9515 47.2' (U_{total} = 5338 ± 2285 µg/g), C9519 46.5' (2886 µg/g), and C9520 43' (1718 µg/g)

1.2. Clay/mica (< 2 micron) XRD to ensure montmorillonite, kaolinite, and muscovite are present (previously identified as major sources of Si, Al): 216-U-8 sediment C9515 47.2 ft

1.3. XANES/EXAFS of untreated/NH_3-treated sediment: 216-U-8 sediment C9520 42.9 ft

1.4. LIFS of untreated/NH_3-treated sediments: C9515 47.2' and untreated C9520 42.9 ft

1.5. Radiography analysis will be conducted to evaluate the spatial heterogeneity of U surface phases on untreated/NH_3-treated sediment from C9520 42.9 ft.

Table 3.5. Sediments for TIC and TOC

Borehole	Depth (ft)	U_{total} (µg/g)	Prev. # extr.	Prev. # leach exp.
C9515	47.2	5338	3	2
	52.8	9.86	3	0
C9519	42.3	383	4	2
	46.5	2886	6	2
	48.5	400	7	2
	54.5	7.5	6	2
C9520	38.0	415	4	0
	42.9	1718	7	4
	47.2	728	7	4
	50.7	67.5	4	0
	54.5	7.81	4	0
	62.0	15.3	4	0
BX102	131	415	8	2
TX104	69	18.4	2	2
C7117	32	1.55	8	4

1.6. TIC of untreated sediments (i.e., vertical profile to measure change in carbonate) were conducted on sediments in Table 3.5. The number of extractions and leach experiments already conducted on specific sediment is indicated in Table 3.5.

1.7. TOC of untreated sediments (i.e., vertical profile to identify presence of organic co-contaminant) was assayed for the sediment samples identified in Table 3.5.

1.8. Alkaline extraction of U surface phases will be conducted on untreated and selected NH_3-treated sediments listed in Table 3.8.

Hypothesis 2:

Using sediments C9520, 47.2' (728 µg/g), C9519 54.7' (7.5 µg/g), C7117 30-33', and TX104 69/110' (four sediments), untreated leach experiments (to 20 pore volumes) were conducted with the following effluent analysis (with details of analysis in Table 3.7):

2.1. U by inductively coupled plasma mass spectrometry (ICP-MS) and selected samples U(VI) by kinetic phosphorescence analysis (KPA)

2.2. Metals by inductively coupled plasma optical emission spectrometry (ICP-OES)

2.3. Anions by ion chromatography (IC)

2.4. Aqueous TIC and TOC

2.5. pH

These four untreated sediments will also be analyzed for:

2.6. Phosphate by extraction (Table 3.6)

2.7. Organic extractions (Table 3.6)

Using the same four sediments at 4% water content, a 5% NH_3/95% N_2 gas treatment (500 pore volumes) will be conducted in eight separate 1-D columns. These experiments are designed to measure an increase in cations during first tens of hours (i.e., compared with untreated sediment), and a subsequent decrease in cation concentration over hundreds of hours. At 24 hours and 650 hours, a deionized water extraction (Table 3.6) will be conducted with aqueous analysis (with details of analysis in Table 3.7). The 650-hour sample is 330 hours of NH_3 treatment followed by 320 hours of air treatment.

2.8. U by ICP-MS and selected samples U(VI) by KPA

2.9. Metals by ICP-OES

2.10. Aqueous TIC and TOC

Hypothesis 3:

Using 216-U-8 sediments C9520, 47.2' (728 µg/g) and C9519 54.7' (7.5 µg/g) at 4% water content, a 100% NH_3 gas treatment (500 pore volumes) will be conducted in eight separate 1-D columns. These experiments are designed to parallel those in Hypothesis 2. At specified times (24, 100, 300, 650 hours), a deionized water extraction (Table 3.6) will be conducted with effluent analysis (details of analysis in Table 3.7). The 650-hour sample is 330 hours of NH_3 treatment followed by 320 hours of air treatment.

3.1. U by ICP-MS and selected samples U(VI) by KPA

3.2. Metals by ICP-OES

3.3. Aqueous TIC and TOC

Selected sediments from 216-U-8 and previous studies will be used in experiments with geochemical extraction and leaching of sediment as described in Table 3.6, and analysis in Table 3.7. A summary of the sediments used in these experimental tasks is given in Table 3.8.

Table 3.6. Geochemical Extraction and Leaching of Sediments

Required Data	Analysis (see Table 3.7)	Method
Deionized water extraction (1:1 sediment: H_2O)	Metals by ICP-OES, U by ICP-MS or U(VI) by KPA	Um et al. 2009b Zachara et al. 2007

Sequential inorganic extractions
  1. Artificial groundwater
  2. Ion exchangeable
  3. pH 5.0 acetate
  4. pH 2.3 acetic acid
  5 Oxalate, oxalic acid
  6. 8M HNO_3, 95°C
	U by ICP-MS or U(VI) by KPA	Gleyzes et al. 2002
		
		Beckett 1989
		
		Larner et al. 2006
		
		Sutherland and Tack 2002
		
		Mossop and Davison 2003

Alkaline extraction for U	U, Th by ICP-MS	Kohler et al. 2004
Phosphate extraction of sediment	PO_4	Hach 8178

Sequential organic extractions
  1. Artificial groundwater
  2. isopropyl alcohol
  3. hexane
	Modified from Amin and Narang 1985, based on MIBK and solvent polarities	Volatile organic compounds by gas chromatography mass spectrometry (GC-MS) (EPA 8260b)

1-D column water leach rate experiment	U by ICP-MS or U(VI) by KPA, metals by ICP-OES, anions by IC, TIC, TOC, pH	Qafoku et al. 2004 Szecsody et al. 2013

Table 3.7. Geochemical Analysis Methods

Data and Instrumentation	Constituents Analyzed	Method
Metals by ICP-OES	Al, Ba, Ca, Fe, K, Mg, Mn, Na, Si, P	PNNL-ESL-ICP-OES, Rev. 4
U by ICP-MS	U, Th	PNNL-ESL-ICP-MS, Rev. 4
U(VI) by KPA	U(VI)	Brina and Miller 1992
Anions by ion chromatography	PO_4^{-2}, Cl-, F-, NO_3^-, NO_2^-, SO_4^{-2}	PNNL-ESL-IC, Rev. 1
Aqueous pH by electrode	pH	PNNL-ESL-pH, Rev. 2
Spectrophotometer	PO_4	Hach 8178
Total carbon and inorganic carbon in water	Total carbon (TC) and TIC	EPA 9060A, OP-DVZ-CHPRC-0006
Total carbon and inorganic carbon in sediment	TC and TIC	OP-DVZ-CHPRC-0006
Volatile organic compounds by GC-MS	Volatile organic compounds	EPA 8260b
XRD	Sediment minerals	For information only
XANES/EXAFS	U mineral phases	For information only
LIFS	U mineral phases	For information only
Radiography	Micron-scale U spatial distribution	For information only

Table 3.8. Sediments Used in Experiments

Borehole	Depth (ft)	U_{tot} (µg/g)	sed., mica XRD	XANES EXAFS, LIFS	Radiography	TIC, TOC[b]	alk. extr.	untr.1-D leach exp.[c]	P, O sed. extraction[d]	5%NH₃, H₂O extr.[e]	100%NH₃ H₂O extr.[f]
C9515	47.2	5338	u, c			u	u				
	52.8	9.86				u	u				
C9519	42.3	383				u	u				
	46.5	2886	u	u		u	u, t				
	48.5	400				u	u				
	54.5	7.5				u	u	u	u	t	t
C9520	38.0	415				u	u				
	42.9	1718	u	u, t	u, t	u	u, t	u	u	t	t
	47.2	728				u	u				
	50.7	67.5				u	u				
	54.5	7.81				u	u				
	62.0	15.3				u	u				
BX102	131	415				u	u, t				
TX104	69	18.4				u	u, t	u	u	t	
C7117	32	1.55				u	u, t	u	u	t	

u = untreated < 2mm sediment, t = NH₃-treated < 2 mm sediment, c = untreated < 2 um sediment (clay)

(a) Whole sediment XRD, clay fraction XRD, XANES/EXAFS, LIFS

(b) Total inorganic carbon (TIC), total organic carbon (TOC)

(c) 1-D leach experiment (20 pore volumes), with analysis of U, metals, anions, TIC, TOC, pH

(d) Sediment extraction for phosphate and organics

(e) 5% NH₃ treatment for 24 h and 650 h, then water extraction and analysis of U, metals, TIC, TOC

(f) 100% NH₃ treatment for 24 h, 100 h, 300 h, and 650 h, then water extraction and analysis of U, metals, TIC, TOC

3.3 Field Test Design and Procedures

The experimental design and procedures are summarized below.

3.3.1   Test Site Background

The DOE Hanford Site is a 1517 km^2 (586 mi^2) federal facility located in southeastern Washington State along the Columbia River. The location of the test, the 216-U-8 crib, is included in the 200-WA-1 OU (Figure 3.2). The 200-WA-1 OU, established in 2011, includes most waste sites located in the 200 West Area of the Hanford Site.

The 216-U-8 crib was selected for the URGS test because (1) historical characterization data indicated that the site contained a significant inventory of uranium that was likely to be in a mobile form, (2) the uranium concentration/distribution was favorable for a test, (3) the test could be conducted with shallow wells, (4) there were minimal logistical issues, and (5) suitable site data were available. Uncertainties for the test site identified in the site selection process were (1) the uranium contaminant concentration/distribution at the scale of the field test and (2) the effectiveness of the ammonia treatment for the sediment mineralogy and uranium phases present at the site. The full site selection process and results are provided in Appendix A. Previous characterization of the 216-U-8 crib region indicates uranium, and other contaminants discharged to the crib, had spread laterally in the vadose zone soils surrounding the crib. Uranium contamination is present in two distinct regions at the 216-U-8 crib (see Figure 3.3). One region is at a relatively shallow depth of approximately 10.6 to 15 m (35 to 50 ft) bgs in the coarser-grained Hanford formation. The second, deeper region is at a depth of approximately 58 m (190 ft) bgs in the fine-grained CCU. The treatability test focused on the shallow contamination in the Hanford formation. The sediments were characterized prior to conducting the treatability test to confirm that site conditions are conducive to the treatment technology.

Figure 3.2. Location of the 216-U-8 Crib Waste Site (DOE 2015a)
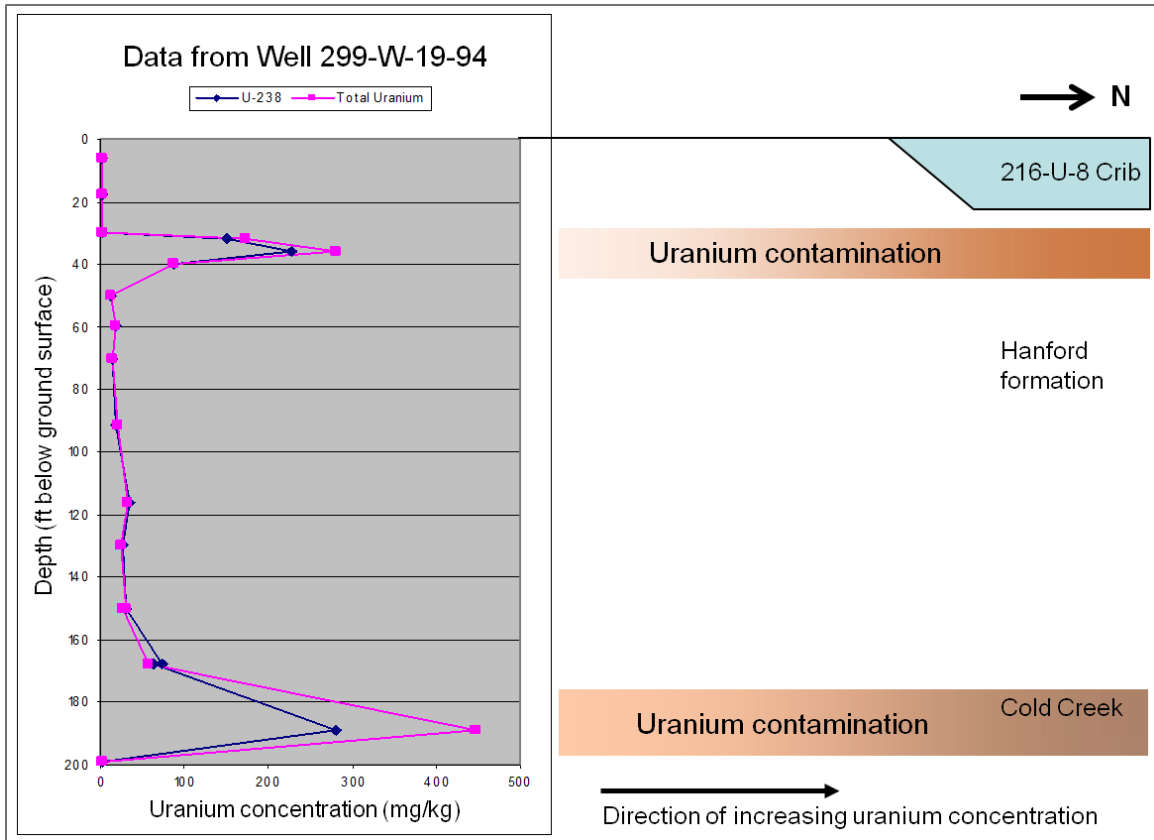
Figure 3.3. Uranium Concentrations in the Sediments beneath the 216-U-8 Crib (DOE 2015a)

3.3.2   Field Test Design Summary

The URGS technology relies on distribution of a 5 vol% ammonia gas mixture to the target treatment zone. Distribution requires multiple pore volumes of injection gas to pass through the treatment zone to deliver sufficient ammonia mass to reach equilibrium partitioning concentrations of ammonia in the pore water. To obtain this type of URGS treatment zone, the field test design used a nitrogen carrier gas supplied by a liquid nitrogen tank that was mixed with a pure ammonia gas stream supplied by liquid ammonia tanks (Figure 3.4). The gas mixture was to be injected into a well screened between 13.4 and 16.5 m bgs (44 and 54 ft bgs) and distributed to a targeted radial distance of 6 m. Progress of the ammonia injection was to be monitored by instrumented boreholes sensing the temperature rise of the ammonia dissolution front and by collecting soil gas samples from multiple sampling ports. Additionally, ERT with both surface electrodes and electrodes placed in all of the site boreholes was planned for tracking the increase in bulk conductivity resulting from dissolution of ammonia into the pore water. Monitoring boreholes also included blank casing to provide access for conducting periodic neutron moisture surveys and cross-borehole ground-penetrating radar (GPR) surveys.
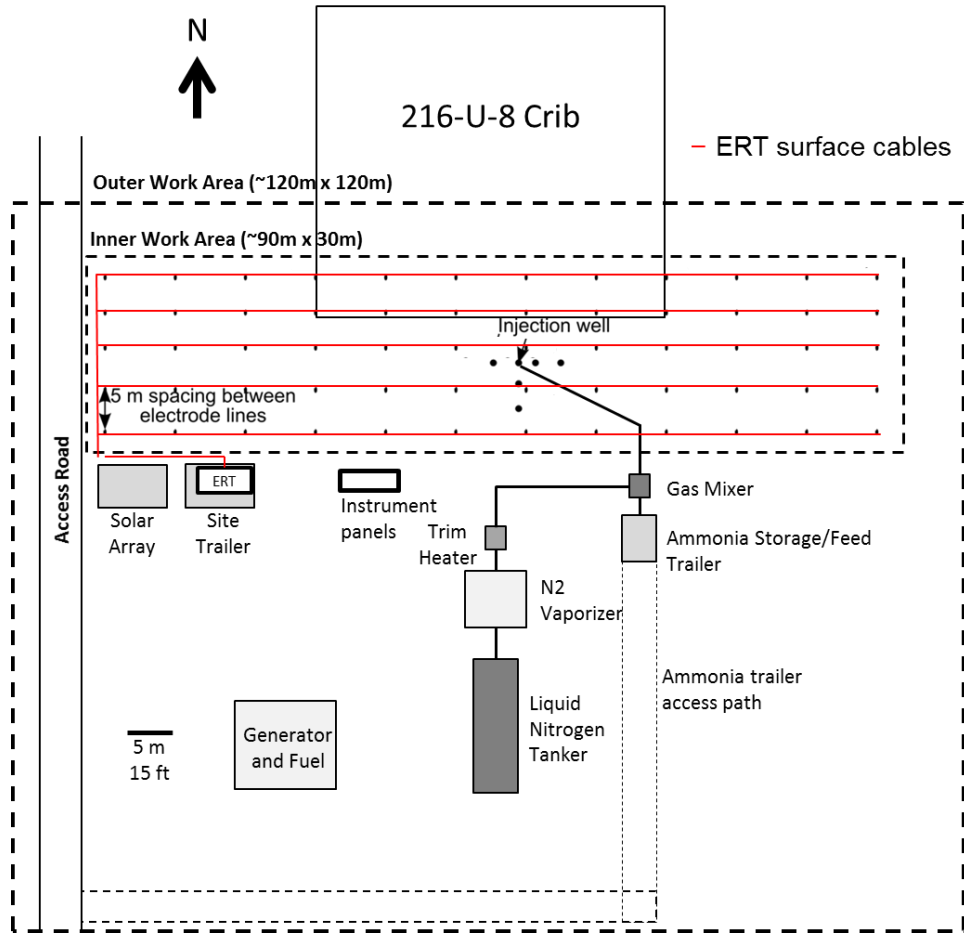
Figure 3.4. Basic Components of the URGS Field Test System

Figure 3.5 depicts the lateral layout of monitoring locations. Distances from the injection well to the monitoring locations are listed in Table 3.9 and monitoring borehole/well names are shown on Figure 3.5.
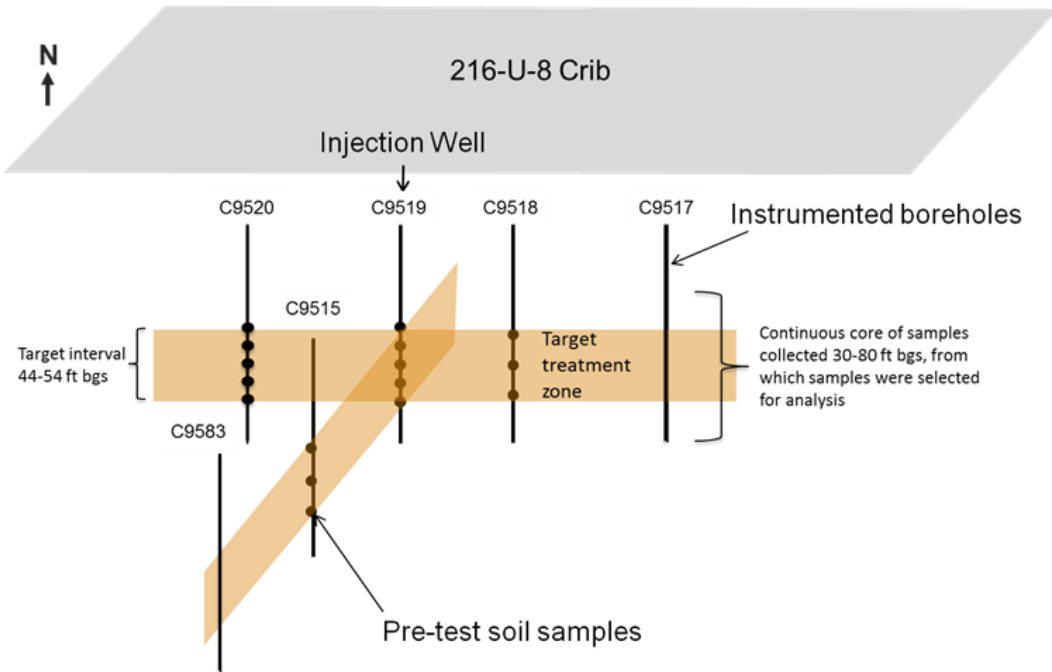
Figure 3.5. Location of Test Site Wells and Monitoring Boreholes.

Table 3.9. Field Site Monitoring Locations

Monitoring Location	Distance from Injection Well (m)
C9515	3.03
C9517	5.07
C9518	2.03
C9520	3.05
C9583	5.99

The system also included provisions to conduct a gas tracer test to evaluate gas flow patterns in the subsurface at the designed gas-injection flow rate. Ammonia sensors were deployed to monitor at ambient test site locations, along ammonia injection piping at all joints, and for internal measurement of ammonia concentrations in the injection system. Oxygen sensors were also included for enclosed spaces as a safety measure due to the use of gases that could displace atmospheric conditions. Injection and ammonia/oxygen sensor inputs were configured for automated data collection and processing, including controls for the injection process and with safety shutdown interlocks.

The following sections provide additional details for the test systems.

3.3.2.1   Aboveground Equipment and Overall Data Collection System

Aboveground equipment and the data collection system are specified in the field test design drawings (CHPRC 2018a, b, c).

3.3.2.2 Borehole Monitoring Equipment Descriptions

A suite of monitoring sensors were installed within each of the five monitoring boreholes.

Borehole gas sampling ports were installed at five discrete depths within each monitoring borehole. Sampling ports were fabricated by attaching porous stainless steel cups to 3/8-inch polypropylene tubing.

Thermistors (USP8242 encapsulated negative temperature coefficient thermistors, U.S. Sensor, Orange, California) were used to monitor temperature. To achieve accurate temperature measurements over the range of interest, a fifth-order polynomial was used to relate resistance to temperature for each of the thermistors used in the field test. The manufacturer's calibration relationship was verified for a subset of the thermistors in a precision water bath spanning the 0°C to 40°C temperature range, with measured accuracies better than 0.07°C.

Due to the corrosive nature of ammonia gas and ammonia hydroxide solutions, electrical resistivity electrode cables were fabricated using only chemically compatible materials. Electrodes were made using stainless steel mesh that was wrapped around the 2-inch PVC access tube and the electrical connection to the surface was accomplished using nylon-coated stainless steel stranded wire.

In addition to thermistors, a fiber optic distributed temperature sensing cable (Paulsson Inc., Van Nuys, CA) was installed to provide an alternative means for temperature measurement. The cable utilized a PVC jacket and was run down and then back up each borehole to provide a continuous temperature measurement while minimizing the risk of ammonia penetrating any downhole junctions.

3.3.2.3 Neutron Moisture Logging Measurements

Soil moisture content determination using neutron scattering probes has become a standard method over the past several decades (Hignett and Evett 2002). A neutron probe consists of a high-energy neutron source, a low-energy or thermal neutron detector, and the electronics required for counting and storing the measured response. A fast neutron source placed within moist soil develops a dense cloud of thermal neutrons around it and a thermal neutron detector placed near the source samples the density of the generated cloud. The concentration of thermal neutrons is affected by both soil density and elemental composition. Elements that absorb neutrons are often in low concentration in the soil solid phase and, when clay content is also low, the neutron probe response is mainly affected by changes in moisture content (Greacen et al. 1981; Hignett and Evett 2002).

Neutron moisture logging was planned using a CPN 503DR Hydroprobe (InstroTek Inc., Raleigh, NC). Neutron probe measurements were to be acquired at depth increments of approximately 7.5 cm using a count time of 30 seconds and then converted to count ratio (C_R) by dividing each measurement by the standard count.

3.3.2.4 Electrical Resistivity Measurements

ERT is a method of remotely imaging the electrical conductivity (EC) of the subsurface. Electrodes installed along the ground surface and/or within boreholes are used to strategically inject currents and measure the resulting potentials to produce a data set that is used to reconstruct the subsurface EC structure (Daily and Owen 1991; Johnson et al. 2010; Slater and Lesmes 2002).

The bulk EC of the subsurface has been widely observed to follow the empirical Archie's law (Archie 1942) in clean (i.e., clay free), non-conductive sands. Archie's law is given by Eq. (3.1):

$$EC = \frac{1}{a} \sigma_f \phi^m S_w^n \tag{3.1}$$

where
a = tortuosity factor
σ_f = fluid conductivity
ϕ = porosity
S_w = water saturation
m = cementation exponent
n = saturation exponent.

3.3.2.5 Cross-Hole Ground-Penetrating Radar Measurements

GPR methods are also commonly used to characterize or monitor subsurface moisture content. GPR systems consist of an impulse generator that repeatedly sends a particular voltage and frequency source to a transmitting antenna. Cross-hole GPR methods involve lowering a transmitter into a wellbore and measuring the energy with a receiving antenna that is lowered down another wellbore, and moving the transmitting and receiving antennas manually to different positions in the wellbores to facilitate transmission of the energy through a large fraction of the targeted area.

3.3.2.6 Gas-Phase Tracer Test System

Gas sampling ports were connected to a sampling and analysis system at the surface to measure soil-gas concentrations of oxygen and ammonia. The system consisted of a diaphragm pump, mass flow controller (MC series, Alicat Scientific Inc., Tucson AZ), oxygen sensor, and percent level infrared absorption (IR) ammonia gas sensor (model E12-15 IR, Analytical Technologies Inc., Collegeville, PA). Gas from individual borehole sampling ports were collected using an array of electrically actuated solenoid valves that allowed for autonomous, unattended sample analysis. The system is suitable for measuring the decrease in oxygen concentration as an indication of movement of injected nitrogen gas in the subsurface away from the injection well. During ammonia injection, the system was also capable of tracking ammonia distribution in the soil gas.

3.3.2.7 Ammonia Sensors

Two types of ammonia sensors were planned for use at the field test site. Percent-level IR ammonia gas sensors (model E12-15 IR, Analytical Technologies Inc., Collegeville, PA) were used to monitor the injection process in injection piping and for soil gas measurements. These sensors were also used to monitoring locations such as the exhaust stack and internal ammonia storage/injection trailer where high

ammonia concentration could result from a system leak. An array of parts-per-million-level ammonia sensors were also used for health and safety monitoring (Model 700 series Detcon Inc., Woodlands, TX). These sensors were deployed at the ground surface to evaluate potential movement of ammonia upward from the subsurface injection zone to the ground-surface and at selected locations for health and safety.

3.3.3   Equipment and Materials

Primary equipment and materials for the test are specified in the field test design drawings (CHPRC 2018a, b, c).

3.3.4   Deviations from Work Plan

The field test plan was followed for the test with the following exceptions. The ammonia injection and all associated monitoring and post-treatment characterization were not completed because of the observed poor treatment effectiveness in the laboratory for field-site sediments. Other deviations were approved prior to test implementation through the change notice process (TPA-CN-0764 and TPA-CN-0766).

4.0   Detailed Results

This section presents the results of the field test. First, the results from technology development efforts and laboratory testing of the field test site sediments are presented in Section 4.1. The data are then assessed with respect to technology effectiveness, implementability, and cost factors in Section 4.2.

4.1   Field Data Summary

This section presents the information collected during treatability test efforts, including technology development data (Section 4.1.1), field site data (Section 4.1.2), investigation of site-specific interferences (Section 4.1.3), and field system functional testing (Section 4.1.4).

4.1.1   URGS Technology Development Data

A series of laboratory tests was conducted to develop and quantify how ammonia treatment of vadose zone sediments can decrease the mobility of uranium contamination. Details of these studies are described in multiple reports and journal manuscripts (Szecsody et al. 2010a,b, 2012; Zhong et al. 2015; Truex et al. 2014). Laboratory evaluation and geochemical modeling were also conducted to examine ammonia treatment mechanisms (Szecsody et al. 2010b, 2012). In summary, laboratory analysis of pore water associated with treated sediment and selected mineral components common in Hanford Site sediments shows the predicted elevated pH conditions, along with significant increases in solute concentrations, including those associated with aluminosilicate and other mineral dissolution and ion exchange processes. Solute concentrations then decline as precipitation occurs. Geochemical modeling confirms these processes. Additional details of these studies and sediment/precipitate analyses are provided in the uranium sequestration study (Szecsody et al. 2010b, 2012).

Laboratory studies (Szecsody et al. 2010a,b, 2012; Zhong et al. 2015; Truex et al. 2014) have also investigated factors impacting distribution of ammonia within the vadose zone. Ammonia distribution is strongly influenced by partitioning to the pore water. With a dimensionless Henry's law coefficient (equilibrium vapor concentration/aqueous concentration) of 6.58×10^{-4}, ammonia readily partitions to the aqueous phase. The partitioning process is rapid (within seconds), and an associated initial rapid pore water pH increase occurs until pH 10 is reached. Partitioning is slower thereafter, but still relatively rapid compared to the expected gas flow rate in the subsurface. Table 4.1 (Zhong et al. 2015) summarizes the relationship between ammonia gas concentration and pH of water in contact with the gas.

Table 4.1. Ammonia Gas Partitioning to Water and Resulting pH (Zhong et al. 2015)

vol% NH$_3$ $_{(g)}$	NH$_3$ (aqueous) Total	pH
100	15.7 mol/L	12.52
30	9.2 mol/L	12.26
10	6.3 mol/L	12.02
5	3.1 mol/L	11.87
1	0.63 mol/L	11.52
0.3	0.19 mol/L	11.26
0.1	6.3×10^{-2} mol/L	11.02
0.01	6.3×10^{-3} mol/L	10.51

The laboratory testing conducted prior to initiating efforts at the field test site demonstrated the treatment process and provided information needed to scale the treatment for field applications. A variety of vadose zone, low-water-content sediments were treated with ammonia to evaluate the treatment (Table 4.2). Sequential extractions ("Sequential U extractions") were applied to assess how the distribution of uranium among aqueous and sediment-associated phases changed during treatment.

For sequential extractions, the sediment was first contacted with simulated groundwater and then the groundwater was removed and analyzed for uranium. This same approach was then sequentially applied with an ion exchange solution, a weak acetic acid, a strong acetic acid, and finally strong acid. Sequential extractions for pre- and post-treatment sediment samples were compared to quantify the effect of the ammonia treatment. Soil column leach tests ("1-D column leach") were also conducted for some sediments when sufficient sediment was available to quantify the amount of uranium that eluted from a sediment when exposed to flowing simulated groundwater. The sediment was placed in a small soil column and simulated groundwater was pumped through the column at a relatively slow rate for about 100 pore volumes. Effluent samples were analyzed for uranium, with comparison of results for pre- and post-treatment sediments.

Large laboratory flow cells were also used to evaluate distribution of ammonia in the gas phase and then to quantify uranium mobility changes at different locations in the flow cell using sequential extractions. These large laboratory tests included sediment packed in a 1-m-long wedge-shaped flow cell and in a 20-ft-long column. Batch laboratory tests were also conducted ("Aqueous U batch"). In the batch tests, pre- and post-treated sediments were placed in contact with water for a long period of time and the uranium concentration in the aqueous phase was periodically measured. The rate of increase in uranium concentration in the aqueous phase is related to the uranium leaching rate. Surface-phase analyses were applied to some sediment samples where uranium concentrations were high enough for instrument detection. Surface analysis techniques including LIFS, XANES, and EXAFS were applied to help identify uranium precipitate forms.

Table 4.2. Pre-Field-Test Uranium Mobility Experiments (as reported in Szecsody et al. 2010b and Zhong et al. 2015)

Sediment and Sample Depth (ft bgs)	Uranium Mobility Experiment
BX-102, 131	(5) sequential U extractions, (2) 1-D column leach
BX-102, 152	(5) sequential U extractions, LIFS
TX-104, 69	(16) sequential U extractions, (4) 1-D column leach
TX-104, 110	(2) sequential U extractions
U-105, 51.8 (C5602)	(2) sequential U extractions
U-105, 52.3'	(2) sequential U extractions, LIFS, XANES/EXAFS
U-105, 67.8'	(2) sequential U extractions
U-105, 68.2'	(2) sequential U extractions
U-105, 82.8'	(2) sequential U extractions
U-105, 83.3'	(2) sequential U extractions
U-105, 91.8'	(2) sequential U extractions
U-105, 92.3'	(2) sequential U extractions
ERDF pit, 20'	(20) aqueous U batch
ERDF pit, 20'	(8) sequential U extractions from a 1-m-long wedge-shaped flow-cell test
300A, 30-33' (C7117)	(2) sequential extractions, (6) 1-D column leach
IDF pit, 30'	(2) sequential U extractions
200-BC-1, 35 (C7540)	(2) sequential U extractions
200-BC-1, 52 (C7534)	(26) sequential U extractions
200-BC-1 (C7540)	(7) sequential U extractions from a 20-ft-long soil column test

Locations: BX-102 and TX-104 – Serne et al. 2008a,b; U-105 – Um et al. 2009a; Environmental Restoration Disposal Facility (ERDF) – sediment obtained from excavation for the Hanford Environmental Restoration Disposal Facility; Integrated Disposal Facility (IDF) sediment obtained from excavation for the Hanford IDF: 200-BC-1 – sediment from the C7534 and C7540 boreholes at the 200-BC-1 operable unit; 300A – sediment from south process pond excavation in the 300-FF-1 operable unit.
Numbers in parentheses are the number of individual experiments conducted.

In general, results showed that injection of ammonia in the gas-phase created high dissolved-phase ammonia concentrations that followed equilibrium partitioning behavior. The injection led to an increase in pH from 8.0 to about 11.5 when the injected gas phase was 5 vol% ammonia. The increase in pore water pH resulted in a large increase in pore water cations and anions from mineral-phase dissolution. Minerals showing the greatest dissolution included montmorillonite, muscovite, and kaolinite. Pore water ion concentrations then decreased with time. Simulations based on initial pore water ion concentrations indicated that quartz, chrysotile, calcite, diaspore, hematite, and Na-boltwoodite (hydrous U silicate) should precipitate.

Of the evaluations shown in Table 4.2, the most important for evaluating ammonia treatment effectiveness were sequential extractions and soil column leach tests. Sequential extractions were applied to assess how the distribution of uranium among aqueous and sediment-associated phases changed during treatment. Soil column leach tests were also conducted for some sediments (when sufficient sediment

was available) to quantify the amount of uranium that eluted from a sediment when exposed to flowing simulated groundwater.

Results of the technology development laboratory tests prior to the testing of field samples showed good ammonia treatment performance. Over 80% of the sequential extraction tests showed good mobility reduction (125 tests on 18 sediments), with mobile phases reduced by an average of 68% and immobile phases increased by an average of 71%. These results are based on information reported by Szecsody et al. (2010b), with a summary of their experimental results shown in

Table 4.3. Positive laboratory results for these ammonia treatment tests are indicated by a decrease in the fraction of uranium for the three least aggressive extractions (extractions 1-3), indicating less mobile uranium after ammonia treatment. Positive results are also indicated by a corresponding increase in the fraction of uranium for the three aggressive extractions (extractions 4-6), indicating more immobile uranium after ammonia treatment. In particular, an increase in the uranium fraction for the most aggressive extraction (extraction 6) is positive because it indicates uranium is bound by very-low-solubility precipitates. These tests were conducted using sediments with several types of initial uranium compounds present in the sediment. Figure 4.1 (from Szecsody et al. 2012) illustrates the decrease in uranium mobility for different initial uranium compounds. In this figure, the fraction of the most mobile uranium (shown as the red colors on the bar chart) decreased and the least mobile uranium fraction from the most aggressive extraction (extraction 6, shown as the dark green color on the bar chart) increased. When present prior to treatment, the moderately mobile uranium phase, indicated by the orange color on the bar chart, also decreased after ammonia treatment.

Table 4.3. Summary of Sequential Extraction Results from Szecsody et al. (2010b) Showing Changes in Uranium Mass Phases between Untreated and Ammonia-Treated Sediments. (Green font shows where favorable results were obtained [a decrease of mobile phases and an increase of low mobility phases] and red font shows unfavorable results.)

Location	Depth (ft bgs)	Total U (µg/g)	Percent change in extracted U mass from untreated to ammonia-treated					
			Mobile Ext. 1	Mobile Ext. 2	Moderately Mobile Ext. 3	Low Mobility Ext. 4	Low Mobility Ext. 5	Immobile Ext. 6
BX-102	152	74.3	-1.3	-0.2	-1.8	-0.1	-4.4	7.3
BX-102	152	74.3	-1.3	-1.1	-1.1	0.2	-2.4	5.1
TX-104	69+110	27.7	-4	-8.8	-10	0.5	2.6	19.5
TX-104	69.3	18.4	-3.8	-6.1	5.8	-4.1	--	8
TX-104	110.3	55	-0.3	-26.4	23.5	6.9	--	-4
U-105	51.8	690	-0.2	-0.2	-0.1	-37.5	--	38.8
U-105	52.3	387	0.1	-0.2	-1.5	-28	--	29.8
U-105	67.8	32.1	-2.8	-3	40	-30.6	--	0.4
U-105	68.3	34.4	-2.7	-4	-1	3.8	--	3.8
U-105	82.8	11	-10.7	-14.1	-3.6	36.6	--	-8
U-105	83.3	13.5	-1	-27.2	21	-14.2	--	21.3
U-105	91.8	0.35	-1	-71.2	47	-1.3	--	25.1
U-105	92.3	0.186	0.2	-0.5	-9.4	-37	--	46.6
ERDF	20	0.181	-6.1	-6.2	-6.8	-4.8	--	-6.6
ERDF	40	0.172	-0.1	-6.1	-0.6	2	--	4.6
IDF	30	3.1	0	0.1	9.1	2.8	--	-12
200-BC-1	35	0.16	-2.7	-0.9	-9	3.8	--	3.8
200-BC-1	52	0.14	0	-4.6	-4.6	5.4	--	13.7
200-BC-1	51	0.15	-1.5	4.6	4.6	-20.9	--	18

Extraction details in Section 3.2.1.1. In summary, Ext. 1 – simulated groundwater; Ext. 2 – ion exchange; Ext. 3 – pH 5 acetic acid; Ext. 4 – pH 2.3 acetic acid; Ext. 5 – oxalic acid; Ext. 6 – nitric acid

Locations: BX-102 and TX-104 – Serne et al. 2008a,b; U-105 – Um et al. 2009a; ERDF – sediment obtained from excavation for the Hanford Environmental Restoration Disposal Facility; IDF sediment obtained from excavation for the Hanford Integrated Disposal Facility: 200-BC-1 – sediment from the C7534 and C7540 boreholes at the 200-BC-1 operable unit.
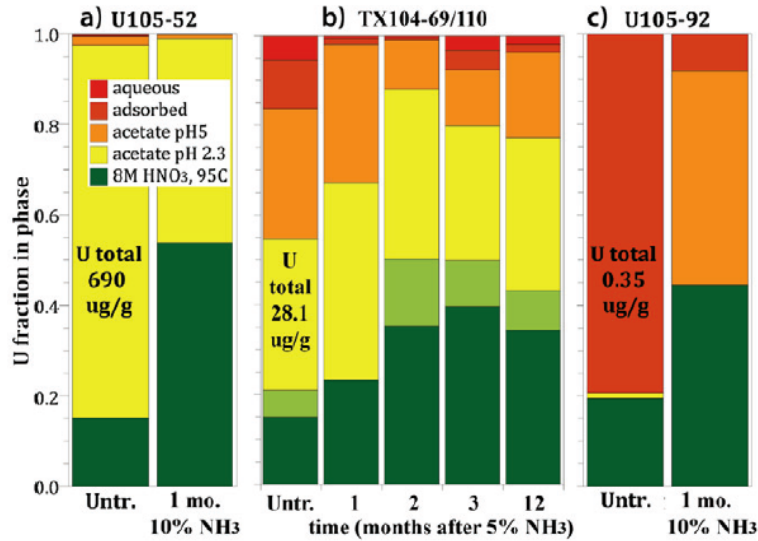
Figure 4.1. Sequential Extraction of Uranium Phases from Contaminated Sediments with and without Ammonia Treatment: a) below the Hanford U-105 Tank as Mainly Na-boltwoodite, b) below the Hanford TX-104 Tank as Uranium-Carbonate, c) below the Hanford U-105 Tank as Primarily Aqueous/Adsorbed Uranium (from Szecsody et al. 2012)

The technology development soil column results also showed good ammonia treatment performance. These results are presented by Szecsody et al. (2012) and Zhong et al. (2015) (Figure 4.2). These tests were consistent with the associated sequential extraction results, showing lower concentrations of uranium in the soil column effluent and about 80% less cumulative uranium leaching from the column over 100 pore volumes due to ammonia treatment. However, testing was limited by two factors. First, because a limited quantity of sediment was available for some types of sediment and soil column testing requires a relatively long time to conduct, only a few sediments were tested with the soil column leaching method. Second, available samples were from limited types of Hanford waste disposal chemistry that did not include acidic disposal, the type of disposal relevant to the 216-U-8 field test site.
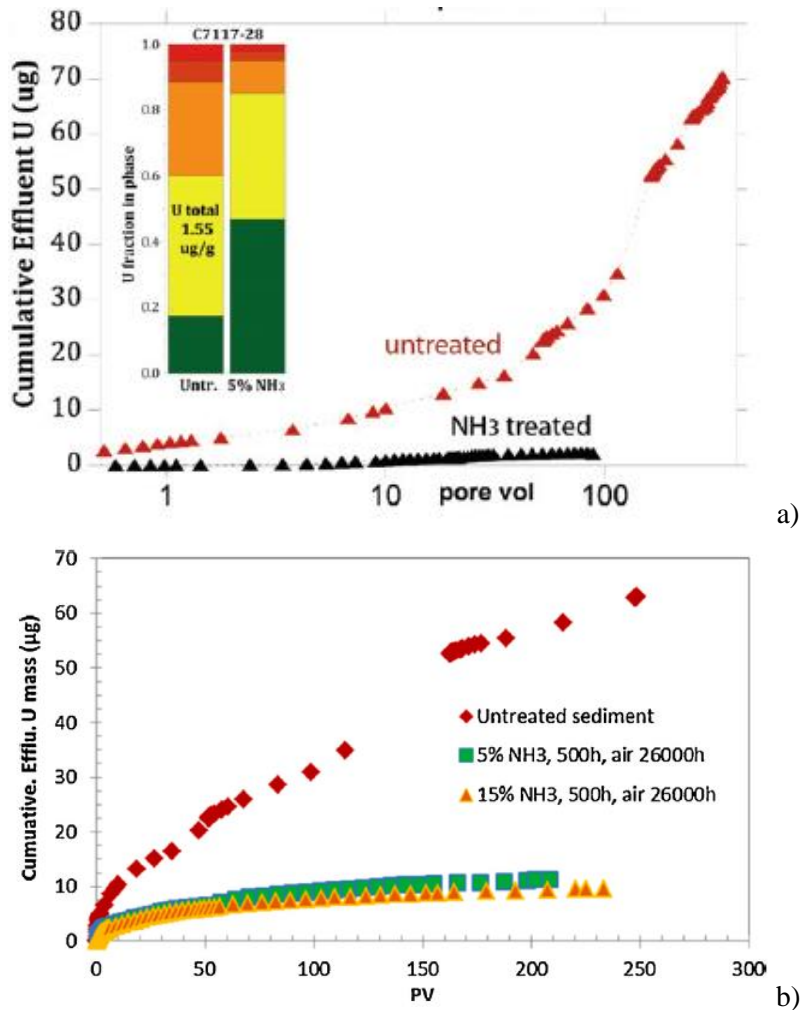
Figure 4.2. Cumulative Uranium Leached from Soil Columns by Simulated Groundwater over Multiple Pore Volumes (PV) from a) Szecsody et al. 2012 and b) Zhong et al. 2015 for Untreated and Ammonia-Treated Sediments

4.1.2   216-U-8 Field Test Site Laboratory Data

Initial activities at the field test site included characterization of site sediments and laboratory dosing and effectiveness testing of site sediments according to the SAP and associated Tri-Party Agreement Change Notice (DOE 2015b, TPA-CN-0764). Sediment characterization was designed to provide site physical and geochemical data as context for evaluating the uranium contamination at the site and the treatment performance. Sediment physical characterization data are shown along with the borehole geophysical logs, sediment sample pictures, and soil resistivity measurements in Appendix B. Sediment geochemical and contaminant data are shown in Table 4.4 (water extract contaminant and cation analyses), Table 4.5 (water extract anion analyses), Table 4.6 (acid extract analyses), Table 4.7 (microwave digestion analyses), and Table 4.8 (total alpha/beta analyses). Air permeability and core sample gamma scan results are presented in Appendix C. Sediment carbon analyses are presented in Appendix E. For boreholes C9520 and C9519, where five samples were used to evaluate the vertical profile, uranium concentrations are highest in the 30 to 50 ft bgs (10 to 15 m bgs) zone, with much lower concentrations below about 50 ft bgs (15 m bgs).

Table 4.4. Contaminant and Cation Results for the Water Extract for Each Sample

Borehole ID	Sample ID	Sample Depth (ft bgs)	Moisture (wt%)	U (µg/g)	Tc-99 (µg/g)	Sr-90 (pCi/g)	Cs-137 (pCi/g)	Ca (µg/g)	Mg (µg/g)	Al (µg/g)	Ba (µg/g)	Fe (µg/g)	K (µg/g)	Si (µg/g)	Na (µg/g)
C9515	B38XK6	47.2 – 47.7	4.66	4.41	ND	--	--	9.05	0.471	ND	ND	ND	ND	1.68	2.3
C9515	B38XK9	48.7 – 49.2	4.85	0.615	ND	--	--	6.82	0.388	ND	ND	ND	ND	1.65	1.49
C9518	B38Y11	47.4 – 47.9	3.39	0.664	ND	--	--	5.09	0.36	0.332	ND	ND	ND	1.17	ND
C9518	B38Y17	48.9 – 49.4	6.47	0.191	ND	--	--	5.71	0.409	ND	ND	ND	ND	2	2.24
C9519	B38YC9	42.3 – 42.8	12.8	0.373	ND	--	--	1.4	0.192	ND	ND	ND	ND	2.92	8.6
C9519	B38YF8	46.5 – 47.0	2.8	0.936	ND	--	--	ND	0.186	ND	ND	ND	ND	0.886	3.18
C9519	B38YH2	48.5 – 49.0	3.1	0.263	ND	--	--	2.41	0.365	0.973	ND	ND	ND	0.881	1.42
C9519	B38YH9	51.9 – 52.4	1.68	0.135	ND	--	--	4.69	0.321	ND	ND	ND	ND	0.984	ND
C9519	B38YK0	54.7 – 55.2	1.66	0.0878	ND	--	--	5	0.531	0.432	ND	ND	ND	0.88	ND
C9520	B32H62	37.5 – 38.0	8.41	0.0246	ND	--	--	4.07	0.514	0.178	ND	0.272	ND	12.9	17.5
C9520	B32H70	42.4 – 42.9	2.5	0.322	ND	--	--	4.11	0.498	0.162	ND	ND	ND	5.96	10.3
C9520	B32H78	46.7 – 47.2	4.79	0.197	ND	--	--	4.21	0.446	ND	ND	0.183	ND	8.31	8.9
C9520	B32H90	54.0 – 54.5	1.97	0.287	ND	--	--	12.1	1.67	ND	ND	ND	2.82	5.79	4.1
C9520	B32HB2	61.5 – 62.0	2.5	0.405	ND	--	--	18.8	1.89	ND	ND	ND	2.88	6.2	3.57

ND = not detected

Table 4.5. Anion Results for the Water Extract for Each Sample

Borehole ID	Sample ID	Sample Depth (ft bgs)	Moisture (wt%)	Bromide (µg/g)	Chloride (µg/g)	Nitrate (µg/g)	Nitrite (µg/g)	Sulfate (µg/g)	pH	SpC (mS/cm)	TIC (µg/g)
C9515	B38XK6	47.2 – 47.7	4.66	ND	ND	ND	ND	ND	7.43	0.0685	ND
C9515	B38XK9	48.7 – 49.2	4.85	ND	ND	ND	ND	ND	7.4	0.056	ND
C9518	B38Y11	47.4 – 47.9	3.39	ND	ND	ND	ND	ND	7.76	0.0314	ND
C9518	B38Y17	48.9 – 49.4	6.47	ND	ND	ND	ND	ND	7.62	0.0964	ND
C9519	B38YC9	42.3 – 42.8	12.8	ND	ND	5.78	ND	ND	7.23	0.0681	ND
C9519	B38YF8	46.5 – 47.0	2.8	ND	ND	ND	ND	ND	7.53	0.0291	ND
C9519	B38YH2	48.5 – 49.0	3.1	ND	ND	ND	ND	ND	7.64	0.0136	ND
C9519	B38YH9	51.9 – 52.4	1.68	ND	ND	ND	ND	ND	7.45	0.0354	ND
C9519	B38YK0	54.7 – 55.2	1.66	ND	ND	ND	ND	ND	8.1	0.0389	ND
C9520	B32H62	37.5 – 38.0	8.41	ND	1.89	11.6	ND	15.9	6.93	1.18	ND
C9520	B32H70	42.4 – 42.9	2.5	ND	1.09	2.95	ND	6.13	7.39	0.99	ND
C9520	B32H78	46.7 – 47.2	4.79	ND	1.98	5.27	ND	8.08	7.16	0.789	ND
C9520	B32H90	54.0 – 54.5	1.97	ND	1.57	15.3	ND	10.5	7.56	1.61	ND
C9520	B32HB2	61.5 – 62.0	2.5	41.9	3.07	ND	ND	12.1	7.52	1.87	ND

Table 4.6. Contaminant and Cation Results for the Acid Extract for Each Sample

Borehole ID	Sample ID	Sample Depth (ft bgs)	Moisture (wt%)	U (µg/g)	Tc-99 (µg/g)	Sr-90 (pCi/g)	Cs-137 (pCi/g)	Ca (µg/g)	Mg (µg/g)	Al (µg/g)	Ba (µg/g)	Fe (µg/g)	K (µg/g)	Si (µg/g)	Na (µg/g)
C9515	B38XK6	47.2 – 47.7	4.66	4480	ND	--	--	3110	1850	3280	19.4	6330	543	ND	ND
C9515	B38XK9	48.7 – 49.2	4.85	24.5	ND	--	--	ND	ND	ND	45.9	ND	ND	ND	ND
C9518	B38Y11	47.4 – 47.9	3.39	238	ND	--	--	4430	1630	2630	22.3	5220	489	ND	ND
C9518	B38Y17	48.9 – 49.4	6.47	13	ND	--	--	8370	3110	4440	56.5	7820	1140	ND	ND
C9519	B38YC9	42.3 – 42.8	12.8	290	ND	--	--	2240	2080	5890	18.3	8700	708	ND	152
C9519	B38YF8	46.5 – 47.0	2.8	1250	ND	--	--	1540	1580	3420	15.8	7740	438	ND	161
C9519	B38YH2	48.5 – 49.0	3.1	294	ND	--	--	1390	1680	3810	18.7	6940	514	ND	148
C9519	B38YH9	51.9 – 52.4	1.68	10.7	ND	--	--	6590	2440	2920	38.2	6410	562	ND	ND
C9519	B38YK0	54.7 – 55.2	1.66	5.77	ND	--	--	7020	2510	2810	30.3	6140	642	ND	202
C9520	B32H62	37.5 – 38.0	8.41	442	ND	414	1.65E +04	4320	2860	6510	27.8	17600	648	ND	339
C9520	B32H70	42.4 – 42.9	2.5	877	ND	286	7.61E +03	3650	3560	5980	33.1	16500	652	ND	253
C9520	B32H78	46.7 – 47.2	4.79	1070	ND	437	7.18E +03	2800	2730	5660	25.8	10600	691	ND	174
C9520	B32H90	54.0 – 54.5	1.97	8.34	ND	32.3	7.84E -01	8550	3410	3990	39.6	10100	709	ND	148
C9520	B32HB2	61.5 – 62.0	2.5	11.6	ND	79.2	4.18E -01	8410	3870	4550	43.2	11100	772	ND	147

Table 4.7. Uranium Results for the Microwave Digest for Each Sample

Borehole ID	Sample ID	Sample Depth (ft bgs)	Moisture (wt%)	U (µg/g)
C9520	B32H62	37.5 – 38.0	8.41	347
C9520	B32H70	42.4 – 42.9	2.5	870
C9520	B32H78	46.7 – 47.2	4.79	853
C9520	B32H90	54.0 – 54.5	1.97	9.96
C9520	B32HB2	61.5 – 62.0	2.5	12

Table 4.8. Acid Extraction Analysis Results for Total Alpha and Total Beta Radiation (all water extraction results were non-detect)

Borehole ID	Sample ID	Sample Depth (ft bgs)	Moisture (wt%)	Total Alpha (pCi/g)	Total Beta (pCi/g)
C9520	B32H62	37.5 – 38.0	8.41	1685	472
C9520	B32H70	42.4 – 42.9	2.5	876	238
C9520	B32H78	46.7 – 47.2	4.79	1243	301
C9520	B32H90	54.0 – 54.5	1.97	ND	ND
C9520	B32HB2	61.5 – 62.0	2.5	ND	ND

Laboratory effectiveness testing with field-site sediments included sediment characterization, sequential extraction analysis, and soil column leach testing of pre- and post-treated sediments (Section 3.0). Sequential extraction results showed a decrease in uranium mobility after ammonia treatment for 17 of 18 samples, based on reductions observed in mobile uranium phases (Table 4.9). These results suggest that uranium mobility was decreased by ammonia treatment. Compared to the technology development sequential extraction results, there was a larger percentage of sediment in the field test samples where there was not an increase in the immobile uranium (harsh acid extraction) phase after ammonia treatment. An increase in the immobile uranium phase is associated with sequestration, based on generation of silicate precipitates. Concentrations of Tc-99, Sr-90, and Cs-137 were also evaluated in selected sequential extraction tests (Appendix D). The Tc-99 concentrations were non-detect. There were minimal to no effects of ammonia treatment on the mobility of Sr-90 and Cs-137.

Table 4.9. Summary of Sequential Extraction Results for Field-Test-Site Sediments Showing Changes in Uranium Mass Phases between Untreated and Ammonia-Treated Sediments (Green font shows where favorable results were obtained [a decrease of mobile phases and an increase of low mobility phases] and red font shows unfavorable results.)

Borehole ID	Depth (ft bgs)	Total U (µg/g)	Percent change in extracted U mass from untreated to ammonia-treated					
			Mobile Ext. 1	Mobile Ext. 2	Moderately Mobile Ext. 3	Low Mobility Ext. 4	Low Mobility Ext. 5	Immobile Ext. 6
C9519	42.3 - 42.8	383.3±51.1	4.553	-0.783	5.729	0.722	-0.708	-0.643
C9519	42.3 - 42.8	383.3±51.1	11.627	-0.302	5.721	0.321	-0.459	-0.649
C9519	46.5 - 47	2886±158	-0.965	-0.981	-0.912	-0.355	0.893	3.647
C9519	46.5 - 47	2886±158	-0.777	-0.923	-0.813	-0.256	2.133	0.875
C9519	48.5 - 49	400.0±68.4	-0.864	-0.845	-0.718	0.361	-0.232	-0.009
C9519	48.5 - 49	400.0±68.4	-0.558	-0.335	-0.647	0.279	0.181	-0.153
C9519	51.9 - 52.4	21.00±7.16	-0.946	-0.985	-0.262	0.355	0.089	-0.082
C9519	51.9 - 52.4	21.00±7.16	-0.778	-0.917	0.210	0.200	0.430	-0.295
C9519	54.7 - 55.2	7.49±1.23	-0.918	-0.980	-0.014	0.072	1.474	0.596
C9519	54.7 - 55.2	7.49±1.23	-0.812	-0.851	0.138	0.153	1.978	0.106
C9518	47.4 - 47.9	820.4±42.7	-0.937	-0.998	-0.474	-0.035	0.365	0.068
C9518	47.4 - 47.9	820.4±42.7	-0.904	-0.991	-0.171	-0.055	0.648	-0.116
C9518	48.9 - 49.4	30.99±7.22	-0.963	-1.000	-0.078	0.367	0.072	-0.301
C9518	48.9 - 49.4	30.99±7.22	-0.961	-0.996	0.471	0.110	0.395	-0.267
C9518	52.9 - 53.4	23.29±2.37	-0.931	-0.993	0.441	-0.147	-0.154	0.472
C9518	52.9 - 53.4	23.29±2.37	0.449	-0.862	0.349	-0.033	0.080	-0.228
C9515	47.2 - 47.7	5338±2285	-0.973	-0.995	-0.760	-0.357	0.547	1.432
C9515	47.2 - 47.7	5338±2285	-0.972	-0.991	-0.610	-0.529	1.641	0.058
C9515	48.7 - 49.2	89.88±56.45	-0.986	-0.999	-0.388	0.328	1.211	-0.612
C9515	48.7 - 49.2	89.88±56.45	-0.992	-0.997	-0.571	-0.039	1.855	-0.423

Borehole ID	Depth (ft bgs)	Total U (µg/g)	Percent change in extracted U mass from untreated to ammonia-treated					
			Mobile Ext. 1	Mobile Ext. 2	Moderately Mobile Ext. 3	Low Mobility Ext. 4	Low Mobility Ext. 5	Immobile Ext. 6
C9515	52.8 - 53.3	9.86±4.25	-0.975	-0.942	-0.510	0.619	1.805	-0.113
C9515	52.8 - 53.3	9.86±4.25	-0.372	-0.963	-0.245	0.213	1.587	-0.276
C9520	38 - 38.5	415.2±84.0	-0.310	-0.949	2.952	0.142	-0.852	0.173
C9520	38 - 38.5	415.2±84.0	10.603	0.087	1.965	0.053	-0.898	0.218
C9520	42.9 - 43.4	1718±693	-0.789	-0.986	-0.831	0.764	-0.682	0.098
C9520	42.9 - 43.4	1718±693	0.114	-0.753	-0.838	0.855	-0.689	-0.041
C9520	47.2 - 47.7	728.2±461.0	-0.804	-0.892	-0.311	1.152	-0.545	-0.255
C9520	47.2 - 47.7	728.2±461.0	-0.505	-0.770	-0.426	1.077	-0.494	-0.247
C9520	50.7 - 51.2	67.50±40.79	-0.977	-0.997	-0.638	0.315	-0.415	0.672
C9520	50.7 - 51.2	67.50±40.79	-0.531	-0.767	-0.604	0.405	-0.451	0.112
C9520	51.7 - 52.2	4.64±0.57	0.342	-0.523	-0.342	0.493	-0.185	-0.149
C9520	51.7 - 52.2	4.64±0.57	-0.558	-0.757	-0.344	0.470	-0.022	0.151
C9520	54.5 - 55	7.81± 1.00	-0.981	-0.981	0.488	0.705	-0.479	0.420
C9520	54.5 - 55	7.81± 1.00	-0.738	-0.745	-0.076	0.674	-0.436	0.542
C9520	62 - 62.5	15.30±5.50	-0.863	-0.956	0.400	0.759	-0.474	0.230
C9520	62 - 62.5	15.30±5.50	-0.730	-0.546	0.086	0.633	-0.570	0.342

Extraction details in Section 3.2.1.1. In summary, Ext. 1 – simulated groundwater; Ext. 2 – ion exchange; Ext. 3 – pH 5 acetic acid; Ext. 4 – pH 2.3 acetic acid; Ext. 5 – oxalic acid; Ext. 6 – nitric acid

In contrast, almost all ammonia-treated samples showed a higher total mass of uranium leached for the same number of pore-volume flushes than was leached for the corresponding untreated sample (Table 4.10). For some samples, part of this difference may be due to different starting uranium concentrations between the untreated and treated subsamples. However, looking across all of the data, this variability does not explain the consistently greater leaching of uranium from ammonia-treated sediments. The soil column leach results were inconsistent with sequential extraction results for mobile uranium phases with respect to total mass leached and the initial uranium concentrations in the column effluent. Most ammonia-treated samples showed a high uranium concentration eluted from the soil column in the first few pore volumes when only the mobile phase of the uranium should elute from the column. For example, Figure 4.3 compares effluent uranium concentrations and cumulative uranium mass eluted from the column for an untreated and ammonia-treated column. In this example, untreated uranium concentrations in the first 5 pore volumes were less than 13,000 µg/L. In contrast, ammonia-treated uranium concentrations in the effluent in the first 5 pore volumes peaked at about 25,000 µg/L. Concentrations of Tc-99, Sr-90, and Cs-137 were also evaluated in selected soil column tests (Appendix D). The Tc-99 concentrations were non-detect. There were minimal to no effects of ammonia treatment on the mobility of Sr-90 and Cs-137. Figures for all of the soil column tests are shown in Appendix D.

Table 4.10. Summary of Soil Column Leaching Tests for Untreated and Ammonia-Treated Field Sediments (Green font shows where favorable results were obtained [a decrease of uranium mobility after ammonia treatment] and red font shows unfavorable results.)

Sample ID	Borehole ID	Depth (ft bgs)	Ammonia Dose (months)	Untreated Leached U (%)	Ammonia-Treated Leached U (%)
B38YC9	C9519	42.3-42.8	2	10.4	52.2
B38YF8	C9519	46.5-47.0	4	0.9	0.9
B38YH2	C9519	48.5-49.0	4	2.4	3.5
B38YH9	C9519	51.9-52.4	2	24	24
B38YK0	C9519	54.7-55.2	4	60	64
B38XK6	C9515	47.2-47.7	4	0.14	0.28
B38Y11	C9518	47.4-47.9	4	1.8	1.2
B32H71	C9520	42.9-43.4	4	1.2	3.7
B32H71	C9520	42.9-43.4	4	2	1.9
B32H79	C9520	47.2-47.7	4	9.6	13.7
B32H79	C9520	47.2-47.7	4	1.3	8.9
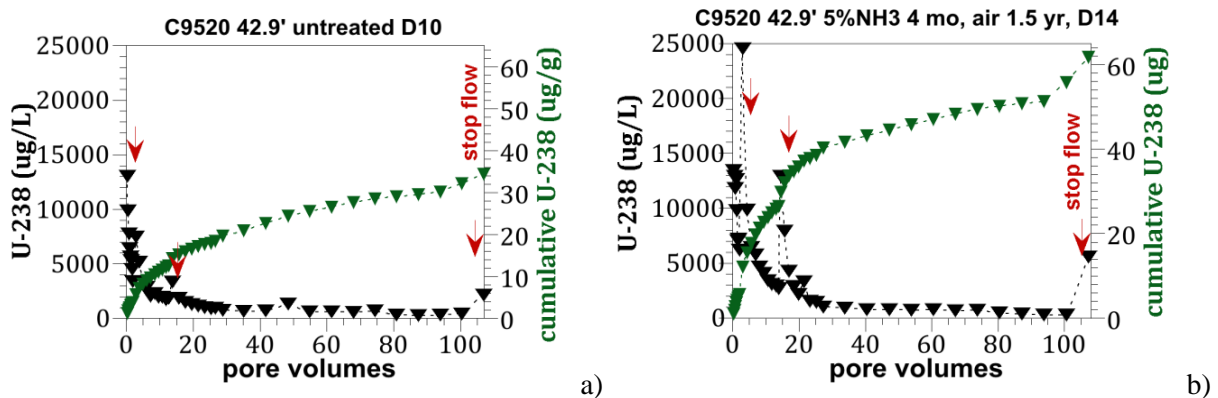
Figure 4.3. Example Soil Column Results for a) Untreated and b) Ammonia-Treated Field Sediments Showing Higher Initial Effluent Uranium Concentrations and High Cumulative Uranium Leached Mass for the Ammonia-Treated Sediment

Ammonia treatment, as indicated by the sequential extraction results, should have significantly decreased the highly mobile uranium phases and the initial eluted uranium concentrations should have been low. Based on previous testing, the ammonia treatment process requires at least 2 to 4 months of incubation time to work. However, reaction times used in for the laboratory tests with the field site sediments are consistent with previous studies (all greater than 2 months) and treatment effectiveness was the same for all of the tested reaction times (Figure 4.4). Thus, observed ammonia treatment results are not due to the reaction time that was used in the test.
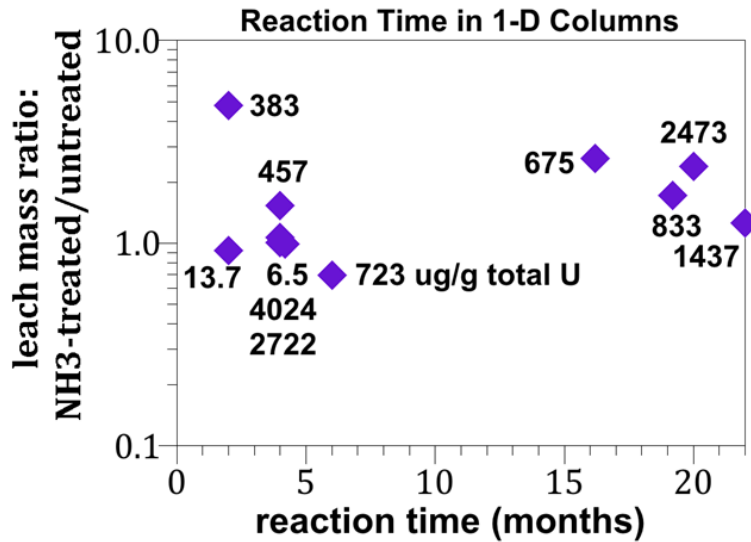
Figure 4.4. Summary of Soil Column Leaching Results Showing the Ratio of Leached Mass for Untreated and Ammonia-Treated Sediment for Different Ammonia Reaction Times

The field-test laboratory results demonstrated that there were site-specific interferences that affect the ammonia treatment effectiveness. These site-specific factors may be caused by the type of uranium phases present, the presence of co-contaminant interferences, or sediment/co-contaminant properties that lead to the need for higher ammonia doses for the treatment to be effective, as described in Section 4.1.3.

4.1.3   216-U-8 Site-Specific Interference Evaluation

Laboratory tests were applied to evaluate potential causes of the poor ammonia treatment effectiveness observed with laboratory dosing of ammonia to field site sediments. Data are provided in Appendix E. Tests showed low sediment carbonate (e.g., calcite) concentrations and low concentrations of uranium associated with the alkaline sediment extraction analysis used to identify carbonate-associated uranium. Sediment carbonate concentrations for 216-U-8 site were, in many cases, less than 250 µg/g inorganic carbon compared to more typical Hanford sediments, such as those evaluated for the 241-BX-102 and 241-TX-104 sites, with greater than 1500 µg/g inorganic carbon. In contrast to sediments from basic to neutral waste sites (i.e., 241-BX-102 and 241-TX-104), alkaline extraction of uranium only removed a few percent of the total sediment uranium from untreated field sediments. Further evidence of low uranium carbonate concentrations was obtained in radiography analysis of untreated sediment where uranium hot spots were in locations of low calcium. Low carbonate and carbonate-associated uranium can affect the uranium compound dissolution that is induced by ammonia treatment, the uranium complexation in the pore water during ammonia treatment, and the pH neutralization process that occurs after ammonia injection is terminated. In tests of ammonia treatment for individual sediment minerals (kaolinite, illite, etc.), Emerson et al. (2018) showed significantly better ammonia treatment effectiveness for tests where carbonate was present in the aqueous solution than for tests with a sodium-chloride solution as the aqueous phase. While these tests are not a direct evaluation of Hanford sediment carbonate concentration impacts, the results are consistent with the hypothesis that low carbonate concentrations hinder ammonia treatment effectiveness.

Another factor potentially related to poor ammonia treatment effectiveness was revealed from X-ray fluorescence two-dimensional surface analysis of untreated sediment where the microscopic uranium distribution on the soil particles was found to be concentrated in localized deposits rather than more uniformly precipitated at the soil surface. Having uranium distributed in sparse hot spots rather than more evenly distributed can affect the uranium compound dissolution that is induced by ammonia treatment. A relatively large deposit would be slower to dissolve than fine, dispersed deposits of uranium. If uranium is not well dissolved during the treatment process, it may not interact with other pore-water constituents to form low-solubility precipitates. In addition, post-ammonia-treatment surface analysis also showed uranium distributed in sparse hot spots, suggesting poor dissolution during ammonia treatment and likely poor coating by aluminosilicates. Sequential liquid extraction data for uranium showing significant variability for sediments with high uranium concentrations was also consistent with the hot-spots of uranium phases observed in X-ray fluorescence data. Laser induced fluorescence spectroscopy identified that uranium was predominantly present as uranophane [$Ca(UO_2)_2(SiO_3OH)_2(H_2O)_5$] with some boltwoodite [$Na(UO_2)(SiO_4)*1.5H_2O$] with very little uranium in other phases. This result is unusual because most Hanford sediments contain a variety of aqueous/adsorbed uranium, uranium associated with carbonates, and uranium in hydrous silicates (i.e., uranophane and boltwoodite). For instance, in a sediment with high uranium beneath the 241-U-105 tank with 690 µg/g uranium, boltwoodite was identified as a dominant uranium phase, but the sediment also contained other U phases comprising about 20% of the uranium content (Um et al. 2009a). This 241-U-105 tank sediment did show effective ammonia treatment in laboratory studies (Szecsody et al. 2012).

Collectively, these conditions, and potentially others, hindered ammonia treatment effectiveness in the laboratory tests using field test site sediments. However, the field test site did not have high organic carbon or phosphate concentrations that might indicate presence of tributyl phosphate or other uranium complexing agents. Other factors were investigated, with some minor evidence that these other factors affected ammonia treatment effectiveness in laboratory tests using field test site samples (Appendix E). Although some potential interference indicators were identified for the 216-U-8 site, other factors such as those listed in the interference hypotheses (Section 3.2.1.3) could affect the treatment process at other sites. In summary, interference testing identified specific concerns at acidic waste discharge sites where the discharge has altered the sediment carbonate concentrations and caused uranium to be deposited in sparse hot spots in the sediment. The overall treatability test results, including these interference tests, leads to a recommendation that site-specific effectiveness testing is needed for evaluation of this technology prior to selection for application at another site because URGS ammonia treatment effectiveness can be impacted by site-specific geochemical factors.

4.1.4   Field System Functional Testing

To ensure proper performance prior to injection of ammonia gas, both the gas delivery and monitoring systems underwent extensive functional testing. Field leak and pressure testing were performed on all mechanical systems and piping. The response of each low level (ppm) ammonia sensor was tested by introducing a known concentration of gas and observing the correct response. The system was designed to automatically shut down gas injection and send out notifications in the event that ammonia gas was detected above defined thresholds. Shut down/notifications were included as part of the system functional testing. Introducing ammonia gas into the subsurface to functionally test borehole sensors was not performed but sensor readings were verified to be within expected ranges under ambient conditions.

4.2 Data Assessment

Treatability test data and associated laboratory and numerical modeling results are interpreted with respect to each of the field test objectives.

4.2.1   Effectiveness Assessment

The change in uranium mobility with URGS ammonia treatment was favorable in some laboratory experiments (Section 4.1.1). The URGS treatment mechanism is based on producing a stable robust precipitated phase that, when produced, would be stable for long time periods. Thus, there is a potential for the URGS ammonia treatment technology to be effective in decreasing uranium mobility in the vadose zone. However, the treatability tests in the laboratory demonstrated that the technology will only be effective under specific conditions.

The URGS treatability tests in the laboratory demonstrated that interactions of the ammonia treatment chemistry and site geochemistry are important with respect to the effectiveness of the treatment for decreasing uranium mobility. Treatability test information suggests that applicability at acidic discharge sites such as the 216-U-8 crib field test site may be poor. Use at basic or neutral discharge sites, or where subsurface geochemistry has not been significantly affected by the waste discharge chemistry, may be possible. Evaluation of the URGS technology for a future application must consider potential effectiveness issues, as observed in the laboratory using samples from the treatability test field site. It is expected that site-specific laboratory testing would be necessary to confirm treatment effectiveness. An initial step in the evaluation of effectiveness would be to consider the waste discharge, associated subsurface geochemistry, and uranium mobility at a site in comparison to the available laboratory data and information herein. Site-specific effectiveness tests would include sequential extraction and soil column leaching tests for untreated and ammonia treated sediments to quantify the change in uranium mobility. This testing would require about 1 year from the time of sediment sample receipt to the reporting of laboratory results.

As described in Section 4.1.3, the ammonia technology may not be applicable for acidic-waste disposal sites because low sediment carbonate concentrations and microscopic uranium concentrated in localized deposits rather than more uniformly precipitated at the soil surface were likely causes of poor ammonia treatment effectiveness in laboratory tests using field test site samples. For deeper ammonia treatment applications at acidic waste sites, the subsurface conditions may be appropriate for use of the technology, but site-specific evaluation would be needed. Other factors affecting ammonia treatment effectiveness were investigated but evidence that they affected ammonia treatment was not found. For instance, the field test site did not have high organic carbon or phosphate concentrations that might indicate presence of tributyl phosphate or other uranium complexing agents. Similarly, tests for the other hypotheses listed in Section 3.2.1.3 did not result in an indicator related to poor ammonia treatment performance. However, those potential concerns (e.g., presence of organic carbon) could affect the treatment process at other sites and site-specific effectiveness evaluation is warranted.

4.2.2   Implementability Assessment

The field design and laboratory testing conducted for the URGS treatability testing and gas-injection experience from the Hanford desiccation field test (Truex et al. 2018), conducted as part of the *Deep*

Vadose Zone Treatability Test Plan for the Hanford Central Plateau (DOE 2008), provide a basis for design of ammonia injection at prospective sites. This information suggests that ammonia injection should be a controllable process able to accommodate moderate subsurface heterogeneities. There are also two anticipated uses of ammonia injection outside Hanford that may also provide relevant information. One of these tests is for a Department of Defense research application evaluating injection of ammonia to increase the rate of alkaline hydrolysis of organic contaminants (Reactive Gas Process for In Situ Treatment of 1,2,3-Trichloropropane in Vadose Zone Soils, ER-201632, https://www.serdp-estcp.org/Program-Areas/Environmental-Restoration/Contaminated-Groundwater/Persistent-Contamination/ER-201632). For another test, ammonia will be injected to provide an electrical conductivity increase in the water within subsurface fractures so that ERT can be used to identify the location of the fractures (PNNL project number 68073). Injection effectiveness is related to the subsurface properties and site-specific ammonia injection trials may also be necessary prior to full implementation at another site. For candidate technology application sites, an ammonia injection design can either be tested as a site-specific treatability study or potentially within a phased implementation approach if the URGS ammonia treatment technology is selected as part of the most promising remedial alternative.

Implementation must also consider the operational and health and safety needs for applying ammonia injection as part of a treatment process. Ammonia is routinely handled for industrial processes and agriculture. Thus, equipment and monitors are available for its use. However, its use requires strict protocols associated with health and safety and engineering rigor with respect to ammonia compatibility and liquid/gas properties. These factors increase the cost of implementation compared to use of non-hazardous amendments and create some project risk associated with potential health and safety issues at the treatment site or at surrounding facilities or sites.

A key project risk is monitoring of ammonia and any potential health and safety incident. One example of a project risk occurred during the treatability test. During functional testing, when there was no ammonia on site, several of the low-level (ppm) ammonia sensors produced readings of ammonia above the notification threshold (12 ppmv). Thus, the ammonia sensor system was sensitive to potential false positive readings, with potential interferences identified by the manufacturer including humidity and electrical noise. False positive readings are a project risk for use of ammonia because notifications of an ammonia detection above the threshold would trigger an expensive response. Additional investigation of sensor sensitivities or other sensor options may be needed prior to use on a field application with the notification thresholds selected for the field test.

4.2.3   Assessment with Respect to CERCLA Feasibility Study Criteria

The following section summarizes the information collected during the URGS treatability test and how they relate to the CERCLA feasibility study evaluation criteria.

4.2.3.1   Threshold Criteria: Protectiveness and ARARs

The URGS ammonia treatment may only meet protectiveness and applicable or relevant and appropriate requirement (ARAR) criteria for sites where there are not site-specific interferences that decrease the effectiveness of the treatment process. At sites like the 216-U-8 crib, the URGS ammonia treatment would not meet these threshold criteria.

In addition to consideration of ammonia treatment effectiveness in decreasing uranium mobility to meet protectiveness and ARAR criteria, nitrate production must also be considered for future remediation applications. As shown in Section 1.1, nitrate mass produced from ammonia injection was estimated to range from about 100 kg for the field test up to 10,000 kg for treatment of an 80×80 m target zone. Thus, evaluation of the protectiveness and ARAR criteria would need to consider whether groundwater protection objectives associated with nitrate would be negatively affected by ammonia treatment. This evaluation would include an assessment of the total mass of nitrate produced at the location of the treatment zone (see estimates and discussion in Section 1.1), and the predicted flux and associated groundwater concentration of nitrate that would be produced.

4.2.3.2   Long-Term Effectiveness and Permanence

For sites such as those tested during technology development (Section 4.1.1), where the URGS ammonia treatment creates low-solubility precipitates that decrease uranium mobility, the treatment would be expected to have good long-term effectiveness and permanence. At sites like the 216-U-8 crib, the URGS ammonia treatment would not meet long-term effectiveness and permanence criteria.

4.2.3.3   Reduction of Volume, Mobility, or Toxicity

For sites such as those tested during technology development (Section 4.1.1), where the URGS ammonia treatment creates low-solubility precipitates that decrease uranium mobility, the treatment would be expected to meet criteria for mobility reduction. At sites like the 216-U-8 crib, the URGS ammonia treatment would not meet the mobility reduction criteria.

In addition to consideration of ammonia treatment effectiveness in decreasing uranium mobility, nitrate production must also be considered for future remediation applications as mobile side-product of ammonia treatment (see discussion of threshold criteria in Section 4.2.3.1).

4.2.3.4   Short-Term Effectiveness

Short-term effectiveness considers potential effects on human health and the environment during the implementation phase of the remedy, and the time required to achieve the remedial action objectives. Ammonia handling has several health and safety issues that would need to be addressed to ensure short-term effectiveness. Thus, there is a risk that ammonia treatment would have poor short-term effectiveness.

4.2.3.5   Implementability

Implementability includes technical and administrative feasibility, and availability of services and materials. The field test design demonstrated that ammonia injection equipment is available for implementation of the technology and that there is an availability of services and materials for the technology. Administrative issues, however, include potential project risks as described in the Lessons Learned section (Section 2.2.2).

4.2.3.6 Cost

Cost elements include rigorous design needs to accommodate hazards and codes, ammonia-compatible equipment, rigorous health and safety monitoring, and emergency planning. High costs for the field test design and construction (see Section 6.0) were driven by these factors, as would a remediation implementation of the ammonia treatment technology. A feasibility study author could use the information in this report and the field test design referenced herein to develop a feasibility study cost estimate within the required +50%/-30% range.

5.0   Quality Assurance Results

A data quality objectives (DQOs) process, as described in *Guidance on Systematic Planning Using the Data Quality Objectives Process* (EPA 2006), was used to develop the sampling and analytical design to support the treatability test. The DQO process is documented in *Data Quality Objectives Summary Report for the Uranium Sequestration Pilot Test* (CHPRC 2010).

Principal study questions (PSQs) for the treatability test are listed below along with a discussion of associated treatability test results.

PSQ #1: Does the planned test interval contain sufficient mobile uranium and have characteristics suitable to evaluate potential treatment effectiveness?

> Untreated samples from the test site were analyzed for uranium concentration and for mobile uranium content using the sequential extraction method. The test site met the criteria listed in the FTP (DOE 2015a), with pore water concentrations greater than 30 μg/L, samples with a uranium mobile fraction (aqueous, sorbed, and rind carbonate) >20% of the total, and a uranium concentration range greater than from 10 to 1000 mg/kg.

PSQ #2: Does laboratory testing of sediments obtained from the planned test interval show reduction in mobile uranium content due to ammonia treatment?

> Laboratory testing of sediments dosed and incubated for 4 months to 1.5 year did not show a decrease in uranium mobility in soil column leaching tests. Almost all of the 22 leaching experiments showed more uranium leached and higher uranium concentrations in the effluent than for the untreated sediments. This information resulted in additional laboratory tests to determine the interference related to the poor effectiveness and the field test was terminated.

PSQ #3: Does laboratory testing of sediments obtained from the planned test interval show reduction in mobile TC-99 content due to ammonia treatment?

> Tc-99 concentrations were below detection at the field test site, so this evaluation could not be completed.

PSQ #4: Will vadose zone geochemical manipulation via ammonia injection result in a reduction of uranium and/or TC-99 mobility?

> This PSQ was for considering the treatability test data with respect to future full-scale applications. Data and interpretation in the treatability test report discuss the challenges for use of ammonia as a treatment technology based on the poor effectiveness observed at the 216-U-8 test site and implementation issues identified during the field tests design and construction activities.

Data collection and evaluation, and laboratory sample analysis, were conducted in accordance with the methods and specifications described in the SAP (DOE 2015b). A data usability assessment report was prepared (CHPRC 2018d).

In addition, work was governed by the *DVZ-AFRI Quality Assurance Plan* (DVZ-QAP). The DVZ-QAP implements the requirements of the United States Department of Energy Order 414.1D, *Quality Assurance* and 10 CFR 830 Subpart A*, Quality Assurance Requirements*. The DVZ-QAP uses ASME NQA-1-2000, *Quality Assurance Requirements for Nuclear Facility Applications* as its consensus standard and NQA-1-2000 Subpart 4.2 as the basis for its graded approach to quality. The work controls were graded as *Applied Research*.

6.0   Cost and Schedule

Overall cost of the URGS test was about $8 million. Major cost elements and associated expenditures are shown in Table 6.1.

Table 6.1. Costs for Treatability Test Activities

Treatability Test Activity	$ (K)
FTP and SAP	300,000
Site characterization	250,000
Laboratory testing of treatment effectiveness (e.g., sequential extractions and soil column tests)	350,000
Borehole drilling and injection well/monitoring borehole construction	1,422,000
Test site preparation	2,250,000
Equipment/instrument design, procurement and installation	3,000,000
Final treatability test report	300,000
Total	**7,872,000**

Costs shown above are not necessarily representative of the cost to implement a URGS remedy because conducting a treatability test required activities needed to collect detailed technology information in support of future feasibility studies.

7.0 References

Amin T and R Narang. 1985. "Determination of volatile organics in sediment at nanogram per gram concentrations by gas chromatography." *Anal. Chem*. 57:648-851.

Archie GE. 1942. "The Electrical Resistivity Log as an Aid in Determining Some Reservoir Characteristics." *Petroleum Transactions of AIME* 146:54–62.

Beckett P. 1989. "The use of extractants in studies on trace metals in soils, sewage sludges, and sludge-treated soils." In *Advances in Soil Science*, Volume 9, Springer-Verlag, New York, p 144-176.

Brina R and AG Miller. 1992. "Direct detection of trace levels of uranium by laser induced kinetic phosphorimetry." *Analytical Chemistry* 64(13):1413-1418.

CHPRC. 2010. *Data Quality Objectives Summary Report for the Uranium Sequestration Pilot Test*, Rev. 0. SGW-46487, CH2M HILL Plateau Remediation Company, Richland, Washington.

CHPRC. 2018a. *Uranium Reactive Gas Sequestration Functional Design Criteria*. SGW-60699, CH2M Hill Plateau Remediation Company, Richland, WA.

CHPRC. 2018b. *URGS – Vendor DWG Release*. ECR-18-000249, CH2M Hill Plateau Remediation Company, Richland, WA.

CHPRC. 2018c. *Uranium Sequestration Drawing Index*. H-2-837215, Rev. 0 (drawing), CH2M Hill Plateau Remediation Company, Richland, WA.

CHPRC. 2018d. *Data Usability Assessment Report for the Deep Vadose Zone Uranium Sequestration Pilot Test on the Hanford Central Plateau*. SGW-62303, CH2M Hill Plateau Remediation Company, Richland, Washington.

Corbin RA, BC Simpson, MJ Anderson, WF Danielson III, JG Field, TE Jones, and CT Kincaid. 2005. *Hanford Soil Inventory Model Rev. 1*. RPP-26744, Rev. 0, CH2M HILL Hanford Group, Inc., Richland Washington.

Daily W and E Owen. 1991. "Cross-Borehole Resistivity Tomography." *Geophysics* 56:1228–1235.

Demirkanli DI, MJ Truex, JE Szecsody, MM Snyder, JJ Moran, MK Nims, AR Lawter, CT Resch, DL Saunders, NP Qafoku, SR Baum, and BD Williams. 2018. *Contaminant Attenuation and Transport Characterization of 200-DV-1 Operable Unit Sediment Samples from Boreholes C9497, C9498, C9603, C9488, and C9513*. PNNL-27524, Pacific Northwest National Laboratory, Richland, Washington.

DOE. 2008. *Deep Vadose Zone Treatability Test Plan for the Hanford Central Plateau*. DOE/RL-2007-56, Rev. 0, U.S. Department of Energy Richland Operations Office, Richland, Washington.

DOE. 2015a. *Field Test Plan for the Uranium Sequestration Pilot Test*. DOE/RL-2010-87, U.S. Department of Energy Richland Operations Office, Richland, Washington.

DOE. 2015b. *Sampling and Analysis Plan for the Uranium Sequestration Pilot Test*. DOE/RL-2010-88, U.S. Department of Energy Richland Operations Office, Richland, Washington.

Dresel PE, DM Wellman, KJ Cantrell, and MJ Truex. 2011. "Review: Technical and Policy Challenges in Deep Vadose Zone Remediation of Metals and Radionuclides." *Environ. Sci. Technol.* 45(10):4207-4216.

EPA. 1992. *Guidance for Conducting Treatability Studies under CERCLA*. EPA/540/R-92/071a, U.S. Environmental Protection Agency, Washington, D.C.

EPA. 2006. *Guidance on Systematic Planning Using the Data Quality Objectives Process*. EPA/240/B-06/001, EPA QA/G-4, Office of Environmental Information, U.S. Environmental Protection Agency, Washington, D.C. Available at: http://www.epa.gov/QUALITY/qs-docs/g4-final.pdf.

Emerson HP, S Di Pietro, Y Katsenovich, and J Szecsody. 2018. "Potential for U sequestration with select minerals and sediments via base treatment." *J Environmental Management* 223:108-114.

Eslinger PW, CT Kincaid, WE Nichols, and SK Wurstner. 2006. *A Demonstration of the System Assessment Capability (SAC) Rev. 1 Software for the Hanford Remediation Assessment Project*. PNNL-16209, Pacific Northwest National Laboratory, Richland, Washington.

Gleyzes C, S Tellier, and M Astruc. 2002. "Fractionation studies of trace elements in contaminated soils and sediments: a review of sequential extraction procedures." *Trends in Analytical Chemistry* 21(6 & 7):451-467.

Greacen EL, RL Correll, RB Cunningham, OC Johns, and KD Nichols. 1981. "Calibration." In *Soil Water Assessment by the Neutron Method*, pp. 50–78, CSIRO, Melbourne, Australia.

Hignett C and SR Evett. 2002. "Neutron Thermalization." In *Methods of Soil Analysis. Part 4 – Physical Methods*. JH Dane and G Clarke Topp (eds.), pp. 501–521, Soil Science Society of America, Madison, Wisconsin.

Johnson TC, RJ Versteeg, A Ward, FD Day-Lewis, and A Revil. 2010. "Improved Hydrogeophysical Characterization and Monitoring Through Parallel Modeling and Inversion of Time-Domain Resistivity and Induced Polarization Data." *Geophysics* 75(4):WA27–WA41.

Kohler M, DP Curtis, DE Meece, and JA Davis. 2004. "Methods for estimating adsorbed uranium (VI) and distribution coefficients of contaminated sediments." *Environ. Sci. Technol.* 38:240-247.

Larner B, A Seen, and A Townsend. 2006. "Comparative study of optimized BCR sequential extraction scheme and acid leaching of elements in certified reference material NIST 2711." *Analytica Chimica Acta* 556:444-449.

Mossop K and C Davison. 2003. "Comparison of original and modified BCR sequential extraction procedures for the fractionation of copper, iron, lead, manganese, and zinc in soils and sediments." *Analytica Chimica Acta* 478:111-118.

Qafoku NP, CC Ainsworth, JE Szecsody, and OS Qafoku. 2004. "Transport-controlled kinetics of dissolution and precipitation in the sediments under alkaline and saline conditions." *Geochimica et Cosmochimica Acta* 68(14):2981-2995.

Serne RJ, MJ Lindberg, SR Baum, GV Last, RE Clayton, KN Geiszler, GW Gee, VL LeGore, CF Brown, HT Schaef, RD Orr, MM Valenta, DC Lanigan, IV Kuthyakov, TS Vickerman, and CW Lindenmeier. 2008a. *Characterization of Vadose Zone Sediment: Borehole 299-E33-45 Near BX 102 in the B-BX-BY Waste Management Area*. PNNL-14083, Rev. 1, Pacific Northwest National Laboratory, Richland, Washington.

Serne RJ, MJ Lindberg, MM Valenta, BN Bjornstad, RE Clayton, IV Kutnyakov, DG Horton, VL LeGore, TS Vickerman, DC Lanigan, KN Geiszler, RD Orr, HT Schaef, SR Baum, CF Brown, and CW Lindenmeier. 2008b. *Characterization of Vadose Zone Sediments Below the T Tank Farm: Boreholes C4104, C4105, 299-W10-196, and RCRA Borehole 299-W11-39*. PNNL-14849, Rev. 1, Pacific Northwest National Laboratory, Richland, Washington.

Simpson BC, RA Corbin, MJ Anderson, CT Kincaid, and JM Zachara. 2006. *Identification and Classification of the Major Uranium Discharges and Unplanned Releases at the Hanford Site Using the Soil Inventory Model (SIM) Rev. 1 Results*. NUV-06-21106-ES-001-DOC, Rev. 1, Novotec, USA Inc., Cincinnati, Ohio.

Slater LD and DP Lesmes. 2002. "Electrical-Hydraulic Relationships Observed for Unconsolidated Sediments." *Water Resources Research* 38:1213–1225.

Sutherland R and F Tack. 2002. "Determination of Al, Cu, Fe, Mn, Pb, and Zn in certified reference materials using the optimized BCR sequential extraction procedure." *Analytica Chimica Acta* 454:249-257.

Szecsody JE, MJ Truex, BD Lee, CE Strickland, JJ Moran, et al. 2017. *Geochemical, Microbial, and Physical Characterization of 200-DV-1 Operable Unit B-Complex Cores from Boreholes C9552, C9487, and C9488 on the Hanford Site Central Plateau*. PNNL-26266, Pacific Northwest National Laboratory, Richland, WA.

Szecsody J, M Truex, N Qafoku, D Wellman, T Resch, and L Zhong. 2013. "Influence of acidic and alkaline co-contaminants on uranium migration in vadose zone sediments." *Journal of Contaminant Hydrology* 151:155-175.

Szecsody JE, MJ Truex, L Zhong, TC Johnson, NP Qafoku, MD Williams, JW Greenwood, EL Wallin, JD Bargar, and DK Faurie. 2012. "Geochemical and Geophysical Changes During NH3 Gas Treatment of Vadose Zone Sediments for Uranium Remediation." *Vadose Zone J.* 11(4) doi:10.2136/vzj2011.0158

Szecsody JE, MJ Truex, L Zhong, MD Williams, and CT Resch. 2010a. *Remediation of Uranium in the Hanford Vadose Zone Using Gas-Transported Reactants: Laboratory-Scale Experiments*. PNNL-18879, Pacific Northwest National Laboratory, Richland, Washington.

Szecsody JE, MJ Truex, L Zhong, NP Qafoku, MD Williams, JP McKinley, CT Resch, JL Phillips, D Faurie, and J Bargar. 2010b. *Remediation of Uranium in the Hanford Vadose Zone Using Ammonia*

Gas: FY10 Laboratory-Scale Experiments. PNNL-20004, Pacific Northwest National Laboratory, Richland, Washington.

Truex MJ, GB Chronister, CE Strickland, CD Johnson, GD Tartakovsky, M Oostrom, RE Clayton, TC Johnson, VL Freedman, ML Rockhold, WJ Greenwood, JE Peterson, SS Hubbard, and AL Ward. 2018. *Deep Vadose Zone Treatability Test of Soil Desiccation for the Hanford Central Plateau: Final Report*. PNNL-26902, Pacific Northwest National Laboratory, Richland, Washington.

Truex MJ, JE Szecsody, NP Qafoku, CE Strickland, JJ Moran, BD Lee, et al. 2017. *Contaminant Attenuation and Transport Characterization of 200-DV-1 Operable Unit Sediment Samples*. PNNL-26208, Pacific Northwest National Laboratory, Richland, Washington.

Truex MJ, JE Szecsody, L Zhong, JN Thomle, and TC Johnson. 2014. *Scale-Up Information for Gas-Phase Ammonia Treatment of Uranium in the Vadose Zone at the Hanford Site Central Plateau*. PNNL-23699, Pacific Northwest National Laboratory, Richland, Washington.

Truex MJ and KC Carroll. 2013. *Remedy Evaluation Framework for Inorganic, Non-Volatile Contaminants in the Deep Vadose Zone*. PNNL-21815, Pacific Northwest National Laboratory, Richland, Washington.

Um W, Z Wang, J Serne, B Williams, C Brown, C Dodge, and A Francis. 2009a. "Uranium Phase in Contaminated Sediments Below Hanford's U Tank Farm." *Environ. Sci. Technol.* 43(12):4280–4286.

Um W, J Serne, M Truex, A Ward, M Valenta, C Brown, C Iovin, K Geiszler, I Kutnyakov, E Clayton, H Chang, S Baum, R Clayton, and D Smith. 2009b. *Characterization of sediments from the soil desiccation pilot test (SDPT) site in the BC Cribs and Trenches area*. PNNL-18800, Pacific Northwest National Laboratory, Richland, Washington.

Zachara JM, CF Brown, JN Christensen, JA Davis, PE Dresel, C Liu, SD Kelly, et al. 2007. *A Site Wide Perspective on Uranium Geochemistry at the Hanford Site*. PNNL-17031, Pacific Northwest National Laboratory, Richland, Washington.

Zhong L, JE Szecsody, MJ Truex, and MD Williams. 2015. "Ammonia Gas Transport and Reactions in Unsaturated Sediments: Implications for Use as an Amendment to Immobilize Inorganic Contaminants." *Journal of Hazardous Materials*. 289:118–129. doi:10.1016/j.jhazmat.2015.02.025

Appendix A

Site Selection

Appendix A

Site Selection

A.1 Deep Vadose Zone Treatability Test: Uranium Treatment Field Test Site Selection

A.1.1   Introduction

The *Deep Vadose Zone Treatability Test Plan for the Hanford Central Plateau* (DOE 2008) provides a strategy and framework for evaluating specific vadose zone remediation technologies. The treatability approach includes laboratory, modeling, and field tests. Testing of reactive gas technology is one component of the overall treatability test plan, with an initial emphasis on uranium contamination. As discussed in the treatability test plan (DOE 2008), there are several potential technologies for vadose zone treatment of uranium. In previous studies associated with evaluating technologies for application to the 200 Area vadose zone at the Hanford Site, technologies requiring the addition of significant amounts of water to the vadose zone were less preferred because of the potential for inducing uncontrolled migration of contaminants, and difficulties in controlling how added water moves through the vadose zone. Thus, treatability testing efforts for uranium are focused on gas-transported reactants.

A range of candidate technologies were identified in the treatability test plan (DOE 2008) and through additional review of current technology information. In fiscal year 2009, for each of the technologies, the potential changes in uranium mobility in the sediment were evaluated based on current knowledge of the reaction mechanism and through proof-of-principle experiments, as appropriate (Szecsody et al. 2010a). This effort identified reactive gas treatment using ammonia gas as a promising candidate for field testing. In summary, when ammonia gas is introduced to the vadose zone, it partitions into the pore water as ammonium ion. This process increases the pH of the pore water and thereby dissolves some mineral phases, notably aluminosilicates. The pH can then be lowered by flushing inert gas through the vadose zone to remove ammonia or through natural buffering capacity. When the pH of the pore water decreases, aluminosilicate minerals precipitate, which, in laboratory tests, rendered the uranium more difficult to extract from the sediment/pore water and thereby less mobile. Additional development of the ammonia technology has been conducted in laboratory and modeling studies (Szecsody et al. 2010b, 2012; Truex et al. 2014a; Zhong et al. 2015) in support of design and interpretation of the planned field test.

Current plans are to proceed with field testing of the ammonia technology for treatment of uranium in the vadose zone. A key first step in preparing for the field test is selection of a suitable field test site. The following sections provide an overview of the field test concept, criteria developed for the field site selection, a review of the site selection approach, and the results of the site selection process.

A.1.2   Field Test Concept

The field test will be designed to collect data that quantify the performance of the ammonia technology and support the treatability test goal of providing information useful for inclusion of the technology in subsequent feasibility studies. Currently, it is envisioned that the test would be conducted using a single vadose zone well for injection of an ammonia gas mixture with monitoring locations surrounding the injection location to monitor the injection process. The primary performance measure will be comparison of uranium in sediment and pore water before and after the treatment. Baseline sediment samples from the test site will also be subjected to ammonia treatment in the laboratory for comparison to field treatment results.

A.1.3   Field Site Selection Criteria

Criteria for selection of the field test site were developed for use in evaluating candidate field sites. These criteria take into account technical and logistical aspects of conducting the test and the intended use of the data to support future feasibility studies. The criteria are listed below in order of importance.

1. Do the data indicate that the site is appropriate for testing the technology based on the uranium concentration, chemistry, and physical properties?
    a. Applicability for treatment will be based on estimates of uranium concentration/sediment chemistry (mobility), waste disposal stream information, and sediment particle size distribution
        1. Essential to have a contaminated zone where a component of the uranium is present in a mobile phase
        2. Prefer site with both coarse and fine grain sediment lenses within contaminated zone
        3. Consider potential impact of waste disposal chemistry (Truex et al. 2014b)
        4. Consider presence of co-contaminants (positive and negative)
    b. Adequacy of existing information, including confirmation by geophysical logging and sample analysis, proximity of boreholes to waste site, depth of drilling and pushes
        1. Absence of characterization data – screened out
        2. Conflicting data (e.g., inventory estimate vs. borehole sample analysis) – screened out
    c. Relation to data from laboratory tests (Szecsody et al. 2010a,b, 2012)
        1. Similarity to uranium concentration in laboratory tests (tens to hundreds μg-U/g-sediment)
        2. Mineralogy similar to sediments used in lab tests
        3. Consider potential for non-neutral pH
        4. Consider moisture content in the target zone

2. Are the size and configuration of the vadose zone contamination suitable for a test location?
    a. Ability to locate a suitable test interval (knowledge of contaminant location)
    b. Depth to suitable test location (shallow but beyond the extent of direct surface flow paths for injected gases is preferred)
    c. Total thickness of contaminated zone (thicker is better)
    d. Areal extent (larger is better)
    e. Uranium inventory (larger is better)
    f. Contamination outside footprint of disposal structures
    g. Consider presence of metallic infrastructure with respect to use of electrical resistivity tomography (ERT)
    h. Consider surface accessibility

3. Are there operational issues that would make testing difficult and/or costly or that would significantly delay initiating the test?
    a. Cost factors
    b. Administrative controls, processes, and restrictions (safety basis, fence lines, potential lead time, etc.), cribs vs. tank farm releases
        1. Inside tank farm – screened out
        2. Restricted area (e.g., cave-in issues) – screened out
    c. ALARA (as low as reasonably achievable), distribution of contaminants within and surrounding the target test interval
    d. No administrative issues with surface modifications for test infrastructure

4. Is the site representative of other sites where the technology may be applied for remediation?
    a. Tank farm or disposal site
    b. Type of waste discharge (e.g., source of waste)
    c. Site geology considering presence of coarse and fine grain sediments and Hanford/ CCU/Ringold materials (evaluate ability to obtain sediment samples of CCU and Ringold if field test is in the Hanford formation)

5. Does the site vadose zone contamination pose a near-term risk for the groundwater?
    a. Is the site a near-term target for remediation?
    b. Is there a priority for activity at the site?

A.1.4   Site Selection Approach

The site selection process was initiated by identifying candidate sites based on information in the treatability test plan (DOE 2008) and knowledge of potentially suitable sites where uranium was disposed. Data and information from reports and interviews of site staff for each candidate site were compiled, as available, to provide input to each of the selection criteria. A series of meetings was convened in 2010 to review the information and evaluate each site with respect to the selection criteria. Attendees of these meetings are listed in Table A.1. Site staff contacted to discuss candidate sites are

listed in Table A.2. The results of the 2010 site selection were reviewed in 2014 by CH2M Hill Plateau Remediation Company (CHPRC) and Pacific Northwest National Laboratory (PNNL) project staff (Table A.3). Refinements to the site selection process have been incorporated into this document.

Table A.4 summarizes general information for candidate sites. Results of the evaluation are documented in Table A.5. A final evaluation of this information was then used to select the target field test site.

Table A.1. Attendees for Site Evaluation Meetings

Attendee	Organization
Glen Chronister	CHPRC
Mark Benecke	CHPRC
Scot Adams	CHPRC
Jeff Serne	PNNL
Mike Truex	PNNL
Wooyong Um	PNNL
Jim Szecsody	PNNL
Mart Oostrom	PNNL
Chris Strickland	PNNL

Table A.2. Contributing Site Staff

Contributor	Organization
Jim Hoover	CHPRC
Bill McMahon	CHPRC
Charles Miller	CHPRC
Jon Lindberg	CHPRC
Dave Erb	CHPRC
Greg Thomas	CHPRC
John McDonald	CHPRC
Dave Ottley	CHPRC
Scott Worley	CHPRC
Bonnie Howard	CHPRC
Les Walker	CHPRC
Scott Petersen	CHPRC
Dave Weekes	CHPRC
William Webber	CHPRC
Carl Connell	CHPRC
Al Rizzo	CHPRC
Rick McCain	Stoller
Paul Henwood	Stoller
Sunil Mehta	Intera
Dave Meyers	Washington River Protection Solutions
Marek H. Zaluski	MSE -Technology Applications
Chris Haas	Freestone Environmental

Table A.3. Attendees for 2014 Site Evaluation Meeting

Attendee	Organization
Glen Chronister	CHPRC
Bruce Williams	CHPRC
Virginia Rohay	CHPRC
Mike Truex	PNNL
Jim Szecsody	PNNL
Chris Strickland	PNNL

A.1.5 Site Selection Results

The following sections describe each step of the site selection process.

A.1.5.1 Site Identification

Table A.4 lists the candidate sites considered in the selection process. The general location of these sites on the Hanford Central Plateau is shown in Figure A.1. This site information was reviewed in 2014 with consideration of vadose zone characterization activities that have occurred between 2010 and 2014. The characterization activities in this period include four wells installed in the B-Complex area, re-inversion of the B-Complex ERT data for vadose zone contamination, wells installed at the S-9 and S-13 sites, and wells installed near U Plant as part of UP-1 operable unit (OU) drilling. In reviewing this characterization information, no changes were identified that impact evaluation of the suitability of a site for the uranium field test. In summary, the UP-1 OU drilling and wells at S-9 and S-13 are not near a candidate test site. The B-Complex well information did not show additional areas of vadose zone uranium contamination. The B-Complex ERT re-inversion did not identify new vadose zone target areas for the test.
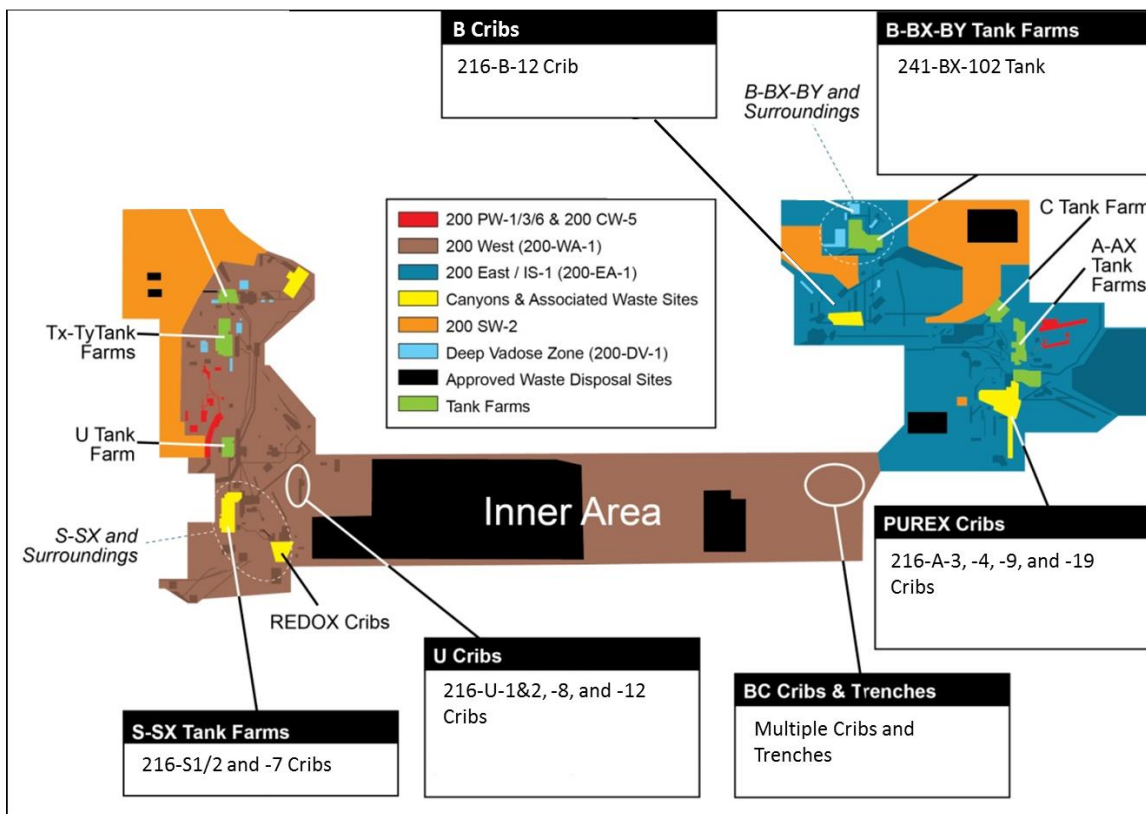
Figure A.1. Location of High Uranium Inventory Sites Considered in the Site Selection Process

Table A.4. Description of Candidate Test Sites

Site	Description
216-A-19 Crib	Waste Stream(s): The site received PUREX startup waste during November and December 1955. Although several references state it also received condenser cooling water from the 241-A-431 building via the 216-A-34 ditch, drawings do not show the 216-A-34 ditch connecting to the 216-A-19 crib. While the U inventory (~43 metric tons) is the largest discharged to any Hanford liquid disposal waste site, all but 31 kg U is estimated to have been discharged as solids (SIM). Cumulative discharge inventory summary (SIM) is: • U: 43,444 kg (depleted) • Na: 27, 671 kg • Fe: 18,345 kg • NO_3: 10,919 kg • CO_3: 5102 kg • SO_4: 4604 kg • Cs-137: 0 Description: The crib is a $7.6 \times 7.6 \times 4.6$ m deep ($25 \times 25 \times 15$ ft deep) excavation with no liquid dispersion structure. Characterization: The only characterization data are from the C3245 borehole drilled through the crib in April 2003. Borehole logging indicates uranium at 20 to 80 pCi/g located from 3.0 to 9.4 m (10 to 31 ft) below ground surface (bgs). Maximum Cs-137 activity level observed was 560 pCi/g at 2.4 m (8 ft) bgs. Sediment sampling showed 51 pCi/g U-238 (max) at 4.4 m (14.5 ft) bgs.
216-U-1&2 Cribs	Waste Stream(s): The cribs received overflow from the 241-U-361 settling tank, which received cell drainage from the 5 to 6 tanks in 221-U and waste from the 224-U building until the uranium recovery process operations shut down in 1957. From July 1957 through May 1967, the 216-U-1&2 cribs received waste from the 224-U facility and equipment decontamination waste and reclamation waste from the 221-U canyon. The waste was low in salt and neutral to basic, except for the highly acidic discharge late in its history. Cumulative discharge inventory summary (SIM) is: • U: 3955 kg • C-137: 1.8 Ci • Na: 8467 kg • K: 127,476 kg • NO_3: 1,669,917 kg • CO_3: 6536 kg • PO_4: 6633 kg • SO_4: 171,222 kg Description: The cribs include two wooden liquid dispersion structures in adjacent excavations $27.1 \times 8.5 \times 4.9$ m deep ($89 \times 28 \times 16$ ft deep) that operated in series. Characterization Data: Characterization borehole 299-W19-96 (A9797) was drilled through the 216-U-1 crib in 1995. The highest zone of contamination was found at a depth of 6 to 12 m (20 to 40 ft). Maximum contamination levels in this zone included 2,400,000 pCi/g Sr-90, 1,430,000 pCi/g Cs-137, and 438 pCi/g Pu- 239/240.

Site	Description
	Three additional characterization boreholes (299-W19-95, 299-W19-96, and 299-W19-97) were drilled near the 216-U-1&2 cribs in 1995. Borehole sediment samples and surface soil samples were collected and analyzed. Uranium-contaminated perched water was observed in the CCU. Shallow push holes surround the crib at various distances. Isopleth maps of uranium and Cs-137 contamination indicate significant lateral contamination spread. There are thought to be two zones of uranium concentration: one that is shallow and another in the deeper Cold Creek silt and carbonate layer. Unusual Occurrence 85-17: Unusual Occurrence 85-17 reports groundwater samples taken in January 1985 from wells 299-W19-03 and 299-W19-11, indicating 60,000 and 85,000 pCi/L of uranium, respectively. Previous routine samples averaged less than 500 pCi/L. Investigation revealed that liquid waste from the 216-U-16 crib, located south of the 216-U-1&2 cribs, had migrated north along a subsurface caliche layer. Existing groundwater monitoring wells around the 216-U-1&2 cribs provided a pathway for the contamination to reach the groundwater.
216-U-8	Waste Stream(s): The cribs received acidic process condensate from the 221-U and 224-U buildings, along with drainage from the 291-U stack via an underground vitrified clay pipeline. The waste was acidic. Discharge inventory summary (SIM) is: • U: 25,512 kg • Tc-99: 2.7 Ci • C-137: 0.05 Ci • Am-241: 4.7 Ci • Na: 7482 kg • K: 3,624,455 kg • Ca: 5852 kg • NO_3: 4,556,685 kg • PO_4: 79,023 kg • F: 7295 kg • Cl: 8192 kg Description: The site consists of three wood timber liquid dispersion structures set in series within a $48.8 \times 15.2 \times 9.7$ m deep ($160 \times 50 \times 32$ ft deep) excavation. Each structure is $4.9 \times 4.9 \times 3.0$ m deep ($16 \times 16 \times 10$ ft). The structures were filled with 1.3 cm (0.5 in.) crushed stone. There is roughly 2070 m^3 (73,000 ft^3) of gravel fill in the cribs. Characterization: During the 1995 Limited Field Investigation, a borehole (299-W19-94) was drilled though the crib to a depth of 60.6 m (199 ft) and abandoned following characterization. Gamma logging detected U-238 (831 pCi/g at 11.4 m [37.5 ft] bgs and 150 pCi/g at 56.4 m [185 ft] bgs) in the borehole. Soil samples showed high concentrations of Cs-137 and Sr-90 near the underground vitrified clay pipeline. Isopleth maps of uranium, Tc-99, and Cs-137 contamination obtained from boreholes drilled to approximately 45 ft deep during 2005 indicate significant lateral spread of contamination.
216-U-12 Crib	Waste Stream(s): From April 1960 to May 1967, the site received 291-U-1 stack drainage, 241-WR vault waste and 224-U process condensate via the C-5 tank. Contaminated water from the 241-WR vault was discharged to the crib in October 1965, which included 3.14 kg (6.9 lb) of thorium. From May 1967 to September 1972, the site received the above wastes (excluding the 241-WR vault waste) and occasional waste via the C-7 tank in the 224-U

Site	Description
	building. From September 1972 to November 1981, the site was inactive. From November 1981 to January 1987, the site received acidic process condensate (typical pH range was 0.5 to 1.5) from the 224-U building. The crib also received miscellaneous storm drain wastes from the 224-U building. Between April 1960 and September 1972, 6.7E+5 kg nitrate was released to the crib from the uranium tri-oxide process. The waste was acidic. Cumulative discharge inventory summary (SIM) is: • U: 6458 kg • Tc-99: 0.7 Ci • Cs-137: 69.6 Ci • Am-241: 1.4 Ci • Na: 3921 kg • K: 1,834,294 kg • Ca: 2965 kg • NO_3: 2,279,820 kg • PO_4: 40,049 kg • F: 3707 kg • Cl: 8192 kg Description: The 216-U-12 crib includes a below-grade, 30 cm (12 in.) diameter vitrified clay pipe running horizontally for the length of the crib within a $30.5 \times 3.0 \times 4.6$ m deep ($100 \times 10 \times 15$ ft deep) excavation that was filled with 264 m^3 gravel. Characterization: Limited characterization data are available from a 1994 borehole placed adjacent to the crib footprint, which showed no contaminants above background. Spectral gamma borehole logging of a borehole through the crib to 53 m (175 ft) bgs indicates Cs-137 from 5 to 18 m (16 to 59 ft) (maximum activity of 16,100 pCi/g at 7 m [23 ft]) and U-238 from 5 to 24 m (17 to 80 ft) (maximum activity of 500 pCi/g at 23 m [76 ft] bgs). Isopleth maps of uranium and Cs-137 contamination obtained from boreholes drilled to approximately 40 to 50 ft deep during 2005 indicate significant lateral contamination spread.
216-B-12	Waste Stream(s): The crib originally received 221-U and 224-U condensate waste transported from 200 West Area via the cross-site transfer line (line V219). Later, the crib received condensate waste from the 221-B Plant. From November 1952 to December 1957, the site received the process condensate waste from the tributyl phosphate uranium recovery processes at the 221-U and 224-U buildings as well as B Plant condensate. From December 1957 to May 1967, the site was inactive. From May 1967 to November 1967, the site received construction waste from the 221-B building. After November 1967, the site received process condensate from the 221-B building. The waste was low in salt and neutral-to-basic. Cumulative discharge inventory summary (SIM) is: • U: 15,112 kg • Na: 14,051 kg • Ca: 8147 kg • K: 2,286,683 kg • NO_3: 2,860,615 kg • CO_3: 11,676 kg • PO_4: 50,066 kg • F: 4743 kg • Sr-90: 120 Ci

Site	Description
	• Tc-99: 1.6 Ci • Cs-137: 326 Ci Description: The unit consists of a series of three cascading, $4.9 \times 4.9 \times 3.0$ m ($16 \times 16 \times 10$ ft) high wooden boxes in a $48.8 \times 15.2 \times 9.1$ m deep ($160 \times 50 \times 30$ ft deep) excavation. A 1.3 cm (0.5 in.) rock backfill lies in the bottom 3.7 m (12 ft) of the excavation and beneath each box is approximately 1.2 m (4 ft) of this rock. The site contains 2900 m³ (3800 yd³) of 1.3 cm (0.5 in.) gravel. Characterization: Wells 299-E28-9, 299-E28-16, 299-E28-65, and 299-E28-66 monitor this unit. Data indicate breakthrough to groundwater has not occurred at this site. Characterization borehole C3246, drilled into the crib in June 2003, was drilled to a depth of 308 ft. Geophysical logging found Cs-137, U-238, and Eu-154. The maximum concentration of Cs-137, 121,000 pCi/g, was found at 35 ft bgs. Approximately 10 pCi/g of U-238 was observed at 36.0 to 36.6 m (118 to 120 ft) bgs. Logging of 299-E28-16 (A6794), located approximately 9.1 m (30 ft) south of the crib, showed ~100 pCi/g of U-238 at 47 m (155 ft) bgs. This hole also indicated ~100,000 pCi/g of Cs-137 at 30.5 m (100 ft) bgs, which may have masked the presence of U-238. Logging of 299-E28-65 (A6816), located in the crib, showed greater than 10,000 pCi/g of Cs-137 from the bottom of the crib to 21 m (70 ft) bgs, with a maximum of approximately 250,000 pCi/g at a depth corresponding to the bottom of the crib.
241-BX-102 overfill event (UPR-200-E-5)	Waste Stream(s): In 1951, this tank was receiving the "metal waste" stream from the bismuth phosphate plutonium separation process at B Plant. On March 20, 1951, a cascade outlet became plugged, resulting in the BX-102 tank overfilling. The bismuth phosphate process released approximately 348,000 L (91,600 gal) of metal waste containing approximately 10.1 metric tons of uranium. Description: Contamination migrated beyond the 241-BX/BY fence, to the northeast and under the road north of the B Farm with increasing depth to the northeast. Some of this waste is contained in the saturated sediments that are perched on the Cold Creek fine-grained interval and is, over time, slowly leaking through and contributing to the groundwater plumes. A groundwater uranium plume that originates beneath the perched zone has flowed to the northwest under the BY cribs. Characterization: There is excellent characterization information available for various depths and locations of holes. Shallow push holes within the tank farm surround the release point. There are several deep boreholes next to the tank and eastward to the point of the projected release to groundwater. The depth of the uranium in the vadose zone increases from the source location to the northeast. Contamination near the CCU is thought to represent the most severe vadose zone threat to groundwater from uranium on the Hanford Site. Well 299-E33-45 (C3269), located west of the BX-102 tank but inside the tank farm fence, revealed silt bands in the upper 51.8 m (170 ft) that exhibit uranium, sodium, nitrate, and Tc-99 contamination. Soil pH is elevated from 22.8 to 51.8 m (75 to 170 ft). U-238 was present between 21.9 and 60.3 m (72 and 198 ft), with a peak value of 240 pCi/g at 41.5 m (136 ft). Tc-99 was noted from 36.6 to 70.1 m (120 to 230 ft), with a maximum of about 30 pCi/g (water extraction) at 51.8 m (170 ft).

Site	Description
	Borehole 299-E33-343, located at the northwest corner of the B tank farm, shows the uranium contamination has migrated deeper within the vadose zone, and appears to be near the perched water zone in the CCU. Boreholes 299-E33-18 (A4844) and 299-E33-345, located approximately 38 m (125 ft) east of 299-E33-343, also revealed high uranium contents in the CCU. Recent wells 299-E33-350 and 299-E33-351 had no vadose zone contamination above the perched water. Well 299-E33-360 also had no vadose zone contamination above the perched water zone, indicating the uranium had moved into this deep zone laterally from near the leaking tank. However, the uranium concentrations within the saturated perched water interval are consistent with other existing perched water concentrations.
BC Cribs and Trenches	Waste Stream(s): The BC cribs and trenches were active in 1956-1957. They received waste produced by the bismuth phosphate separations process that was reprocessed at 221-U to recover the uranium from the waste. After the uranium was removed, the Cs-137 and Sr-90 contents of the effluent were reduced by precipitation. A total of 6 cribs and 16 unlined trenches received scavenged tank waste from the uranium recovery process. Trenches 216-B-53A, 216-B-53B, 216-B-54, and 216-B-58 received laboratory and Plutonium Recycle Test Reactor waste from the 300 Area. The scavenged tank waste was high in salt and neutral-to-basic. Cumulative discharge inventory summary (SIM) to the 216-B-17 crib (example) is: - U: 104 kg - Na: 279,059 kg - Ca: 503 kg - K: 1984 kg NO_3: 561,917 kg NO_2: 18,709 kg CO_3: 19,658 kg PO_4: 20,064 kg SO_4: 37,363 kg - F: 6111 kg - Cl: 9944 kg - Sr-90: 82.9 Ci - Tc-99: 9.8 Ci - Cs-137: 119.7 Ci Description: The 216-B-17 crib is constructed of a single wood/concrete block/steel plate liquid dispersion structure measuring $3 \times 3 \times 0.9$ m ($10 \times 10 \times 3$ ft) high that is set below grade on a 1.5 m (5 ft) thick bed of 3-inch gravel. The 216-B-26 trench is an unlined trench 154 m (500 ft) long, 3 m (10 ft) wide, and 2.4 m (8 ft) deep. Earthen dams divide the trench into three sections. Characterization: In 2005, characterization borehole C4191 was drilled through the 216-B-26 trench to groundwater. Two regions of contamination were found: a near-surface region of Cs-137 and Sr-90 associated with the bottom of the trench and a deeper region of Tc-99 and nitrate from 27.4 to 41.1 m (90 to 135 ft) bgs. Maximum near-surface contamination concentrations observed were Cs-137: 529,000 pCi/g, Sr-90: 974,000 pCi/g, Am-241: 41 pCi/g, Pu: 95 pCi/g. Spectral-gamma logging system (SGLS) logging of boreholes installed to support a subsequent excavation-focused treatability test revealed a highly contaminated region (~1 ft thick) at a depth of approximately 3.3 to 3.6 m (11 to 12 ft) with Cs-137 concentrations exceeding 1E+06 pCi/g.

Site	Description
	In 2008, borehole C5923 was drilled to groundwater near the 216-B-17 crib. No near-surface contamination was observed because it was intentionally located outside the footprint of the crib. Peaks of Tc-99 contamination were observed at approximately 15.2, 27.4, 38.1, and 68.6 m (50, 90, 125, and 225 ft) bgs, indicating significant lateral spread, as well as deep mobile contamination. Maximum mobile U contamination observed was ~40 μg/L at approximately 21.3 m (70 ft) bgs.
216-A-3, and -9 Cribs	**216-A-3 Crib** Waste Stream(s): Until November 1967, the site received wastes from the silica-gel regeneration in the 203-A building, the UNH storage pit drainage, and the liquid waste from the 203-A pump house. After November 1967, the site received UNH storage pit drainage, liquid drainage, liquid waste from the 203-A building enclosure sumps, and the heating coil condensate from the P1 through P4 UNH tanks. Between 1967 and 1970, the site discontinued receiving discharge from silica-gel regeneration wastes. The waste included uranium, Cs-137, Sr-90 and Ru-106. The site was taken out of service in April 1981. Description: The unit contains a 10 cm (4 in.) diameter Schedule 10 perforated 304 stainless steel pipe placed horizontally 2.4 m (8 ft) below grade and two 6.1 m (20 ft) lengths of this pipe placed perpendicularly to the first pipe, forming an H pattern in a $6.1 \times 6.1 \times 4.9$ m deep ($20 \times 20 \times 16$ ft deep) excavation. The site has approximately 2.4 m (8 ft) of gravel fill with a volume of 280 m^3 (10,000 ft^3) and has been backfilled. **216-A-9 Crib** Waste Stream(s): Until February 1958, the site received acid fractionator condensate and condenser cooling water from the 202-A building. In February 1958, the crib was judged to have reached its capacity and was taken out of service. In April 1966, the crib was approved for disposal of liquid N Reactor decontamination waste, which continued to October 1966. From October 1966 to August 1969, the site was inactive. In August 1969, the site again received acid fractionator condensate from the 202-A building. The waste was acidic. Description: The site contains a 25 cm (10 in.) diameter Schedule 30 steel perforated pipe, placed horizontally, 2.7 m (9 ft) below grade in a $420 \times 20 \times 13$ ft deep excavation. The site has 1840 m^3 (65,000 ft^3) of gravel fill and has been backfilled. Characterization: Groundwater wells 299-E24-3, E24-4, E24-5, and E24-63 monitor this unit. The data indicate that no breakthrough to groundwater has occurred at this site.
216-A-4 Crib	Waste Stream(s): The site received the laboratory cell drainage from the 202-A building. (The site was reported to have also received 291-A-1 stack drainage.) The 216-A-4 crib also received waste solution from the 216-A-2 waste collection tank, the U cell U-3 and U-4 laboratory waste receiver tanks (located in the acid storage vault), the dissolver off-gas scrubbers, and the 241-A-151 diversion box catch tank. The waste was low in salt and neutral-to-basic. Cumulative discharge inventory summary (SIM) is: • U: 5388 kg • K: 75,974 kg • NO$_3$: 95,373 kg • PO$_4$: 1691 kg • Cs-137: 4.9 Ci

Site	Description
	Description: Excavation was $20 \times 20 \times 26$ ft deep. Two 6.1 m (20 ft) lengths of 15 cm (6 in.) perforated vitrified clay pipe form a horizontal cross pattern and are located 5.5 m (18 ft) below grade. The excavation has 2.4 m (8 ft) of coarse rock fill with a volume of 280 m^3 (10,000 ft^3) and has been backfilled. Characterization: Characterization borehole C4560 was drilled into the crib in 2004. Drilling was suspended due to an unexpected extremely high zone of radiological contamination encountered. Dose rates of 2.2 R at 6.7 m (22 ft) and 2.4 R at 7.0 m (23 ft) were observed. Borehole C5301 (299-E24-23), drilled in late 2006/early 2007, was placed south of the southwest corner of the crib and drilled 109.7 m (360 ft) deep. Cs-137 was the only manmade isotope detected.
216-S-1&2	Waste Stream(s): This unit was used as a subsurface liquid distribution system that received cell drainage and process condensate from the REDOX facility. The waste had a pH of 2.1. The waste was discharged to the cribs in batches, with each batch being approximately 19,000 L (4940 gal.), and an average of 10 batches discharged each day. When the crib was abandoned, it had received approximately 750,000 Ci of mixed fission products. The site received cell drainage from the D-1 receiver tank and process condensate from the D-2 receiver tank in the 202-S building. The waste was acidic. Cumulative discharge inventory summary (SIM) is: • U: 2220 kg • Na: 9778 kg • NO$_3$: 210,879 kg • Sr-90: 959 Ci • Tc-99: 2.6 Ci • Cs-137: 827 Ci Description: The excavation includes two open-bottomed crib boxes, each measuring 3.7×3.7 m (12 ft $\times$ 12 ft), made of timber, and placed in a 3.0 m (10 ft) thick gravel bed in a $27.4 \times 12.2 \times 10.4$ m deep ($90 \times 40 \times 34$ ft deep) excavation. The cribs are connected in series where overflow from the crib box S1 flows into crib box S2 via an underground pipe. Characterization: Core samples from wells drilled in 1956 determined that Cs-137 was contained in the upper strata beneath the cribs, but that Sr-90 had reached groundwater. Core samples from five additional wells drilled near the 216-S-1&2 cribs in 1966 indicated that 90% of the Cs-137 and less than 10% of the Sr-90 was contained in the soil between 4.8 m (16 ft) and 10 m (33 ft) below the cribs. Geophysical logging performed in 1984 indicated that Cs-137 concentrations were highest just below the bottom of the crib and decreased rapidly with depth. There has been little change in the gamma activity profiles since 1958.
216-S-7	Waste Stream(s): From January 12, 1956, to April 12, 1959, the unit received REDOX cell drainage from the D-1 receiver tank, process condensate from the D-2 receiver tank, and condensate from the H-6 condenser in the 202-S building. A buildup of beta activity in this crib prompted the rerouting of H-6 waste material to the underground waste storage tanks. The crib continued to receive waste from D-1 and D-2 vessels until July 1965. The waste was acidic. Cumulative discharge inventory summary (SIM) is: • U: 3411 kg • Na: 11,760 kg • NO$_3$: 432,149 • Sr-90: 1471 Ci

Site	Description
	- Tc-99: 2.5 Ci - Cs-137: 979 Ci - Pu-239/240: 83.7 Ci Description: The unit consists of two wooden structures measuring 4.9 m (16.1 ft) square and 1.6 m (5.2 ft) high. The structures are set 15.2 m (50 ft) apart, center to center, in a 30.5 × 15.2 × 6.7 m deep (100 × 50 × 22 ft deep) excavation. The structures were set in gravel and covered with backfill. The two structures are connected in parallel by a pipe, allowing the flow to be equally distributed to both cribs. Characterization: Characterization borehole C4557 was installed in late 2004 and completed in early 2005. Geophysical logging indicated maximum Cs-137 of two million pCi/g at 7.8 m (25 ft) bgs. No other manmade radionuclides were detected. SGLS characterization of 299-W22-33, located in the crib footprint, indicated 300 pCi/g of Cs-137 at 8.4 m (27.5 ft). No other manmade radionuclides were detected.

A.1.5.2   Site Evaluation

Evaluation of each candidate site with respect to the selection criteria was conducted in technical meetings. A summary of the evaluation findings is documented in Table A.5.

Table A.5. Summary of Candidate Site Evaluation

Site	Do the data indicate that the site is appropriate for testing the technology based on the uranium concentration, chemistry, and physical properties?	Are the size and configuration of the vadose zone contamination suitable for a test location?	Are there administrative, operational, or ALARA issues that would make testing difficult and/or costly or that would significantly delay initiating the test?	Is the site representative of other sites where the technology may be applied for remediation?	Does the site vadose zone contamination pose a near-term risk for the groundwater?

216-U-8/12	• Uranium in preferred range for U-8 and low for U-12 outside of crib
	  - Sediment data available and have concentration contours to guide site selection
	  - Limited set of sediment analytical data available
	• Chemistry may be different than lab tests (acidic disposal)
	• Hanford formation but fines present
	• Sediment samples are available from boreholes through cribs and laterally outside
		• Large inventory
		• Likely have a zone in the 15 to 1000 mg/kg range
		• Uranium in 45 to 70 ft depth interval
		• 3-D data interpretation available
			• Good access and logistics
			• Cs low outside crib in likely target test area
				• Representative of acidic waste	• Yes

216-U-1/2	• Uranium in preferred range for U-1 and low for U-2 outside of crib
	  - Outside crib there are reasonable concentrations, but risk being on the high side of lab tests
	  - May be beneficial to have both high and low concentrations in test zone
	  - Sediment data available and have concentration contours to guide site selection
	  - Limited set of sediment analytical data available
	• Chemistry may be different than lab tests
	• Hanford formation but fines present
	• Sediment samples are available from boreholes through cribs and laterally outside
		• Moderately large inventory
		• Likely have a zone in the 15 to 5000 mg/kg range
		• Uranium in 40 to 60 ft depth interval
		• 3-D data interpretation available
			• Moderately good access and logistics
			  - Limited space between crib exclusion area and the street
			  - Close to other work sites and roadways
			• Cs low outside crib in likely target test area
				May not be representative of acidic waste because Waste Information Data System says neutral/basic; however, likely followed by acidic waste
				• May have some organic constituents that were added in some waste streams, but not all
				• Higher uranium concentration in the crib than anywhere else based on SGLS
				• Has both shallow and deep test opportunities for Hanford and CCU targets
					• Yes

A.16

Site	Do the data indicate that the site is appropriate for testing the technology based on the uranium concentration, chemistry, and physical properties?	Are the size and configuration of the vadose zone contamination suitable for a test location?	Are there administrative, operational, or ALARA issues that would make testing difficult and/or costly or that would significantly delay initiating the test?	Is the site representative of other sites where the technology may be applied for remediation?	Does the site vadose zone contamination pose a near-term risk for the groundwater?
241-BX-102 (UPR-200-E-5)	• Uranium in preferred range - Primary contaminant issue is the CCU (just above water table) - Excellent sediment data available • Chemistry similar to lab tests • Gas treatment to large silt zones (CCU) not yet tested in lab • Hanford formation but fines present – except for portion of contaminants in CCU (silt) • Sediment samples available	• Large inventory • Non-CCU uranium in 120 to 200 ft depth interval – relatively deep test location • Prefer not to test in CCU due to sediment particle size and depth	• Poor access and logistics, especially for Hanford formation test • Marginal access and logistics for CCU test, but deep (different location for CCU test than Hanford formation test) • Multiple contractor interfaces required - Adjacent to tank farms, bad logistics shallow, better logistics for deeper plume but still need to interact with tank farm • Low co-contaminant concentrations	• Representative of basic waste except it contained some inorganic complexing ligands (bismuth phosphate process waste example) - Perceived as worst case scenario	• Yes, previous documented releases
216-B-12	• Uranium in preferred range only in small bands - Limited sediment data available - Limited set of sediment analytical data available • Chemistry similar to lab tests • Hanford formation but fines present • Sediment samples likely available (new borehole being installed)	• Large inventory • Deep contamination • Uncertainty on vadose zone plume compared to large inventory (borehole drilled through crib showed low uranium concentration)	• Good access and logistics	• Representative of basic waste	• Maybe

Site	Do the data indicate that the site is appropriate for testing the technology based on the uranium concentration, chemistry, and physical properties?	Are the size and configuration of the vadose zone contamination suitable for a test location?	Are there administrative, operational, or ALARA issues that would make testing difficult and/or costly or that would significantly delay initiating the test?	Is the site representative of other sites where the technology may be applied for remediation?	Does the site vadose zone contamination pose a near-term risk for the groundwater?

216-A-19	• Uranium in preferred range but may only be so in a small area
	  - Limited sediment data available
	  - Limited set of sediment analytical data available
	• Likely similar chemistry to lab tests except for presence of solids
	• Hanford formation but fines present
	• Archive sediment likely not available
		• Concentration and extent of mobile uranium may be low
		  - Only 31 kg dissolved uranium in inventory per SIM; the remainder is listed as solids
		• Shallow, 20 to 30 ft depth for testing
		• Solid uranium is an interference in testing and not representative of uranium carried into vadose zone in pore water
			• Minimal co-contaminants, so can test directly in waste site (25 x 25 ft)
			• Easy access
			• Good logistics
				• Not representative due to solids and startup waste
				• Waste was startup waste and therefore could be atypical (e.g., high suspended solids component of uranium)
					• Maybe

BC Cribs and Trenches	• Low uranium concentration • Good data set • Tc-99 site candidate	• Low uranium inventory	• Good access and logistics	• Not applicable for uranium • Representative for Tc-99	• No, uranium • Yes, Tc-99
216-A- 4	• Low uranium concentration - C5301 borehole to groundwater, uranium very low, similar to background	• High uranium inventory • Small lateral spread	• Uranium associated with Cs, Am • Borehole in the crib shows area is highly radioactive	No data	No data
216-S-1&2	• Uranium in preferred range only in small bands - Deep data sparse with low-to-medium confidence on data	• Moderate uranium inventory	• Cave-in potential • Cs, Sr hit groundwater	• Very high acid site	No data

Site	Do the data indicate that the site is appropriate for testing the technology based on the uranium concentration, chemistry, and physical properties?	Are the size and configuration of the vadose zone contamination suitable for a test location?	Are there administrative, operational, or ALARA issues that would make testing difficult and/or costly or that would significantly delay initiating the test?	Is the site representative of other sites where the technology may be applied for remediation?	Does the site vadose zone contamination pose a near-term risk for the groundwater?
216-S-7	• Low uranium concentration	• Uranium inventory uncertain	• Uranium associated with Cs, Am • Cave-in potential • Cs, Sr hit groundwater	• Acidic waste	No data
216-A-3 and -9	No data	• Low uranium inventory	No data	No data	No data
216-B-43 through 49 (BY Cribs)	• Low uranium concentration • Thin bands of contamination	• Same waste as BC cribs • Low uranium inventory	No data	• Not applicable for uranium	No data
216-B- 50	• Same location as BY cribs, but different waste stream. Not a uranium site for vadose zone contamination	• Same waste as BC cribs • Low uranium inventory	No data	• Not applicable for uranium	No data

A.1.6   Site Selection

Based on the evaluation presented in the previous section, the U cribs, in particular the 216-U-8 crib, best meet the criteria for a field test site. In summary, this site is best suited for the treatability test because of the favorable uranium concentration/distribution, ability to conduct the test with shallow wells, minimal logistical issues, and the availability of suitable data. In contrast, the BX-102 overfill event site is less favorable because of the depth of contamination, proximity to a tank farm, and uncertainty regarding potential for unintended consequences with the contaminated perched water zone in the CCU near the water table. Other sites evaluated have more significant issues with respect to the selection criteria.

As with all of the sites evaluated, there are still technical uncertainties, and therefore technical risks, with the 216-U-8 site with respect to its suitability for the field test. The primary uncertainties are (1) the uranium contaminant concentration/distribution at the scale of the field test and (2) the effectiveness of the ammonia treatment for the sediment mineralogy and uranium phases present at the site. These uncertainties need to be addressed through the initial field test site characterization whereby the uranium concentration/distribution is assessed and sediments are collected for use in laboratory verification that the ammonia treatment will be effective.

The 216-U-8 crib is the preferred field test site.

A.2 References

DOE. 2008. *Deep Vadose Zone Treatability Test Plan for the Hanford Central Plateau*. DOE/RL-2007-56, Rev. 0, U.S. Department of Energy Richland Operations Office, Richland, Washington.

Szecsody JE, MJ Truex, L Zhong, TC Johnson, NP Qafoku, MD Williams, JW Greenwood, EL Wallin, JD Bargar, and DK Faurie. 2012. "Geochemical and Geophysical Changes During NH_3 Gas Treatment of Vadose Zone Sediments for Uranium Remediation." *Vadose Zone J.* 11(4). doi:10.2136/vzj2011.0158

Szecsody, JE, MJ Truex, L Zhong, MD Williams, and CT Resch. 2010a. *Remediation of Uranium in the Hanford Vadose Zone Using Gas-Transported Reactants: Laboratory-Scale Experiments*. PNNL-18879, Pacific Northwest National Laboratory, Richland, Washington.

Szecsody JE, MJ Truex, L Zhong, NP Qafoku, MD Williams, JP McKinley, CT Resch, JL Phillips, D Faurie, and J Bargar. 2010b. *Remediation of Uranium in the Hanford Vadose Zone Using Ammonia Gas: FY10 Laboratory-Scale Experiments*. PNNL-20004, Pacific Northwest National Laboratory, Richland, Washington.

Truex MJ, JE Szecsody, L Zhong, JN Thomle, and TC Johnson. 2014a. *Scale-Up Information for Gas-Phase Ammonia Treatment of Uranium in the Vadose Zone at the Hanford Site Central Plateau*. PNNL-23699, Pacific Northwest National Laboratory, Richland, Washington.

Truex MJ, JE Szecsody, N Qafoku, and JR Serne. 2014b. *Conceptual Model of Uranium in the Vadose Zone for Acidic and Alkaline Wastes Discharged at the Hanford Site Central Plateau*. PNNL-23666, Pacific Northwest National Laboratory, Richland, Washington.

Zhong L, JE Szecsody, MJ Truex, and MD Williams. 2015. "Ammonia Gas Transport and Reactions in Unsaturated Sediments: Implications for Use as an Amendment to Immobilize Inorganic Contaminants." *Journal of Hazardous Materials* 289:118–129. doi:10.1016/j.jhazmat.2015.02.025

Appendix B

Geologic Logs, Core Photographs, Particle Size Distribution, and Soil Resistivity

Appendix B

Geologic Logs, Core Photographs,
Particle Size Distribution, and Soil Resistivity

Figure B.1 shows the location of the boreholes. The combination borehole geophysical logs for boreholes C9515, C9518, C9519, and C9520 are shown in Figure B.2 to Figure B.5 with selected sample locations shown on the log.
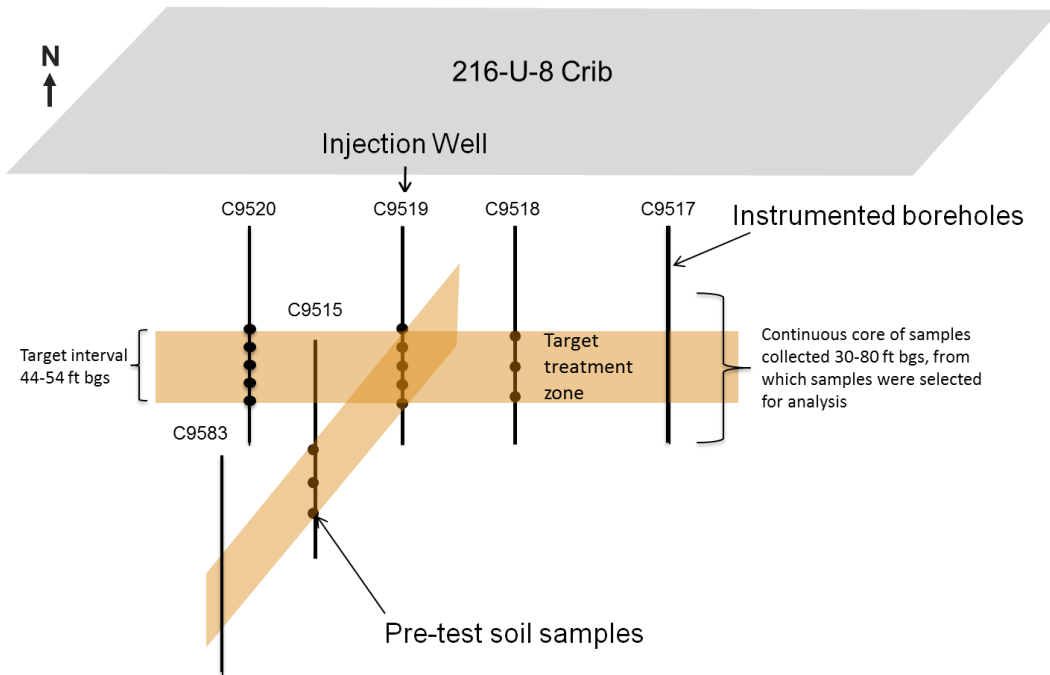
Figure B.1. Borehole Layout and Sampling Interval
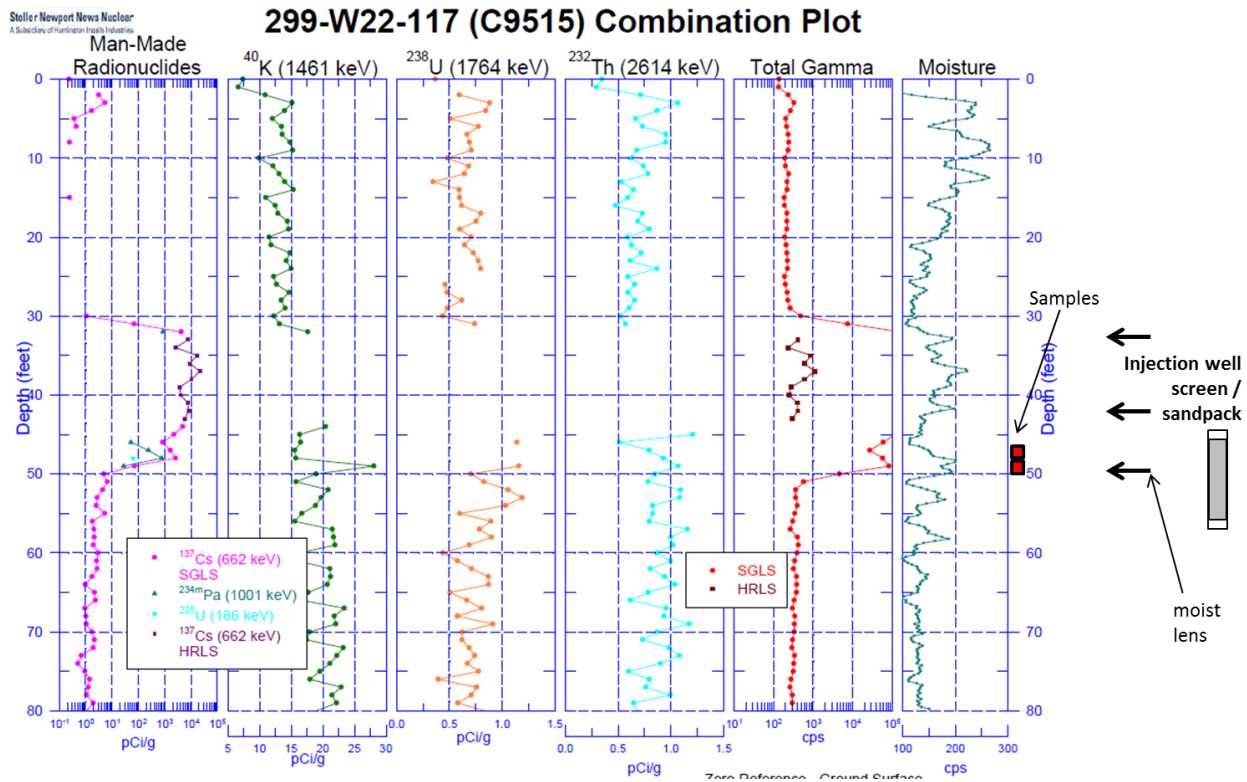
Figure B.2. C9515 Combination Log with Annotations for Samples Selected for Analyses
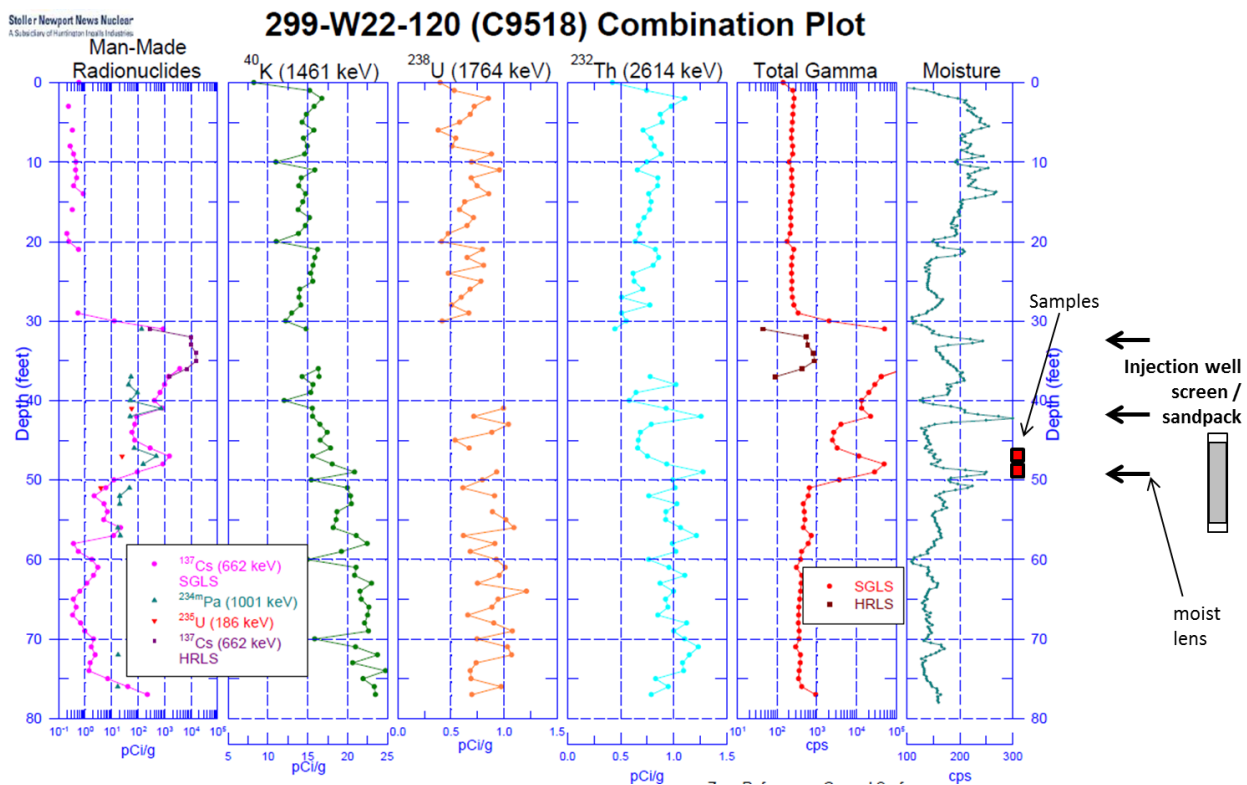
Figure B.3. C9518 Combination Log with Annotations for Samples Selected for Analyses
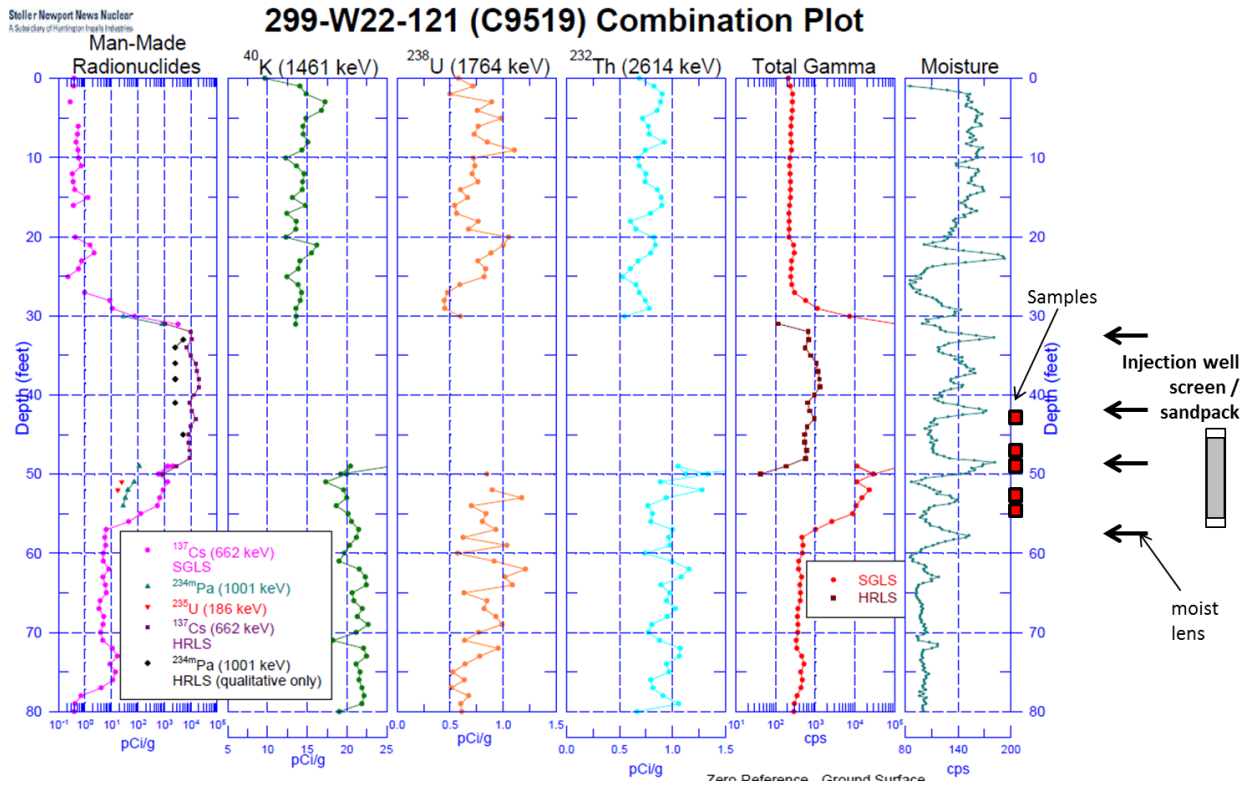
Figure B.4. C9519 Combination Log with Annotations for Samples Selected for Analyses
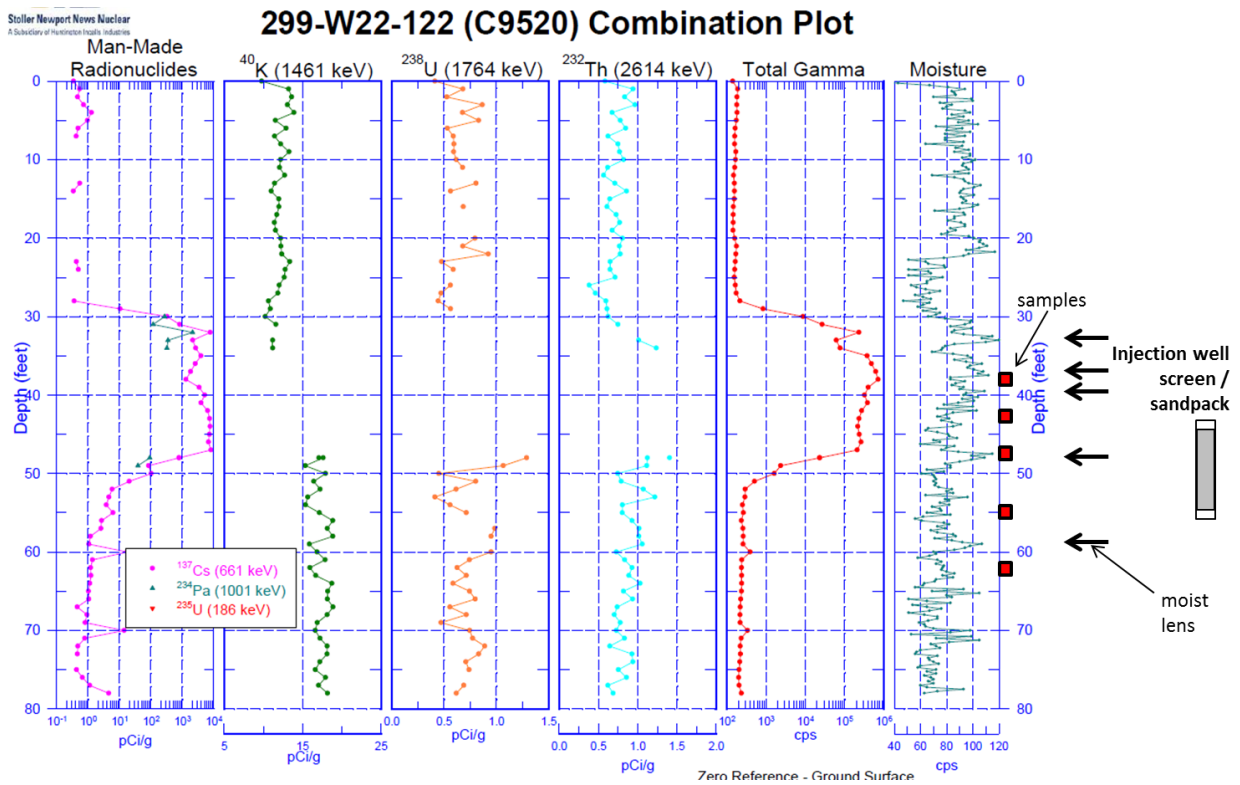
Figure B.5. C9520 Combination Log with Annotations for Samples Selected for Analyses

B.3

B.1 Geologic Logs

Geologic logs were prepared for each of the core sections used for analysis. Geologic logs are provided below for the selected samples from boreholes C9515, C9518, C9519, and C9520.

Pacific Northwest National Laboratory

BOREHOLE SAMPLE LOG

Boring/Well No ____
Location ____

Depth 41.2 - 41.2'   Date 3/31/18   Sheet 1 of 1

Logged by ____ Jeanette Snyder
Reviewed by ____
Lithologic Class. Scheme ____ Folk-Wentworth

Project ____ ARH Inyection

Drilling Contractor ____
Driller ____
Drill Method ____

Procedure ____   Date ____   Rev ____

DEPTH (ft)	SAMPLES		MOIS TURE	GRAPHIC LOG				LITHOLOGIC DESCRIPTION (particle size distribution, sorting, mineralogy, roundness, color, reaction to HCl, maximum grain size, consolidation, structure, etc.)	COMMENTS
	TYPE	ID NUMBER			C	M	S	G		
41.2 - 41.2	C	B3BX60	SM					s – 5% 2, 95% fine to coarse sand. Some consolidated pieces up 2. Well-sorted. Loose. 2.5Y 4/2 (light brownish gray)	6" core - removed from liner, put into tupperware
41.2 - 41.2	C	B3BX69	SM					s – Same as above. ~ 10% 2, 90% fine to medium sand	

C = Core, G = Grab   D = Dry, M = Moist, W = Wet

2015/GW/Remediation Group/Procedures/Sampling/001 (02/06)

Pacific Northwest National Laboratory

BOREHOLE SAMPLE LOG

Boring/Well No ___C3518___
Location ___U-8___

Depth _41.4 - 41.4'_ Date _2/13/17_
Project _N14 injection_

Sheet _1_ of _1_

Logged by ___Winnie Spear___
Reviewed by ___

Lithologic Class. Scheme ___Folk-Wentworth___

Drilling Contractor ___
Driller ___
Drill Method ___

Date ___
Rev ___

Procedure ___

DEPTH (Ft)	TYPE	ID NUMBER	MOIS-TURE	GRAPHIC LOG C 2 1 5 16	LITHOLOGIC DESCRIPTION (particle size distribution, sorting, mineralogy, reaction, color, reaction to HCl, maximum grain size, consolidation, structure, etc.)	COMMENTS
414	C	B-3841	D		S - 5%, Z, 95% fine to coarse sand. Some slightly consolidated pieces w/ Z, otherwise loose. Well-sorted - 2.5 Y 4/2 light brownish gray.	4" core - returned + put into plastic tube
414	C	B-3847	SM		mud5 413 5' UM - slightly muddy sand. 2 - 10% fines 90% fine to medium sand. slightly consolidated pieces w/ Z, the rest loose. Well-sorted - 2.5 Y 5/4 light olive brown.	
414						

BOREHOLE SAMPLE LOG

Pacific Northwest National Laboratory

Field	Value
Boring/Well No	C9519
Location	B2B-4-8 River Stage
Depth	413 – 66.2'
Date	3/13/18
Sheet	1 of 1

Logged by: _Michelle Snyder_   Drilling Contractor: _____
Reviewed by: _____   Driller: _____   Date: _____
Lithologic Class. Scheme: _Folk / Wentworth_   Procedure: _____   Rev: _____   Project: _____   Drill Method: _____

LITHOLOGIC DESCRIPTION
(particle size distribution, sorting, mineralogy, roundness, color, reaction to HCl, maximum grain size, consolidation, structure, etc.)

DEPTH (ft.)	SAMPLES TYPE	ID NUMBER	MOIS TURE	GRAPHIC LOG C 1 2 S G	LITHOLOGIC DESCRIPTION	COMMENTS
41.3–42.0	C	B38V09 (A			(m)S – Slightly mucky Sand. 20% Z, 80% Fine to medium Sand. Well sorted. 2.5Y 4/3 (olive brown).	Samples removed from well break, broke into pieces cohesive
41.6–42.0	C	B38V08	D		(gm)S – Slightly muddy, gravelly sand – 10% Z, 5% G, 85% Fine to coarse Sand. Poorly Sorted. Max G ~ 5mm (sand). 2.5Y 4/3 Light yellowish brown	
46.5–47.0	C	B38V12	D		(m)S – Slightly muddy Sand. 10% Z, 90% v. Fine to medium sand. Z slightly consolidated. Sand loose. 2.5Y 4/2 (light brownish gray).	
51.9–52.4	C	B38V11	D		(gm)S – 10% Z, 5% G, 85% Fine to coarse Sand. Max G ~ 5mm. Poorly Sorted. 2.5Y 4/2 (light brownish gray).	
56.7–66.2	C	B38V10			(gm)S – 20% Z, 5% G, 75% Fine to coarse Sand – Max G ~ 5mm. Poorly Sorted. Slight consolidation of Z. Some caliche visible w/Z. 2.5Y 7/3 (pale yellow).	

C = Core, G = Grab   D = Dry, M = Moist, W = Wet

Pacific Northwest National Laboratory

BOREHOLE SAMPLE LOG

| Boring/Well No | C9520 | Depth | 61.6 - 62.5 | Date 11/05/15 | Sheet 1 of 2 |

Location 216-U-B Crib

Logged by G.V. LAST

Reviewed by _____ Date _____

Lithologic Class. Scheme Folk/Wentworth

Procedure PNNL-ESL-GEOLOGY Rev 1

Drilling Contractor _____
Driller _____
Drill Method _____

Project _____

DEPTH (FT)	SAMPLES TYPE	SAMPLES ID NUMBER	MOIS-TURE	GRAPHIC LOG C 2 S G	LITHOLOGIC DESCRIPTION (particle size distribution, sorting, mineralogy, roundness, color, reaction to HCl, maximum grain size, consolidation, structure, etc.)	COMMENTS
61.5						
.6	C	B32HB2	D		SAND 5% fine to very fine pebble, 90% Coarse-to Medium Sand, 5% Silt. Max gravel = 1cm. Grains is mostly basaltic angular. Sand is 65% quartz, 45% feldspar. Color is 2.5Y5/2 dry. No reaction to 10% HCl. No obvious sedimentary structure, trace. Compacted but not cemented.	Top = 2,000 DPM; Sample knocked out into tray
.7						
.8						
.9						
62.0						
62.1	C	B32HB3	D		SAND 10% fine to very fine Pebble, 82% Very coarse to Medium Sand, 9% silt. Max 0.5cm. quartz. Sample gets a little finer or buff color through. color is 2.5Y5/2 to 5/3 dry. No reaction to 10% HCl. Sand is 65% quartz, 45% feldspar.	Bottom = 2,500 DPM; Top = 2,000 DPM; Core only 80% full; Knocked out into tray
.2						
.3					X		
.4							
62.5						Bottom = 2,000 DPM

C = Core, G = Grab   D = Dry, M = Moist, W = Wet

Pacific Northwest National Laboratory — BOREHOLE SAMPLE LOG

Boring/Well No	C9520
Location	216-U-8 Crib
Depth	54.1 – 55.0
Date	11/05/15
Project	

Logged by GVLAST
Reviewed by
Lithologic Class. Scheme: Folk/Wentworth
Procedure: PNNL-ESL-GEOLOGY Rev 1

Drilling Contractor
Driller
Drill Method
Date

DEPTH (FT)	TYPE	ID NUMBER	MOIS-TURE	C	Z	S	G	LITHOLOGIC DESCRIPTION (particle size distribution, sorting, mineralogy, roundness, color, reaction to HCl, maximum grain size, consolidation, structure, etc.)	COMMENTS
54.0									
54.1	C	B32H90	D			0		SAND. 10% fine Pebble, 85% Very Coarse to Medium Sand, 5% silt (pretty clean)	Top = 1,500 DPM
54.2						0		Max Gravel = 2cm. Gravel mostly basalt, subrounded. Sand is 60% mafic	Core was full, knocked in to tray
54.3						0		40% Felsic. Some stratifications of finer (ie, medium increase sand. Color is	
54.4						0		2.5Y 5/2, dry. No reaction to 10% HCl.	
54.5						G			Bottom = NM
54.6	C	B32H91	D			0		SAND. 5% Very fine pebble, 90% Very coarse to Medium Sand, 5% (max gravel)	Top = 1,500 DPM
.7						0		= 1cm. Gravel mostly basalt. Sand is 40% mafic, 60% felsic. Color is 2.5Y5/2,	Core was previously sampled,
.8						0		dry. No reaction to 10% HCl. No obvious sed structures. Congested.	Designation ~9.5'-9.5'
.9						0			
55.0									Bottom = NM

Pacific Northwest National Laboratory

BOREHOLE SAMPLE LOG

Boring/Well No _C9520_ Depth _46.8 – 47.7_ Date _11/6/15_

Location _216-U-8 Crib_ Sheet _3_ of _2_

Logged by _G.V. Last_

Reviewed by _A.V. Pael_ Date ____

Lithologic Class. Scheme _Folk/Wentworth_ Procedure _PNNL-ESL-GEOLOGY_ Rev _1_

Drilling Contractor ____

Driller ____

Drill Method ____

DEPTH (FT)	SAMPLES		MOIS-TURE	GRAPHIC LOG				LITHOLOGIC DESCRIPTION (particle size distribution, sorting, mineralogy, roundness, color, reaction to HCl, maximum grain size, consolidation, structure, etc.)	COMMENTS
	TYPE	ID NUMBER		C	Z	S	G		
46.7									
.8	C	B32H78	D-M					SAND. Mostly medium to fine sand, 95% -5% silt. Sand is ~35% mafic; 65% felsic. Color is 2.5Y5/2 to 4/3. No reaction to 10% HCl. Moderately compacted.	TOP = 82,000 DPM
.9									Core is full. Dumped into tray.
47.0								No obvious sed. structures.	
.1									
.2									Bottom = 79,000 DPM
47.3	C	B32H79	D-M					SAND. Mostly medium to fine sand, <5% silt. Sand is ~40% mafic; 60% felsic.	TOP = 77,000 DPM
.4								Color is 2.5Y4/2 to 4/3. No reaction to 10% HCl. Moderate compaction.	Core was previously sampled. Originally 9.0'.
.5								No obvious sed. structures.	full. Dumped in tray.
.6									Bottom = 85,000 DPM
47.7									

Pacific Northwest National Laboratory

BOREHOLE SAMPLE LOG

Boring/Well No	C9520
Location	216-U-B CRIB
Depth	42.5 - 43.4
Date	11/6/15
Sheet	4 of 21

Logged by GV LAST

Reviewed by _____

Lithologic Class. Scheme Folk/Wentworth

Procedure PNNL-ESL-Geology   Rev 1

Project _____

Drilling Contractor _____

Driller _____

Date _____

Drill Method _____

DEPTH (FT.)	SAMPLES TYPE	ID NUMBER	MOIS-TURE	GRAPHIC LOG C Z S G	LITHOLOGIC DESCRIPTION (particle size distribution, sorting, mineralogy, roundness, color, reaction to HCl, maximum grain size, consolidation, structure, etc.)	COMMENTS
42.4						
.5	C	B32H7D	M		SAND, 10% Gravel up to 2cm, 85% Sand, 5% Silt. Sand is mostly very coarse to coarse, changing to coarse to med (w/out pebbles). Gravel is 5% basalt, 5% quartzite. Sand is 50% mafic, 50% felsic. Fabric is 5L5/3 to 4/3, mod. No reaction to 10% HCl. Transitions at about 42.7' (graded?).	Top = 82,000 DPM
.6						Core is full. Pumped into tray.
.7						
.8						
42.9						
43.0	C	B32H71	M		SAND <5% Pebble. 90% Sand <5% Silt. Sand is mostly Very coarse to medium. 45% mafic, 55% felsic. Pebbles are 50% basalt, 50% quartzite (w/lithic. Color is 5L5/2 to 4/3. No reaction to 10% HCl. No obvious soil structures. Compact. Originally B33 full.	Bottom = 70,000 DPM Top = 70,000 DPM Previously sampled.
.1						
.2						
.3						
.4						Bottom = 85,000 DPM

C = Core, G = Grab   D = Dry, M = Moist, W = Wet

2015/GVL/GeosciencesGroup/Procedures/SampleLog/001 (02/06)

B.11

Pacific Northwest National Laboratory

BOREHOLE SAMPLE LOG

Boring/Well No **C9520**
Location **216-U-B CRB**
Depth **37.6 - 38.5**
Date **11/1/2015**

Project

Logged by **G.V.LAST**

Reviewed by

Lithologic Class. Scheme **Folk/Wentworth**

Procedure **TANN-ISL-GEOLOG** Rev **1**

Drilling Contractor

Driller

Drill Method

Date

DEPTH (FT)	SAMPLES		MOIS-TURE	GRAPHIC LOG				LITHOLOGIC DESCRIPTION (particle size distribution, sorting, mineralogy, roundness, color, reaction to HCl, maximum grain size, consolidation, structure, etc.)	COMMENTS
	TYPE	ID NUMBER		C	Z	S	G		
37.5									
.6	C	B32H62	M-W					SILTY SAND, Mostly Medium to Fine sand at top. A silty layer ~1.5cm thick near	TOP = 200,000 DPM
.7								top of core. Bottom 80-90% is coarse to medium sand, very little silt. Color is	Full sample.
.8								2.5Y 4/2. Reaction to HCl is None. The silty layer is ~20% silt, 80% Fine to very	
.9								Fine sand, color is 2.5Y 4/3 moist. No reaction to 10% HCl. Some stratification	
38.0									Bottom = 175×100×10 DPM
38.1	C	B32H63	M-W					SAND, Mostly coarse to medium sand, some silt (~5-10%). Sand is ~90% fine.	TOP = 150,000 DPM
.2								50% coarse. One layer of fine to very fine sand (silt) about 2cm thick. Coarse to Med	Previously sampled not
.3								sand composite is 2.5Y 4/2 moist. No reaction to 10% HCl. Stratified. Fine layer	full.
.4								very compacted.	
.5									Bottom = 125,000 DPM

C = Core, G = Grab   D = Dry, M = Moist, W = Wet

2015/GVL/GeosciencesGroup/Procedures/SampleLog/001 [02/06]

B.12

Pacific Northwest National Laboratory

BOREHOLE SAMPLE LOG

Boring/Well No __C9520__

Location __216-U-8 CRD__

Depth __29.8 – 31.7__   Date __11/2/2015__

Project ____

Logged by __G.V. LAST__

Reviewed by ____

Lithologic Class. Scheme __Folk/Wentworth__

Procedure __PNNL-EL-GEOLOGY__ Rev __1__   Date ____

Drilling Contractor ____

Driller ____

Drill Method ____

DEPTH (FT)	SAMPLES		MOIS-TURE	GRAPHIC LOG				LITHOLOGIC DESCRIPTION (particle size distribution, sorting, mineralogy, roundness, color, reaction to HCl, maximum grain size, consolidation, structure, etc.)	COMMENTS
	TYPE	ID NUMBER		C	Z	S	G		
29.7									
.8	C	B32H48	M					SLOUGH, SANDY GRAVEL. GRAVEL up to 3 cm.	TOP = 2,500 DPM
.9									NOT TRAP, SLOUGH?
.0								SANDY GRAVEL. 60% Gravel, 40% Sand, trace of Silt. Gravel up to 4 cm, 70% basaltic. Sand mostly coarse to Med. Color is 2.5Y 3/2. Weak reaction.	TOP = 4,000 DPM
.1								20% felsic, subrounded.	
30.2	C	B32H49	M-W					SANDY GRAVEL. 50% Gravel up to 3 cm, 45% Sand, mostly coarse to medium. Color is 2.5Y 4/2. Weak Rx to w/ HCl. Gravel is 60% basalt, subround. Sand is 50% mafic, 50% felsic. Stratified, weakly compacted.	TOP = 2,500 DPM
.3									
.4									
.5									
.6									
30.7	C	B32H50	M-W					Coarse to Medium SAND. Grades upward to Medium to Fine Sand. Color 2.5Y 4/2, weak Rx. SAND, mostly coarse to Medium. Stratified, one 1.5 cm thick silty very fine sand layer. Another less of silty very fine sand, mafic-chunk near top. Fine layer, coarse sand 2.5Y 3/2 wet, coarse to med. sand is 2.5Y 4/2. Weak reaction to 10% HCl.	Bottom = 20,000 DPM. TOP = 22,000 DPM
.8									
.9									
31.0									
.1									
31.2	C	B32H51						SAND. Mostly Coarse to Medium Sand, some silty very fine inclusions. Stratified, one thin fine sand layer ~ 1 cm thick. Sand is 50% felsic, 50% mafic. Color is 2.5Y 3/2. No reaction to 10% HCl.	Bottom = 40,000 DPM. TOP = 45,000 DPM. Not full - dumped out in bottom - loose
.3									
.4									
.5									
.6									Bottom = 40,000 DPM
.7									

B.13

Pacific Northwest National Laboratory

BOREHOLE SAMPLE LOG

Boring/Well No __C9520__   Depth __32.4 - 34.4__   Date __11/24/15__

Location __216-U-8 CRIB__   Sheet __7__ of __21__

Logged by __G.V. LAST__

Reviewed by ____

Lithologic Class. Scheme __Folk/Wentworth__

Procedure __PNNL-ESL-GEOLOG__ Rev __1__

Drilling Contractor ____

Driller ____

Drill Method ____

Project ____

Date ____

DEPTH (FT)	SAMPLES		MOIS-TURE	GRAPHIC LOG C Z S G	LITHOLOGIC DESCRIPTION (particle size distribution, sorting, mineralogy, roundness, color, reaction to HCl, maximum grain size, consolidation, structure, etc.)	COMMENTS
	TYPE	ID NUMBER				
32.4						
.5	C	B32H52	D		GRAVELLY SAND. 30% Gravel up to 3cm-broken basalt. Sand is mostly coarse to medium. Sand is 50 to 60% mafic to 50% felsic. Color is 2.5Y 5/2, dry. None to weak reaction to 10% HCl.	TOP = 45,000 DPM
.6						Description at top only. Could be slough?
.7						
.8						Not removed from liner
.9						BOTTOM = 175,000 DPM
33.0	C	B32H53	M-W		SAND. mostly coarse to medium. More moist, no reaction. Color is 2.5Y 6/2.	TOP = 150,000 DPM
.1					SAND. Mostly medium sand. Color is 2.5Y 4/2 to 5/2. Sand is 50% mafic, 50% felsic. No reaction to 10% HCl.	
.2						Not removed from liner
.3					Fine to very fine sand. Color is 2.5Y 5/2 (mottled). Some lenses of gray silty w/ sand.	Moisture sample of fines.
.4					No reaction to 10% HCl. Transition is uneven, still near inside core sleeve. W/ structures.	Bottom = 25,000 DPM
33.5	C	B32H54	M-W		SILTY SAND. 60% very fine sand, 40% silty. Color is 2.5Y 6/4 mottled. One silty clast (2.5Y 5/2). Some vertical structures (clastic dike like). Weak to no reaction to 10% HCl. Silty clast had weak to strong reaction.	TOP = 20,000 DPM
.6						
.7						
.8					SAND. mostly coarse to medium sand 50% mafic, 50% felsic. Transition is not seen - inside liner. Color is 2.5Y 5/2 to 5/4. Weak reaction to 10% HCl.	Not removed from liner. Bottom = 20,000 DPM
.9						TOP = 25,000 DPM
34.0	C	B32H55	M-W		SAND. mostly coarse to medium. 60% mafic, 40% felsic. Color is 2.5Y 6/2. Coarsens downward to very coarse to medium sand w/ some very fine pebble to 1/2 cm. Sand is 70% mafic, 30% felsic. Color is 2.5Y 5/2. No reaction to 10% HCl. Transition.	Not full. Not removed from liner.
.1						
.2						
.3						Bottom = 20,000 DPM
.4						

C = Core, G = Grab   D = Dry, M = Moist, W = Wet

Descriptions based on top to bottom of cores only.

BOREHOLE SAMPLE LOG

Pacific Northwest National Laboratory

Boring/Well No C9520

Location 216-U-8 CRIB

Depth 34.4 - 36.4   Date 12/1/15

Sheet 8 of 21

Logged by G.V. LAST

Reviewed by _____

Lithologic Class. Scheme Folk/Wentworth

Drilling Contractor _____
Driller _____

Date _____

Project _____

Procedure PNNL-EG-GEOLOGY   Rev 1

Drill Method _____

DEPTH (FT)	SAMPLES TYPE	SAMPLES ID NUMBER	MOISTURE	GRAPHIC LOG C Z S G	LITHOLOGIC DESCRIPTION (particle size distribution, sorting, mineralogy, roundness, color, reaction to HCl, maximum grain size, consolidation, structure, etc.)	COMMENTS
34.4						
.5	C	B32H56	D-M		GRAVELLY SAND. Mostly medium Sand. Gravel up to 2.5cm. Gravel clasts are subround where unbroken, mostly basaltic. Sand is mostly ~65% mafic, ~35% felsic.	TOP = 37,500 DPM
.6					Color is 2.5Y6/2. Fairly compacted. Sand seems to be coarser at bottom.	Not full. Not removed from liner.
.7						
.8					No reaction to 10% HCl	
.9						Bottom = 68,000 DPM
35.0	C	B32H57	M-W		GRAVELLY SAND. 5% Gravel, 95% Sand. Gravel is mostly very fine pebble.	TOP = 85,000 DPM
.1					Slightly Sand is mostly coarse to medium. Color is 2.5Y5/2. No reaction.	Not removed from liner.
.2						
.3					SAND. Mostly Medium to fine sand. Color is 2.5Y5/4. No reaction.	Moisture Sample from fines
.4						Bottom = 150,000 DPM
35.5	C	B32H58	M-W		SAND, mostly fine sand, some med to coarse along core edges. Color is 2.5Y5/4.	TOP = 175,000 DPM
.6					Some silt (minor). Sand is mostly felsic (75%), some (25%) mafic. No reaction to 10% HCl.	Not removed from liner.
.7						
.8					SAND. Mostly coarse to Medium Sand. 60% mafic, 40% felsic. 2.5Y5/2. No	Bottom = 85,000 DPM
.9					reaction. Contact approx. not observed - still in liner.	
36.0		B32H59	M-W		SAND. Mostly Coarse to Medium Sand. 50% mafic, 50% felsic. Color is 2.5Y5/2.	TOP = 90,000 DPM
.1					Sand gets finer at the bottom => Medium Sand, mace felsic (60%). Color is	Not full. Not removed from liner.
.2					2.5Y5/4. No reaction to 10% HCl.	
.3						
.4						Bottom = 95,000 DPM
						Descriptions based on top and bottom of core only.

C = Core, G = Grab   D = Dry, M = Moist, W = Wet

2015/GVL/GeosciencesGroup/Procedures/SampleLog/001 (02/06)

BOREHOLE SAMPLE LOG

Pacific Northwest National Laboratory

Boring/Well No **C9520** Depth **36.5 - 40.0** Date **12/8/15** Sheet **9** of **21**

Location **216-U-8 CRIB** Project _____

Logged by **G.V. LAST**

Reviewed by _____

Lithologic Class. Scheme **Folk/Wentworth**

Drilling Contractor _____

Driller _____ Date _____

Procedure **PNNL-ESL-Geolog** Rev **1**

Drill Method _____

DEPTH (FT)	\[SAMPLES\] TYPE	\[SAMPLES\] ID NUMBER	MOIS-TURE	GRAPHIC LOG	LITHOLOGIC DESCRIPTION (particle size distribution, sorting, mineralogy, roundness, color, reaction to HCl, maximum grain size, consolidation, structure, etc.)	COMMENTS
36.5						
.6	C	B32H60	W-M		SAND. Mostly medium sand. Color is 2.5Y4/4 to 4/2. Sand is 60% felsic, 40% mafic. No reaction 16% HCl.	Top = 150,000 DPM
.7						Not removed from liner. Inspection of top and bottom only
.8						
.9						Bottom = 175,000 DPM
37.0						
.1	C	B32H64	M-M		SAND. Mostly medium sand. Mostly felsic (60-70%). Color is 2.5Y4/4 to 4/2.	Top = 200,000 DPM
.2					1 pebble, finer at bottom with some coarse sand intermixed. No reaction to 16% HCl.	Not removed from liner
.3						
.4						
.5						Bottom = 200,000
39.1	C	B32H66				Top half empty. Dumped into tray. Loose.
.2						
.3						
.4			M		SAND. Mostly coarse to medium sand. Some very coarse sand and a few fine to very fine pebbles. Color is 2.5Y4/2. No reaction to HCl.	Tray = 20,000
.5						
39.6	C	B32H67	M		SAND. Mostly coarse to medium sand. Color is 2.5Y5/2. Sand is mostly felsic (60-70%), 30-40% mafic. No reaction to 16% HCl.	Not full. Dumped in bottom. Loose.
.7						
.8						Tray = 125,000
.9						
40.0						

C = Core, G = Grab   D = Dry, M = Moist, W = Wet   2015/GVL/GeoscienceGroup/Procedures/SampleLog/001 (02/06)

B.16

Pacific Northwest National Laboratory

BOREHOLE SAMPLE LOG

Boring/Well No. C9520
Location 216-U-8 CRIB
Depth 41.4 – 45.2
Date 12/9/15

Logged by G.V. LAST
Reviewed by
Lithologic Class. Scheme Folk/Wentworth

Drilling Contractor
Driller
Project
Procedure PNNL-TECH-GEOLOGY Rev 1

Date: by VLast

DEPTH (FT)	SAMPLES		MOIS-TURE	GRAPHIC LOG				LITHOLOGIC DESCRIPTION (particle size distribution, sorting, mineralogy, roundness, color, reaction to HCl, maximum grain size, consolidation, structure, etc.)	COMMENTS
	TYPE	ID NUMBER		C	2	S	G		
41.4									
.5	C	B32H68	m					SAND. Mostly medium, well sorted. Mostly felsic (70%?), 30% mafic.	TOP = 150,000 dpm
.6								coarser at bottom, going to coarse to medium sand. Color is 2.5Y 5/2 to 5/4.	Liner is full, some
.7								No reaction to 10% HCl. No obvious sed. structures. Can not observe transitions.	teflon tape in sample.
.8									Not removed from liner.
.9								contact.	Bottom = 150,000 dpm
42.0	C	B32H69	m-d					SAND. Mostly coarse to medium, some very coarse, mostly felsic (60%, 40% mafic).	TOP = 150,000 dpm
.1								Color is 2.5Y 5/2 to 5/4. Gets even coarser at bottom, going to very coarse sand	Not removed from liner.
.2								with occasional very fine to fine pebbles, some medium to coarse sand. No reaction	Most sample torn from top &
.3								to 10% HCl. No obvious sed. structures – can not see transition contact.	bottom.
42.4									Bottom = 110,000 dpm
43.8	C	B32H72	m					SAND. Mostly medium sand, some fine to coarse sand. Mostly felsic (70%, 30% mafic).	TOP = 150,000 dpm
.9								Some vertical sed structures in bottom (an artifact of drilling?), one coarse to	Liner is full. Some white
.0								medium ped in bottom. Color 2.5Y 5/2 to 5/4. Less fines in bottom. No	teflon tape. Not removed
.1								reaction to 10% HCl.	from liner.
44.2									Bottom = 150,000 dpm
.3	C	B32H73	m					SAND. Mostly medium, some fine sand and silt. Some vertical structure same	TOP = 160,000 dpm
.4								as above. One fine ped (very fine sand & silt?). Color is 2.5Y 6/2. Gets coarser and	Not removed from liner.
.5								more poorly sorted at bottom – going to mostly coarse sand, some very coarse and	
.6								occasional very fine pebbles. Some fines. No reaction to 10% HCl.	
44.7									Bottom = 130,000 dpm
.8	C	B32H74	m					SAND. Mostly coarse to fine sand, with occasional pebbles up to 1cm. Color is 2.5Y 6/2.	TOP = 125,000 dpm
.9								Not well sorted. Gets a little coarser (less fine sand) at bottom. No reaction to HCl.	Not removed from liner.
.3								No pebble at bottom and more very coarse sand. No sed. structure observed.	
.1								observed.	
45.2									Bottom = 250,000 dpm

C = Core, G = Grab   D = Dry, M = Moist, W = Wet   2015/GVL/GeosciencesGroup/Procedures/Samplelog/001 (02/06)

B.17

Pacific Northwest National Laboratory

BOREHOLE SAMPLE LOG

Boring/Well No **C9520**
Location **216-U-8 crib**
Depth **45.2 - 48.9**   Date **12/9/15**
Sheet **1 of 2**

Logged by **GV Last**
Reviewed by ____
Lithologic Class. Scheme **Folk/Wentworth**
Procedure **PNNL-ESL-Geology** Rev **1**

Drilling Contractor ____   Date ____
Driller ____
Drill Method ____

DEPTH (FT)	TYPE	ID NUMBER	MOIS-TURE	GRAPHIC LOG (C Z S G)	LITHOLOGIC DESCRIPTION (particle size distribution, sorting, mineralogy, roundness, color, reaction to HCl, maximum grain size, consolidation, structure, etc.)	COMMENTS
45.2						
.3	C	B32H75	M		SAND. Mostly coarse to medium. Some very coarse and fine sand. Color is 2.5Y7/2. Mostly (75%) felsic, 25% mafic. No reaction to 10% HCl.	TOP = 200,000 dpm
.4						Not removed from liner.
.5						Not Full.
.6						
45.7						Bottom = 125,000 dpm
.8	C	B32H76	M		SAND. Poorly sorted. Coarse sand with some silt (loess?). Bottom of core is well sorted coarse to medium sand. 50% felsic, 50% mafic. Color 2.5Y 5/2 to 6/2. No reaction to 10% HCl.	TOP = 150,000 dpm
.9						Full but highly compacted.
.0						Not removed from liner
.1						
46.2						Bottom = 350,000 dpm
.3	C	B32H77	M		SAND. Mostly medium sand, fairly well sorted. 50% mafic, 50% felsic. Not very compacted - loose. Color is 2.5Y 5/2. No reaction to 10% HCl. Might get a little finer - less coarse sand - at bottom.	TOP = 350,000 dpm
.9						Not removed from liner.
.5						
.6						
46.7						Bottom = 100,000 dpm
47.7						
.0	C	B32H80	M			Not Full.
.1						Removed from liner.
.2						TRAY = 85,000 dpm
.3					SAND. Coarse to fine sand. Color is 2.5Y5/2. Weak to no reaction to 10% HCl. Some calic nodules. Loose.	
48.4						
.5	C	B32H81	M		SAND. Coarse to fine sand at top, very little - fell out at liner. Transitions to fine sand with some mottling, harder, some silt? No reaction at top.	TOP = 74,000 dpm
.6						
.7						
.8					Fine to very fine sand at bottom. Color is 2.5Y4/4. Weak reaction to 10% HCl.	
48.9						Bottom = 17,000 dpm

C = Core, G = Grab   D = Dry, M = Moist, W = Wet

2015/GVL/GeoscienceGroup/Procedures/SampleLog/001 (02/06)

Pacific Northwest National Laboratory

BOREHOLE SAMPLE LOG

Boring/Well No __C9520__ Depth __48.9 - 52.2__ Date __12/9/15__

Location __216-U-8 CRIB__ Project _____

Logged by __G V LAST__ Drilling Contractor _____

Reviewed by _____ Driller _____

Lithologic Class. Scheme __FOLK/WENTWORTH__ Procedure __PNNL-ESL-GEOLOG Rev)__ Drill Method _____

G V Last Date _____

DEPTH (FT)	SAMPLES TYPE	ID NUMBER	MOIS-TURE	GRAPHIC LOG	LITHOLOGIC DESCRIPTION (particle size distribution, sorting, mineralogy, roundness, color, reaction to HCl, maximum grain size, consolidation, structure, etc.)	COMMENTS
48.9						
.0	C	B32H82	M		SAND. Mostly Fine to Very Fine Sand. Mostly felsic. Color is 2.5Y6/4. Gets coarser at bottom — goes to mostly medium Sand, well sorted. Color goes to 2.5Y6/2. No reaction to 10% HCl.	TOP = 12,500 dpm
.1						Not removed from liner.
.2						
.3						
49.4						
.5	C	B32H83	M		SAND. Mostly medium sand, well sorted. 50% felsic, 50% mafic. Some coarse to very fine sand. Color is 2.5Y6/2, to 6/4. Might be a little darker at the bottom. Top has a weak reaction to 10% HCl. Bottom has no reaction.	Bottom = 12,500 dpm
.6						TOP = 10,000 dpm
.7						Sample mostly say #84 — 50+ (should be 49.97)
.8						Not removed from liner
.9						Bottom = 8,500 dpm
50.1						
50.8	C	B32H84	M-D		SAND. Top is poorly sorted, could be slough. Sand ranges from Very coarse to very fine — mostly fine to medium. Color is 25Y7/2. Dry. Bottom is Coarse to Very Coarse Sand. Color is 2.5Y6/2. Some very fine pebble up to 1 cm. No sed structures or contacts observed.	TOP = 3,000 dpm Top could be slough. Not removed from liner.
.9						
.0						
.1						Bottom = < 1,000 dpm
51.2	C	B32H85	D		SLIGHTLY GRAVELLY SAND. 10% Gravel—mostly fine to Very fine pebble. Sand is mostly coarse. Color is 2.5Y7/2. Gravel is 50% mafic, 50% felsic. Sand is 70% felsic, 30% mafic. No reaction to 10% HCl.	TOP = < 1,000 dpm Not removed from liner
.3						
.4						
.5						
.6						
51.7	C	B32H86	M-D		SLIGHTLY GRAVELLY SAND. 10% Fine to Very Fine Pebble. Gravel is 70% mafic, 30% felsic. Sand is mostly coarse. 75% felsic, 25% mafic. Very loose. Bottom is SAND. Mostly coarse to medium. Sand is 10% felsic, 30% mafic. Color is 2.5Y 6/2. Weak to no reaction to HCl. No obvious sed structures or contacts observed.	Bottom = < 1,000 dpm TOP = < 1,000 dpm
.8						
.9						
.0						
.1						Bottom = 1500 dpm
52.1						

C = Core, G = Grab   D = Dry, M = Moist, W = Wet

B.19

BOREHOLE SAMPLE LOG

Pacific Northwest National Laboratory

Field	Value
Boring/Well No	C9520
Depth	52.2 – 56.2
Date	12/9/15
Sheet	13 of 21
Location	216-U-8CRIB
Project	
Logged by	G.V. Last
Reviewed by	
Lithologic Class. Scheme	Folk/Wentworth
Procedure	PNNL-ESL-Geology Rev 1
Date	
Drilling Contractor	
Driller	
Drill Method	

DEPTH (FT)	SAMPLES TYPE	ID NUMBER	MOIS-TURE	GRAPHIC LOG	LITHOLOGIC DESCRIPTION (particle size distribution, sorting, mineralogy, roundness, color, reaction to HCl, maximum grain size, consolidation, structure, etc.)	COMMENTS
52.2 .3 .4 .5 .6 .7	C	B32487	M		SAND. Mostly coarse to medium. 75% felsic, 30% mafic. Fairly well sorted. Color is 2.5Y 6/2. Sand get finer at bottom - going to medium sand - less coarse sand. Weak to no reaction to 10% HCl.	TOP = 1500 dpm. Depths are off - says 52.2 - 52.2 but should be 52.7? Not full. Not removed from liner. Bottom = 1750 dpm
53.0 .1 .2 .3 .4	C	B32488	M		SAND. Poorly sorted - very coarse to fine sand. Color is 2.5Y 6/2 to 6/4. Could be slough. Sand at bottom is mostly fine, some medium, mostly felsic. Color is 2.5Y 6/4. Weak to strong reaction to 10% HCl. Contact not observed.	TOP = 2000 dpm. Full, compacted - top could be slough. Not removed from liner. Bottom = 3000 dpm
53.5 .6 .7 .8 .9 54.0	C	B32489	M		SAND. Mostly medium to fine sand. Mostly felsic (80%?). Color is 2.5Y 6/2-6/4. Sand is coarser at bottom - going to very coarse to medium sand. Contact not observed. Color is 2.5Y 7/2 to 6/2. Top sands have weak to strong reaction. Bottom sands have weak to no reaction.	TOP = 3000 dpm. Not removed from liner. Bottom = 3000 dpm
55.3 .4 .5 .6	C	B32492	M-D		SAND. Poorly sorted, mostly coarse to fine. Mostly felsic. Color is 2.5Y 7/2. Some very fine pebble, up to 0.5cm. Sand is mostly felsic. Weak to strong reaction to 10% HCl.	TOP = 1000 dpm. Full but top could be slough. Not removed from liner.
55.7 .8 .9 .0 .1 56.2	C	B32493	M-D		SAND. Mostly coarse to fine sand, poorly sorted. Some very coarse sand and very fine pebble. Color is 2.5Y 7/2. Very coarse sand to fine pebble is mostly mafic. Top has more fine sand and weak reaction to HCl. Bottom is better sorted (clean) and has weak to no reaction to 10% HCl.	Bottom = <1000 dpm. TOP = 1000 dpm. Not removed from liner. Bottom = <1000 dpm

C = Core, G = Grab   D = Dry, M = Moist, W = Wet

2015/GVL/GeosciencesGroup/Procedures/Samplelog/001 (02/06)

Pacific Northwest National Laboratory

BOREHOLE SAMPLE LOG

Boring/Well No C9520
Depth 56.2 – 58.9
Date 12/10/15

Location 216-U-8 CRIB
Project

Logged by G.V. LAST
Reviewed by

Drilling Contractor
Driller
Drill Method

Lithologic Class. Scheme Folk/Wentworth
Procedure PNNL-ESL-GEOLOGY Rev 1
Date

DEPTH (FT)	SAMPLES TYPE	ID NUMBER	MOIS-TURE	GRAPHIC LOG C Z S G	LITHOLOGIC DESCRIPTION (particle size distribution, sorting, mineralogy, roundness, color, reaction to HCl, maximum grain size, consolidation, structure, etc.)	COMMENTS
56.2						
.3	C	B32H94	M-D		SAND. Mostly Medium to coarse sand. Loose. Some very coarse sand. Sand is mostly felsic - very coarse sand has more mafic/basalt. Color is 2.5Y 7/2.	TOP = <1000 dpm
.4						Not removed from liner
.5					Gets a little finer at bottom - less to no very coarse sand - mostly coarse to	
.6					medium. Can not observe contact. Weak to no reaction to 10% HCl.	
56.7						Bottom = <1000 dpm
.8	C	B32H95	M-D		SAND. Mostly coarse to medium sand. Mostly felsic (7%). Color is 2.5Y 7/2.	TOP = <1000 dpm
.9					Gets finer at bottom - going mostly medium sand, less felsic (60%). Color the	Not full. Not removed
.0					same. Can not see contact. Weak to no reaction to 10% HCl.	from liner.
.1						
57.2						Bottom = 1000 dpm
.3						
57.4						
.5	C	B32H96	M-D		SAND. Mostly medium to fine sand. Color is 2.5Y 7/2. Mostly felsic sands.	TOP = 1500 dpm
.6					might get a little coarser at bottom, more coarse sand and some very coarse.	Full, but could be slough
.7					Weak reaction to 10% HCl.	in top. Not removed from
.8						liner.
57.9						Bottom = 2500 dpm
.0	C	B32H97	M		SAND. Mostly medium sand. Ranges up to very coarse sand. Color is 2.5Y 6/2. Some	TOP = 3,000 dpm
.1					vertical structure, finer sand darker, vis. coarser and lighter colored - no clay skins.	Not removed from liner.
.2					(drilling artifact?). Seds are more moist and darker - perhaps finer - no very coarse sand.	
.3					Color is 2.5Y 6/4. Weak reaction to 10% HCl.	
58.4						Bottom = 2,500 dpm
.5	C	B32H98	M		SAND. Mostly medium to fine. Color is 2.5Y 6/4. More moist - gets a little coarser	TOP 3000 dpm
.6					less fine sand - color get grayer (2.5Y 6/2). Weak to no reaction to 10% HCl.	Not removed from liner.
.7						
.8						
58.9						Bottom = 2500 dpm

C = Core, G = Grab
D = Dry, M = Moist, W = Wet

BOREHOLE SAMPLE LOG

Pacific Northwest National Laboratory

Boring/Well No __C9520__   Depth __589 – 63.6__   Date __12/10/15__

Location __216-U-8 CRIB__   Project _____   Sheet __15__ of __(2)__

Logged by __G.V. LAST__

Reviewed by _____

Lithologic Class. Scheme __Folk/Wentworth__   Procedure __PNNL-EY-GEOLOG__ Rev __1__

Drilling Contractor _____
Driller _____
Drill Method _____

DEPTH (FT)	SAMPLES TYPE	ID NUMBER	MOIS-TURE	GRAPHIC LOG C Z S G	LITHOLOGIC DESCRIPTION (particle size distribution, sorting, mineralogy, roundness, color, reaction to HCl, maximum grain size, consolidation, structure, etc.)	COMMENTS
58.9						
.0	C	B32H99	M-W		SAND, mostly medium sand, 65% felsic, 35% mafic. Color is 2.5Y4/4, gets a little coarser, more coarse sand. Some silty peds near bottom – could be an artifact of drilling? Weak reaction to 10% HCl.	Top = 4000 dpm
.1						Not removed from liner.
.2						
.3						
57.4						Bottom = 4500 dpm
60.6	C	B32H80	M-D		SAND. Poorly sorted very coarse to fine sand – some silt? Color is 2.5Y7/2, gets a little coarser – mostly very coarse to medium. Coarser sand is more mafic (50%?) Top of sample is more reactive – weak to strong – to 10% HCl. Bottom has weak to no reaction.	Top = 4500 dpm
.7						Full but top could be
.8						sloughi. Not removed from liner.
.9						
61.0						Bottom = 3500 dpm
.1	C	B32H81	M		SAND, mostly coarse, ranges from fine to very coarse. 60% felsic, 40% mafic. Some very fine to fine pebbles up to 0.5 cm. Color is 2.5Y6/2, more moist at bottom. Weak to no reaction to 10% HCl.	Top = 4500 dpm
.2						Not removed from liner.
.3						
.4						
.5						Bottom = 3500 dpm
62.7	C	B32H84	M		SAND. Poorly sorted very coarse to fine. Color is 2.5Y6/2 to 6/4, mostly coarse to medium sand. Sand is mostly (60% felsic). Poorly sorted, some fine to very fine sizeable at bottom. Also more fine sand. Weak to strong reaction to 10% HCl. Fairly dry.	Top = 4500 dpm
.8						Full but top may be
.9						sloughi. Not removed from liner.
.0						
63.1						Bottom = 5000 dpm
.2	C	B324B5	M-D		SAND, mostly medium sand, ranges up to very coarse sand. Color is 2.5Y6/2 to 7/2. poorly sorted. Occasional fine to very fine pebble – mostly mafic, at bottom. Color is 2.5Y6/2 at bottom – weak to strong reaction to 10% HCl.	Top = 4,500 dpm
.3						Not removed from liner.
.4						
.5						
63.6						Bottom = 4,000 dpm

C = Core, G = Grab   D = Dry, M = Moist, W = Wet

Borehole Sample Log

Pacific Northwest National Laboratory

BOREHOLE SAMPLE LOG

Boring/Well No C9520
Location 216-U-8 cr-B
Depth 63.6 –
Date 12/10/15
Sheet 16 of 21

Logged by G.V. Last
Reviewed by _____
Lithologic Class. Scheme Folk/Wentworth
Procedure PNNL-ESL-GEOLOGY Rev 1

Drilling Contractor _____
Driller _____
Drill Method _____
Project _____
Date _____

DEPTH (FT)	SAMPLES TYPE	ID NUMBER	MOISTURE	GRAPHIC LOG	LITHOLOGIC DESCRIPTION (particle size distribution, sorting, mineralogy, roundness, color, reaction to HCl, maximum grain size, consolidation, structure, etc.)	COMMENTS
63.6						
.7	C	B32HB6	M		SAND, mostly medium to coarse ranges up to very coarse sand. 70% felsic. Color is 2.5Y 7/2.	TOP = 3,000 dpm
.8					sand gets more mafic at the bottom. Fairly loose. Some mica. Weak to strong	Not removed from liner.
.9					reaction to 10% HCl.	
.0						
64.1						Bottom = 4,000 dpm
.2	C	B32HB7	M		SAND. Mostly coarse to medium, some very coarse. 50% mafic, 50% felsic.	TOP = 3,500 dpm
.3					Color is 2.5Y 6/2. Weak reaction to 10% HCl	Not removed from liner.
.4						
.5						
64.6						
64.7						Bottom = 3,000 dpm
.8	C	B32HB8	M-D		SAND. Partly sorting coarse to medium sand. Some very fine sand and tr. of silt.	TOP = 4,500 dpm
.9					Very mostly felsic sands (~10%). Color is 2.5Y 7/2. Weak to strong reaction to 10% HCl	Full, but top may contain
.0						slough. Not removed
.1					Sand at bottom is coarser – less medium to fine sand – less very fine sand and silt.	from liner.
65.2					Sand is 50% felsic, 50% mafic. Color 2.5Y 7/2. Weak to strong reaction to 10% HCl.	Bottom = 3,500 dpm
.3	C	B32HB9	M		SAND. Coarse to medium sand (mostly). 60% felsic, 40% mafic. Color is 2.5Y 7/2	TOP = 3,000 dpm
.4					Gets coarser at bottom more very coarse sand – going to very coarse to coarse	Not removed from
.5					sand – more mafic – 50%, 50% felsic. Top of core has weak to strong reaction.	liner.
.6					bottom has weak to no reaction. Can not see contact.	
65.7						Bottom = 3,000 dpm
.8	C	B32HC0	M		SAND. Very coarse to medium, mostly coarse. 50% mafic, 50% felsic. Very loose at	TOP = 3,000 dpm
.9					top of core. Color is 2.5Y 6/2. No reaction to 10% HCl	
.0						
.1						
66.2						Bottom =

C = Core, G = Grab
D = Dry, M = Moist, W = Wet

Pacific Northwest National Laboratory

BOREHOLE SAMPLE LOG

Boring/Well No __C9520__   Depth _66.2 – 70.1_   Date _12/1/15_

Location __216-U-8 CRIB__   Sheet _17_ of _21_

Logged by __GV Last__

Reviewed by ____

Lithologic Class. Scheme __Folk/Wentworth__

Procedure __PNNL-ESL-GEOLOGY__ Rev _1_

Drilling Contractor ____
Driller ____
Drill Method ____
Project ____

WPot   Date ____

DEPTH (FT)	SAMPLES TYPE	SAMPLES ID NUMBER	MOIS-TURE	GRAPHIC LOG C Z S G	LITHOLOGIC DESCRIPTION (particle size distribution, sorting, mineralogy, roundness, color, reaction to HCl, maximum grain size, consolidation, structure, etc.)	COMMENTS
66.2						
.3	C	B32HC1	M		SAND. Mostly coarse to medium sand. Very loose. Color is 2.5Y 6/2 to 7/2. 5% mafic, 5% felsic. Some very coarse sand.	TOP = 4000 dpm
.4					Particularly at bottom. No to weak reaction to 10% HCl.	Not removed from liner. Not full (A liner).
.5						
.6						
66.7						BOTTOM = 3500 dpm
68.2	C	B32HC2	M-D		SAND. Mostly coarse to medium, dries. Color is 2.5Y 7/2. Mostly felsic (70%). Weak reaction to 10% HCl.	TOP = 2000 dpm
.3						Full, but top could have
.4						slough (D liner). Not removed
.5					Sand at bottom is a bit cleaner – less very fine sand & silt. Color is 2.5Y 6/2 to 7/2. Sand is 5% mafic / 50% felsic. Weak to no reaction.	from liner.
68.6						BOTTOM = 2000 dpm
68.7	C	B32HC3	M		SAND. Mostly coarse to medium. 80% felsic, 10% mafic. Color is 2.5Y 7/2. Might have some coarser lenses. Color at bottom is a bit darker and more moist. 2.5Y 6/2 to 7/2. Weak to no reaction at top, no reaction at bottom.	TOP = 2000 dpm
.8						Not removed from liner.
.9						
.0						
69.1						BOTTOM = 2000 dpm
.2	C	B32HC4	M		SAND. Mostly coarse to medium sand, clean – very few fines. 50% mafic, 5% felsic. (salt and pepper) Very loose. Color is 2.5Y 6/2 to 7/2. Sample seems more moist at bottom. Some very coarse sand. No reaction – to weak.	TOP = 2000 dpm
.3						Not removed from liner.
.4						
.5						
69.6						BOTTOM = 2000 dpm
.7	C	B32HC5	M		SAND. Mostly coarse to medium sand. Very coarse. 50% mafic, 50% felsic. Clean – very little very fine sand or silt. Color is 2.5Y 6/2. A finer stringer on one side. One carbonate clast ~ 1.5 cm, makes this weak to no reaction.	TOP = 1000 dpm
.8						Not removed from liner.
.9						Not full (A liner).
.0				D		
70.1						BOTTOM = 1000 dpm

C = Core, G = Grab   D = Dry, M = Moist, W = Wet

Pacific Northwest National Laboratory	BOREHOLE SAMPLE LOG	Boring/Well No C9520	Depth 69.9 - 71.9	Sheet 18 of 21
		Location 216-U-B crib	Date 12/11/15	

Logged by GY Last

Reviewed by _____

Lithologic Class. Scheme Folk/Wentworth

Drilling Contractor _____

Driller _____ Date _____

Procedure PNNL-ESL-GEOLOG Rev 1

Drill Method _____

Project _____

Signature: by V. Last

DEPTH (FT)	SAMPLES		MOIS-TURE	GRAPHIC LOG				LITHOLOGIC DESCRIPTION (particle size distribution, sorting, mineralogy, roundness, color, reaction to HCl, maximum grain size, consolidation, structure, etc.)	COMMENTS
	TYPE	ID NUMBER		C	2	S	G		
69.9									
.0	C	B32HC6	M-D					SAND. Poorly sorted and drier. Very coarse to very fine sand, mostly coarse to medium. Color is 2.5Y7/2.	Top = 2500 dpm
.1									Full, but may have slough in top - depth on WPS with punched sample. Not removed from liner.
.2									
.3								Sand is cleaner at bottom - maybe more medium sand, and fine pebble. Color is 2.5Y 7/2. Weak reaction to 10% HCl.	
70.4									Bottom= 2000 dpm
.5	C	B32HC7	M-D					SAND. Mostly coarse to fine sand, some very coarse sand. Color is 2.5Y 8/2, perhaps some caliche mottling. More compacted/tight. Looks coarser or pea balls	Top = 2600 dpm
.6									Not removed from liner.
.7								cleaner - less fine to very fine sand and silt. Color is 2.5Y 7/2 at bottom.	
.8								Top has strong reaction to 10% HCl, bottom has weak reaction.	
70.9									Bottom= 1000 dpm
.0	C	B32HC8	M					SAND. mostly coarse to very coarse. Very-fine fines (very fine sand or silt), 50% to 60% finer. 50% mafic. Some very fine pebble. Gets finer at bottom - grout to coarse to fine sand. Color is 2.5Y 6/2. Weak to no reaction to 10% HCl.	Top = 1000 dpm. Not removed from liner.
.1									
.2									
.3									
71.4									Bottom= 1000 dpm
.5	C	B32HC9	M					SAND. Mostly medium sand. Color of core is poorly sorted - Very coarse sand to very fine sand and silty matrix (artifact of drilling?). Color is 2.5Y 6/2. Bottom is a coarse to medium sand. One thin stringer of liner is very fine sand with 3,500 dpm. Color of lens is 2.5Y5/4. Less is 0.5cm thick. Weak reaction to 10% HCl.	Top = 2000 dpm Not full (A liner) not removed from liner.
.6									
.7									
.8									
71.9									Bottom= 3500 dpm

C = Core, G = Grab   D = Dry, M = Moist, W = Wet

Pacific Northwest National Laboratory	BOREHOLE SAMPLE LOG	Boring/Well No C9520	Depth 72.7 – 74.7	Date 12/11/2015

Location 216-U-8 CRIB   Project

Logged by GV. LAST

Reviewed by _____ _A.V. Last_ _____ Date _____ Drilling Contractor _____

Lithologic Class. Scheme Folk/Wentworth   Procedure PNNL-ESL-GEOLOG Rev)   Driller _____

Drill Method _____

DEPTH (FT)	SAMPLES			GRAPHIC LOG				LITHOLOGIC DESCRIPTION (particle size distribution, sorting, mineralogy, roundness, color, reaction to HCl, maximum grain size, consolidation, structure, etc.)	COMMENTS
	TYPE	ID NUMBER	MOIS-TURE	C	Z	S	G		
72.7									
.8	C	B32HD0	M-D					SAND. Mostly coarse to medium, maybe heavier on the medium. 60% felsic, 40% mafic. Color is 2.5Y7/2. Perhaps a little coarser (more coarse sand) and more	Top = 2,500 dpm
.9								moist at bottom, color is darker 2.5Y6/2. Top of sample has weak reaction to	Top could have slough (D liners). Not removed from liner.
.0								10% HCl. Bottom has no reaction.	
.1									
73.2									Bottom = 1,500 dpm
.3	C	B32HD1	M					SAND. Mostly coarse to medium, 60% felsic, 40% mafic. Color is 2.5Y7/2.	Top = 1,500 dpm
.4								Some very coarse sand (mostly basalt).	Not removed from liner.
.5									
.6									
73.7									Bottom = 1,500 dpm
.8	C	B32HD2	M					SAND. Mostly coarse to medium sand. Some very coarse sand. Sand is 50% mafic,	Top = 2000 dpm
.9								50% felsic. Color is 2.5Y7/2. Loose. Weak to no reaction to 10% HCl.	Not removed from liner.
.0									
.1									
74.2									Bottom = 1000 dpm
.3	C	B32HD3	M					SAND. Mostly coarse to medium. Very heavy. 60% felsic, 40% mafic – some reddish	Top = 1000 dpm
.4								grains. Color is 2.5Y7/2.	Not removed from liner.
.5									Not full (A liner).
.6									
74.7									Bottom = 1000 dpm

C = Core, G = Grab   D = Dry, M = Moist, W = Wet

BOREHOLE SAMPLE LOG

Boring/Well No C9520
Location 216-U-8 CRIB
Depth ___
Date 12/15/2005
Project ___

Logged by G.V.LAST
Reviewed by ___
Lithologic Class. Scheme Folk/Wentworth
Procedure PNNL-ESL-GEOLOGY Rev 1

Drilling Contractor ___
Driller ___
Drill Method ___

DEPTH (FT)	SAMPLES TYPE	ID NUMBER	MOIS-TURE	GRAPHIC LOG	LITHOLOGIC DESCRIPTION (particle size distribution, sorting, mineralogy, roundness, color, reaction to HCl, maximum grain size, consolidation, structure, etc.)	COMMENTS
74.9						
.0	C	B32HD4	D		SAND. Poorly sorted, mostly coarse to fine sand. Bottom appears to be coarser, more very coarse sand, mostly medium. Color is 2.5Y3/2. Some occasional very few pebbles. Weak reaction to 1e2? HCl. Loose on top.	Top= 1000 dpm. Not full likely has slough in top/ID know? Not remelted from liner. Bottom= 1000 dpm
.1						
.2						
.3						
75.4						
.5	C	B32HD5	M-D		SAND. Mostly coarse to medium sand. Some very coarse sand w/very fine pebble (few.) Color is 2.5Y7/2. More medium than coarse sand. Sand is 60% felsic, 40% mafic. Loose. Weak to no reaction to 10% HCl.	Top= 1000 dpm. Not remelted from liner
.6						
.7						
.8						
75.9						
.0	C	B32HD6	M		SAND. Mostly coarse to medium sand, well sorted. Sand is 50% felsic, 50% mafic. Fairly loose. Color is 2.5Y7/2. Some very fine pebble in bottom. Weak to no reaction to 10% HCl.	Bottom=<1000 dpm. Top= <1000 dpm. Not remelted from liner.
.1						
.2						
.3						
76.4						
.5	C	B32HD7	M		SAND. Mostly coarse to medium sand. 50% mafic, 50% felsic. Loose. Occasional very fine to fine pebble (<1/2cm), might be a little finer at bottom - more fine sand. Color is 2.5Y7/2. Weak reaction, more reaction at bottom.	Bottom=<1000 dpm. Top=<1000 dpm. Not felsic. Not removed from liner. Bottom=<1000 dpm.
.6						
.7						
.8						
76.9						

C = Core, G = Grab
D = Dry, M = Moist, W = Wet

2015/GVL/GeoscienceGroup/Procedures/SampleLog/001 (02/06)

Pacific Northwest National Laboratory

BOREHOLE SAMPLE LOG

Boring/Well No C9520	Depth 77.6 to 79.6	Date 12/15/15
Location 216-α-8 CRIB	Project	Sheet 21 of 21

Logged by G.V. Last

Reviewed by _____

Lithologic Class. Scheme Folk / Wentworth

Drilling Contractor _____
Driller _____
Drill Method _____

Procedure PNNL-ESL-GEOLOGY Rev 1   Date _____

DEPTH (FT)	SAMPLES TYPE	SAMPLES ID NUMBER	MOIS-TURE	GRAPHIC LOG C Z S G	LITHOLOGIC DESCRIPTION (particle size distribution, sorting, mineralogy, roundness, color, reaction to HCl, maximum grain size, consolidation, structure, etc.)	COMMENTS
77.6						
.7	C	B330H0	M-D		SAND. Poorly sorted, mostly medium to fine sand. Color is 2.5Y 7/2. Some coarse sand – poorly sorted, some very fine pebble. Weak weathering reaction.	TOP = <1000 dpm
.8						Nearly full but likely contains slough. Not
.9						removed from liner.
.0					Sand at bottom is cleaner – less fine to very fine sand. Mostly coarse to medium. Color is 2.5Y 7/2. Weak to no reaction to 10% HCl.	BOTTOM = <1000 dpm
78.1						
.2	C	B330H1	M		SAND. Mostly medium sand. 50% mafic, 50% felsic. Color is 2.5Y 7/2.	TOP = <1000 dpm
.3					Get a little coarser at bottom, mostly coarse sand. Weak reaction at top.	Not removed from liner.
.4					No reaction at bottom.	
.5						
78.6						Bottom = <1000 dpm
.7	C	B330H2	M-D		SAND. Mostly very coarse to medium sand, maybe 5% very fine pebble.	TOP = <1000 dpm
.8					Some layers (strata) of coarser and finer sand. Maybe a little finer at bottom –	Not removed from
.9					more medium sand, less pebble. Color 2.5Y 7/2. Weak reaction to 10% HCl.	liner.
.0						
79.1						Bottom = <1000 dpm
.2	C	B330H3	M-D		SAND. Mostly coarse to medium, some coarser and finer strata. Color is 2.5Y	TOP = <1000 dpm
.3					7/2. 50% mafic, 50% felsic. Weak reaction to 10% HCl.	Not removed from liner.
.4						Not full.
.5						
79.6						Bottom = <1000 dpm

C = Core, G = Grab   D = Dry, M = Moist, W = Wet   2015/GVL/GeosciencesGroup/Procedures/SampleLog/001 (02/06)

B.2 Core Photographs

Core photographs are provided for analyzed samples from boreholes C9515, C9518, C9519, and C9520.

Figure B.6. Borehole C9515 Sample B38XK6

Figure B.7. Borehole C9515 Sample B38XK9

Figure B.8. Borehole C9518 Sample B38Y11
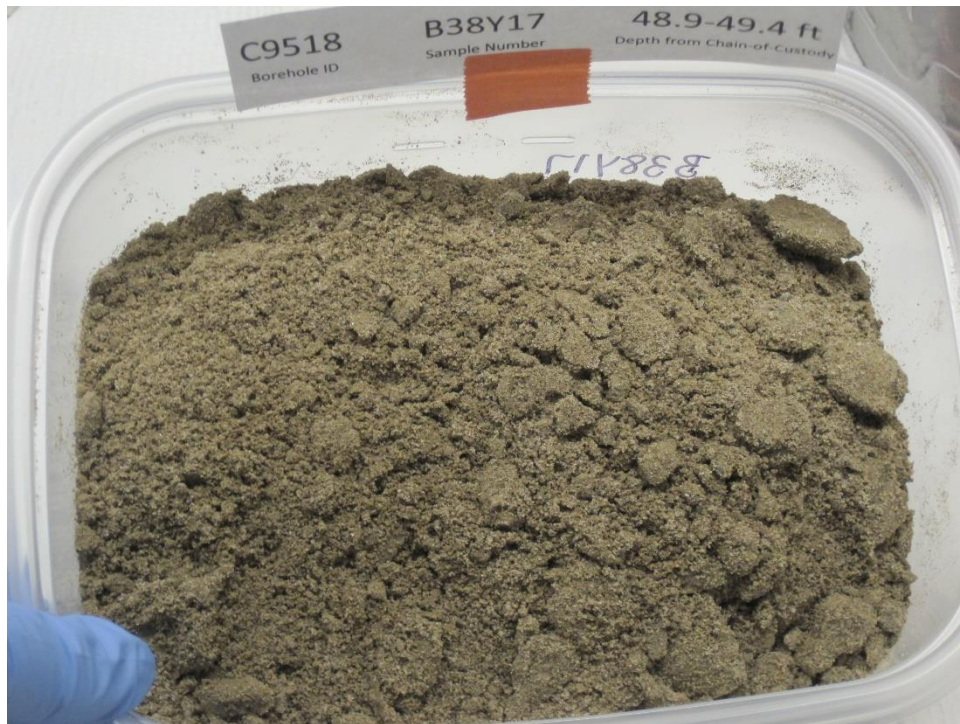
Figure B.9. Borehole C9518 Sample B38Y17

Figure B.10. Borehole C9519 Sample B38YC9

Figure B.11. Borehole C9519 Sample B38YF8

B.31

Figure B.12. Borehole C9519 Sample B38YH2

Figure B.13. Borehole C9519 Sample B38YH9

Figure B.14. Borehole C9519 Sample B38YK0

Figure B.15. Borehole C9520 Sample B32H62

Figure B.16. Borehole C9520 Sample B32H70
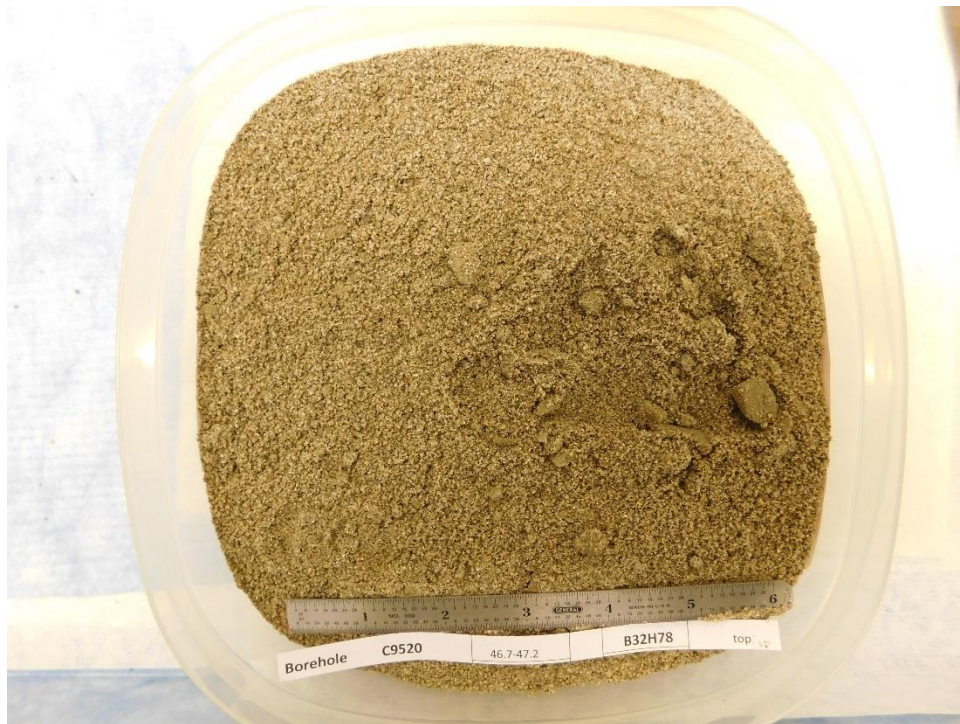
Figure B.17. Borehole C9520 Sample B32H78
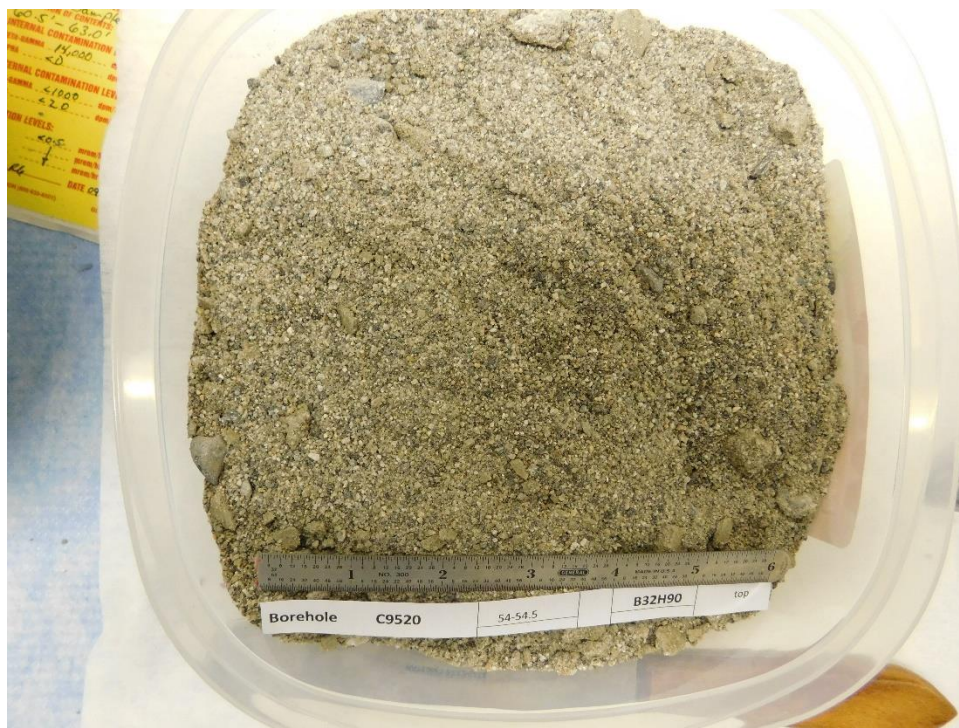
Figure B.18. Borehole C9520 Sample B32H90
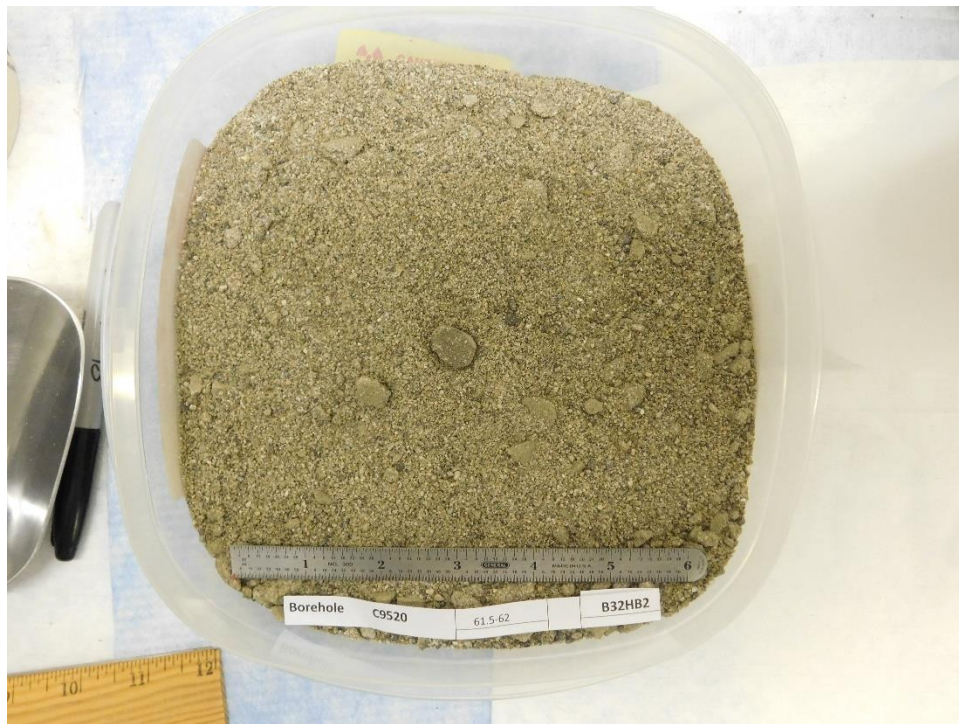
Figure B.19. Borehole C9520 Sample B32HB2

B.3 Particle Size Distribution (PSD)
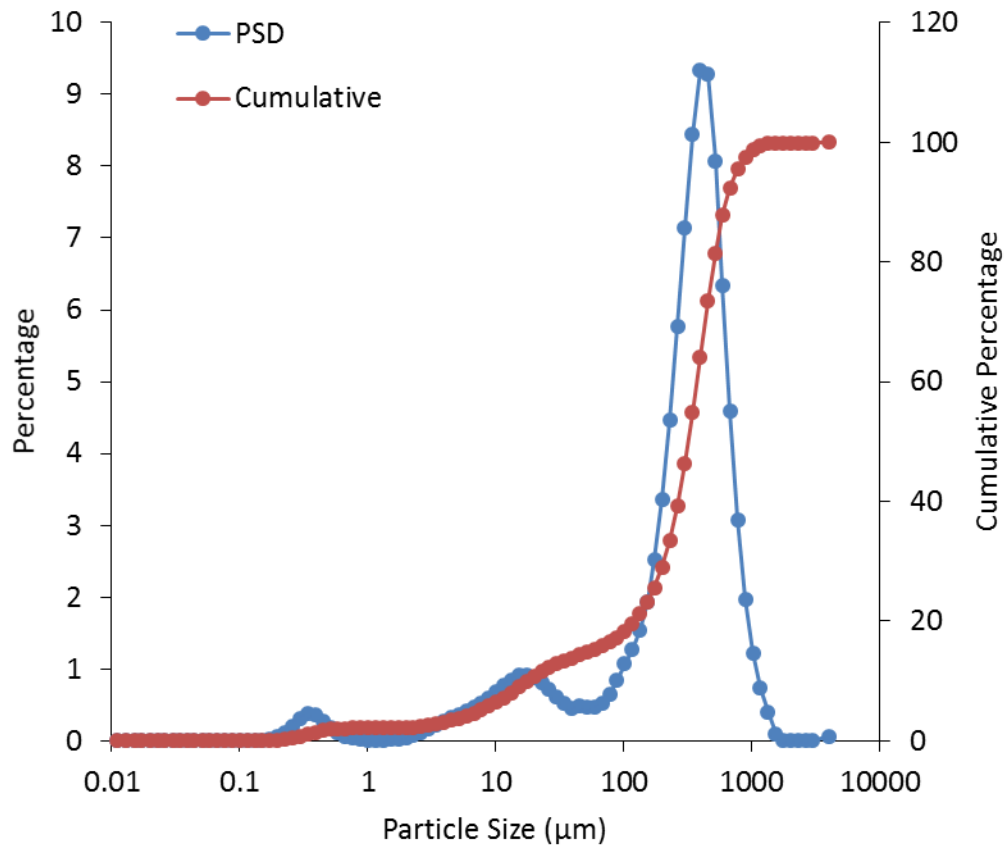
Figure B.20. Borehole C9515 Sample B38XK6
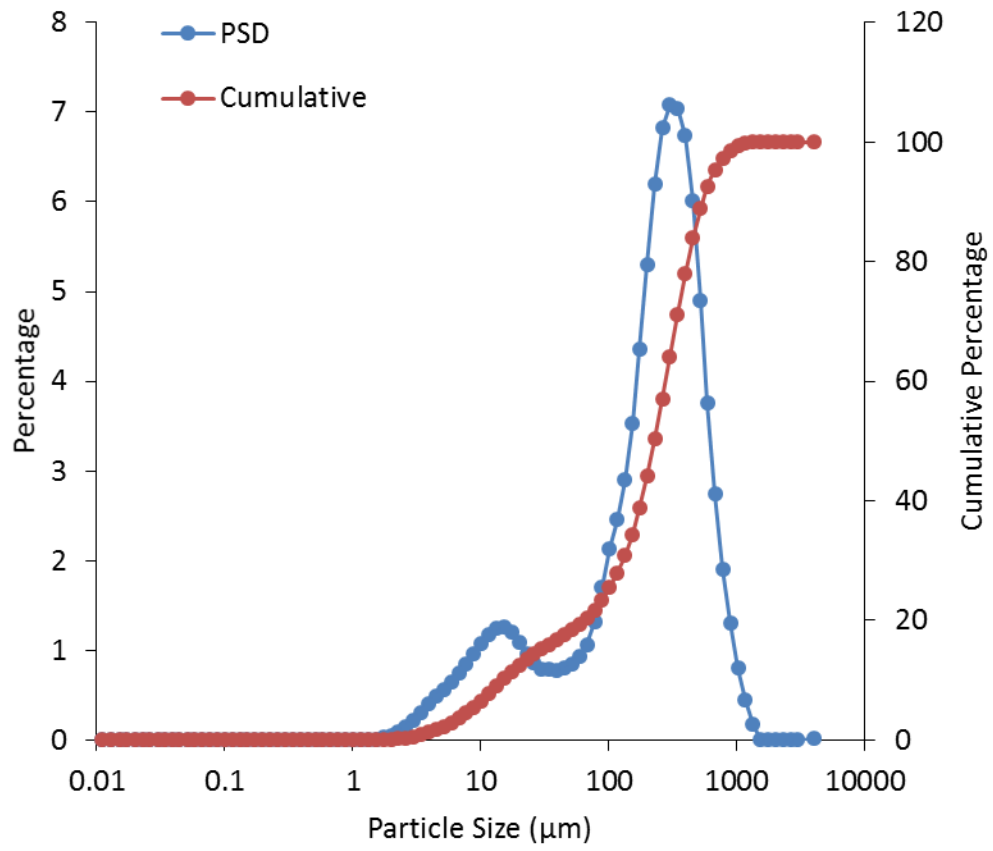
Figure B.21. Borehole C9515 Sample B38XK9
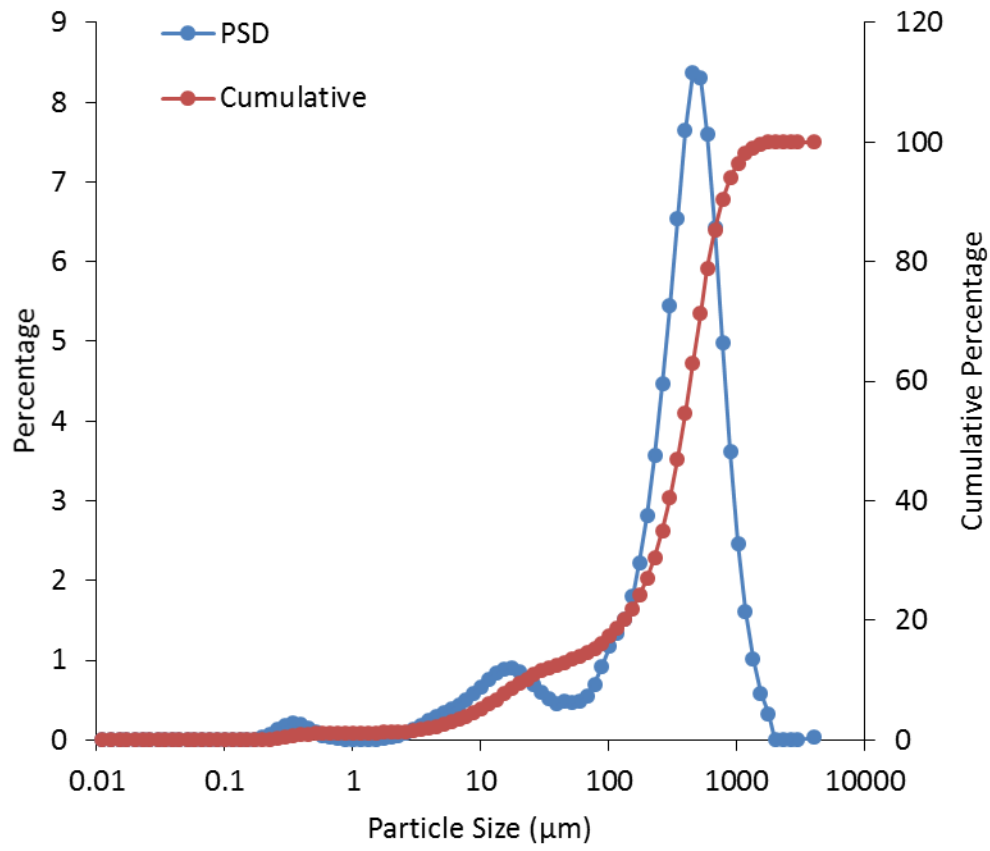
Figure B.22. Borehole C9518 Sample B38Y11
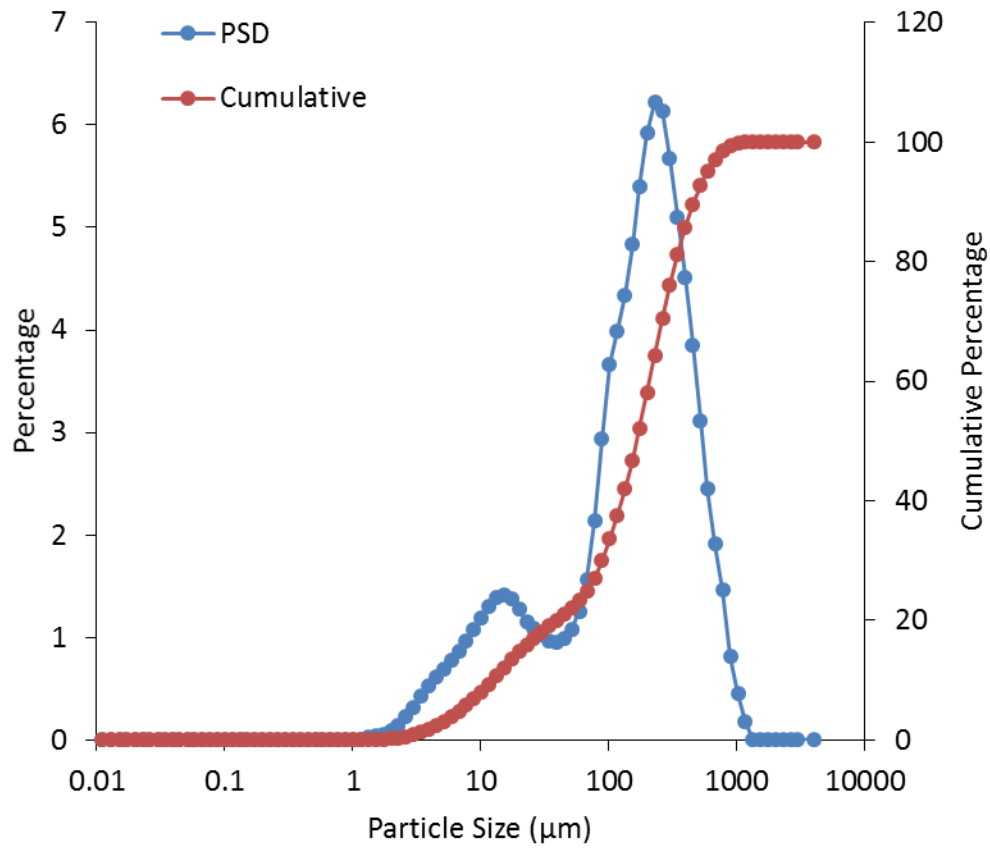
Figure B.23. Borehole C9518 Sample B38Y17
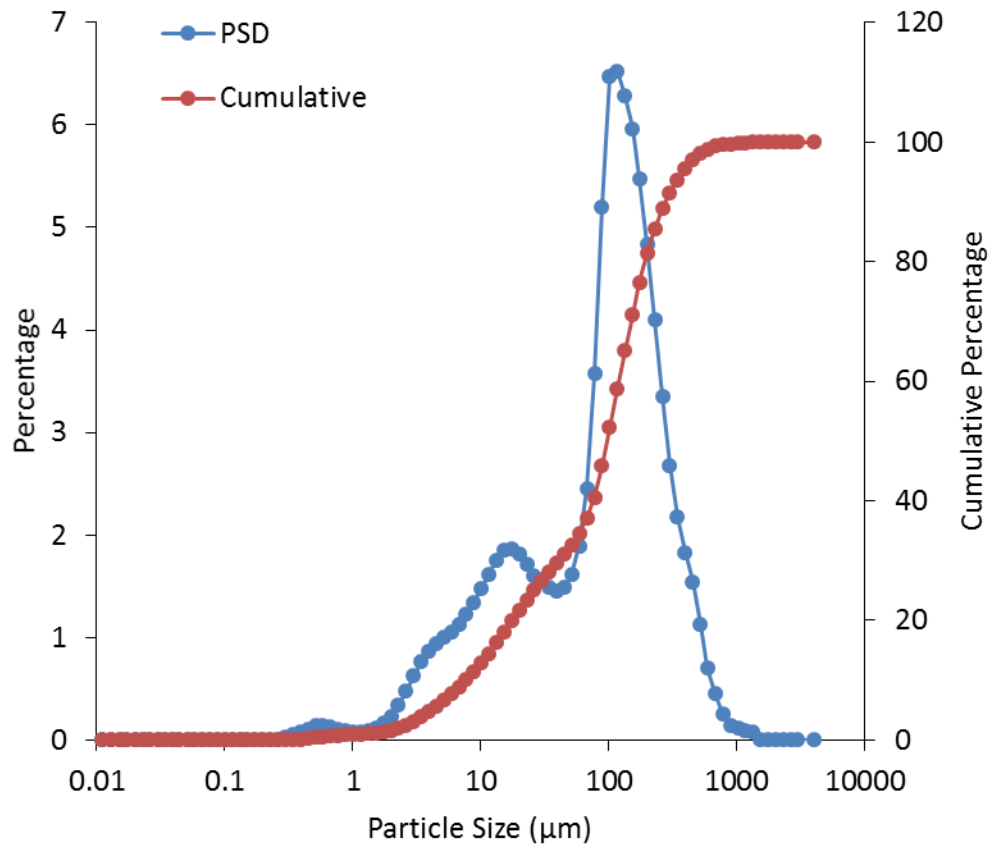
Figure B.24. Borehole C9519 Sample B38YC9
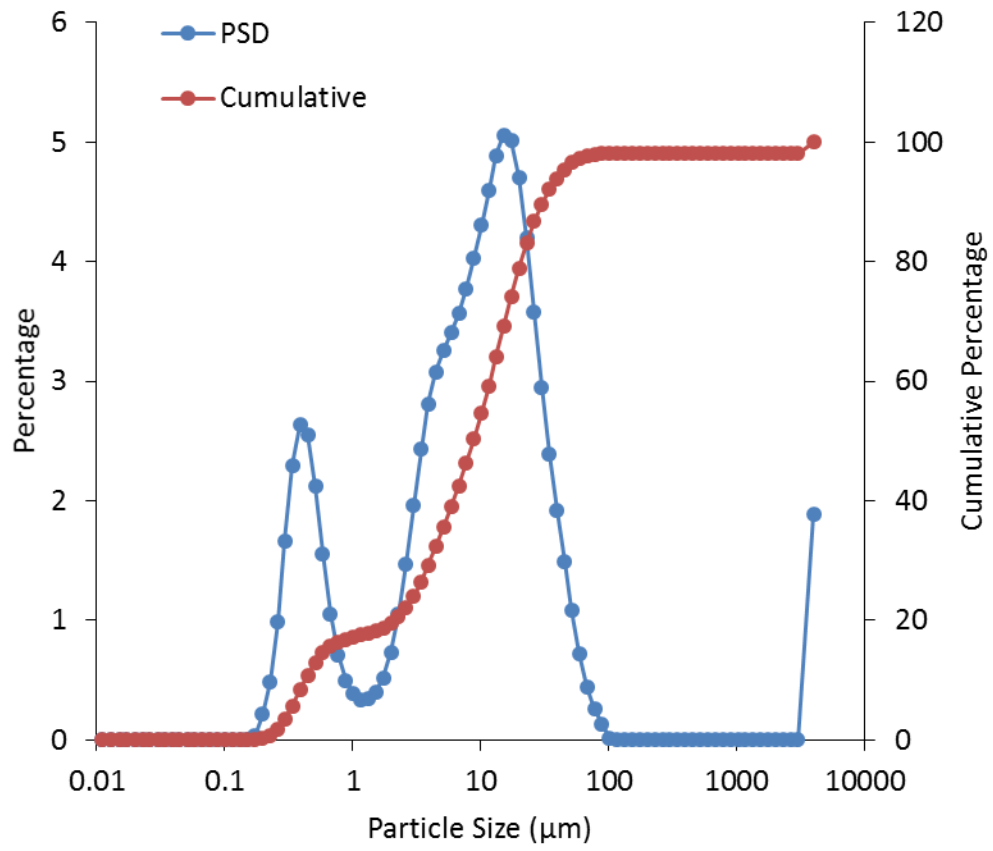
Figure B.25. Borehole C9519 Sample B38YF8
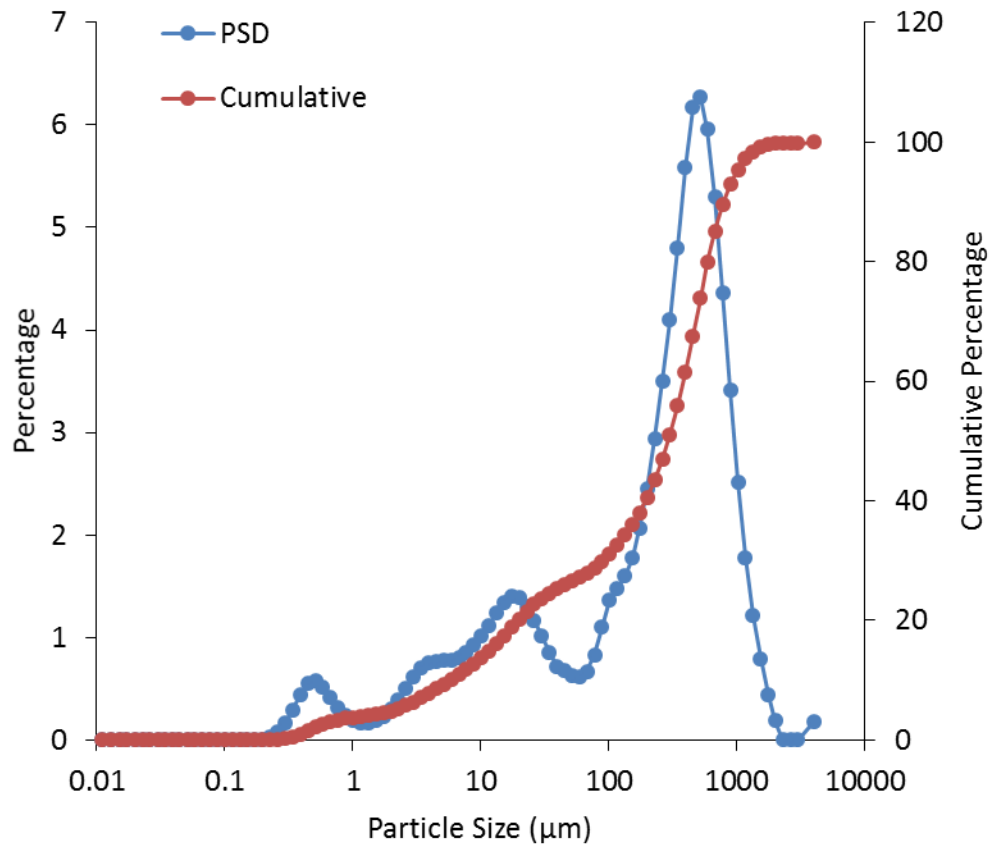
Figure B.26. Borehole C9519 Sample B38YH2
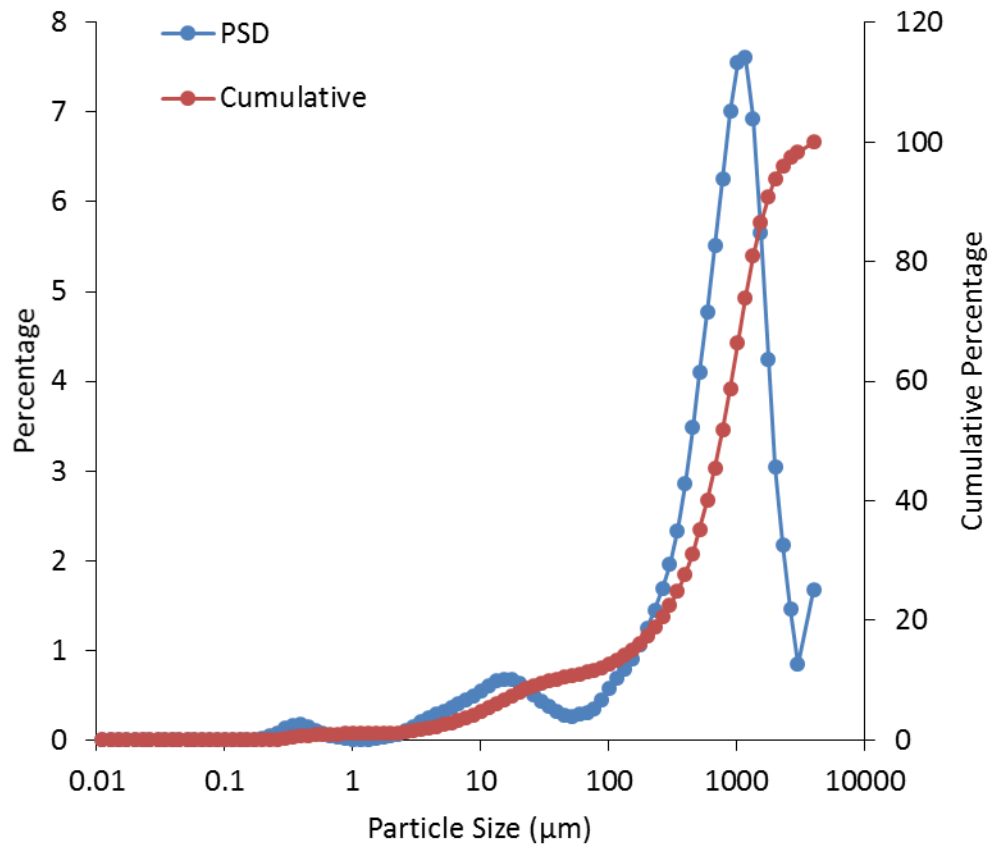
Figure B.27. Borehole C9519 Sample B38YH9
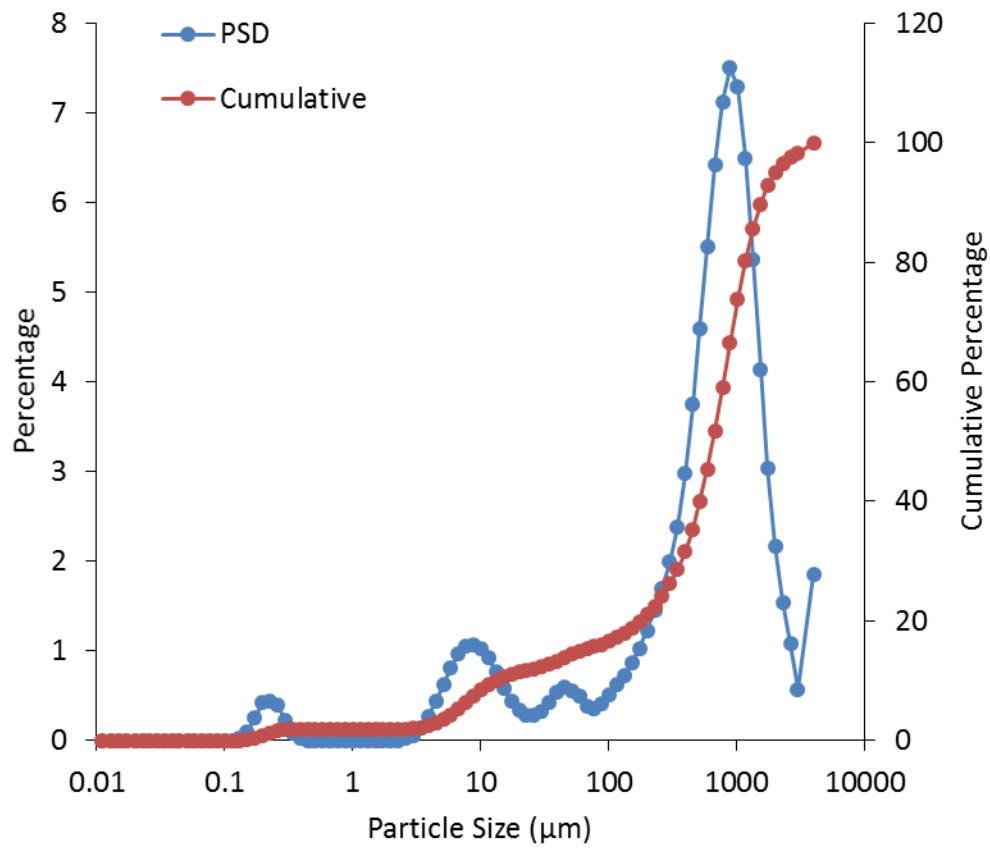
Figure B.28. Borehole C9519 Sample B38YK0
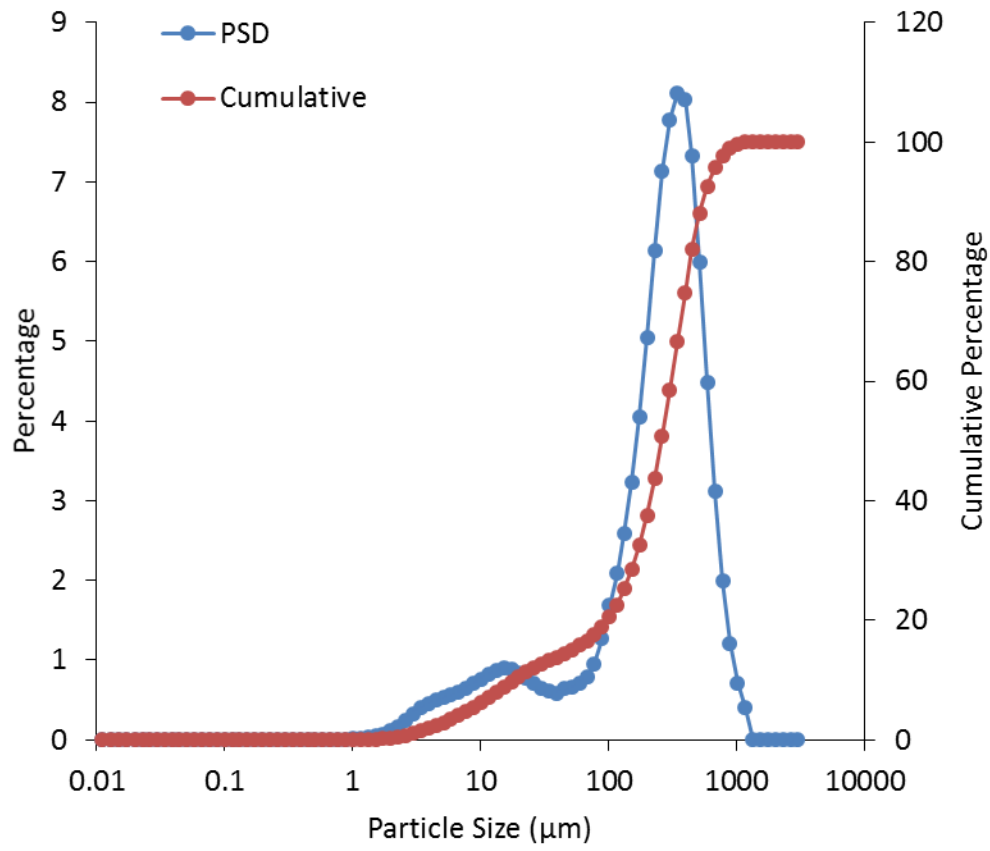
Figure B.29. Borehole C9520 Sample B32H63
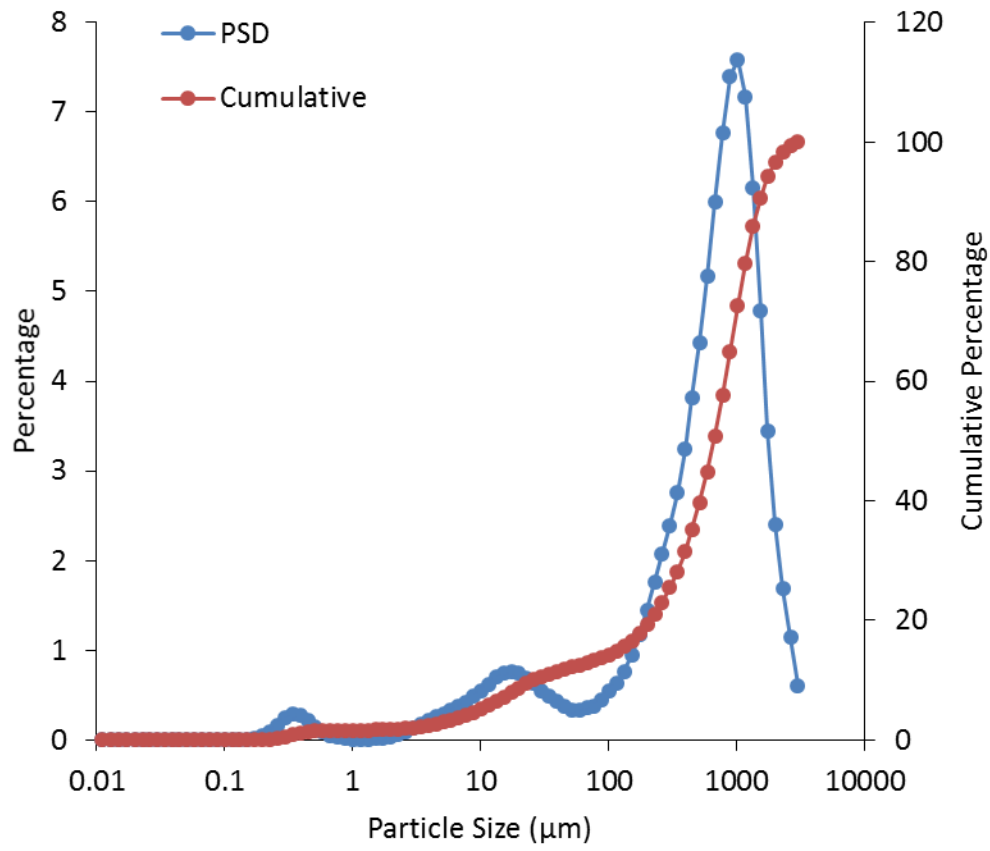
Figure B.30. Borehole C9520 Sample B32H71
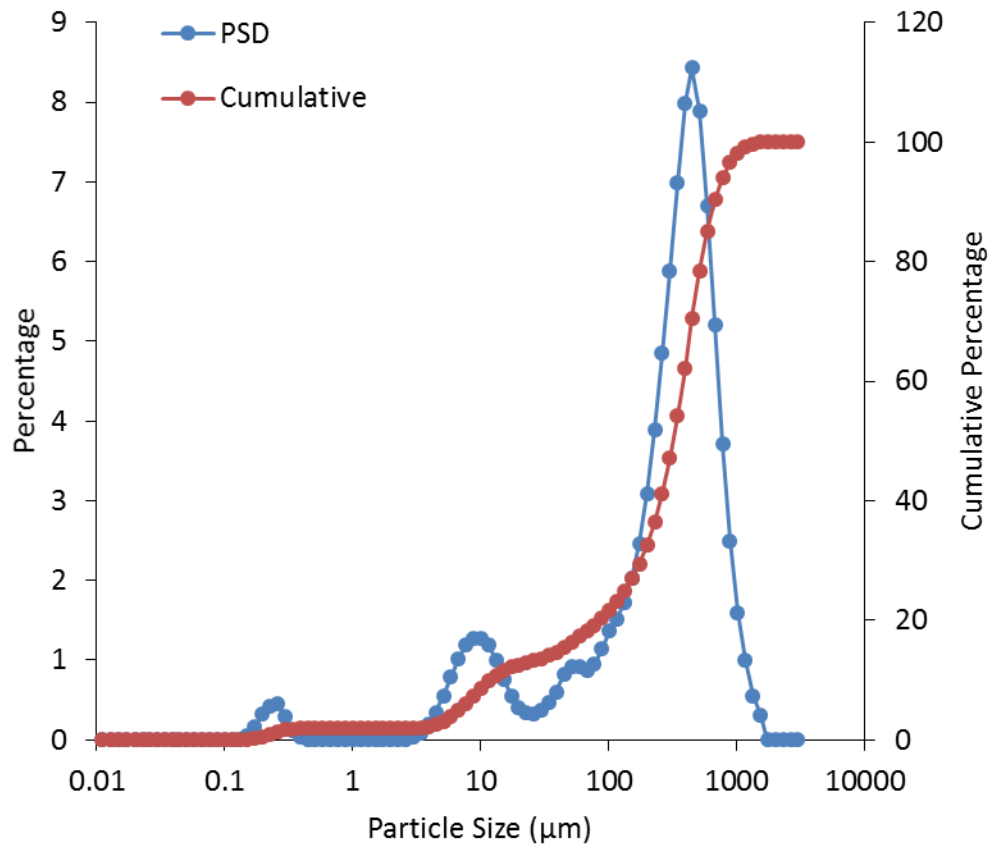
Figure B.31. Borehole C9520 Sample B32H79
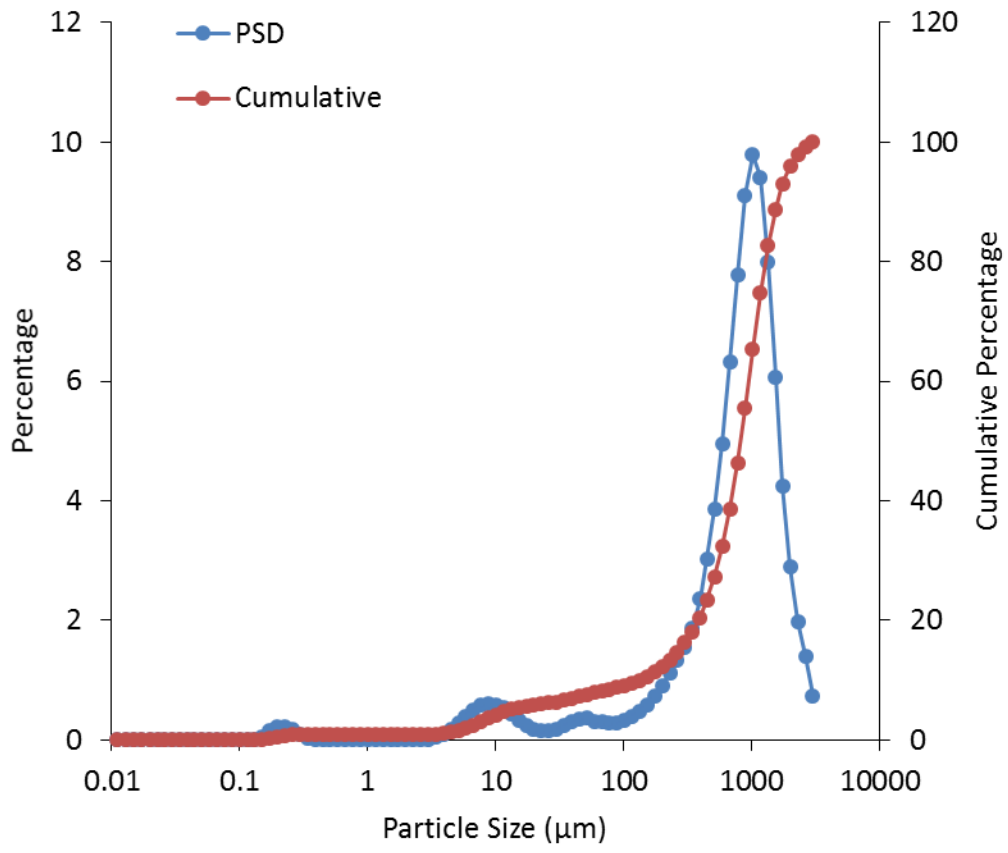
Figure B.32. Borehole C9520 Sample B32H91
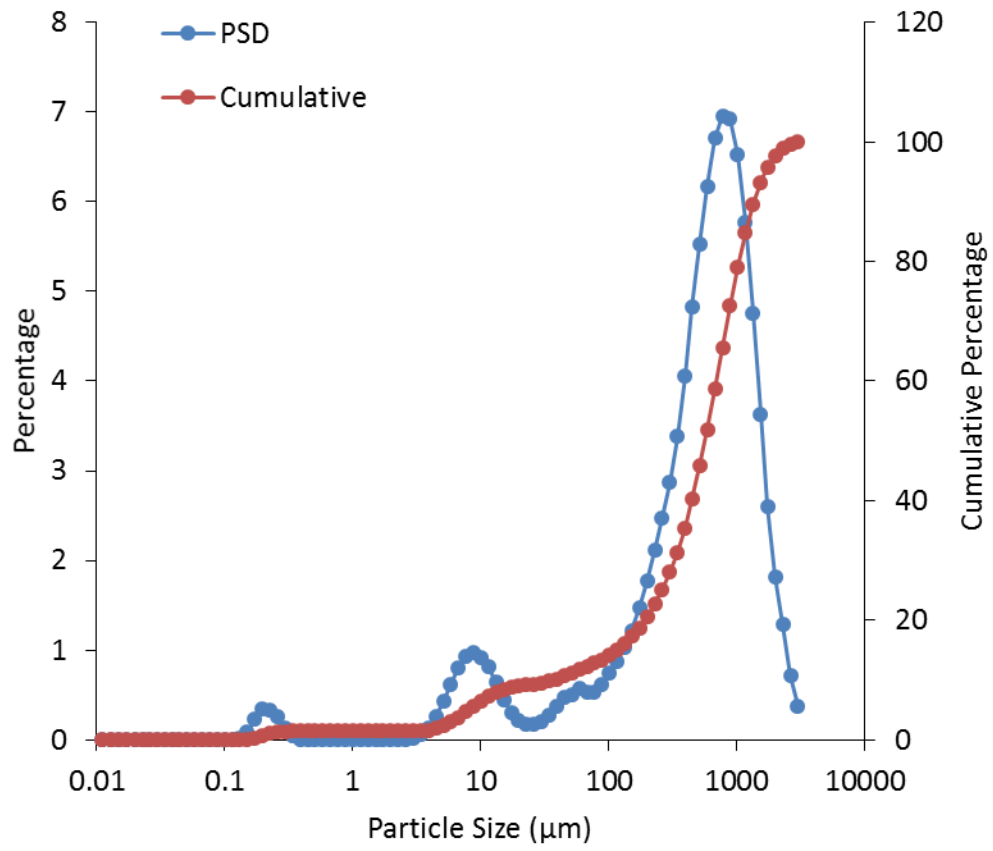
Figure B.33. Borehole C9520 Sample B32HB3

Table B.1. Particle Size Data for Boreholes C9515, C9518, and C9519

Diameter (µm)	C9515 B38XK6		C9515 B38XK9		C9518 B38Y11		C9518 B38Y17		C9519 B38YC9		C9519 B38YF8		C9519 B38YH2		C9519 B38YH9		C9519 B38YK0	
	PSD	Cumulative	PSD	Cumulative	PSD	Cumulative	PSD	Cumulative	PSD	Cumulative	PSD	Cumulative	PSD	Cumulative	PSD	Cumulative	PSD	Cumulative
0.011	0	0	0	0	0	0	0	0	0	0	0	0	0	0	0	0	0	0
0.013	0	0	0	0	0	0	0	0	0	0	0	0	0	0	0	0	0	0
0.015	0	0	0	0	0	0	0	0	0	0	0	0	0	0	0	0	0	0
0.017	0	0	0	0	0	0	0	0	0	0	0	0	0	0	0	0	0	0
0.02	0	0	0	0	0	0	0	0	0	0	0	0	0	0	0	0	0	0
0.023	0	0	0	0	0	0	0	0	0	0	0	0	0	0	0	0	0	0
0.026	0	0	0	0	0	0	0	0	0	0	0	0	0	0	0	0	0	0
0.03	0	0	0	0	0	0	0	0	0	0	0	0	0	0	0	0	0	0
0.034	0	0	0	0	0	0	0	0	0	0	0	0	0	0	0	0	0	0
0.039	0	0	0	0	0	0	0	0	0	0	0	0	0	0	0	0	0	0
0.044	0	0	0	0	0	0	0	0	0	0	0	0	0	0	0	0	0	0
0.051	0	0	0	0	0	0	0	0	0	0	0	0	0	0	0	0	0	0
0.058	0	0	0	0	0	0	0	0	0	0	0	0	0	0	0	0	0	0
0.067	0	0	0	0	0	0	0	0	0	0	0	0	0	0	0	0	0	0
0.076	0	0	0	0	0	0	0	0	0	0	0	0	0	0	0	0	0	0
0.087	0	0	0	0	0	0	0	0	0	0	0	0	0	0	0	0	0	0
0.1	0	0	0	0	0	0	0	0	0	0	0	0	0	0	0	0	0	0
0.115	0	0	0	0	0	0	0	0	0	0	0	0	0	0	0	0	0	0
0.131	0	0	0	0	0	0	0	0	0	0	0	0	0	0	0	0	0.022	0.022
0.15	0	0	0	0	0	0	0	0	0	0	0	0	0	0	0	0	0.093	0.115
0.172	0.021	0.021	0	0	0.012	0.012	0	0	0	0	0.033	0.033	0	0	0.005	0.005	0.259	0.375
0.197	0.053	0.074	0	0	0.035	0.048	0	0	0	0	0.215	0.248	0	0	0.020	0.025	0.418	0.793
0.226	0.110	0.184	0	0	0.070	0.118	0	0	0	0	0.487	0.735	0.033	0.033	0.043	0.068	0.440	1.233
0.259	0.207	0.391	0	0	0.126	0.244	0	0	0	0	0.991	1.726	0.076	0.109	0.082	0.150	0.392	1.625
0.296	0.314	0.706	0	0	0.185	0.429	0	0	0.025	0.025	1.664	3.390	0.160	0.268	0.130	0.280	0.226	1.851
0.339	0.378	1.083	0	0	0.217	0.646	0	0	0.047	0.073	2.294	5.684	0.289	0.558	0.168	0.448	0.086	1.937
0.389	0.359	1.442	0	0	0.203	0.849	0	0	0.075	0.147	2.634	8.318	0.438	0.996	0.175	0.623	0.023	1.960

Diameter (µm)	C9515 B38XK6		C9515 B38XK9		C9518 B38Y11		C9518 B38Y17		C9519 B38YC9		C9519 B38YF8		C9519 B38YH2		C9519 B38YH9		C9519 B38YK0	
	PSD	Cumulative	PSD	Cumulative	PSD	Cumulative	PSD	Cumulative	PSD	Cumulative	PSD	Cumulative	PSD	Cumulative	PSD	Cumulative	PSD	Cumulative
0.445	0.276	1.718	0	0	0.155	1.004	0	0	0.098	0.245	2.551	10.869	0.550	1.546	0.149	0.772	0	1.960
0.51	0.179	1.897	0	0	0.101	1.105	0	0	0.138	0.384	2.121	12.990	0.574	2.120	0.108	0.880	0	1.960
0.584	0.104	2.001	0	0	0.060	1.165	0	0	0.137	0.521	1.559	14.549	0.514	2.634	0.069	0.949	0	1.960
0.669	0.058	2.060	0	0	0.034	1.199	0	0	0.122	0.643	1.056	15.605	0.412	3.046	0.042	0.991	0	1.960
0.766	0.034	2.093	0	0	0.020	1.219	0	0	0.104	0.747	0.710	16.315	0.312	3.358	0.026	1.018	0	1.960
0.877	0.022	2.115	0	0	0.006	1.225	0	0	0.090	0.836	0.498	16.813	0.237	3.595	0.018	1.036	0	1.960
1.005	0.011	2.126	0	0	0	1.225	0	0	0.082	0.918	0.384	17.196	0.191	3.785	0.010	1.046	0	1.960
1.151	0	2.126	0	0	0	1.225	0	0	0.083	1.001	0.336	17.533	0.169	3.954	0.010	1.056	0	1.960
1.318	0.010	2.136	0	0	0	1.225	0.025	0.025	0.093	1.094	0.342	17.875	0.168	4.122	0.010	1.066	0	1.960
1.51	0.020	2.156	0	0	0.006	1.231	0.035	0.060	0.118	1.211	0.398	18.273	0.188	4.309	0.018	1.084	0	1.960
1.729	0.028	2.184	0.028	0.028	0.020	1.251	0.055	0.115	0.162	1.373	0.517	18.790	0.230	4.539	0.026	1.110	0	1.960
1.981	0.044	2.229	0.050	0.078	0.033	1.284	0.089	0.204	0.234	1.608	0.733	19.523	0.299	4.838	0.041	1.152	0	1.960
2.269	0.071	2.299	0.088	0.167	0.055	1.339	0.144	0.348	0.340	1.947	1.050	20.573	0.393	5.232	0.067	1.218	0	1.960
2.599	0.110	2.409	0.146	0.312	0.088	1.427	0.223	0.570	0.475	2.422	1.472	22.045	0.505	5.737	0.103	1.322	0.019	1.980
2.976	0.160	2.569	0.222	0.534	0.133	1.560	0.321	0.891	0.624	3.046	1.959	24.004	0.615	6.351	0.150	1.472	0.057	2.036
3.409	0.217	2.786	0.309	0.844	0.185	1.746	0.427	1.318	0.762	3.808	2.431	26.435	0.700	7.051	0.201	1.673	0.134	2.170
3.905	0.271	3.057	0.398	1.242	0.239	1.984	0.526	1.844	0.869	4.678	2.812	29.247	0.749	7.800	0.249	1.921	0.261	2.432
4.472	0.321	3.378	0.483	1.724	0.289	2.273	0.614	2.458	0.945	5.622	3.078	32.326	0.768	8.568	0.290	2.211	0.432	2.864
5.122	0.365	3.743	0.565	2.290	0.337	2.610	0.693	3.151	1.001	6.624	3.257	35.583	0.772	9.341	0.325	2.536	0.624	3.488
5.867	0.411	4.154	0.651	2.941	0.386	2.996	0.774	3.925	1.058	7.681	3.403	38.986	0.780	10.121	0.359	2.895	0.811	4.298
6.72	0.464	4.618	0.747	3.687	0.443	3.439	0.864	4.789	1.130	8.811	3.567	42.553	0.805	10.925	0.397	3.293	0.963	5.262
7.697	0.526	5.144	0.853	4.541	0.509	3.948	0.966	5.755	1.226	10.037	3.775	46.329	0.853	11.778	0.442	3.735	1.055	6.317
8.816	0.600	5.744	0.965	5.506	0.586	4.534	1.079	6.834	1.345	11.382	4.029	50.357	0.926	12.704	0.494	4.229	1.071	7.388
10.097	0.681	6.425	1.076	6.582	0.669	5.203	1.192	8.026	1.478	12.861	4.305	54.662	1.016	13.721	0.548	4.777	1.023	8.411
11.565	0.768	7.193	1.181	7.763	0.758	5.961	1.303	9.329	1.618	14.479	4.599	59.261	1.119	14.840	0.604	5.381	0.927	9.338
13.246	0.851	8.044	1.252	9.015	0.839	6.800	1.388	10.717	1.754	16.233	4.888	64.148	1.238	16.078	0.654	6.035	0.767	10.105
15.172	0.908	8.952	1.259	10.274	0.892	7.692	1.415	12.132	1.848	18.081	5.059	69.208	1.343	17.421	0.681	6.715	0.587	10.692
17.377	0.918	9.870	1.198	11.472	0.897	8.588	1.372	13.505	1.870	19.950	5.009	74.217	1.400	18.821	0.673	7.388	0.434	11.127
19.904	0.880	10.750	1.089	12.560	0.855	9.444	1.276	14.781	1.819	21.770	4.707	78.924	1.386	20.207	0.632	8.020	0.334	11.461
22.797	0.804	11.554	0.966	13.526	0.782	10.225	1.156	15.937	1.721	23.490	4.198	83.121	1.304	21.512	0.571	8.591	0.287	11.748

B.51

Diameter (μm)	C9515 B38XK6		C9515 B38XK9		C9518 B38Y11		C9518 B38Y17		C9519 B38YC9		C9519 B38YF8		C9519 B38YH2		C9519 B38YH9		C9519 B38YK0	
	PSD	Cum-ulative	PSD	Cum-ulative	PSD	Cum-ulative	PSD	Cum-ulative	PSD	Cum-ulative	PSD	Cum-ulative	PSD	Cum-ulative	PSD	Cum-ulative	PSD	Cum-ulative
26.111	0.710	12.265	0.854	14.381	0.694	10.919	1.092	17.029	1.601	25.092	3.577	86.698	1.171	22.683	0.502	9.093	0.287	12.035
29.907	0.614	12.879	0.793	15.174	0.606	11.525	1.028	18.057	1.561	26.653	2.949	89.647	1.013	23.696	0.435	9.528	0.331	12.366
34.255	0.527	13.406	0.793	15.967	0.526	12.050	0.971	19.028	1.484	28.137	2.388	92.035	0.855	24.550	0.375	9.903	0.420	12.786
39.234	0.454	13.860	0.777	16.744	0.456	12.507	0.954	19.983	1.454	29.590	1.915	93.950	0.712	25.262	0.324	10.227	0.533	13.318
44.938	0.483	14.342	0.799	17.543	0.491	12.998	0.990	20.973	1.491	31.081	1.490	95.440	0.682	25.944	0.276	10.503	0.595	13.913
51.471	0.465	14.807	0.845	18.388	0.475	13.473	1.077	22.049	1.608	32.690	1.086	96.526	0.622	26.566	0.257	10.760	0.551	14.464
58.953	0.474	15.281	0.926	19.314	0.490	13.962	1.254	23.303	1.891	34.580	0.725	97.250	0.611	27.178	0.289	11.049	0.503	14.967
67.523	0.525	15.806	1.066	20.380	0.553	14.515	1.571	24.873	2.454	37.034	0.444	97.694	0.667	27.845	0.298	11.347	0.382	15.348
77.34	0.639	16.446	1.315	21.695	0.695	15.210	2.134	27.007	3.569	40.603	0.258	97.951	0.828	28.673	0.349	11.696	0.351	15.699
88.583	0.835	17.281	1.701	23.396	0.927	16.137	2.937	29.944	5.204	45.807	0.136	98.088	1.101	29.775	0.451	12.147	0.407	16.106
101.46	1.069	18.350	2.132	25.528	1.173	17.310	3.668	33.612	6.475	52.283	0.011	98.099	1.367	31.142	0.582	12.729	0.509	16.615
116.21	1.269	19.619	2.459	27.987	1.334	18.644	3.990	37.603	6.527	58.810	0.008	98.107	1.479	32.621	0.689	13.418	0.622	17.237
133.103	1.540	21.158	2.900	30.886	1.519	20.163	4.342	41.944	6.284	65.093	0	98.107	1.599	34.220	0.786	14.204	0.731	17.969
152.453	1.939	23.097	3.535	34.421	1.800	21.962	4.836	46.781	5.962	71.055	0	98.107	1.778	35.998	0.908	15.112	0.862	18.831
174.616	2.525	25.621	4.358	38.778	2.221	24.183	5.398	52.179	5.475	76.531	0	98.107	2.059	38.058	1.057	16.169	1.025	19.856
200	3.361	28.982	5.301	44.079	2.810	26.993	5.922	58.101	4.833	81.364	0	98.107	2.449	40.506	1.239	17.409	1.225	21.081
229.075	4.463	33.445	6.193	50.272	3.569	30.562	6.223	64.324	4.098	85.462	0	98.107	2.941	43.447	1.450	18.858	1.453	22.533
262.376	5.774	39.219	6.826	57.098	4.462	35.025	6.142	70.466	3.355	88.817	0.007	98.114	3.503	46.950	1.684	20.542	1.702	24.235
300.518	7.150	46.370	7.080	64.178	5.446	40.470	5.674	76.139	2.678	91.495	0	98.114	4.096	51.045	1.958	22.500	1.990	26.225
344.206	8.444	54.814	7.042	71.220	6.533	47.004	5.102	81.241	2.176	93.671	0	98.114	4.803	55.848	2.332	24.832	2.386	28.611
394.244	9.340	64.153	6.735	77.955	7.647	54.650	4.516	85.757	1.828	95.500	0	98.114	5.583	61.431	2.857	27.688	2.977	31.588
451.556	9.282	73.435	6.013	83.968	8.374	63.024	3.855	89.613	1.541	97.041	0	98.114	6.173	67.604	3.481	31.169	3.745	35.333
517.2	8.071	81.506	4.898	88.866	8.302	71.326	3.114	92.727	1.126	98.167	0	98.114	6.268	73.871	4.100	35.270	4.586	39.919
592.387	6.340	87.846	3.753	92.619	7.601	78.927	2.456	95.183	0.707	98.874	0	98.114	5.956	79.827	4.770	40.040	5.506	45.425
678.504	4.589	92.435	2.740	95.359	6.432	85.359	1.913	97.096	0.459	99.333	0	98.114	5.299	85.126	5.508	45.547	6.421	51.847
777.141	3.079	95.514	1.908	97.267	4.981	90.341	1.462	98.557	0.256	99.589	0	98.114	4.368	89.494	6.249	51.797	7.122	58.969
890.116	1.975	97.489	1.309	98.577	3.615	93.956	0.812	99.369	0.137	99.726	0	98.114	3.409	92.903	7.009	58.806	7.502	66.471
1019.515	1.219	98.708	0.800	99.377	2.467	96.423	0.451	99.821	0.110	99.836	0	98.114	2.516	95.419	7.552	66.358	7.285	73.756
1167.725	0.730	99.438	0.444	99.821	1.610	98.033	0.176	99.997	0.090	99.926	0	98.114	1.778	97.197	7.606	73.964	6.498	80.254
1337.481	0.406	99.844	0.169	99.989	1.020	99.054	0	99.997	0.075	100.00	0	98.114	1.215	98.412	6.928	80.892	5.360	85.614

B.52

Diameter (µm)	C9515 B38XK6		C9515 B38XK9		C9518 B38Y11		C9518 B38Y17		C9519 B38YC9		C9519 B38YF8		C9519 B38YH2		C9519 B38YH9		C9519 B38YK0	
	PSD	Cum-ulative	PSD	Cum-ulative	PSD	Cum-ulative	PSD	Cum-ulative	PSD	Cum-ulative	PSD	Cum-ulative	PSD	Cum-ulative	PSD	Cum-ulative	PSD	Cum-ulative
1531.914	0.097	99.941	0	99.989	0.590	99.643	0	99.997	0	100.00	0	98.114	0.791	99.203	5.659	86.550	4.137	89.750
1754.613	0	99.941	0	99.989	0.327	99.971	0	99.997	0	100.00	0	98.114	0.439	99.642	4.247	90.797	3.042	92.792
2009.687	0	99.941	0	99.989	0	99.971	0	99.997	0	100.00	0	98.114	0.188	99.830	3.050	93.847	2.170	94.962
2301.841	0	99.941	0	99.989	0	99.971	0	99.997	0	100.00	0	98.114	0	99.830	2.178	96.024	1.543	96.505
2636.467	0	99.941	0	99.989	0	99.971	0	99.997	0	100.00	0	98.114	0	99.830	1.459	97.483	1.075	97.580
3000	0	99.941	0	99.989	0	99.971	0	99.997	0	100.00	0	98.114	0	99.830	0.846	98.329	0.568	98.149
4000	0.061	100.00	0.011	100.00	0.031	100.00	0.005	100.00	0	100.00	1.888	100.00	0.173	100.00	1.672	100.00	1.854	100.00

Table B.2. Particle Size Data for Borehole C9520

Diameter (µm)	B32H63 PSD	B32H63 Cumulative	B32H71 PSD	B32H71 Cumulative	B32H79 PSD	B32H79 Cumulative	B32H91 PSD	B32H91 Cumulative	B32HB3 PSD	B32HB3 Cumulative
0.011	0	0	0	0	0	0	0	0	0	0
0.013	0	0	0	0	0	0	0	0	0	0
0.015	0	0	0	0	0	0	0	0	0	0
0.017	0	0	0	0	0	0	0	0	0	0
0.02	0	0	0	0	0	0	0	0	0	0
0.023	0	0	0	0	0	0	0	0	0	0
0.026	0	0	0	0	0	0	0	0	0	0
0.03	0	0	0	0	0	0	0	0	0	0
0.034	0	0	0	0	0	0	0	0	0	0
0.039	0	0	0	0	0	0	0	0	0	0
0.044	0	0	0	0	0	0	0	0	0	0
0.051	0	0	0	0	0	0	0	0	0	0
0.058	0	0	0	0	0	0	0	0	0	0
0.067	0	0	0	0	0	0	0	0	0	0
0.076	0	0	0	0	0	0	0	0	0	0
0.087	0	0	0	0	0	0	0	0	0	0
0.1	0	0	0	0	0	0	0	0	0	0
0.115	0	0	0	0	0	0	0	0	0	0
0.131	0	0	0	0	0	0	0.013	0.013	0.020	0.020
0.15	0	0	0	0	0.050	0.050	0.056	0.070	0.084	0.103
0.172	0	0	0.016	0.016	0.166	0.216	0.151	0.220	0.228	0.332
0.197	0	0	0.041	0.057	0.332	0.548	0.225	0.446	0.346	0.678
0.226	0	0	0.085	0.142	0.428	0.976	0.211	0.657	0.327	1.006
0.259	0	0	0.158	0.300	0.453	1.429	0.167	0.824	0.259	1.265
0.296	0	0	0.240	0.540	0.301	1.730	0.082	0.906	0.127	1.391
0.339	0	0	0.288	0.828	0.123	1.853	0.026	0.932	0.039	1.430
0.389	0	0	0.276	1.104	0.032	1.885	0	0.932	0	1.430
0.445	0	0	0.214	1.318	0	1.885	0	0.932	0	1.430
0.51	0	0	0.140	1.458	0	1.885	0	0.932	0	1.430
0.584	0	0	0.083	1.541	0	1.885	0	0.932	0	1.430
0.669	0	0	0.047	1.588	0	1.885	0	0.932	0	1.430
0.766	0	0	0.028	1.616	0	1.885	0	0.932	0	1.430
0.877	0	0	0.018	1.634	0	1.885	0	0.932	0	1.430
1.005	0.019	0.019	0.009	1.643	0	1.885	0	0.932	0	1.430
1.151	0.023	0.042	0	1.643	0	1.885	0	0.932	0	1.430
1.318	0.031	0.074	0.005	1.648	0	1.885	0	0.932	0	1.430
1.51	0.046	0.119	0.017	1.665	0	1.885	0	0.932	0	1.430
1.729	0.070	0.190	0.024	1.689	0	1.885	0	0.932	0	1.430
1.981	0.110	0.300	0.038	1.726	0	1.885	0	0.932	0	1.430
2.269	0.169	0.469	0.060	1.786	0	1.885	0	0.932	0	1.430
2.599	0.244	0.713	0.092	1.878	0	1.885	0	0.932	0	1.430
2.976	0.327	1.040	0.133	2.012	0.032	1.917	0.016	0.948	0.018	1.448
3.409	0.402	1.441	0.179	2.191	0.086	2.003	0.043	0.990	0.053	1.501

Diameter	B32H63		B32H71		B32H79		B32H91		B32HB3	
(µm)	PSD	Cumulative	PSD	Cumulative	PSD	Cumulative	PSD	Cumulative	PSD	Cumulative
3.905	0.459	1.901	0.222	2.413	0.189	2.192	0.095	1.085	0.128	1.629
4.472	0.499	2.400	0.261	2.674	0.348	2.540	0.175	1.259	0.253	1.882
5.122	0.529	2.929	0.296	2.969	0.554	3.094	0.278	1.538	0.425	2.307
5.867	0.560	3.489	0.331	3.301	0.788	3.882	0.393	1.930	0.622	2.929
6.72	0.598	4.087	0.373	3.674	1.016	4.897	0.498	2.428	0.808	3.737
7.697	0.646	4.733	0.424	4.097	1.193	6.090	0.572	3.001	0.935	4.672
8.816	0.704	5.438	0.484	4.581	1.279	7.369	0.599	3.600	0.970	5.642
10.097	0.766	6.203	0.551	5.132	1.273	8.642	0.581	4.181	0.922	6.564
11.565	0.826	7.029	0.624	5.756	1.196	9.838	0.531	4.712	0.819	7.382
13.246	0.877	7.907	0.696	6.452	1.004	10.842	0.434	5.146	0.640	8.023
15.172	0.899	8.806	0.749	7.201	0.764	11.606	0.324	5.469	0.451	8.474
17.377	0.883	9.689	0.767	7.968	0.553	12.158	0.232	5.702	0.304	8.778
19.904	0.835	10.524	0.745	8.713	0.412	12.570	0.174	5.876	0.215	8.992
22.797	0.771	11.295	0.693	9.407	0.341	12.911	0.148	6.024	0.175	9.167
26.111	0.706	12.001	0.624	10.031	0.330	13.242	0.149	6.173	0.172	9.339
29.907	0.650	12.651	0.552	10.583	0.373	13.614	0.176	6.349	0.203	9.542
34.255	0.607	13.258	0.484	11.067	0.468	14.082	0.231	6.580	0.273	9.816
39.234	0.578	13.836	0.427	11.494	0.604	14.686	0.305	6.885	0.376	10.192
44.938	0.645	14.481	0.378	11.872	0.821	15.507	0.358	7.243	0.468	10.660
51.471	0.662	15.143	0.327	12.199	0.914	16.421	0.359	7.601	0.502	11.162
58.953	0.702	15.846	0.333	12.532	0.917	17.338	0.299	7.900	0.568	11.730
67.523	0.787	16.633	0.356	12.888	0.876	18.214	0.310	8.210	0.531	12.261
77.34	0.959	17.592	0.381	13.269	0.947	19.161	0.278	8.488	0.537	12.798
88.583	1.269	18.861	0.447	13.716	1.137	20.299	0.285	8.773	0.613	13.411
101.46	1.688	20.549	0.543	14.259	1.374	21.672	0.332	9.104	0.749	14.160
116.21	2.085	22.634	0.638	14.897	1.518	23.190	0.398	9.502	0.879	15.040
133.103	2.585	25.219	0.765	15.662	1.724	24.914	0.478	9.980	1.029	16.069
152.453	3.233	28.452	0.939	16.601	2.027	26.941	0.593	10.573	1.219	17.288
174.616	4.052	32.504	1.168	17.769	2.467	29.408	0.737	11.310	1.466	18.754
200	5.049	37.554	1.445	19.214	3.088	32.496	0.913	12.223	1.771	20.525
229.075	6.141	43.695	1.761	20.975	3.897	36.393	1.118	13.341	2.111	22.636
262.376	7.137	50.832	2.080	23.055	4.852	41.245	1.328	14.670	2.476	25.112
300.518	7.777	58.609	2.392	25.447	5.889	47.134	1.548	16.217	2.871	27.984
344.206	8.114	66.724	2.757	28.204	6.984	54.118	1.876	18.093	3.379	31.362
394.244	8.040	74.763	3.239	31.442	7.993	62.110	2.352	20.445	4.057	35.420
451.556	7.330	82.093	3.816	35.258	8.428	70.538	3.025	23.470	4.827	40.247
517.2	5.987	88.081	4.430	39.689	7.889	78.428	3.863	27.333	5.520	45.767
592.387	4.488	92.569	5.169	44.858	6.697	85.125	4.959	32.292	6.173	51.939
678.504	3.112	95.681	6.001	50.859	5.207	90.332	6.323	38.615	6.711	58.650
777.141	1.989	97.670	6.767	57.626	3.709	94.042	7.776	46.391	6.955	65.605
890.116	1.214	98.884	7.395	65.021	2.498	96.539	9.110	55.501	6.924	72.528
1019.515	0.717	99.601	7.590	72.611	1.600	98.139	9.787	65.287	6.520	79.048
1167.725	0.398	100.000	7.175	79.786	0.999	99.138	9.409	74.697	5.774	84.821
1337.481	0	100.000	6.149	85.935	0.555	99.693	7.984	82.680	4.756	89.577
1531.914	0	100.000	4.780	90.715	0.308	100.001	6.058	88.739	3.631	93.208

Diameter	B32H63		B32H71		B32H79		B32H91		B32HB3	
(μm)	PSD	Cumulative	PSD	Cumulative	PSD	Cumulative	PSD	Cumulative	PSD	Cumulative
1754.613	0	100.000	3.450	94.166	0	100.001	4.252	92.990	2.605	95.813
2009.687	0	100.000	2.405	96.570	0	100.001	2.890	95.880	1.816	97.629
2301.841	0	100.000	1.683	98.254	0	100.001	1.980	97.860	1.282	98.912
2636.467	0	100.000	1.143	99.396	0	100.001	1.400	99.260	0.712	99.624
3000	0	100.000	0.604	100.001	0	100.001	0.740	100.001	0.377	100.001
4000	0	100.000	0	100.001	0	100.001	0	100.001	0	100.001

Table B.3. Soil Resistivity Measurements for Borehole C9520

Sample ID	Depth (ft bgs)	Resistivity (ohm-m)	Standard Deviation (ohm-m)
B32H62	37.75	59.04	0.02
B32H63	38.25	97.50	0.82
B32H70	42.65	1188.14	0.31
B32H71	43.15	947.66	4.66
B32H78	46.95	402.88	2.56
B32H79	47.45	242.30	0.59
B32H90	54.25	549.48	1.17
B32H91	54.75	1075.78	4.88
B32HB2	61.75	255.30	0.83
B32HB3	62.25	245.77	2.71

Appendix C

Additional Core Analysis Data

Appendix C

Additional Core Analysis Data

Several categories of additional data were collected for the C9520 borehole as shown below.

Table C.1. Air Permeability Data for Core C9520 (For Information Only)

Sample ID	Soil Bulk Density (g/cm³)	Gravimetric Moisture Content (g/g)	Air Permeability (darcy)	Stand Deviation (darcy)	Percent Error
B32H90	1.64	0.019	52.26	3.98	7.61
B32HB2	1.66	0.026	0.28	0.00	1.09
B32HB3	1.29	0.028	31.38	2.79	8.89
B32H78	1.55	0.042	21.99	0.59	2.68
B32H70	1.77	0.027	38.74	11.37	29.34
B32H71	1.18	0.032	30.90	7.75	25.09
B32H62	1.61	0.065	0.75	1.11	147.34
B32H49	1.78	0.044	23.09	0.92	4.00
B32H50	1.63	0.095	14.73	6.29	42.69
B32H52	1.80	0.038	2.45	0.82	33.49
B32H53	1.55	0.136	1.94	0.73	37.41
B32H54	1.65	0.091	0.06	0.02	29.95
B32H56	1.73	0.038	10.33	5.58	54.02
B32H58	1.45	0.135	15.61	9.25	59.24
B32H57	1.49	0.121	0.92	0.40	43.07
B32H60	1.69	0.075	4.67	2.97	63.47
B32H61	1.63	0.104	1.04	0.70	67.01
B32H68	1.61	0.055	3.58	1.17	32.83
B32H69	1.60	0.047	9.10	1.10	12.05
B32H72	1.75	0.063	1.81	0.48	26.67
B32H73	1.71	0.049	1.64	0.19	11.36
B32H74	1.82	0.036	1.13	1.17	104.20
B32H75	1.45	0.031	8.31	2.97	35.77
B32H76	1.68	0.044	0.49	0.28	57.60
B32H77	1.57	0.041	4.34	0.54	12.39
B32H81	1.64	0.052	4.32	0.53	12.20
B32H82	1.48	0.115	0.24	0.16	65.77
B32H83	1.46	0.063	6.17	0.87	14.03
B32H84	1.82	0.026	2.93	0.30	10.34

Sample ID	Soil Bulk Density (g/cm^3)	Gravimetric Moisture Content (g/g)	Air Permeability (darcy)	Stand Deviation (darcy)	Percent Error
B32H85	1.67	0.024	20.96	2.98	14.23
B32H86	1.67	0.034	41.88	2.32	5.53
B32H87	1.34	0.040	15.54	2.34	15.05
B32H88	1.75	0.105	4.96	1.83	36.86
B32H89	1.65	0.040	0.26	0.01	3.68
B32H92	1.76	0.025	1.39	0.46	33.09
B32H93	1.64	0.022	2.57	0.33	13.01
B32H94	1.55	0.019	27.90	5.48	19.64
B32H96	1.73	0.028	1.60	1.00	62.32
B32H97	1.57	0.052	1.61	0.62	38.39
B32H98	1.50	0.055	6.80	0.63	9.26
B32HB0	1.71	0.017	1.02	0.54	52.87
B32HB1	1.61	0.026	25.91	1.93	7.45
B32HB4	1.81	0.023	2.70	0.75	27.99
B32HB5	1.79	0.025	1.34	0.73	54.07
B32HB6	1.62	0.026	8.74	1.62	18.51
B32HB8	1.73	0.025	1.89	0.20	10.83
B32HB9	1.64	0.027	2.53	1.27	50.32
B32HC0	1.55	0.018	37.23	5.39	14.47
B32HC1	1.24	0.024	48.40	6.27	12.97
B32HC2	1.63	0.016	2.19	0.17	7.93
B32HC3	1.55	0.020	23.79	6.27	26.34
B32HC4	1.55	0.023	53.75	1.59	2.96
B32HC6	1.76	0.026	1.84	0.71	38.39
B32HC7	1.63	0.020	0.92	0.58	62.90
B32HC8	1.60	0.025	21.49	1.59	7.40
B32HC9	1.46	0.044	28.82	21.07	73.10
B32HD0	1.73	0.029	5.76	1.02	17.78
B32HD1	1.59	0.021	14.71	0.60	4.05
B32HD2	1.60	0.017	48.86	3.50	7.16
B32HD3	1.36	0.023	41.70	9.94	23.84
B32HD4	1.70	0.018	0.35	0.25	70.59
B32HD5	1.60	0.025	10.54	1.97	18.69
B32HD6	1.58	0.020	37.76	0.93	2.47
B33OH0	1.72	0.018	1.41	0.09	6.67
B33OH1	1.60	0.021	28.31	3.26	11.52
B33OH2	1.58	0.024	42.75	6.10	14.26

Table C.2. Core Gamma Scan Data for Borehole C9520 (For Information Only)

Core ID	Depth	Count Rate[a] (dpm)
B32H62	37.5-38	60000
B32H63	38-38.5	60000
B32H70	42.4-42.9	50000
B32H71	42.9-43.4	40000
B32H78	46.7-47.2	45000
B32H79	47.2-47.7	40000
B32H90	54-54.5	1500
B32H91	54.5-55	1500
B32HB2	61.5-62	1500
B32HB3	62-62.5	1500
B32H48	29.7-30.2	2500
B32H49	30.2-30.7	2500/20000
B32H50	30.7-31.2	22000/40000
B32H51	31.2-31.7	45000/40000
B32H52	32.4-32.9	45000/175000
B32H53	32.9-33.4	15000/25000
B32H54	33.4-33.9	20000/20000
B32H55	33.9-34.4	25000/20000
B32H56	34.4-34.9	37500/68000
B32H57	34.9-35.4	80000/150000
B32H58	35.4-35.9	175000/85000
B32H59	35.9-36.4	90000/95000
B32H60	36.5-37.0	150000/175000
B32H61	37-37.5	200000/200000
B32H66	39-39.5	80000
B32H67	39.5-40	125000
B32H68	41.4-41.9	150000/150000
B32H69	41.9-42.4	150000/110000
B32H72	43.7-44.2	150000/150000
B32H73	44.2-44.7	160000/130000
B32H74	44.7-45.2	125000/250000
B32H75	45.2-45.7	300000/125000
B32H76	45.7-46.2	150000/350000
B32H77	46.2-46.7	350000/100000
B32H80	47.9-48.4	85000
B32H81	48.4-48.9	70000/17000
B32H82	48.9-49.4	12500/12500

Core ID	Depth	Count Rate[a] (dpm)
B32H83	49.4-50.4	10000/8500
B32H84	50.7-51.2	3000/<1000
B32H85	51.2-51.7	<1000
B32H86	51.7-52.2	<1000/1500
B32H87	52.2-53.2	1500/1750
B32H88	53.0-53.5	2000/3000
B32H89	53.5-54	3000/3000
B32H92	55.2-55.7	1000/<1000
B32H93	55.7-56.2	1000/<1000
B32H94	56.2-56.7	<1000/<1000
B32H95	56.7-57.2	<1000/1000
B32H96	57.4-57.9	1500/2500
B32H97	57.9-58.4	3000/2500
B32H98	58.4-58.9	3000/2500
B32H99	58.9-59.4	4000/4500
B32HB0	60.5-61	4500/3500
B32HB1	61-61.5	4500/3500
B32HB4	62.6-63.1	4500/5000
B32HB5	363.1-63.6	4500/4000
B32HB6	63.6-64.1	3000/4000
B32HB7	64.1-64.6	3500/3000
B32HB8	64.7-65.2	4500/3500
B32HB9	65.2-65.7	3000/3000
B32HC0	65.7-66.2	3000/3000
B32HC1	66.2-66.7	4000/3500
B32HC2	68.1-68.6	2000/2000
B32HC3	68.6-69.1	2000/2000
B32HC4	69.1-69.6	2000/2000
B32HC5	69.6-70.1	1000/1000
B32HC6	69.9-70.4	2500/2000
B32HC7	70.4-70.9	2000/1000
B32HC8	70.9-71.4	1000/1000
B32HC9	71.4-71.9	2000/3500
B32HD0	72.7-73.2	2500/1500
B32HD1	73.2-73.7	1500/1500
B32HD2	73.7-74.2	2000/1000
B32HD3	74.2-74.7	1000/1000
B32HD4	74.9-75.4	1000/1000

Core ID	Depth	Count Rate[a] (dpm)
B32HD5	75.4-75.9	1000/<1000
B32HD6	75.9-76.4	<1000/<1000
B32HD7	76.4-76.9	<1000/<1000
B33OH0	77.6-78.1	<1000/<1000
B33OH1	78.1-78.6	<1000/<1000
B33OH2	78.6-79.1	<1000/<1000
B33OH3	79.1-79.6	<1000/<1000

(a) Where one number is presented, it is a measurement for the top of the core sample. Where two numbers are presented, they are the top/bottom measurements

Appendix D

Sequential Extraction and Soil Column Data for the 216-U-8 Field Site Samples

Appendix D

Sequential Extraction and Soil Column Data for the 216-U-8 Field Site Samples

Sequential extractions and soil column leaching tests were conducted for field site sediments for untreated and ammonia-treated conditions. Sequential extraction results are reported in tabular form in the main text and using stacked bar charts in this appendix. Soil column results are provided as figures with column effluent concentrations and cumulative leached mass included on each figure. Figures for pre- and post-leaching sequential extraction results and soil column results for samples are grouped together in this appendix. Uranium data are presented first, followed by data for Cs-137 and Sr-90. Data for Tc-99 were all below detection limits.

Untreated   Treated

Pre-Leach
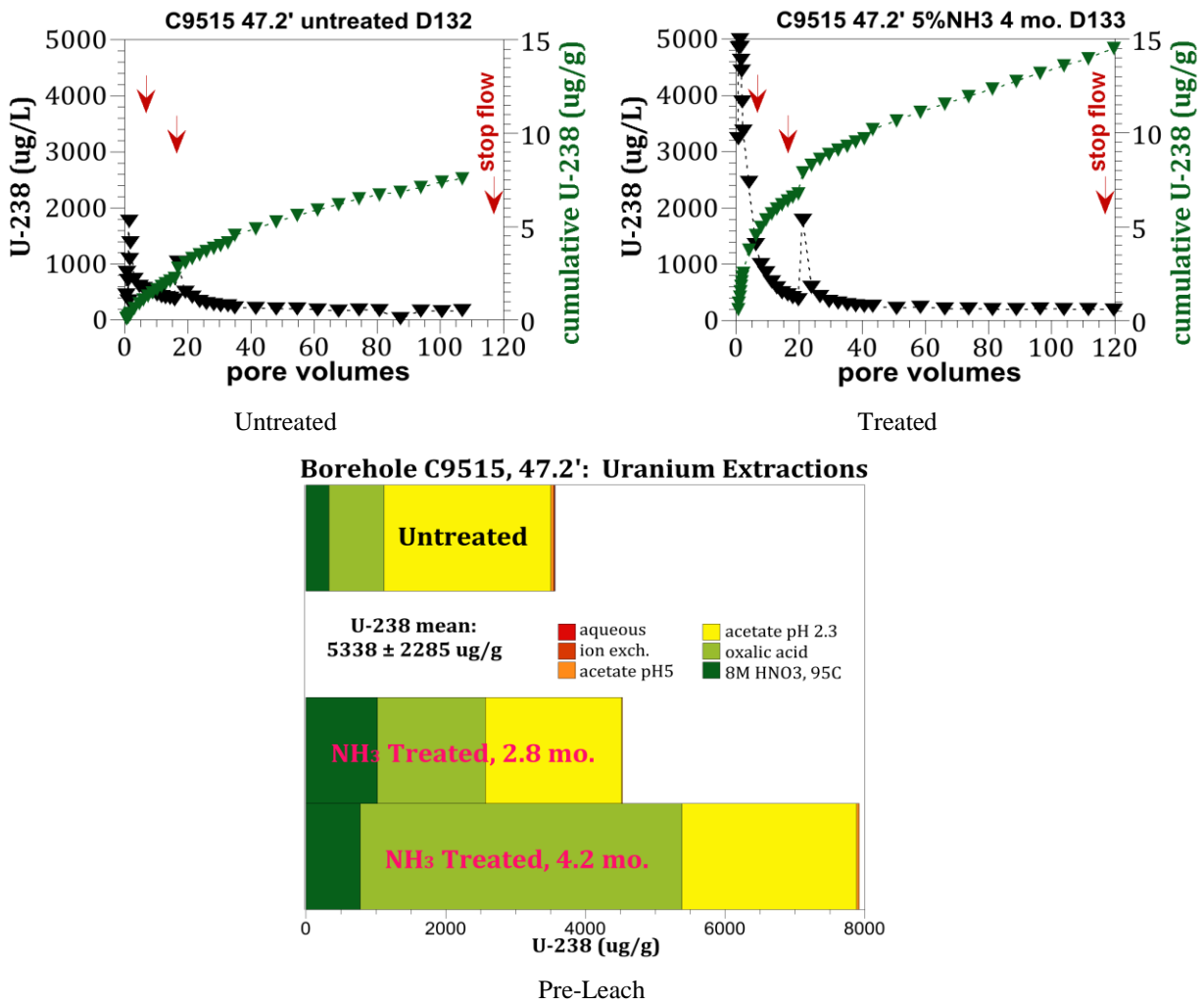
Figure D.1. Borehole C9515 Sample B38XK6
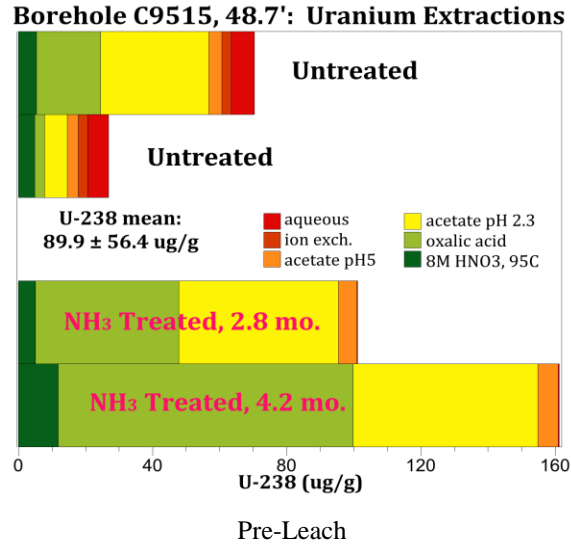
Figure D.2. Borehole C9515 Sample B38XK9
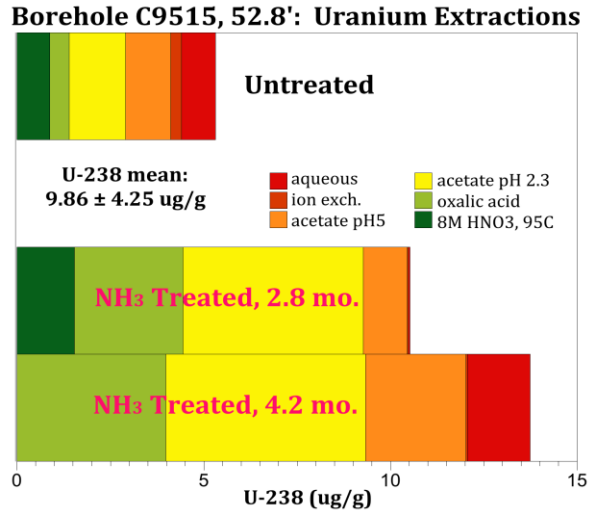
Figure D.3. Borehole C9515 Sample B38XM5
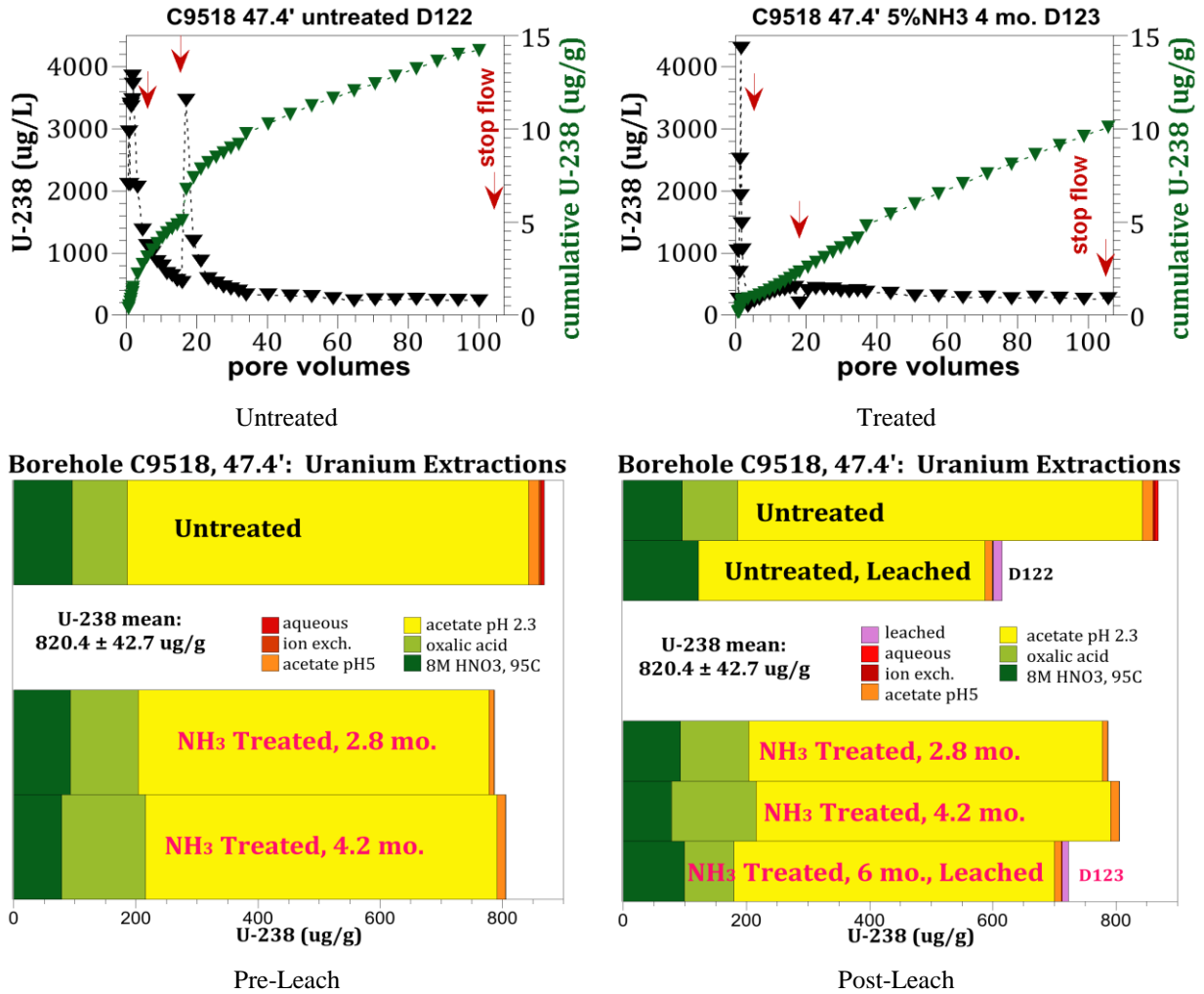
Figure D.4. Borehole C9518 Sample B38Y11

Borehole C9518, 48.9': Uranium Extractions
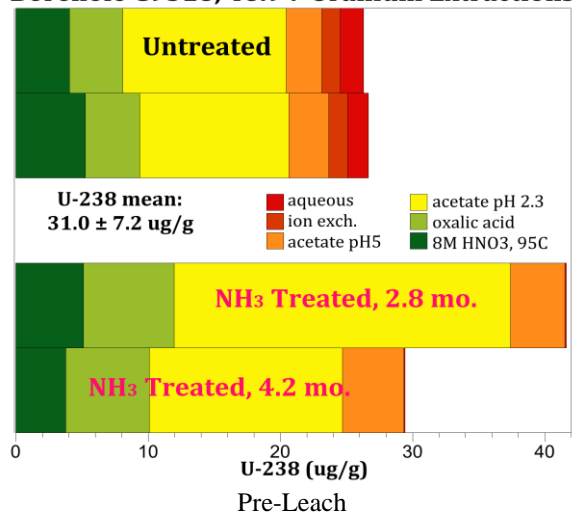
Figure D.5. Borehole C9518 Sample B38Y17

Borehole C9518, 52.9': Uranium Extractions
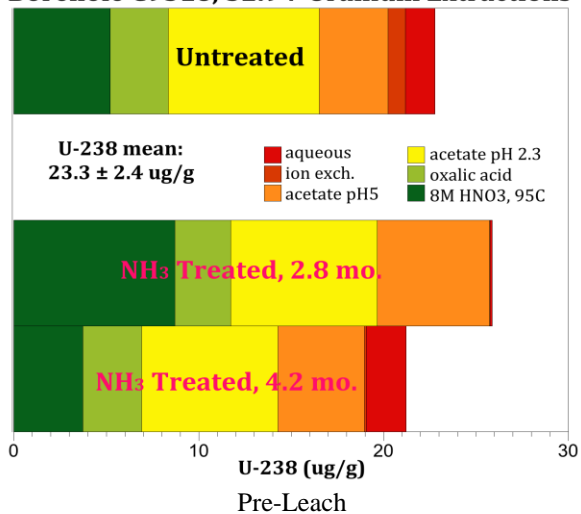
Figure D.6. Borehole C9518 Sample B38Y29
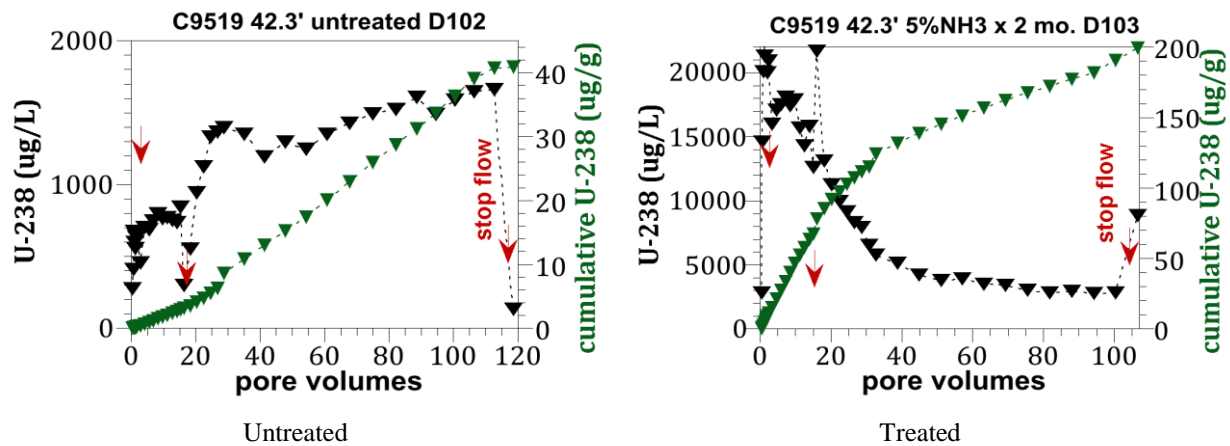
Untreated   Treated
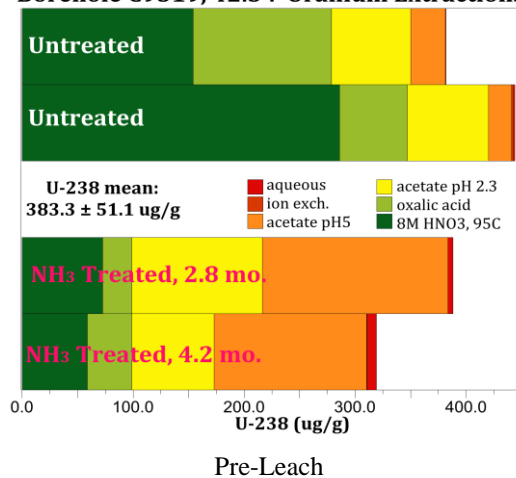
Pre-Leach

Figure D.7. Borehole C9519 Sample B38YC9

Untreated   Treated

Pre-Leach   Post-Leach
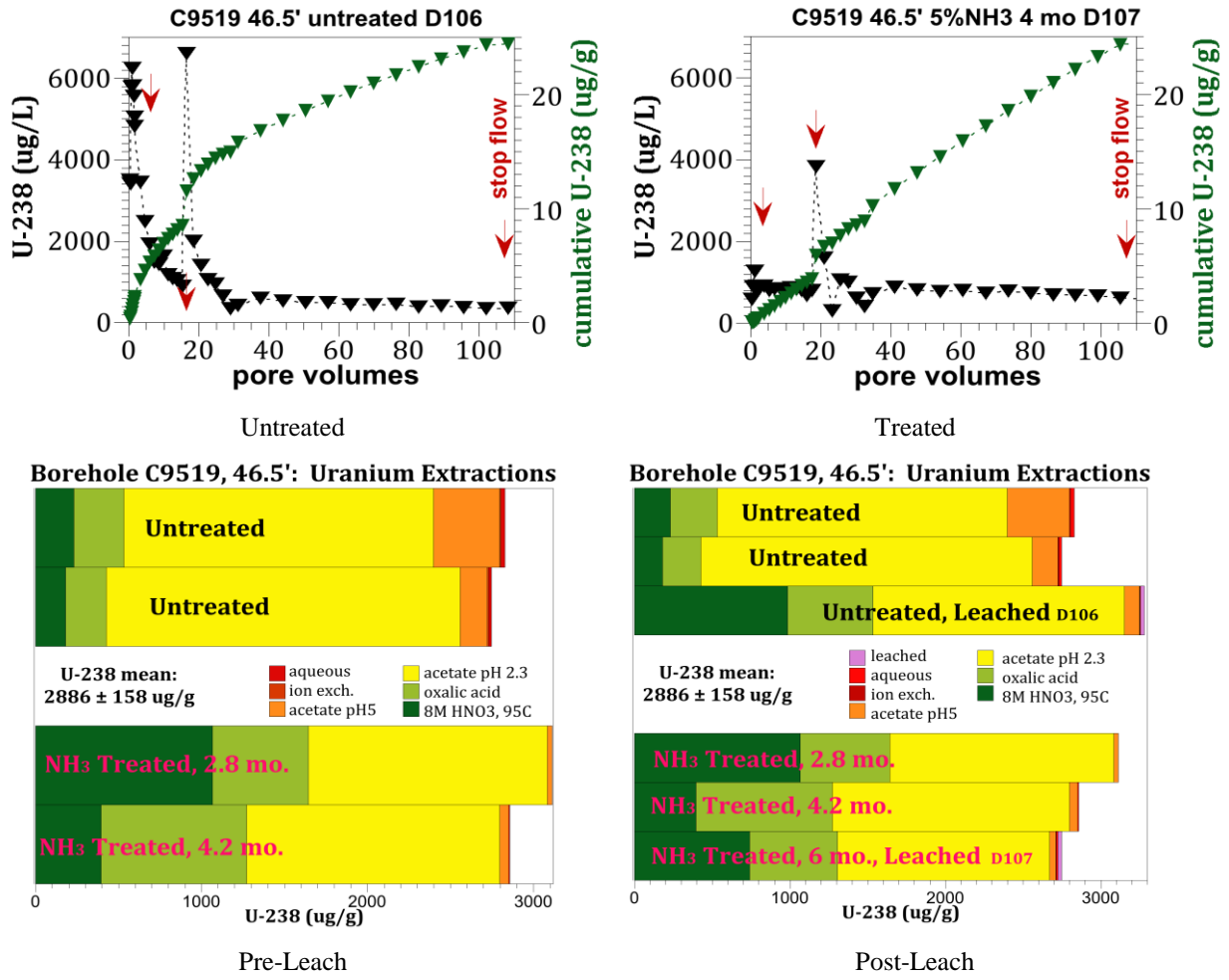
Figure D.8. Borehole C9519 Sample B38YF8

Untreated
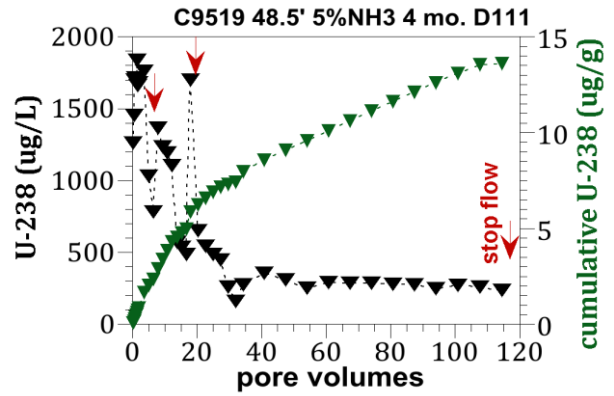
Treated

Pre-Leach

Post-Leach

Figure D.9. Borehole C9519 Sample B38YH2

Untreated   Treated
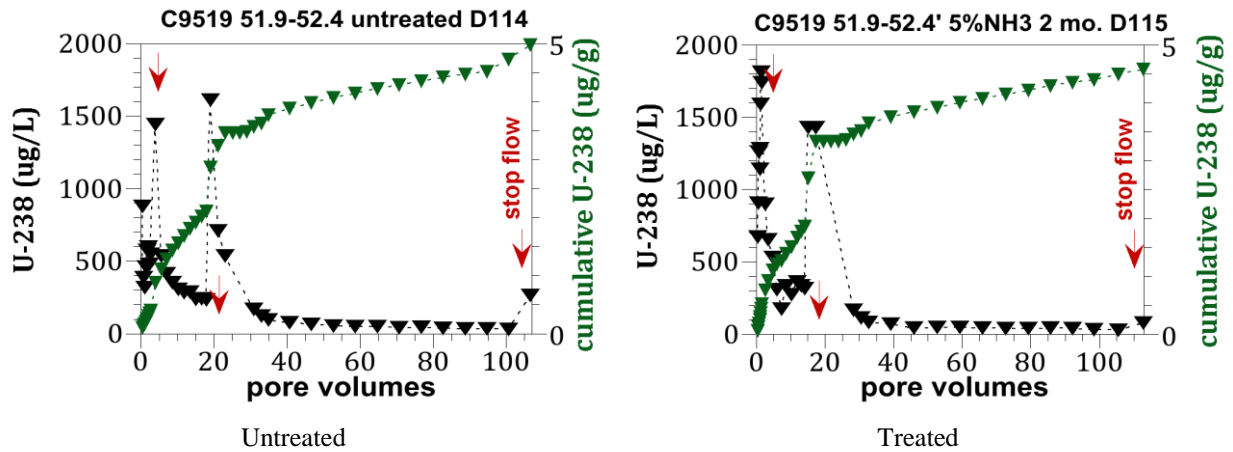
Borehole C9519, 51.9': Uranium Extractions
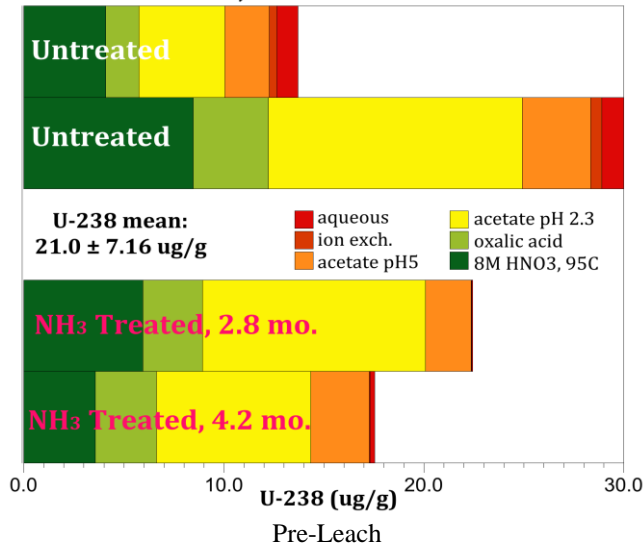
Figure D.10. Borehole C9519 Sample B38YH9

Figure D.11. Borehole C9519 Sample B38YK0

D.9

Untreated · Treated

Pre-Leach · Post-Leach
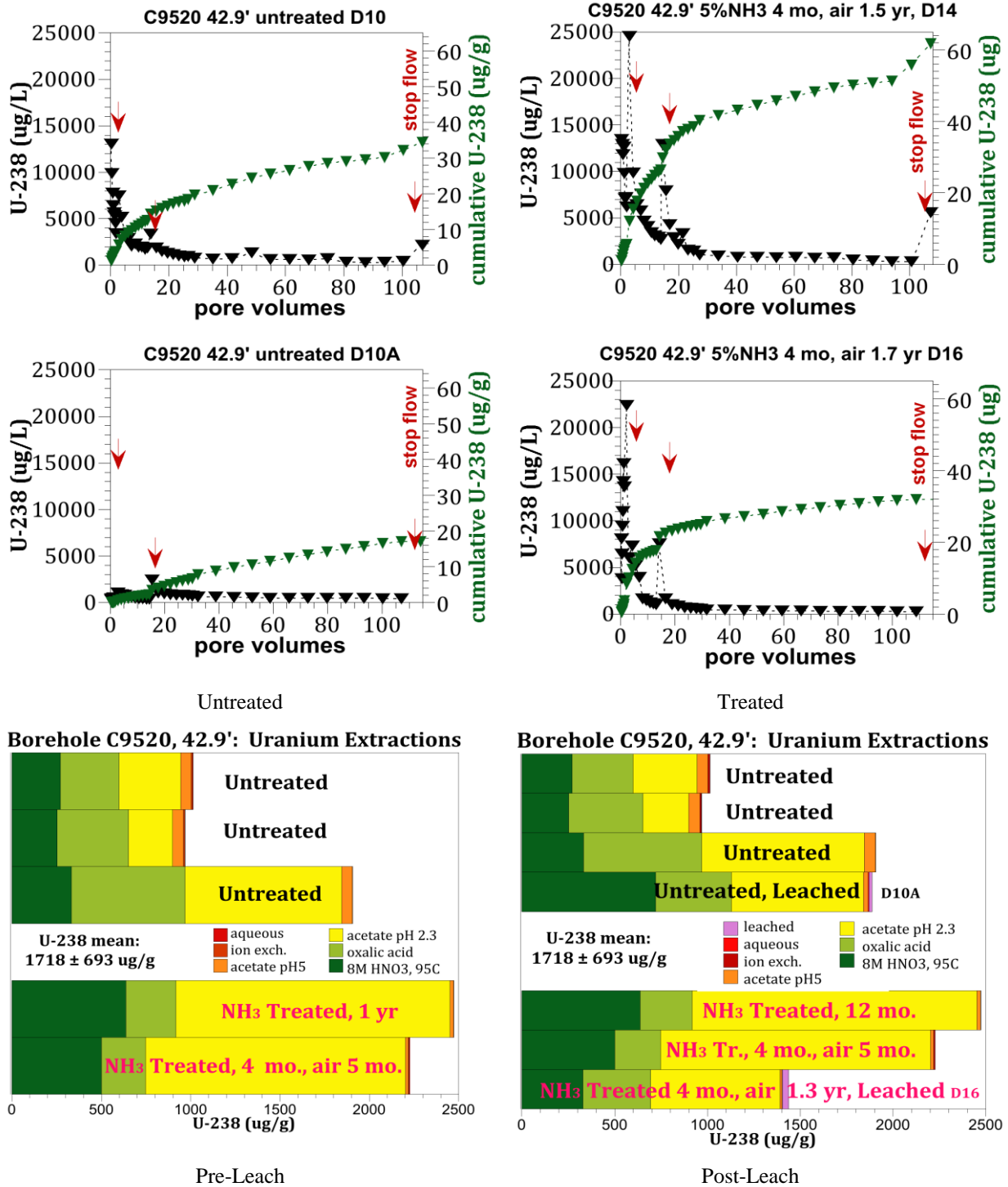
Figure D.12. Borehole C9520 Sample B32H70

Figure D.13. Borehole C9520 Sample B32H78

Figure D.14. Borehole C9515 Sample B38XK6

Figure D.15. Borehole C9518 Sample B38Y11

Figure D.16. Borehole C9519 Sample B38YC9

Figure D.17. Borehole C9519 Sample B38YF8
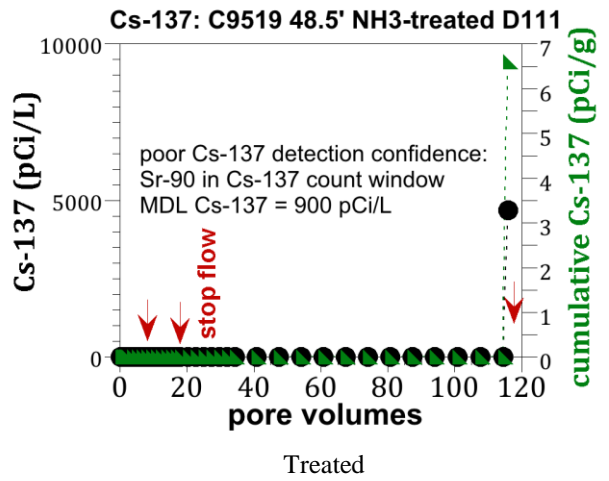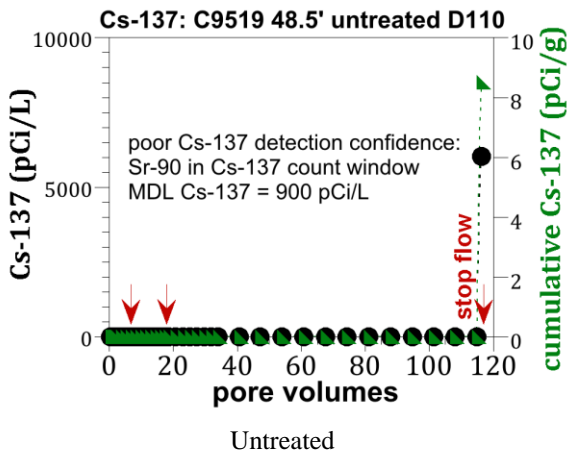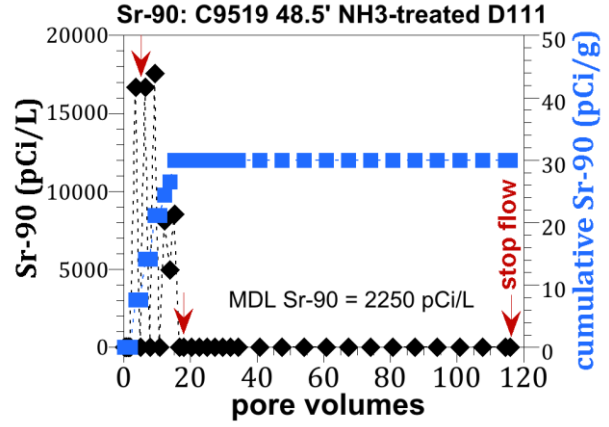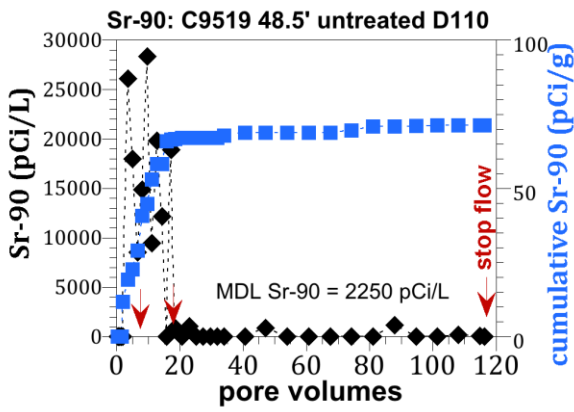
Figure D.18. Borehole C9519 Sample B38YH2

Figure D.19. Borehole C9519 Sample B38YH9

Untreated   Treated
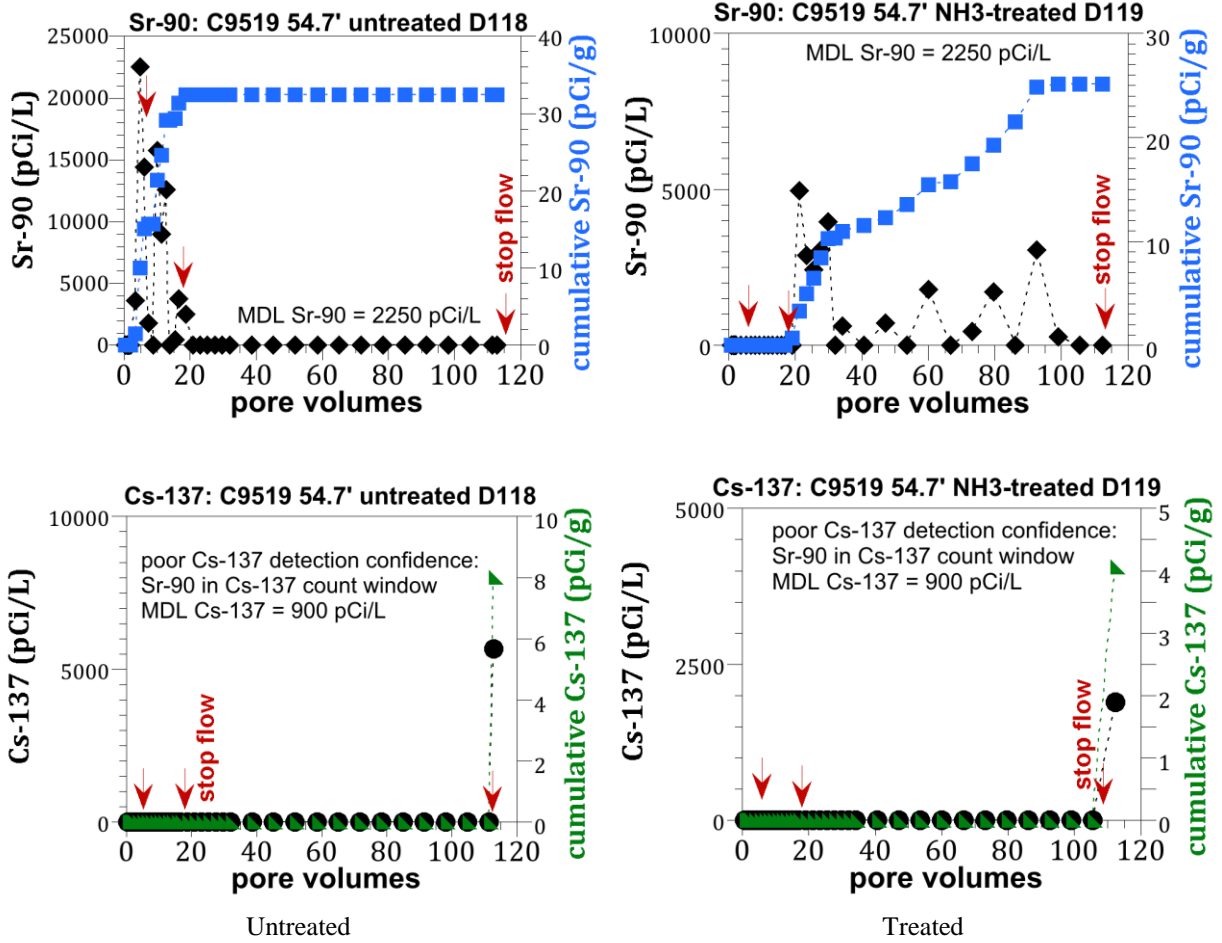
Figure D.20. Borehole C9519 Sample B38YK0
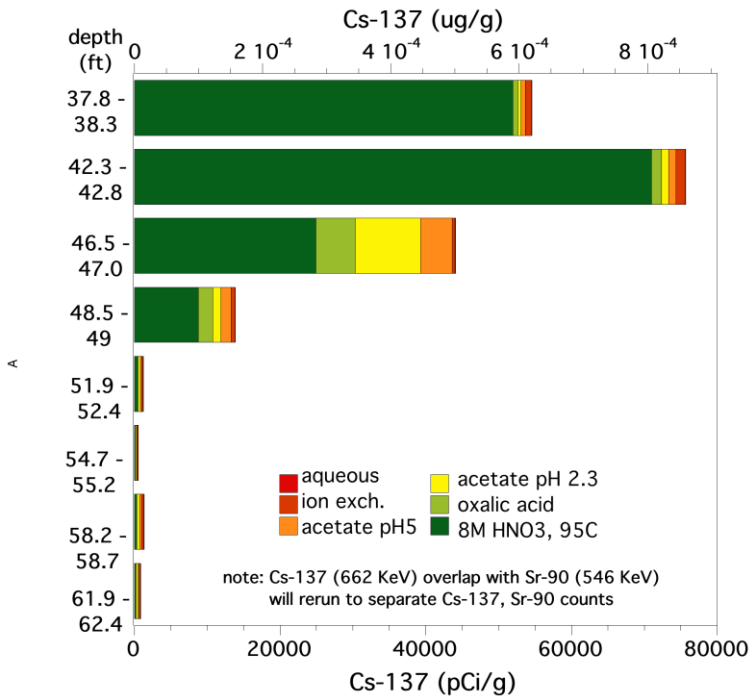
Borehole C9519: Cs-137 Extractions
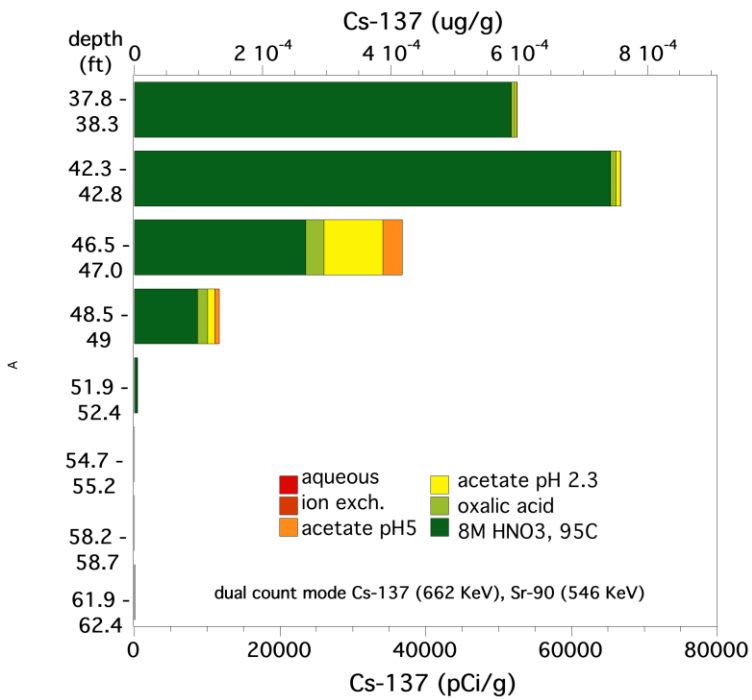
Borehole C9519: Cs-137 Extractions
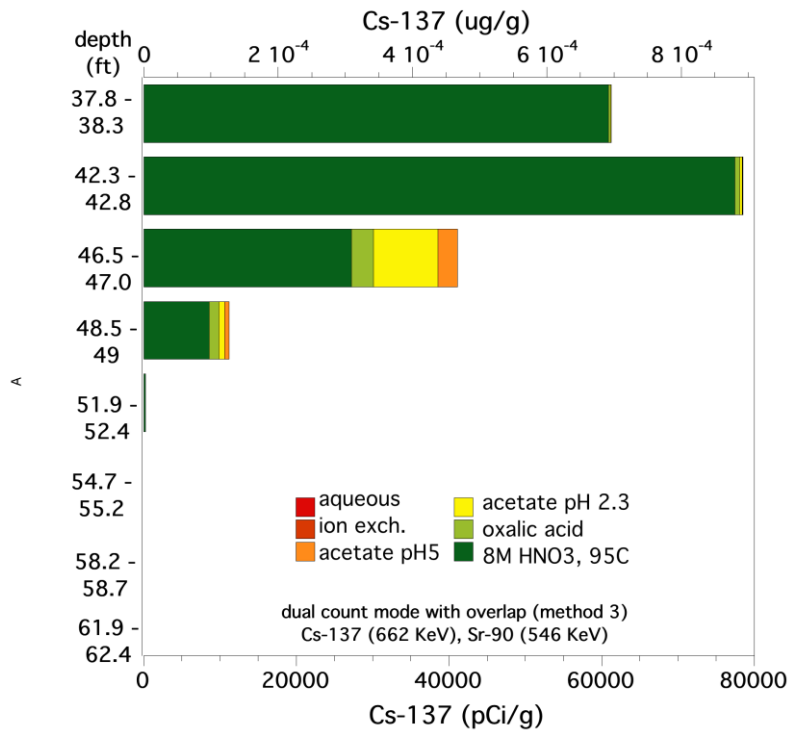
Figure D.21. Borehole C9519 Cs-137 extraction results
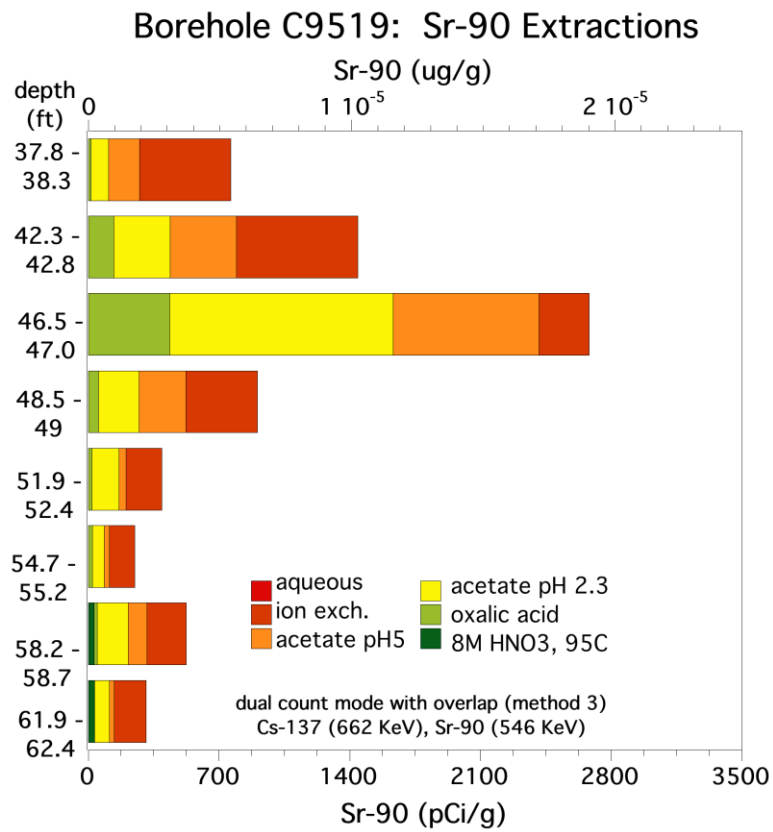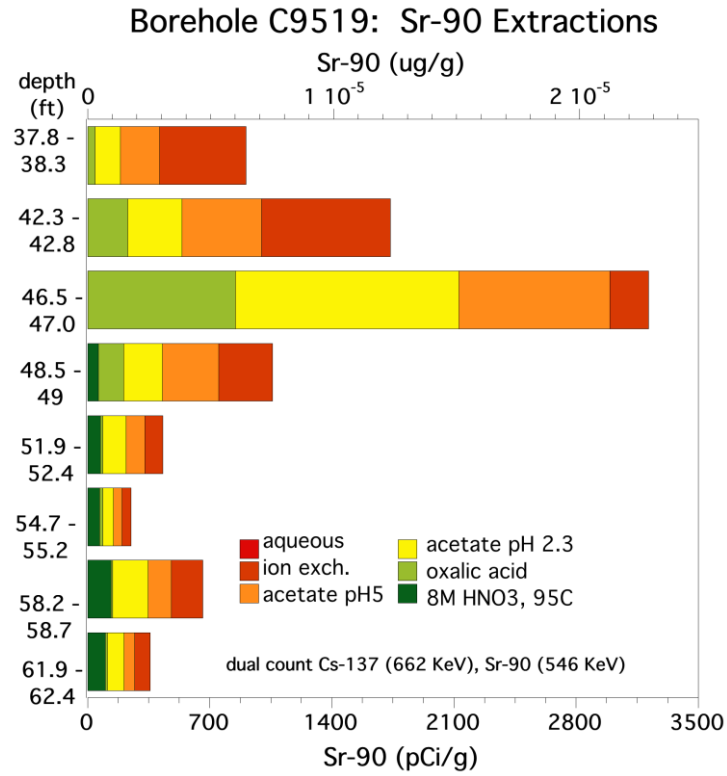
Figure D.22. Borehole C9519 Sr-90 extraction results

Figure D.23. Borehole C9520 Sample B32H70
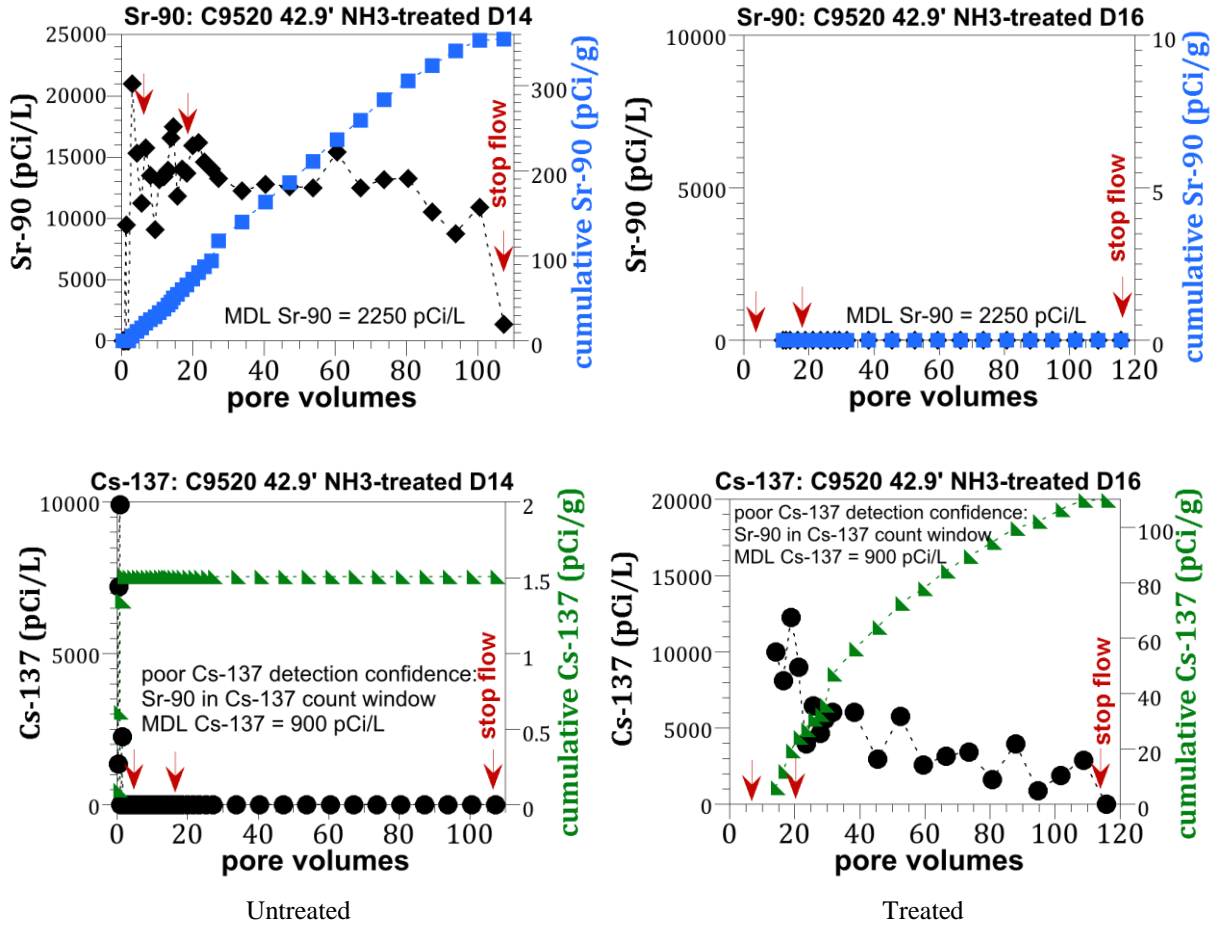
Figure D.24. Borehole C9520 Sample B32H70

Figure D.25. Borehole C9520 Sample B32H78

Figure D.26. Borehole C9520 Sample B32H78

Appendix E

216-U-8 Site-Specific Interference Study Results

Appendix E

216-U-8 Site-Specific Interference Study Results

E.1 Summary

Laboratory tests were applied to evaluate potential causes of the poor ammonia treatment effectiveness observed with laboratory dosing of ammonia to field site sediments. Data are provided in this appendix. Tests showed low sediment carbonate (i.e., calcite) concentrations and low concentrations of uranium associated with the alkaline sediment extraction analysis used to identify carbonate-associated uranium. Sediment carbonate concentrations for 216-U-8 site were in many cases less than 250 µg/g inorganic carbon compared to more typical Hanford sediments such as those evaluated for the BX-102 and TX-104 sites with greater than 1500 µg/g inorganic carbon. In contrast to sediments from basic to neutral waste sites (i.e., BX-102 and TX-104), alkaline extraction of uranium only removed a few percent of the total sediment uranium from untreated field sediments. Further evidence of low uranium carbonate concentrations was obtained in radiography analysis of untreated sediment where uranium hot spots were in locations of low calcium. Low carbonate and carbonate-associated uranium can affect the uranium compound dissolution that is induced by ammonia treatment, the uranium complexation in the pore water during ammonia treatment, and the pH neutralization process that occurs after ammonia injection is terminated. In tests of ammonia treatment for individual sediment minerals (e.g., kaolinite, illite), Emerson et al. (2018) showed significantly better ammonia treatment effectiveness for tests where carbonate was present in the aqueous solution than for tests with a sodium-chloride solution as the aqueous phase. While these tests are not a direct evaluation of Hanford sediment carbonate concentration impacts, the results are consistent with the hypothesis that low carbonate concentrations hinder ammonia treatment effectiveness.

Another factor potentially related to poor ammonia treatment effectiveness was revealed from X-ray fluorescence (XRF) two-dimensional surface analysis of untreated sediment where the uranium was found to be distributed as localized hot spots in the sediment matrix. Having uranium distributed in sparse hot spots rather than more evenly distributed can affect the uranium compound dissolution that is induced by ammonia treatment. A relatively large deposit would be slower to dissolve than fine dispersed deposits of uranium. If uranium is not well dissolved during the treatment process, it may not interact with other pore-water constituents to form low-solubility precipitates. In addition, post-ammonia-treatment surface analysis also showed uranium distributed in sparse hot spots, suggesting poor dissolution during ammonia treatment and likely poor coating by aluminosilicates. Sequential liquid extraction data for uranium showing significant variability for sediments with high uranium concentrations was also consistent with the hot spots of uranium phases observed in XRF data. Laser induced fluorescence spectroscopy (LIFS) identified that uranium was predominantly present as uranophane [$Ca(UO_2)_2(SiO_3OH)_2(H_2O)_5$] with some boltwoodite [$Na(UO_2)(SiO_4)*1.5H_2O$], with very little uranium in other phases. This result is unusual because most Hanford sediments contain a variety of aqueous/adsorbed uranium, uranium associated with

carbonates, and uranium in hydrous silicates (i.e., uranophane and boltwoodite). For instance, in a sediment with high uranium beneath the U-105 tank with 690 µg/g uranium, boltwoodite was identified as a dominant uranium phase, but the sediment also contained other U phases comprising about 20% of the uranium content (Um et al. 2009). This U-105 tank sediment did show effective NH_3 treatment in laboratory studies (Szecsody et al. 2012).

Collectively, these conditions, and potentially others, hindered ammonia treatment effectiveness for the field test site sediments. However, the field test site did not have high organic carbon or organic phosphate concentrations that might indicate the presence of tributyl phosphate or other uranium complexing agents. Other factors were investigated, with some minor evidence that these other factors affected ammonia treatment at the field test site. For instance, a comparison of 5% ammonia (planned for use at field scale) and 100% ammonia treatments for the field site sediments clearly indicates the higher ammonia concentration treatment results in greater mineral dissolution and more rapid aluminosilicate precipitation (one of two mechanisms decreasing U mobility). The change in mobile uranium in these 5% and 100% treatments over time did not parallel the regular decrease in aqueous pH, Si, and Al concentrations. Therefore, while both 5% and 100% ammonia treatments are effective at dissolving (at short time) then precipitating aluminosilicates (at longer time), the lack of decreased uranium mobility may be due to the inability of aluminosilicates to precipitate on (i.e., coat) the uranium hot spots (predominantly uranophane) and/or precipitate as in low-solubility forms in the low carbonate water.

Although some potential interference indicators were identified for the 216-U-8 site, other factors such as those listed in the interference hypotheses (Section 3.2.1.3) could affect the treatment process at other sites. In summary, interference testing identified specific concerns at acidic waste discharge sites where the discharge has altered the sediment carbonate concentrations and caused uranium to be deposited in sparse hot spots in the sediment. The overall treatability test results, including these interference tests, leads to a recommendation that uranium reactive gas sequestration ammonia treatment effectiveness can be impacted by site-specific geochemical factors and site-specific effectiveness testing is needed for evaluation of this technology.

E.2 Hypothesis 1 - U Surface Phase(s) in U-8 Sediments Compared with Previous Sediments

It was hypothesized that the waste chemistry at the U-8 site caused uranium distribution in a way that includes U surface phases different from those present in other previously tested sites or U contained in microfractures, and when ammonia treatment (high pH) is applied, U does not re-precipitate as silicates or get coated by alumino-silicates. The type of data collected to address this hypothesis included a) whole sediment X-ray diffraction (XRD), b) clay-size fraction XRD, c) X-ray absorption near edge structure/extended X-ray absorption fine structure (XANES/EFAFS) U surface phase/valence state identification of untreated and ammonia-treated U-8 sediments, d) LIFS U surface phase identification of untreated and NH_3-treated U-8 sediments, e) XRF U and other element mapping of the spatial heterogeneity of the U on sediment mineral grains, f) total inorganic carbon and total organic carbon on U-8 and other sediments, and g) alkaline extraction of U on U-8 and other sediments.

E.2.1   Mineral Identification by X-ray Diffraction

XRD identification of the U-8 minerals indicates a similar range of major minerals (Figure E.1a, b) that are typically found in the Hanford formation (Table E.1). Of concern was whether the acidic co-contaminants resulted in dissolution of sufficient clay or calcite that would influence the alkaline NH_3 treatment. The 1:1 clay kaolinite was identified by XRD, but calcite was not (typically present at a few percent concentration). Total inorganic carbon extractions of the sediments (following section) more accurately identify low carbonate for the U-8 sediments. The clay-size fraction mineralogy (Figure E.1c) with a high total uranium concentration (5338 µg/g) showed identification of alpha-uranophane.
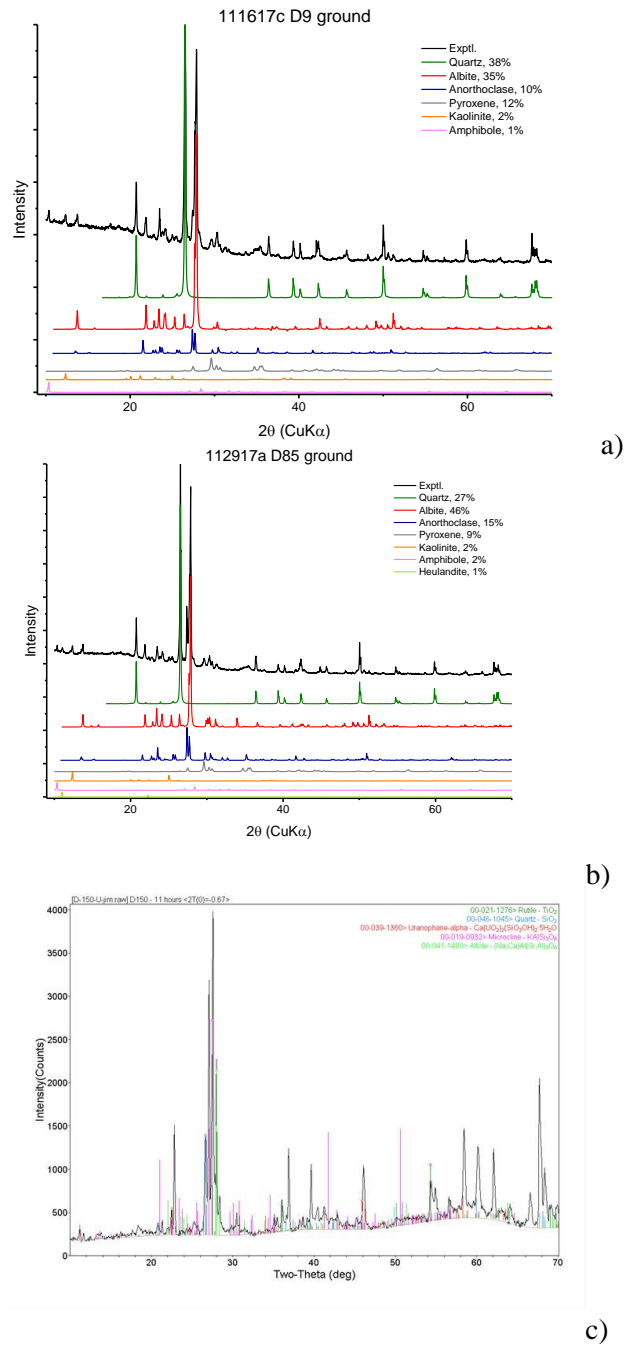
Figure E.1. XRD and mineral identification of a) C9520 42.9' untreated sediment, b) C9519 46.5' untreated sediment, and c) C9515 47' clay-size fraction 5% ammonia-treated 9-months, air 13 months. (For Information Only)

Table E.1. Average mineralogy of Hanford and Ringold formation, as identified by 22 XRD (Xie et al. 2003).

mineral	formula	both Fm (% wt)	Hanford Fm (% wt)	Ringold Fm (% wt)
quartz	SiO_2	37.7 ± 12.4	38.4 ± 12.8	37.03 ± 12.4
microcline	$KAlSi_3O_8$	17.0 ± 6.7	15.3 ± 4.4	18.7 ± 8.0
plagioclase	$NaAlSi_3O_8$-$CaAl_2Si_2O_8$	18.7 ± 7.7	22.2 ± 7.2	15.5 ± 6.8
pyroxenes	$(Ca,Mg,Fe)Si_2O_6$	3.03 ± 5.99	5.01 ± 7.83	1.14 ± 2.52
calcite	$CaCO_3$	4.97 ± 7.19	1.91 ± 1.71	0.68 ± 0.92
magnetite	Fe_3O_4	5.09 ± 4.37	4.46 ± 4.12	5.68 ± 4.63
amphiboles	$Ca_2(Mg, Fe, Al)_5 (Al, Si)_8O_{22}(OH)_2$	5.55 ± 5.97	5.46 ± 5.67	5.64 ± 6.40
apatite	$Ca_{10}(PO_4)_6(OH)_2$	0.60 ± 1.04	0.52 ± 0.92	0.67 ± 1.16
mica*	$(K, Na,Ca)(Al, Mg, Fe)_{2-3}(Si,Al)_4O_{10}(O, F, OH)_2$	2.07 ± 4.47	2.46 ± 3.74	1.71 ± 5.15
ilmenite	$FeTiO_3$	2.51 ± 2.66	1.28 ± 1.51	3.67 ± 3.00
epidote	$\{Ca_2\}\{Al_2Fe^{3+}\}[O\|OH\|SiO_4\|Si_2O_7]$	1.65 ± 2.98	1.78 ± 3.75	1.52 ± 2.14

* muscovite, biotite, phlogopite, lepidolite, clintonite, illite, phengite

E.2.2   Mineral Identification by Extended X-ray Techniques (XANES/EXAFS)

XANES conducted at Stanford Synchrotron Radiation Lightsource (SSRL) and Advanced Photon Source (APS) showed that U(VI) was the dominant phase (74% to 84%) in the untreated and ammonia-treated C9520 43' sediment samples, indicating uranium was present as the uranyl cation in a mineral such as Na-boltwoodite or uranophane (Figure E.2, Table E.2). Two standard spectra were used in the linear combination analysis fitting of the sample XANES spectra: UO_2 and UO_3. Each standard was diluted in cellulose to minimize the effects of self-absorption. Both standards contributed to each sample fit; however, UO_3 was the most dominating phase in all samples. A slight increase in UO_2 and decrease in UO_3 is observed in the ammonia-treated sample.
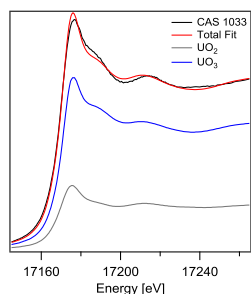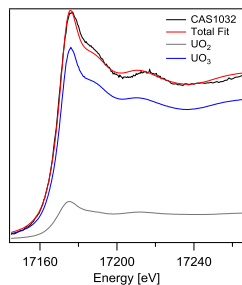
a)

b)

Figure E.2. U L3-edge XANES spectrum [black] and total linear combination fit (LCF) fit [red] for PNNL00033 (CAS 1032), for the C9520 43' untreated (a) and 5% NH_3 treated sample; (b) fraction-adjusted standards contributing to the LCF fit shown for UO_2 [grey] and UO_3 [blue]. (For Information Only)

Table E.2. Uranium valance state (U^{IV} in UO_2, U^{VI} in UO_2) in U-8 sediment samples. (For Information Only)

Sample	D9, C9520 43', Untreated	D12, C9520 43', NH_3 treated
APS CAS #	*CAS 1032*	*CAS 1033*
PNNL#	*PNNL00033*	*PNNL00034*
UO_2 Fraction	0.16(4)	0.26(4)
UO_3 Fraction	0.84(4)	0.74(4)

E.2.3   Mineral Identification by Cryogenic Laser Fluorescence Spectroscopy (TRLIFS)

Cryogenic time-resolved laser induced U(VI) fluorescence spectroscopic (TRLIFS) measurements of the selected sediment samples were performed at near liquid helium temperature (LHeT, 8 ±2 ˚K) using methods described by Wan et al. (2009) and Wang et al. (2004). A picture of the spectrometer apparatus is shown in Figure E.3. Sediment solids were placed inside a 2 mm × 4 mm × 25 mm fused quartz cuvette, sealed with a silicone stopper, further wrapped with parafilm, and attached to the cold-finger of a Cryo Industries model RC-152 cryogenic workstation and cooled with helium vapors to lower the sample temperature.

For spectral and lifetime measurements, the samples were excited at 415 nm using a Spectra-Physics Nd:YAG laser pumped Lasertechnik-GWU MOPO laser. The emitted light was collected at 85˚ to the excitation beam, dispersed through an Acton SpectroPro 300i double monochromator spectrograph, and detected with a thermoelectrically cooled Princeton Instruments PIMAX intensified CCD camera that was triggered by the delayed output of the laser pulse and controlled by the WinSpec data acquisition software. Luminescence decay curves were constructed by plotting the spectral intensity of a series of time-delayed fluorescence spectra as a function of the corresponding delay time. The emission spectra and decay data were analyzed using commercial software, IGOR®, from Wavematrix, Inc.
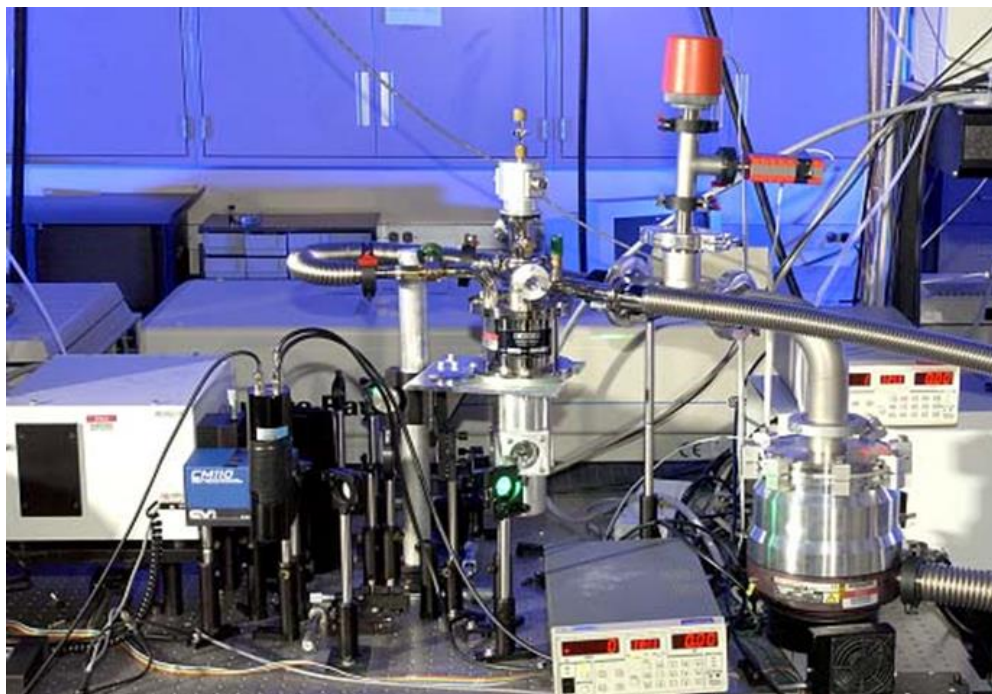
Figure E.3. Spectrometer system

Three U-8 sediment samples were analyzed by LIFS: a) C9520 42.9' untreated (D9, total U = 1807 µg/g), b) C9520 42.9' 5% NH3 treated for 4 months then air for 15 months (D15, total U = 1807 µg/g), and c) C9515 47.2' untreated (D132, total U = 5338 µg/g). All three samples show similar luminescence spectral profiles at near LHeT (Figure E.4a, Figure E.5a and Figure E.6a).   All three samples show the

typical five-band U(VI) luminescence spectra with the first peak located in the range from 504 to 508 nm (Table E.3). Some spectral shifts are observed among the three samples. However, all the bands shifted consistently with little variations in the relative intensities of the vibronic bands for each sample (Table E.4). These band positions and the general spectral profiles match well with those of synthetic boltwoodite and/or uranophane (Wang et al. 2005, 2008). Secondary U(VI) minerals of uranophane/boltwoodite have also been observed 119 to 142 feet underneath the BX-102 high-level waste tank, where a significant leak of the highly basic liquid waste occurred in 1951, and those at similar depth in the U-tank farm (Wang et al. 2005; Um et al. 2009). Therefore, these results suggest that under the present conditions, highly basic solutions dissolved silicate minerals in the sediments and the high concentrations of silicates and uranium (VI) lead to secondary precipitates of uranium silicate minerals, in this case uranophane and/or boltwoodite. Consistent with this assignment, the measured vibronic spacings between the vibronic bands for all three samples fall between 754 and 791 cm^{-1}, again, consistent with the vibronic spacings of uranium silicate minerals (Wang et al. 2008).

Time-resolved spectral data indicated that at decay times reaching 3.9 ms, at which the spectral intensity reaches almost zero, the same spectral profiles were maintained for each of the three samples, although minor changes in the relative intensities of the vibronic appears noticeable (Figure E.4b and c, Figure E.5b and c, and Figure E.6b and c). Such minor variation along with the obvious spectral shoulders that are apparent on shorter wavelength side of the first vibronic band the luminescence spectra (Figure E.4a, Figure E.5a, and Figure E.6a) suggest that while uranophane and boltwoodite constitute the primary U(VI) mineral phase, either other minor U(VI) species are present or slight variations in the hydration or crystallinity of the same uranophane/boltwoodite are present in these sediments. Indeed, fit of the luminescence decay curves of two of the three samples (D9 and D132; Figure E.4d and Figure E.6d) require a double exponential function. While the decay curve of D15 can be simulated by a single exponential function (Figure E.5d), inclusion of a second exponential function also improved the fitting parameters (data not shown).

Table E.3. LHeT luminescence spectral characteristics and lifetime data. (For Information Only)

Band Position		Peak Spacing	Lifetimes	
(nm)	(cm-1)	(cm-1)	T1 (µs)	T2 (µs)
C9520 42.9', untreated (D9)				
503.55	19859	787.77	332.23	95.24
524.35	19071	780.33	295.86	71.43
546.72	18291	731.33	361.01	99.01
569.49	17560			
		766.5 ± 30.7	329.7 ± 32.6	88.56 ± 14.95
C9520 42.9', NH3 treated (D15)				
508.07	19682	711.67	198.02	
527.13	18971	788.83	214.59	
550.00	18182	775.38	181.16	
574.50	17406			
508.36	19671	700.45		
527.13	18971	797.76		
550.27	18173	752.51		
574.04	17420			
		754.4 ± 41.2	197.9 ± 16.7	
C9515 47.2' untreated (D132)				
507.71	19696	805.55	324.68	91.74
529.36	18891	798.72	353.36	169.78
552.73	18092	776.30	274.73	43.29
577.51	17316			
506.09	19759	828.90		
528.25	18930	802.67		
551.64	18128	731.92		
574.85	17396			
		790.7 ± 15.3	317.6 ± 39.8	101.6 ± 63.8
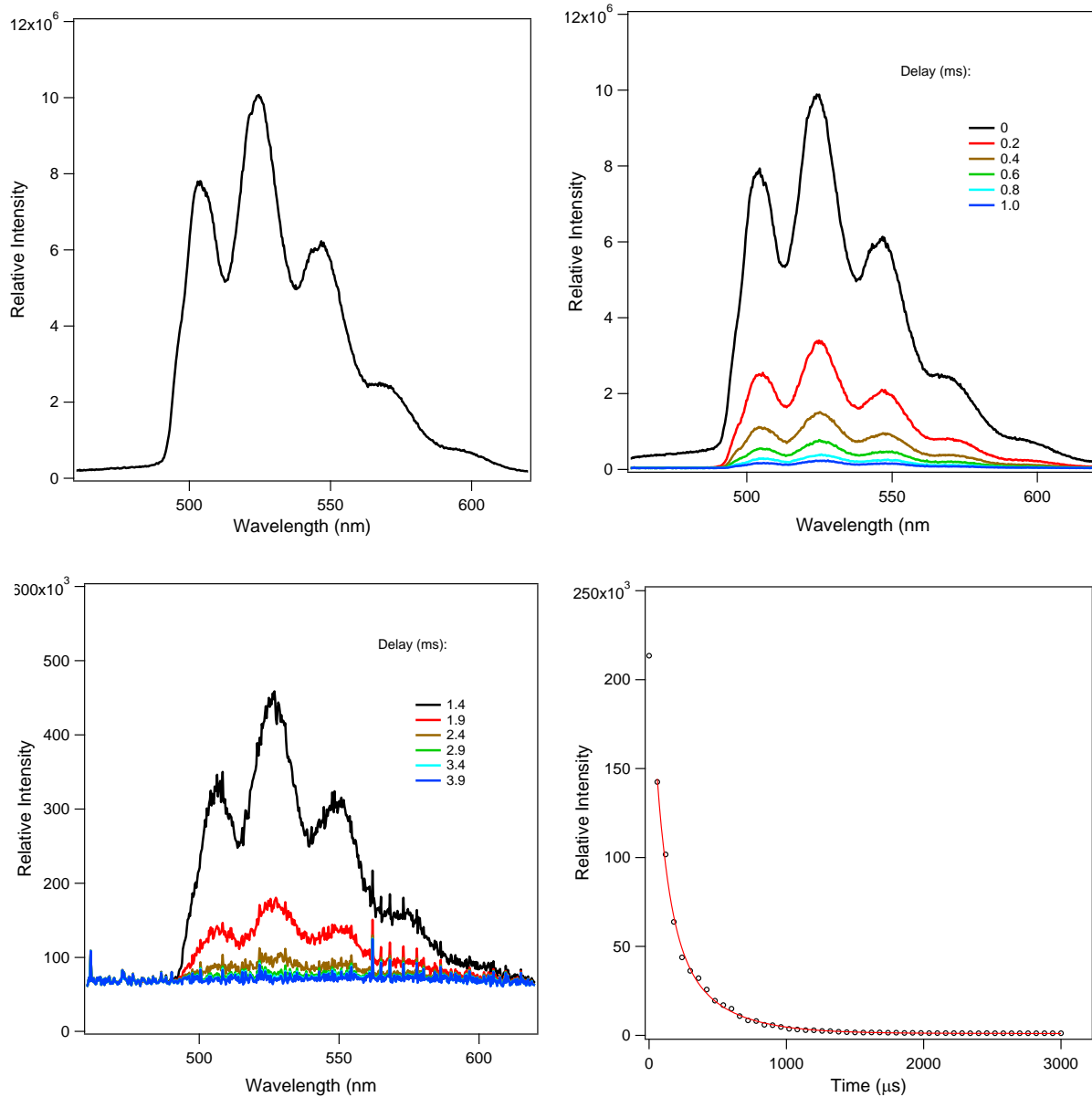
Figure E.4. LHeT luminescence spectra of C9520 42.9' untreated sediment (D-9) in a, b, and c, and the time-resolved LHeT luminescence decay and fit (d). (For Information Only)
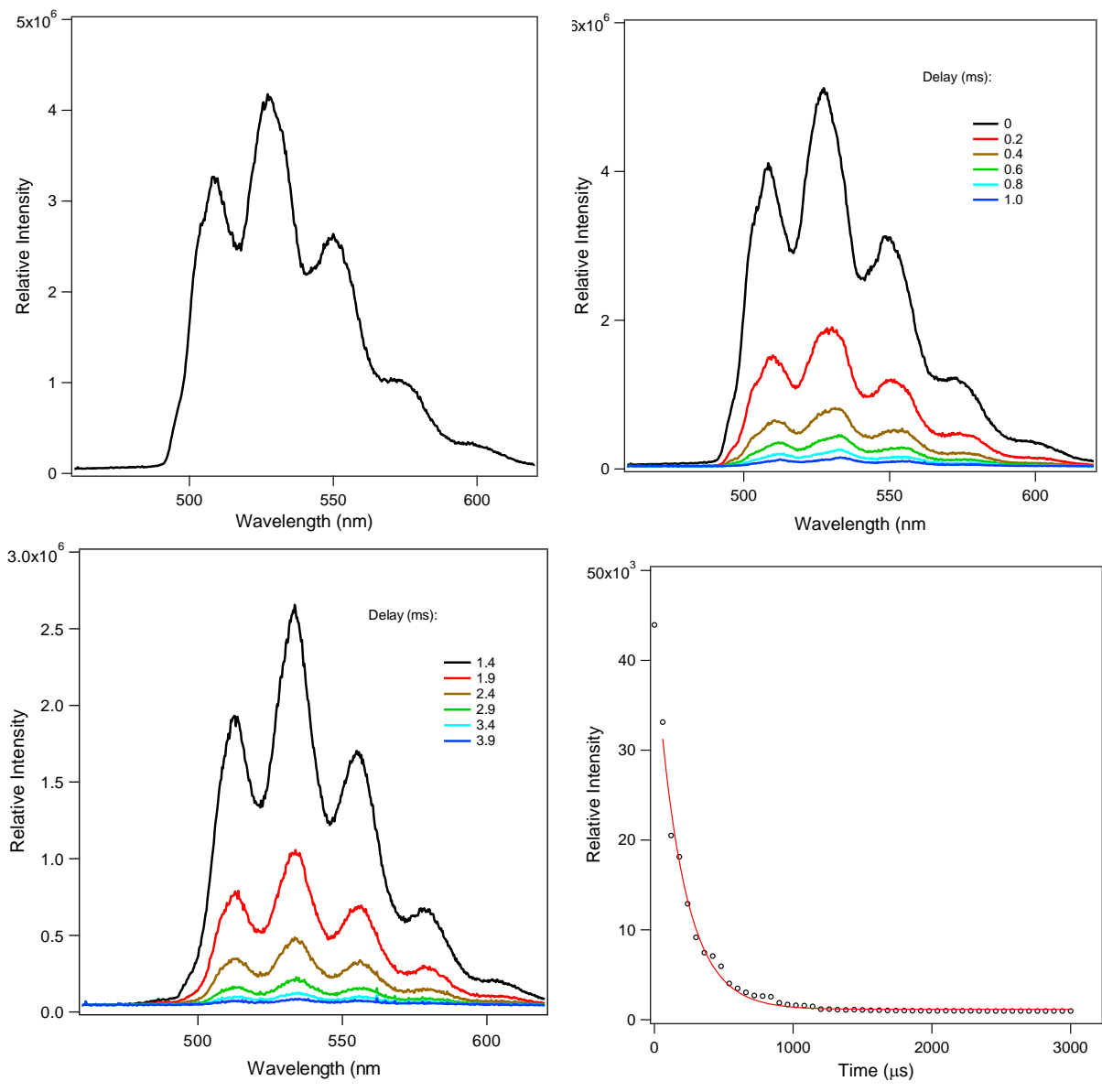
Figure E.5. LHeT Luminescence spectra of C9520 42.9' NH$_3$/air-treated sediment (D-15) in a, b, and c, and the time-resolved LHeT luminescence decay and fit (d). (For Information Only)
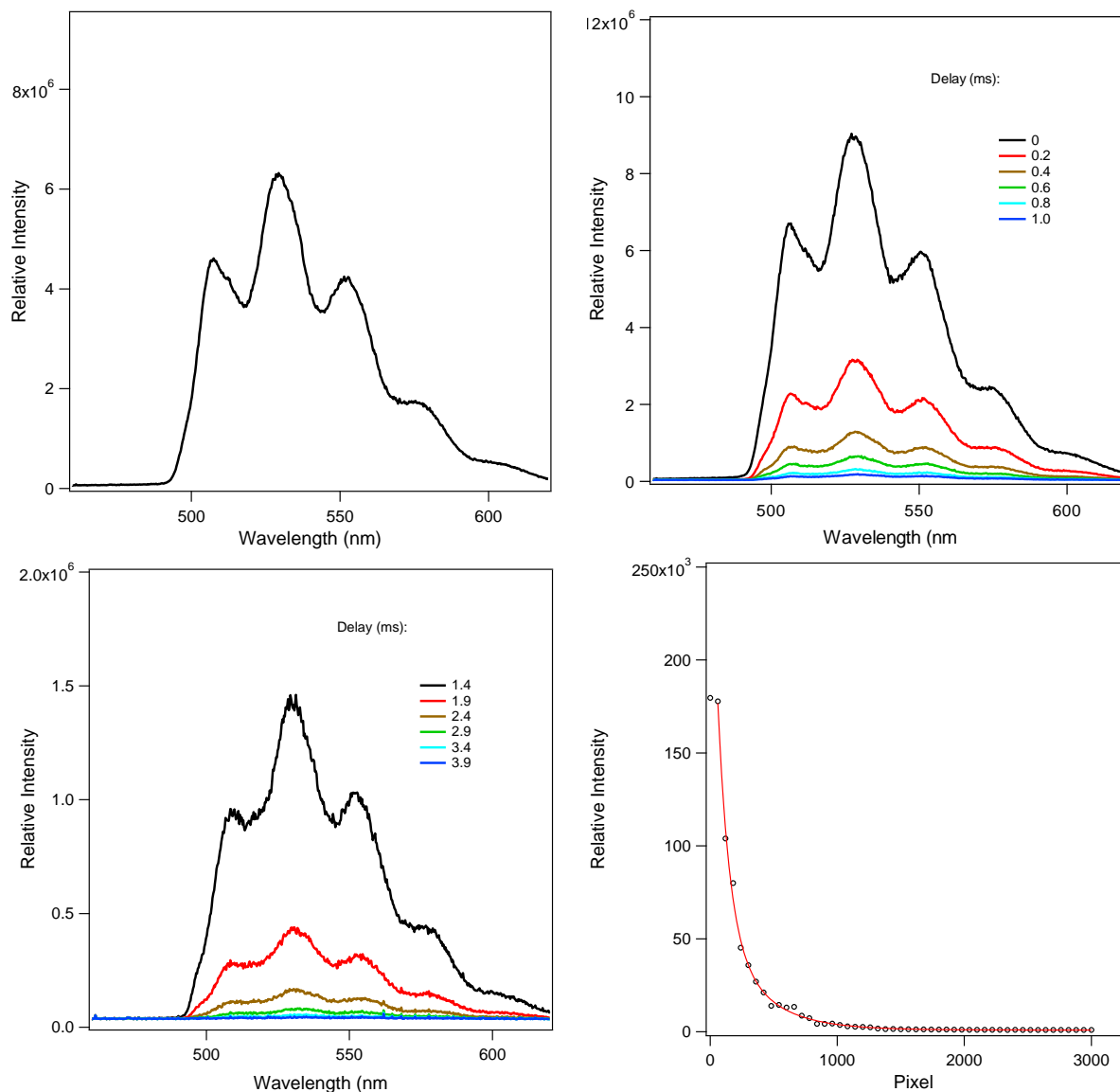
Figure E.6. LHeT Luminescence spectra of C9515 47.2' untreated sediment (D-132) in a, b, and c, and the time-resolved LHeT luminescence decay and fit (d). (For Information Only)

E.2.4   Spatial Distribution of Elements in Sediments by 2-D X-ray Fluorescence

X-ray fluorescence was conducted on four sediment samples: a) full grain size C9520, 42.9-43.9' (1718 µg/g U) untreated, b) < 10 micron C9520, 42.9-43.9' (1718 µg/g U) untreated, c) full grain size C9520, 42.9-43.9' (1718 µg/g U) with 5% NH_3 for 4 months then air for 15 months and d) < 10 micron C9520, 42.9-43.9' (1718 µg/g U) with 5% NH_3 for 4 months then air for 15 months. The sediment sample (particles) are mounted in an epoxy cylinder, surface cut, and polished to ~1 micron flatness, so there are cross sections of particle grains. The mount is 22 mm round. Elemental concentration is presented in color with blue (lowest concentration) to green, yellow, and red (highest concentration). The full 22 mm image has a 60 micron resolution. This scan took about 2 days. Higher resolution scans (smaller resolution, greater time collecting data on each point) were also conducted on portions of the mount.

Elemental images for U, Si, Ca, Fe, and P for the untreated full grain size distribution (Figure E.7 and Figure E.8) show uranium is present as surface precipitates (i.e., as a rind on the outside of particles, as shown best with the particle near the center of Figure E.7a). The spatial distribution of uranium was uneven, with high concentrations on a few particles distributed throughout the series of particles. It is estimated that 5% of minerals contained a high uranium concentration. In terms of mineral associations, uranium in precipitates is present in carbonates (i.e., calcite) and silicates (Na-boltwoodite, uranophane), co-precipitated in iron oxides, and possibly associated with phosphate (i.e., present in autunite, if phosphate were present). Elemental maps of Si, Fe, and P all show a relatively even spatial distribution, and thus are not useful for identifying an association with uranium. The Ca spatial distribution (Figure E.7c) does show some spatial distribution, and some areas of high Ca are associated with areas of high U. For example, the rind of U around a particle (center of image) appears to be high in Ca, and thus may be calcite or anorthite. However, other zones of high U are associated with low Ca. Higher resolution imaging of some of the high-U-containing particles (Figure E.8) also shows that U is at a high concentration on some particle exteriors, and these minerals have high Si content (and thus may be clays).
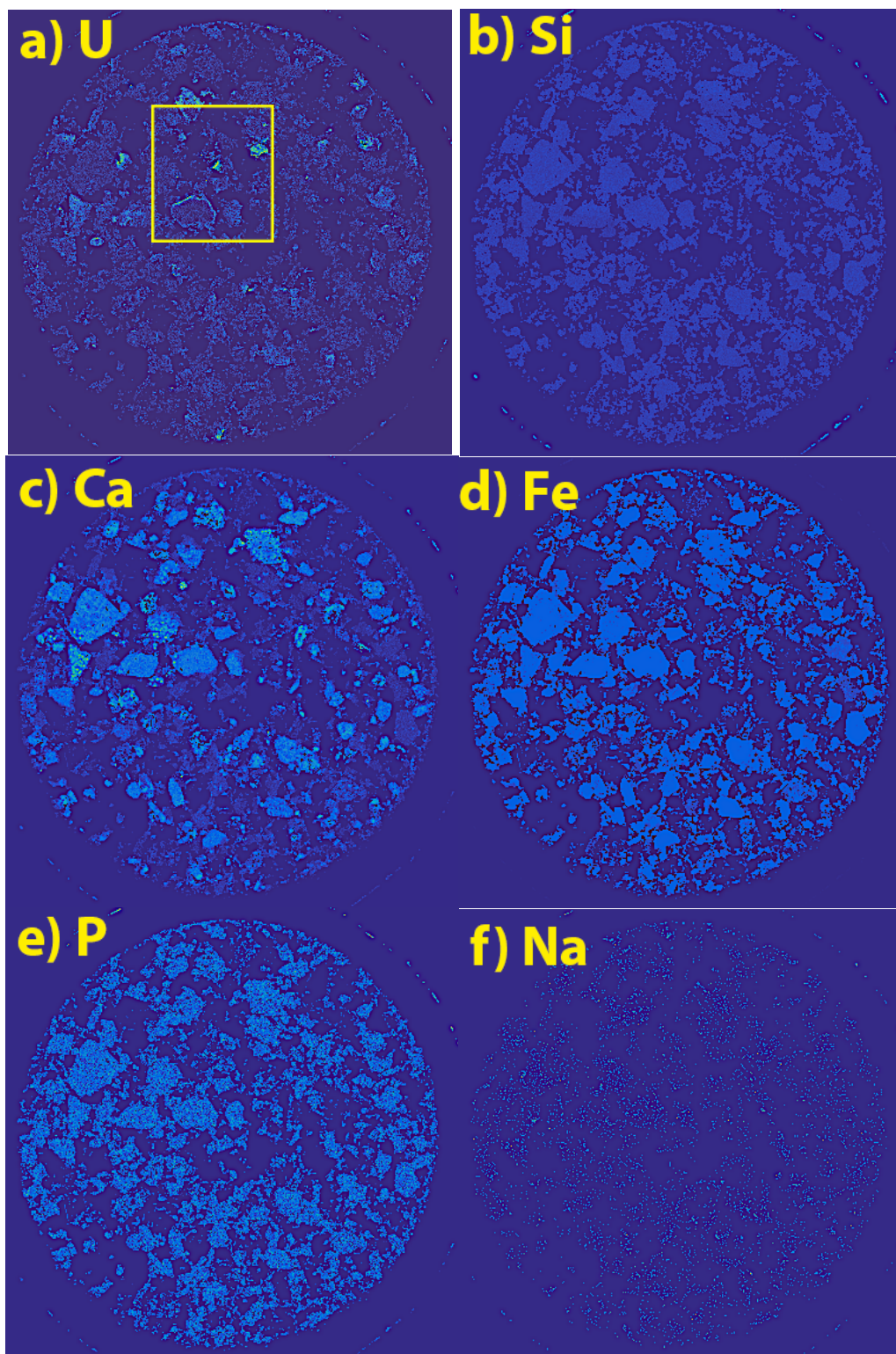
Figure E.7. XRF elemental images of the full grain size C9520, 42.9-43.9' (1718 µg/g U) untreated in a 22 mm round epoxy mount showing elements: a) U, b) Si, c) Ca, d) Fe, e) P, and f) Na with 60-micron resolution. Uranium was additionally mapped at a 30-micron resolution with the location shown by the yellow rectangle in (a). (For Information Only)
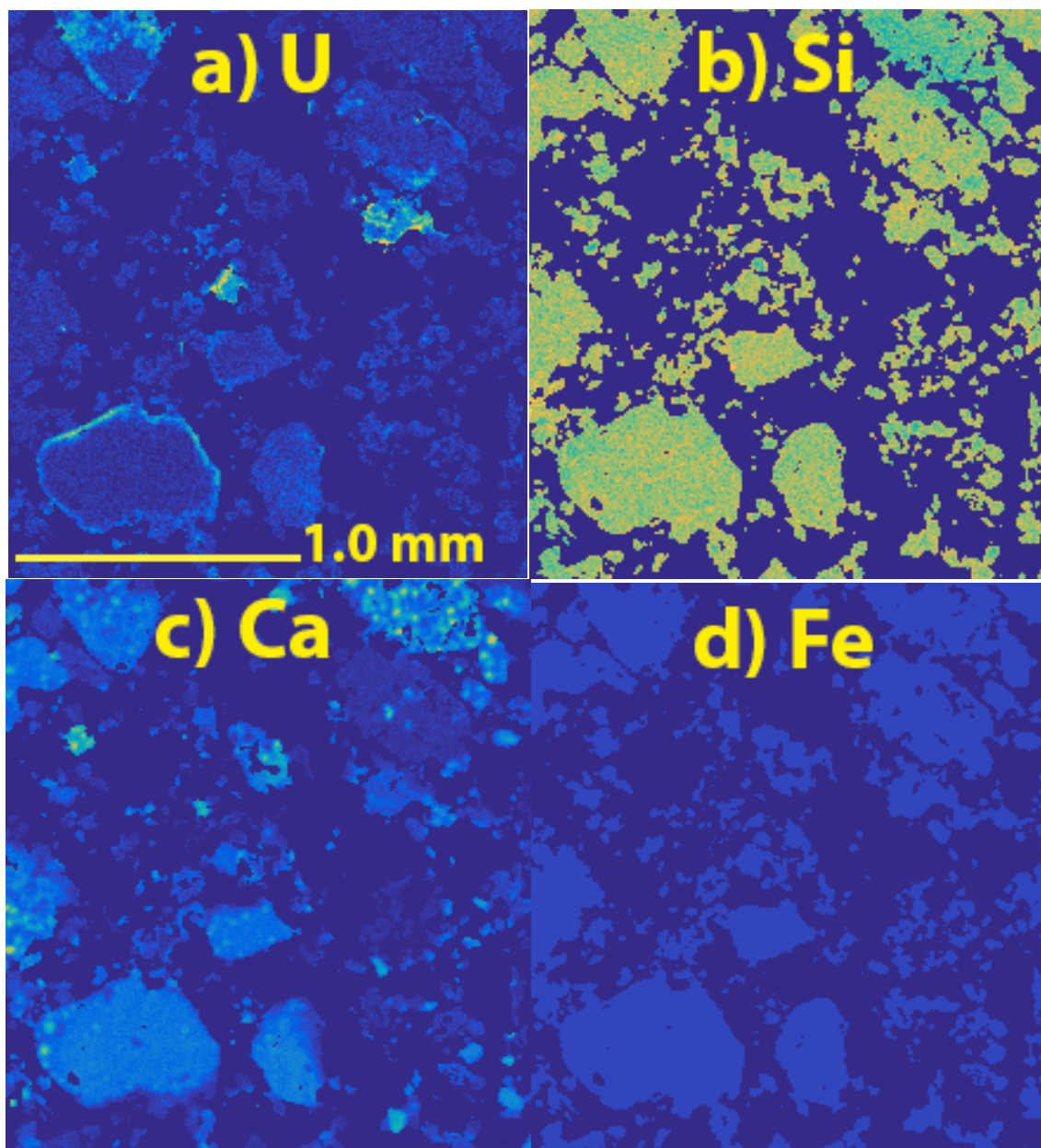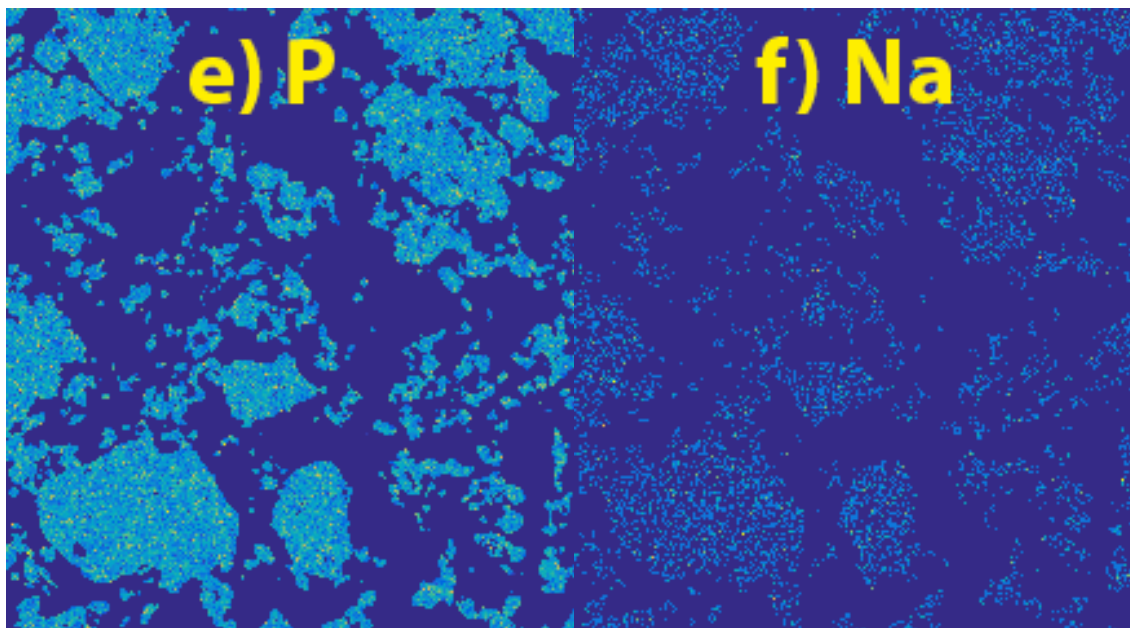
Figure E.8. XRF elemental images of the full grain size C9520, 42.9-43.9' (1718 µg/g U) untreated in a 1.9 by 0.8 mm epoxy thin section showing elements: a) U, b) Si, c) Ca, d) Fe, e) P, and f) Na with 30-micron resolution. (For Information Only)

Elemental images for U, Si, Ca, Fe, and P for the NH$_3$/air-treated full grain size distribution (Figure E.9 and Figure E.10) also show uranium is present as surface precipitates (i.e., as a rind on the outside of particles, as shown best with the particle slightly left of center in Figure E.9a). The spatial distribution of uranium was uneven, with high concentrations on a few particles distributed throughout the series of particles. The higher resolution map of uranium (Figure E.10a) also shows uranium is at a high concentration at the outer edges of particles. This spatial distribution was similar to that of the untreated sample (Figure E.8a). In terms of mineral associations, uranium in precipitates is present in carbonates (i.e., calcite) and silicates (Na-boltwoodite, uranophane), co-precipitated in iron oxides, and possibly associated with phosphate (i.e., present in autunite, if phosphate were present). Elemental maps of Si, Fe, and P all show a relatively even spatial distribution, and thus are not useful for identifying an association with uranium. Ca (Figure E.9d) does show some spatial distribution, and some areas of high Ca are associated with areas of high U. However, locations of the highest Ca concentration are not associated with U. Higher resolution imaging (Figure E.10) of U-containing particles indicates uranium is present on the outer surface of particles, likely as a precipitate, and is highly unevenly distributed. A high-resolution map of Na does not show any association (Figure E.10b) with uranium.
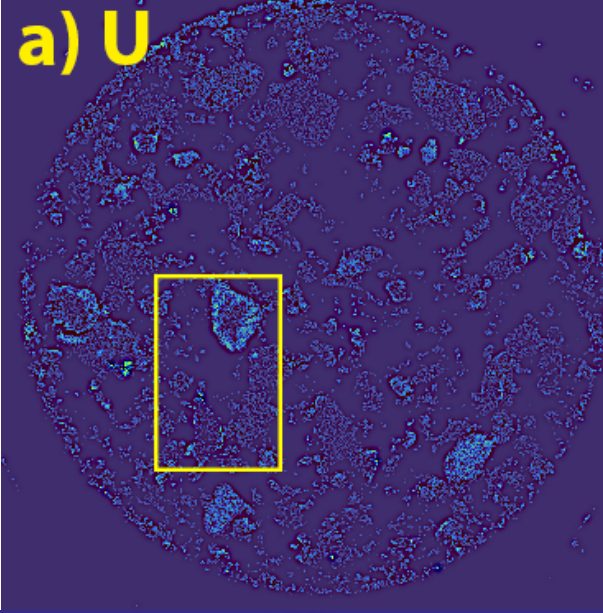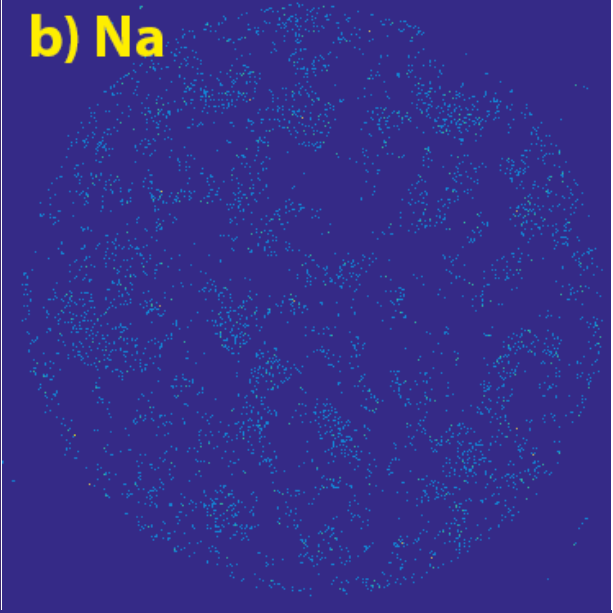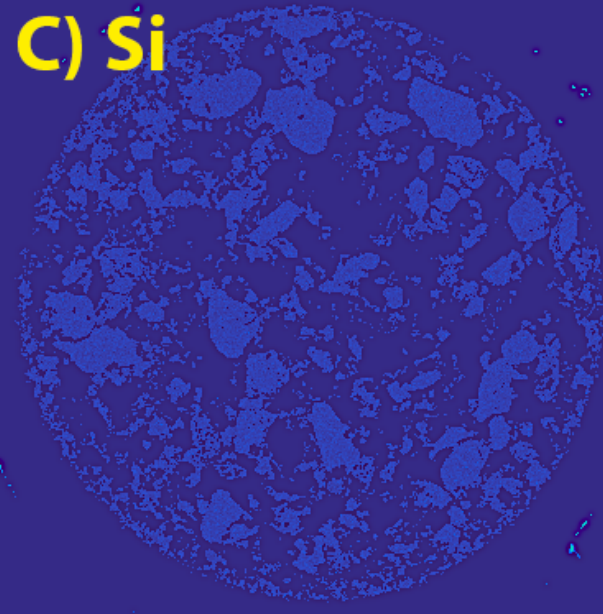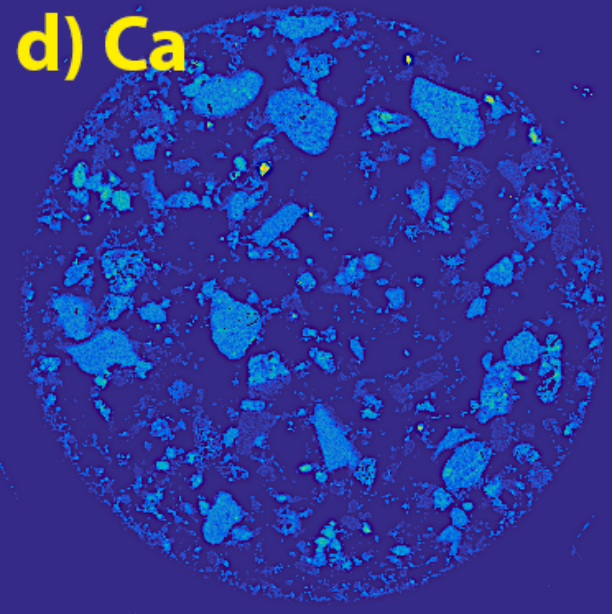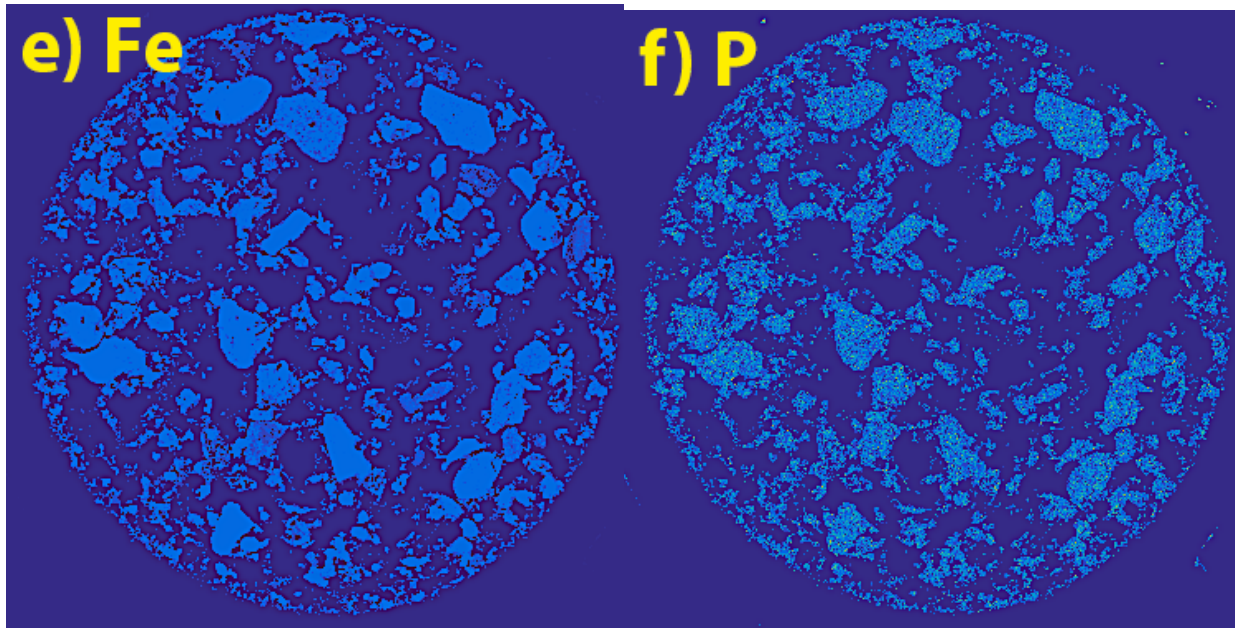
Figure E.9. XRF elemental images of the full grain size C9520, 42.9-43.9' (1718 µg/g U) NH$_3$/air-treated sample in a 22 mm round epoxy mount showing elements: a) U, b) Na, c) Si, d) Ca, e) Fe, and f) P with 60-micron resolution. Uranium was additionally mapped at a 30-micron resolution, with the location shown by the yellow rectangle in (a). (For Information Only)
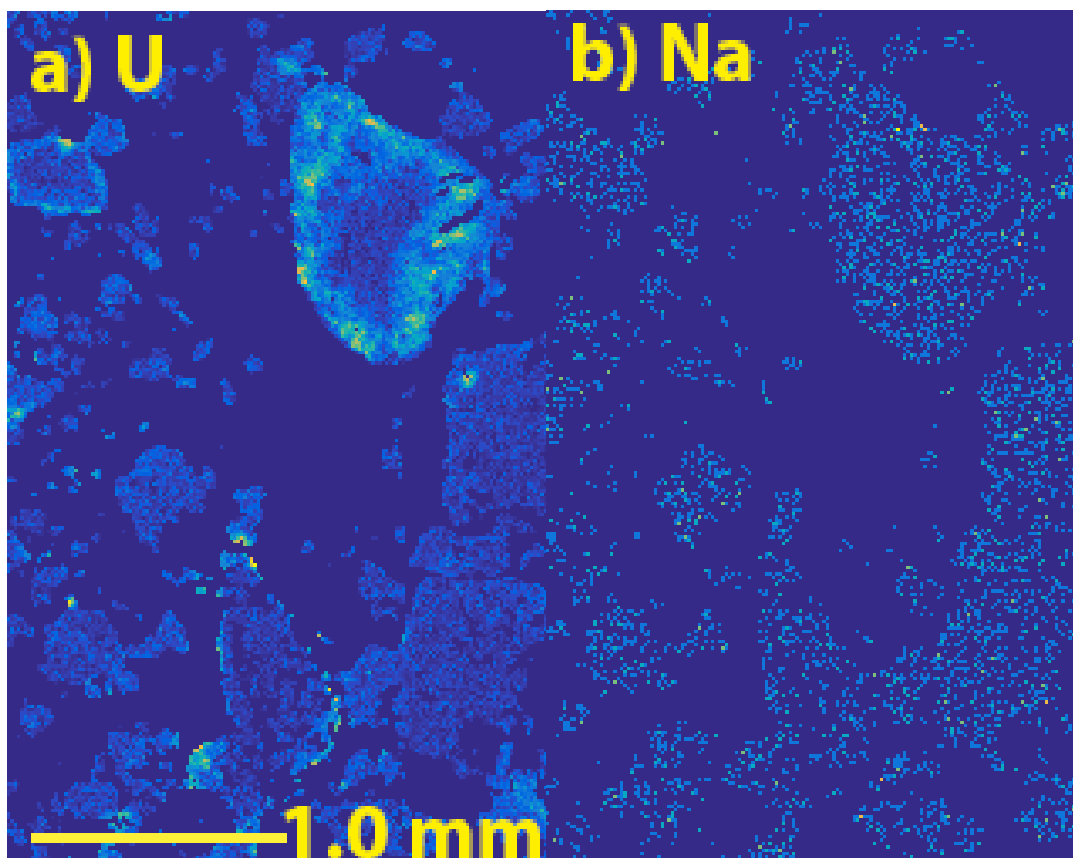
Figure E.10. XRF elemental images of the full grain size C9520, 42.9-43.9' (1718 µg/g U) NH$_3$/air-treated in a 1.5 by 0.7 mm epoxy thin section showing elements: a) U and b) Na with 30-micron resolution. (For Information Only)

E.2.5   Inorganic and Organic Extractions of Sediments

It was hypothesized that the acidic co-contaminants disposed of in the U-8 crib may have led to a decrease in the calcite in sediments directly under the crib. Carbonates are needed for the NH$_3$ treatment process, as a recent study indicates a lack of aqueous carbonates during the dissolution processes results in a substantial (~10x) increase in aqueous uranium (Emerson et al. 2018), as shown in Figure E.11.
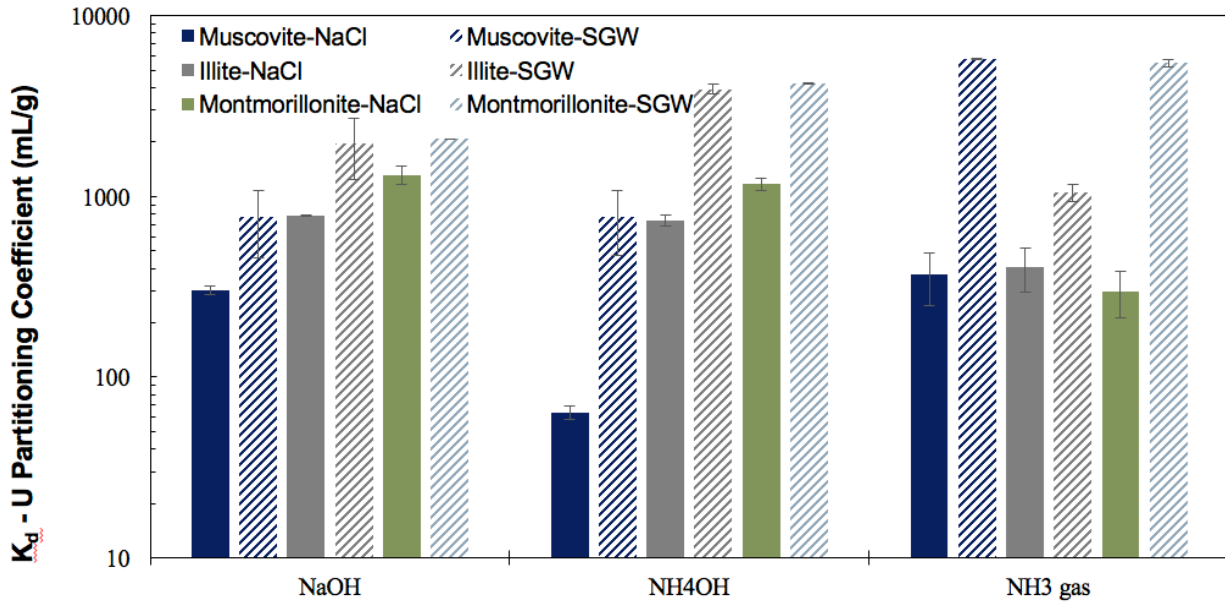
Figure E.11. Difference in U uptake in different mineral-alkaline treatments in water containing only Na+ and Cl- (solid bars) and synthetic groundwater containing 154 mg/L carbonate (cross hatched bars; Emerson et al. 2018).

Total inorganic carbon and total organic carbon were extracted from 16 sediments from U-8, and sediments and previous NH_3-treatment studies (Table E.4) showed low (below detection limits of 294 μg C/g or 0.03%) inorganic carbon in U-8 sediments. Non-U-8 sediments all had significant inorganic carbon (0.1% to 0.3%). Therefore, the lack of carbonate in samples could be a contributing factor to elevated aqueous uranium in NH_3-treated U-8 sediments.

Table E.4. Alkaline uranium, total carbon, and total inorganic carbon extractions of sediments used in current and previous NH₃ studies.

Borehole	depth (ft)	#	Total U (µg/g)	U Alk. Extr. (µg/g)	mobile U (µg/g)	Total C (µg/g)	TIC (µg/g)	TOC (µg/g)
C9515	47.2	D151	5338 ± 2285	122.2	60	ND	ND	ND
C9515	47.2	D151 dup	5338 ± 2285	117.7	60	ND	ND	ND
	52.8	D152	9.86 ± 4.25	4.08	2.4	2490	2140	350
C9519	42.3	D153	383.3±51.1	264.7	40	266	ND	
	46.5	D154	2886 ± 158	213.0	300	228	ND	
	48.5	D155	400.0 ± 68.4	79.8	70	ND	ND	
	54.7	D156	13.02 ± 8.32	5.147	4.5	3060	2320	740
C9520	38	D157	415.2±84.0	122.8	14	204	ND	
	42.9	D158	1808 ± 616	70.48	70	ND	ND	
	47.2	D159	728. ± 461.	66.08	33	ND	ND	
	50.7	D160	67.5 ± 40.8	8.175	7.1	1280	1040	240
	54.5	D161	7.81 ± 1.00	3.607	3.2	1850	1490	360
	62	D162	15.30 ± 5.50	6.843	6.2	1920	1420	500
BX102	131	D163	376.6 ± 6.15	160.5	20.0	2110	1890	220
TX104	69	D164	8.49 ± 0.29	2.911	3.9	3970	1900	2070
C7117	32	D165	1.573±0.159	0.916	0.2	1080	2630	
				MDL 0.006		MDL 200	MDL 294	

The possibility of using CO_2 gas treatment during NH_3 treatment (to provide carbonate) or CO_2 gas treatment sequentially after NH_3 treatment to accelerate pH neutralization was previously investigated (Szecsody et al. 2010). In a limited number of experiments, neither of these mixed CO_2/NH_3 treatments was effective (Figure E.12).
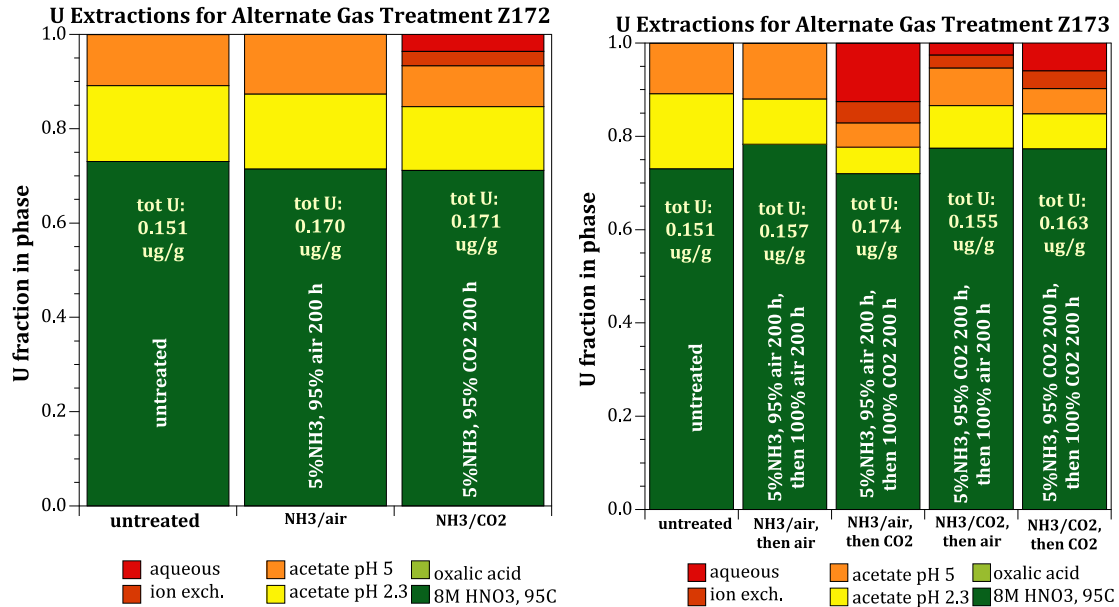
Figure E.12. Sequential gas treatments showing a) mixed NH_3 /CO_2 treatment, and b) sequential treatments.

It was also hypothesized that organic co-contaminants may be present in U-8 sediments. Total organic carbon calculated from the total carbon minus total inorganic carbon analysis (Table E.4) showed very low organic carbon in U-8 sediments (samples results ranged from nondetect to $< 0.07\%$). Thus, sequential extractions using water (polarity index 10.2), then isopropyl alcohol (polarity index 4), then cyclohexane (polarity index 0.2) with gas chromatography mass spectrometry (GC-MS) analysis of the extraction solution for organic compounds were not conducted.

Because of the high variability in sequential acidic extractions (Table E.4), total U with standard deviation listed), a 1000-hour alkaline extraction was conducted on sediment samples to evaluate whether the alkaline extraction could provide a more reliable total uranium concentration in the sediment. The alkaline extraction results (Table E.4) for total uranium averaged $25.9 \pm 21.3\%$ that of the total sequential acidic extractions, with a range of 2.1% to 69%, and thus were not a useful for determining total uranium extraction. The results had been previously been used as a measure of the total labile uranium (Zachara et al. 2007). However, this 1000-hour alkaline extraction accurately predicts the mass of mobile uranium (from aqueous + adsorbed + pH 5 acetate or leached) for untreated sediments, but not for the NH_3-treated sediments.

E.3 Hypothesis 2 - Constituents Present in U-8 Sediments Complex with U during NH_3 Treatment

E.3.1 Phosphate and Organic Extractions

It was hypothesized that due to inorganic or organic co-contaminants that may be present in the U-8 sediments, the alkaline NH_3 treatment is not as effective. This hypothesis was addressed by the following experiments: a) 1-D leach experiments with untreated U-8 (C9520, 42.9') and untreated TX104 69' sediments with U, Th, pH, metals, anions, total organic carbon, and total inorganic carbon analysis; b) phosphate extractions of sediments; c) sequential organic extractions of sediments; and d) a comparison of 5% NH_3 treatment on U-8 sediments (C9520 42.9' and C9519 54.7') and TX104 sediments (69', 110') with batch extractions at selected times with U, pH, metals, anions, total organic carbon, and total inorganic carbon analysis.

The phosphate extractions of sediments (0.5M HNO_3 for 15 minutes contact with sediment) are designed to dissolve labile phosphate present in surface precipitates and minimize dissolution of additional P in minerals such as microcline (see Table E.1). Results indicated that there was a fair amount of phosphate in U-8 and TX104 sediments (Table E.5), which was predominantly orthophosphate with little (or none) organic-phosphate. Orthophosphate was measured colorimetrically (Hach 8178 method, Szecsody et al. 2010) and total P (reported as PO_4) was measured by inductively coupled plasma optical emission spectrometry.

Table E.5. Orthophosphate and total phosphate extractions of sediments.

Borehole	Depth (ft)	#	Ortho PO$_4$ (mg/g)	Total PO$_4$ (mg/g)
C9520	42.9	D166P	0.452	0.506
C9519	54.7	D167P	0.545	0.705
TX104	69	D168P	1.182	1.465
TX104	110	D169P	ND	0.528[*]
Pasco Sand	10	D188P	1.756	2.070

[*]outside calibration range

Sequential organic extractions consist initially of an aqueous extraction (1:2 sediment:liquid) for 24 hours followed by an isopropyl alcohol extraction for 24 hours, then followed by a cyclohexane extraction for 24 hours. These liquids span the polarity index from most polar (water, 10.2) to some polarity (isopropyl alcohol, 4.0), to nonpolar (cyclohexane, 0.2), and thus should be effective at removing different organic compounds from the sediments. The GC-MS analysis conducted on these extraction liquids also included blanks (i.e., artificial groundwater, isopropyl alcohol, cyclohexane) to be able to subtract out organic compounds present in these solvents from organic compounds present in the sediments. Water-extracted compounds (Table E.6), isopropyl alcohol-extracted organics (Table E.7), and cyclohexane-extracted organics (Table E.8) show a small list of low molecular weight compounds. Even though these compounds were not detected in the blank solvents, there were similar compounds found in U-8 and TX104 sediments (for isopropyl and cyclohexane extractions). Because this cyclohexane extraction was conducted after the isopropyl alcohol extraction and compounds were in all samples, there is some residual isopropyl alcohol in the sediment, which contributed to the measured compounds that are not in the cyclohexane blank. An organic compound qualitatively identified only in the U-8 crib sediments is 2-2-(dimethylamino)-ethyl)-pyridine, and an organic compound qualitatively identified only in the TX104 sediments is N-formylglycine. Results are qualitative because standards were not used to quantify the concentration of these compounds. It should be noted that while qualitative, no organic compounds were detected by GC-MS in these liquid extractions at any significant concentration (i.e., all >20 µg/L or 0.04 µg/g), so in general, these results show essentially no organics present in the U-8 and TX104 sediments.

Table E.6. Organic compounds extracted from sediments with artificial groundwater. (For Information Only)

#	Borehole/Depth	Water Extracted Organic Name	Formula	Confidence[(a)]
D169RA	C3832 110' (TX104)	Tetrahydrofuran	C4H8O	60%

(a) Confidence in GC-MS identification of the compound

Table E.7. Organic compounds extracted from sediments with isopropyl alcohol. (For Information Only)

#	Borehole/Depth	Isopropyl Alcohol Extracted Organic Name	Formula	Confidence[a]
D166RB	C9520 42.9' (U-8 crib)	4-methyl-2-pentanol	C6H14O	95%
		2,3-dimethyl-2-butanol	C6H14O	85%
		2-methyl-2-pentanol	C6H14O	95%
D167RB	C9510 54.7' (U-8 crib)	2-methyl-2-pentanol	C6H14O	90%
		4-methyl-2-pentanol	C6H14O	90%
		2-methyl-3-pentanol	C6H14O	90%
D168RB	C3832 69' (TX104)	2,3-dimethyl-2-butanol	C6H14O	85%
D169RB	C3832 110' (TX104)	2-methyl-2-pentanol	C6H14O	95%
		3-methyl-3-pentanol	C6H14O	90%
		4-methyl-2-pentanol	C6H14O	95%
		2-methyl-3-pentanol	C6H14O	90%

(a) Confidence in GC-MS identification of the compound

Table E.8. Organic compounds extracted from sediments with cyclohexane. (For Information Only)

Borehole/Depth	Cyclohexane Extracted Organic Name	Formula	Confidence[a]
C9520 42.9' (U-8 crib)	2,2,3,3,-tetramethylbutane	C8H18	90%
	cyclopentane	C8H16	90%
	boric acid-tris(1-methylethyl)ester	C9H21BO3	90%
	xylene isomer	C8H10	90%
	2-2-(dimethylamino)-ethyl)-pyridine	C9H14N2	40%
	1,1'-bicyclohexyl	C12H22	99%
C9510 54.7' (U-8 crib)	2,2,3,3,-tetramethyl butane	C8H18	95%
	2-methyl-2-pentanol	C6H14O	90%
	1,2,4-trimethylcyclopentane	C8H16	95%
	1,2,3-trimethylcyclopentane	C8H16	90%
	6-methyl-2-heptene	C8H16	85%
	1,2-dimethyl-cyclohexane	C8H16	99%
	boric acid-tris(1-methylethyl)ester	C9H21BO3	95%
C3832 69' (TX104)	2,2,3,3,-tetramethyl butane	C8H18	99%
	2,3-dimethyl-2-butanol	C6H14)	80%
	cyclopentane	C8H16	90%
	1,2,3-trimethylcyclopentane	C8H16	90%
	boric acid-tris(1-methylethyl)ester	C9H21BO3	90%
	0-xylene	C8H10	99%
	2-hexen-1-ol	C6H12O	95%
	N-formylglycine	C3H5NO3	95%
	1,1'-bicyclohexyl	C12H22	99%
C3832 110' (TX104)	2,2,3,3,-tetramethyl butane	C8H18	99%
	2-methyl-2-pentanol	C6H14O	99%
	cyclopentane	C8H16	90%
	boric acid-tris(1-methylethyl)ester	C9H21BO3	90%
	ethylbenzene	C8H10	100%
	2-hexen-1-ol	C6H12O	95%
	3-ethyl-2-pentene	C7H14	90%
	N-formylglycine	C3H5NO3	85%
	1,1'-bicyclohexyl	C12H22	99%

(a) Confidence in GC-MS identification of the compound

E.3.2   Untreated Sediment Leach Experiments

The four untreated sediment leach experiments were conducted to compare uranium, pH, cations, and anion leaching between U-8 and TX104 sediments. These leach experiments were conducted to 30 pore volumes. Additional uranium leach data from previous sediments with the same sediments is shown for comparison.

Leaching synthetic groundwater through the C9520, 42.9' sediment (with a total U of 1807 µg/g) in three different experiments shows generally similar behavior, with a) a peak initial U concentration of 1.5 to 14 mg/L, b) subsequent lower U concentration at greater pore volumes, c) slow U release from sediments as indicated by U concentration increase at stop flow events, and d) cumulative U by 30 pore volumes of 5.2 to 20 µg/g (Figure E.13). Metals and anion concentrations (Figure E.14) showed predominantly Na and sulfate, with a decreasing silica concentration from 16.7 mg/L (at 0.2 pore volumes) to 7.7 mg/L at 30 pore volumes. All leach experiments had nondetectable aqueous organic carbon and total carbon, which was consistent with batch studies. Leach studies also had nondetectable aqueous phosphate and phosphate. Other metals were analyzed (Sr, Sn, B, Fe, Mn, Zn), but were below detection limits. All untreated and NH_3-treated sequential U extractions conducted on this sediment (Figure E.15) pre- and post-leaching show an average U of 1807 ± 616 µg/g. The large variation in total uranium between sediment samples is consistent with uranium apparently present in high concentration on a small fraction of minerals as shown above. The fraction of uranium that is considered "mobile" (i.e., aqueous plus adsorbed plus pH 5 acetate extractable) is small ($< 2\%$) and the fraction of uranium leached from the samples is similarly small. The fraction of mobile uranium is significantly smaller than that leached from TX104 sediments (i.e., TX104, 69' shows 10% to 30% leached; TX104 110' shows 35% leached). Thorium-232 was below the detection limits (0.48 µg/g) in all aqueous effluent samples measured.
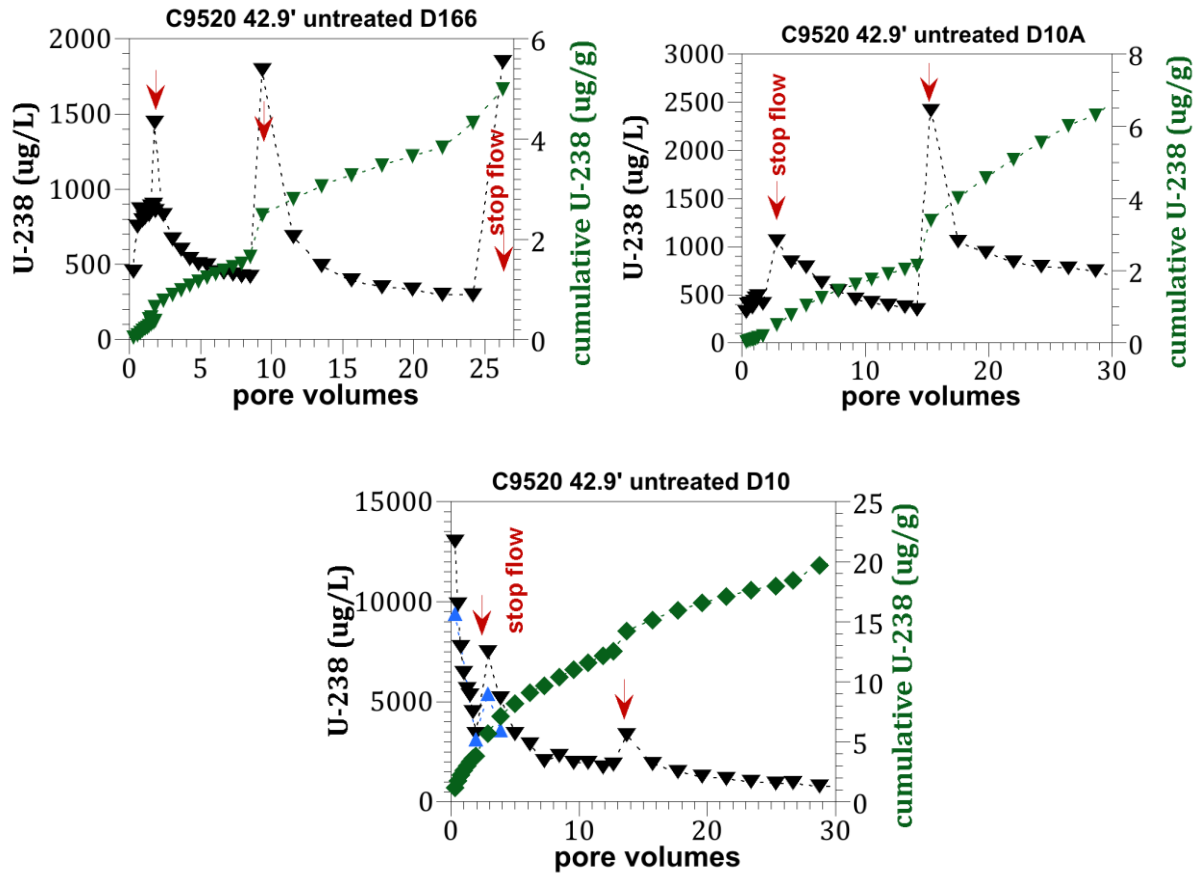
Figure E.13. 1-D leaching of C9520 42.9 untreated sediment with artificial groundwater, showing effluent uranium concentration.
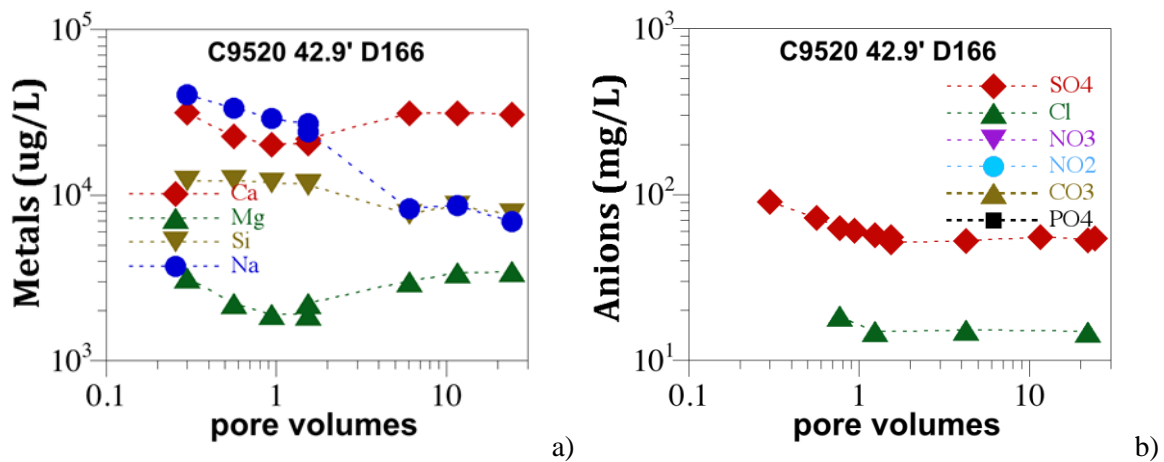
Figure E.14. 1-D leaching of C9520 42.9 untreated sediment with artificial groundwater, showing effluent metals a) and anion b) concentrations.
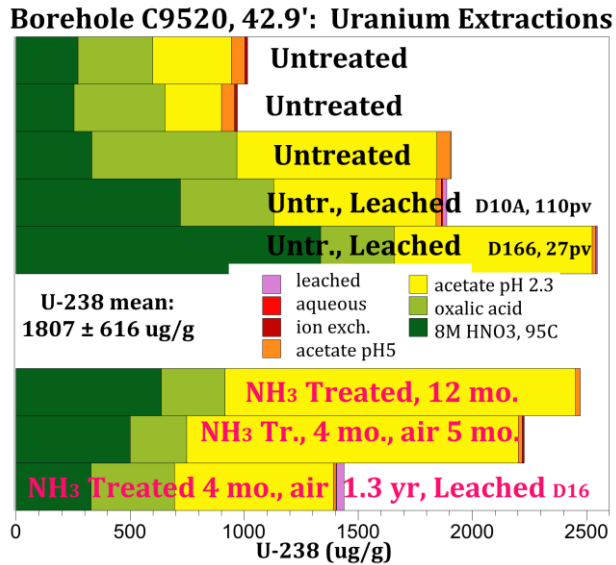
Figure E.15. Sequential liquid extractions conducted on C9520 42.9' depth sediment.

In contrast to the U-8 high-U sediment above, leaching synthetic groundwater through the C9519 54.7 sediment (with a total U of 12.0 µg/g) in three different experiments shows very similar behavior, with a) a peak initial U concentration of 2.5 mg/L, b) subsequent lower U concentration at greater pore volumes, c) slow U release from sediments as indicated by U concentration increase at stop flow events, and d) cumulative U by 30 pore volumes of 3.3 µg/g (Figure E.16). Metals and anion concentrations (Figure E.17) showed predominantly Ca, sulfate, and nitrate with a constant silica concentration of 8 to 13 mg/L. Other metals were analyzed (Sr, Sn, B, Fe, Mn, Zn), but were below detection limits. All untreated and NH₃-treated sequential U extractions conducted on this sediment (Figure E.18) pre- and post-leaching show an average U of 12.0 ± 8.33 µg/g. The fraction of uranium that is considered "mobile" (i.e., aqueous plus adsorbed plus pH 5 acetate extractable) is similar (20% to 35%) to TX104 sediments (i.e., TX104, 69' shows 10% to 30% leached; TX104 110' shows 35% leached). Thorium-232 below the detection limits (0.48 µg/g) in all aqueous effluent samples measured.
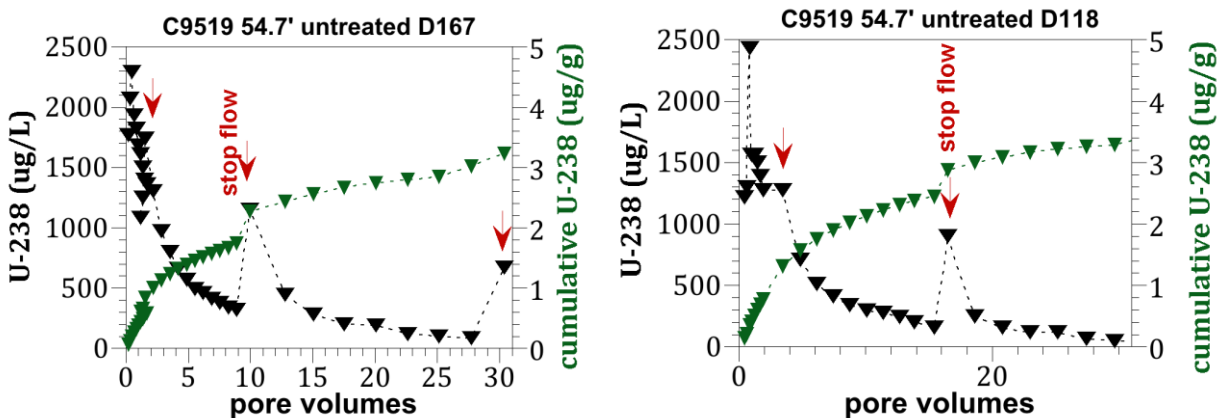
Figure E.16. 1-D leaching of C9519 54.7' untreated sediment with artificial groundwater, showing effluent uranium concentration.
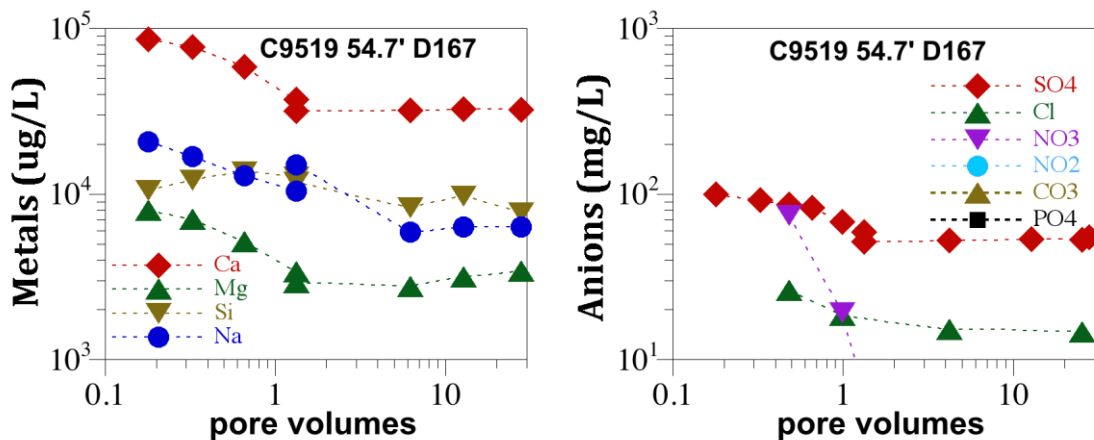
Figure E.17. 1-D leaching of C9519 54.7' untreated sediment with artificial groundwater, showing effluent metals a) and anion b) concentrations.
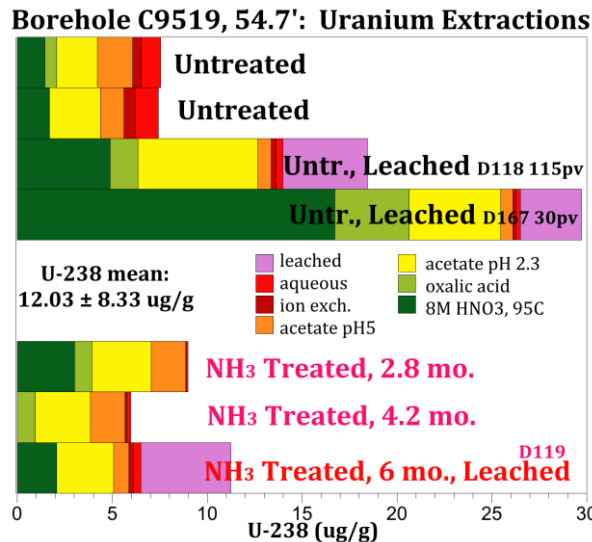
Figure E.18. Sequential liquid extractions conducted on C9519 54.7' depth sediment.

Similar to the U-8 low-U sediment (Figure E.15 through Figure E.18, total U of 12.0 µg/g), leaching synthetic groundwater through the TX104 (borehole 3832) 69' depth sediment (with a total U of 8.49 µg/g) in three different experiments shows very similar behavior, with a) a peak initial U concentration of 0.4 to 2.5 mg/L (untreated sediments in Figure E.19a, b), b) subsequent lower U concentration at greater pore volumes, c) slow U release from sediments as indicated by U concentration increase at stop flow events, and d) cumulative U by 30 pore volumes of 1 to 3 µg/g (Figure E.19). Metals and anion concentrations (Figure E.20) showed predominantly Na and sulfate with a constant silica concentration of 8 to 11 mg/L. Other metals were analyzed (Sr, Sn, B, Fe, Mn, Zn), but were below detection limits. All untreated and NH₃-treated sequential U extractions conducted on this sediment (Figure E.21) pre- and post-leaching show an average U of 12.0 ± 8.33 µg/g. The fraction of uranium that is considered "mobile" (i.e., aqueous plus adsorbed plus pH 5 acetate extractable) is similar (20% to 35%) to TX104 sediments (i.e., TX104, 69' shows 10% to 30% leached; TX104 110' shows 35% leached). Thorium-232 was below the detection limits (0.48 µg/g) in all aqueous effluent samples measured.
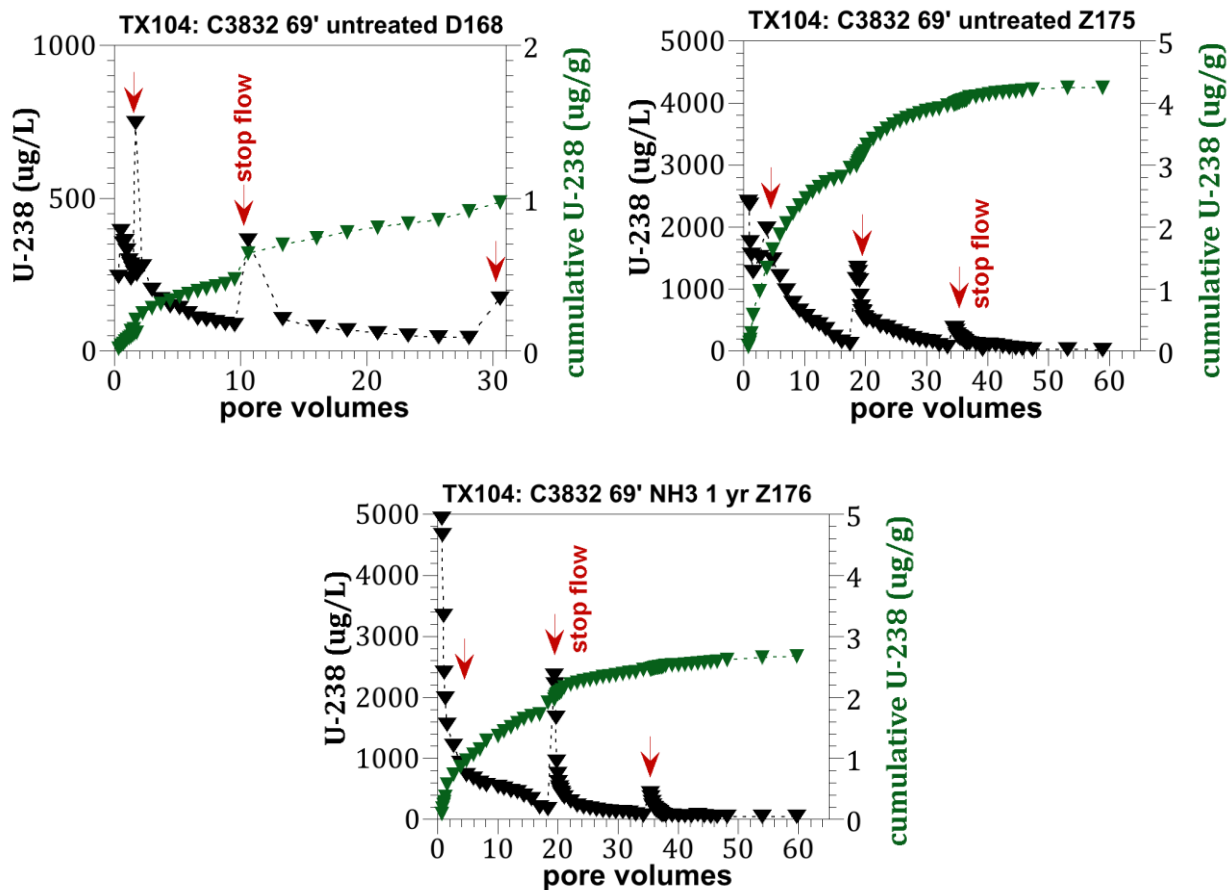
Figure E.19. 1-D leaching of TX104, C3832 69' untreated (a, b) and NH$_3$-treated c) sediment with artificial groundwater, showing effluent uranium concentration.
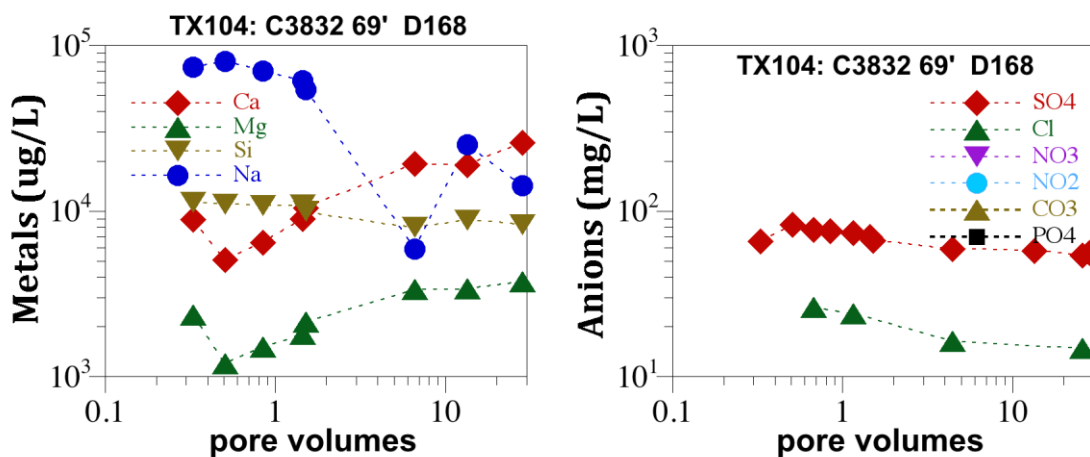
Figure E.20. 1-D leaching of TX104, C3832 69' untreated sediment with artificial groundwater, showing effluent metals a) and anion b) concentrations.
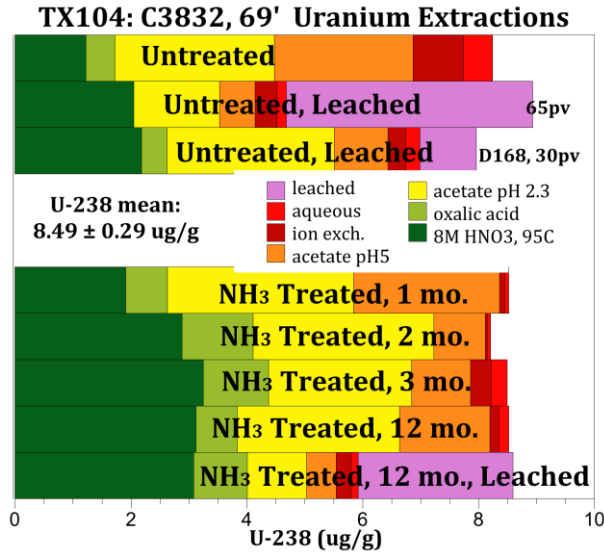
Figure E.21. Sequential liquid extractions conducted on TX104, C3832 69' depth sediment.

Similar to the U-8 low-U sediment (Figure E.15 through Figure E.18, total U of 12.0 µg/g) and TX104 69' sediment (Figure E.19 through Figure E.21, total U of 8.49 µg/g), leaching synthetic groundwater through the TX104 (borehole 3832) 110" depth sediment (with a total U of 65.4 µg/g) shows very similar behavior, with a) a peak initial U concentration of 7.5 mg/L, b) subsequent lower U concentration at greater pore volumes, c) slow U release from sediments as indicated by U concentration increase at stop flow events, and d) cumulative U by 30 pore volumes of 23 µg/g (Figure E.22). Metals and anion concentrations (Figure E.23) showed a higher Ca and sulfate with a decreasing silica concentration of 18 to 10 mg/L. Other metals were analyzed (Sr, Sn, B, Fe, Mn, Zn), but were below detection limits. All untreated and NH$_3$-treated sequential U extractions conducted on this sediment (Figure E.24) pre- and post-leaching show an average U of 60.2 ± 7.35 µg/g. The fraction of uranium that is considered "mobile" (i.e., aqueous plus adsorbed plus pH 5 acetate extractable) of 35% is similar to the TX104, 69' (10% to 30% leached) and C9519 54.7' (12% leached). Thorium-232 was below the detection limits (0.48 µg/g) in all aqueous effluent samples measured.
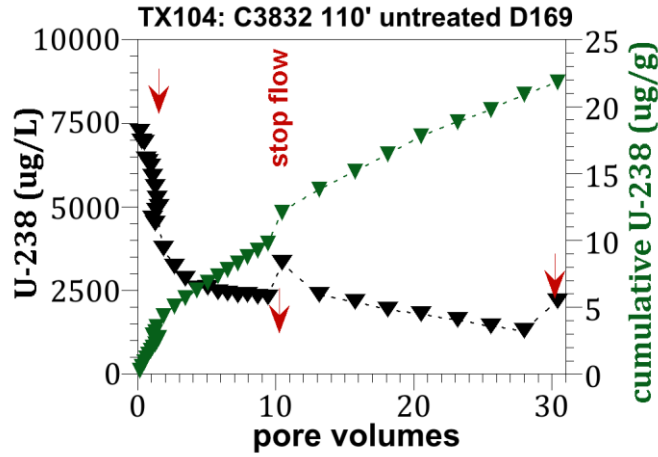
Figure E.22. 1-D leaching of TX104, C3832 110' untreated sediment with artificial groundwater, showing effluent uranium concentration.
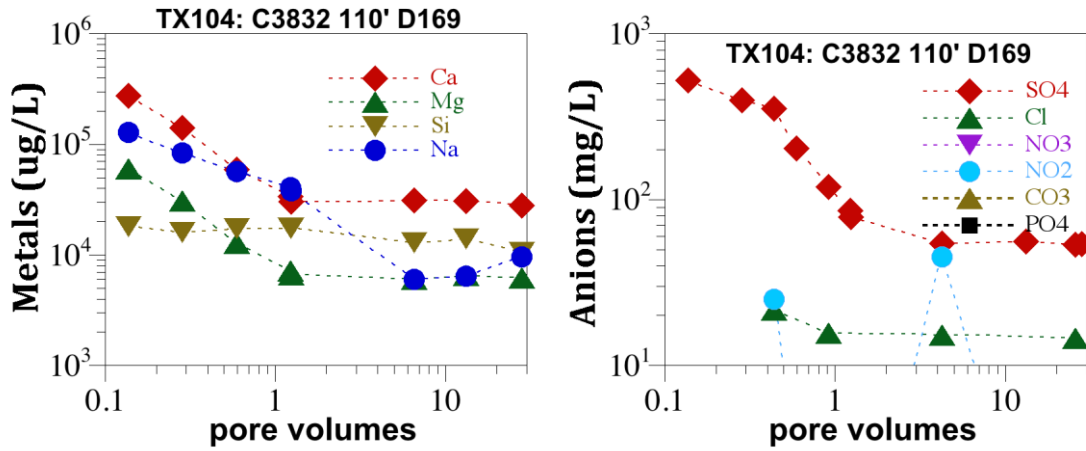
Figure E.23. 1-D leaching of TX104, C3832 110' untreated sediment with artificial groundwater, showing effluent metals a) and anion b) concentrations.
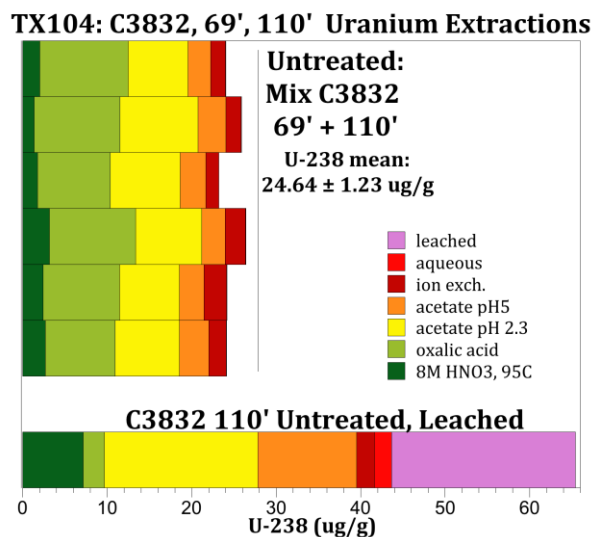
Figure E.24. Sequential liquid extractions conducted on TX104, C3832 110' depth sediment.

In summary, the U-8 sediment with a high uranium concentration (C9520 42.9', U = 1808 µg/g) exhibited unusual behavior with <2% leached. This was dissimilar to lower U sediments (U-8, C9519 54.7 12.0 µg/g; TX104 69' 13.0 µg/g; TX104 110' 60.2 µg/g), which all showed 10% to 35% of the total uranium leached and more reproducible leaching and/or extractions. It is hypothesized that the high uranium precipitates concentrated on a few mineral grains shown for C9520 42.9' (see above) may be more difficult to coat with aluminosilicates. It is likely that the C9520 42.9' depth sediment contains a high concentration of uranophane [$Ca(UO_2)_2(SiO_3OH)_2(H_2O)_5$], based on XRD and XANES analysis. Although sequential liquid extractions accurately identify aqueous and adsorbed uranium phases, the remaining four extractions may dissolve one or more uranium surface phases. The pH 5 acetate extraction dissolves some calcite that may contain uranium and a smaller fraction of U silicates such as Na-boltwoodite [$Na(UO_2)(SiO_4)*1.5H_2O$] and uranophane. The pH 2.3 acetic acid extraction dissolves most carbonates and remaining uranium silicates. A previous sequential extraction of a Na-boltwoodite and synthesized U-substituted carbonate shows that the pH 5 acetate extraction dissolved 15% of Na-boltwoodite and 85% of the U-substituted carbonate (Figure E.25).
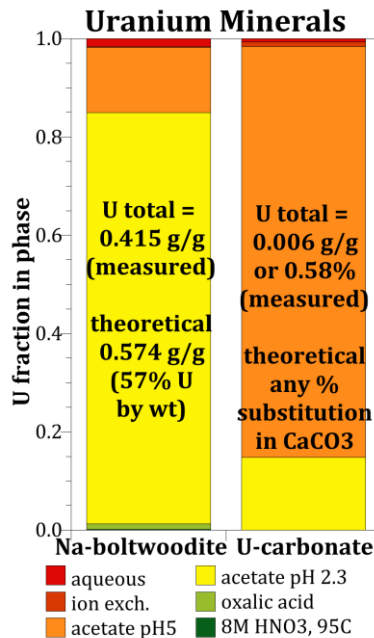
Figure E.25. Sequential liquid extractions conducted on Na-boltwoodite and a synthesized U-substituted calcite.

E.3.3   5% NH₃ Treatment of U-8 and TX104 Sediments

To evaluate differences in mineral dissolution (releasing Si, Al, U, and other metals) at early times and subsequent mineral precipitation, a series of eight 1-D columns containing U-8 and TX104 sediments at 4% water content were treated with 5% NH_3 (and 95% N_2) for times ranging from 24 to 671 hours. At the selected time interval, deionized water was mixed with the sediment and the solution was analyzed for U, pH, metals, anions, total carbon, and total inorganic carbon. Previous studies showed that the uranium concentration increased in the first 100 hours with metals concentration, then subsequently decreased (Figure E.26, Szecsody et al. 2012). Silica concentrations increased in a variety of Hanford formation sediment samples (Figure E.27, Szecsody et al. 2010).
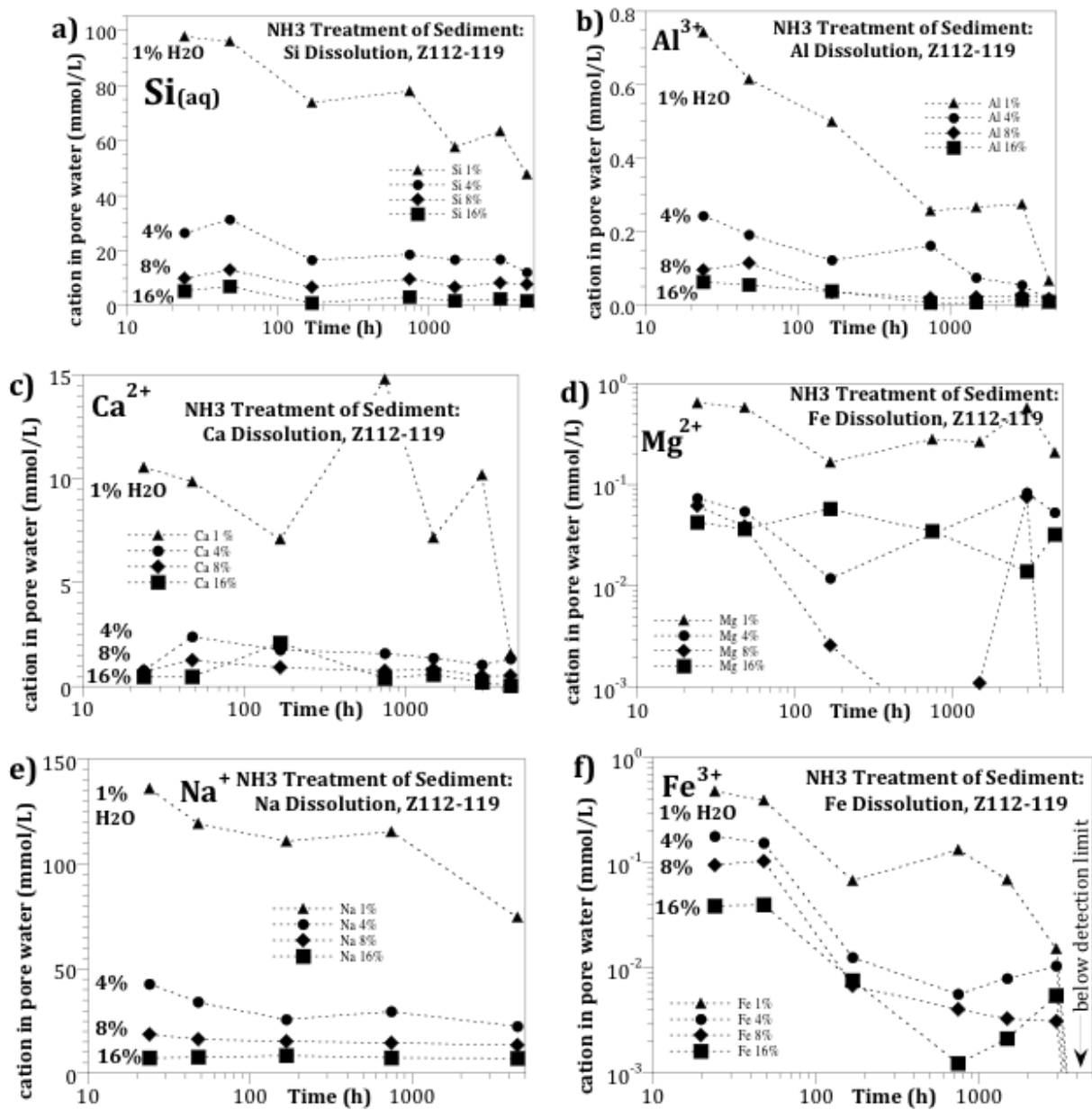
Figure E.26. Sediment pore water metals concentration change over time during 5% NH₃ treatment of the Hanford formation Environmental Restoration Disposal Facility pit sediment (Szecsody et al. 2012).
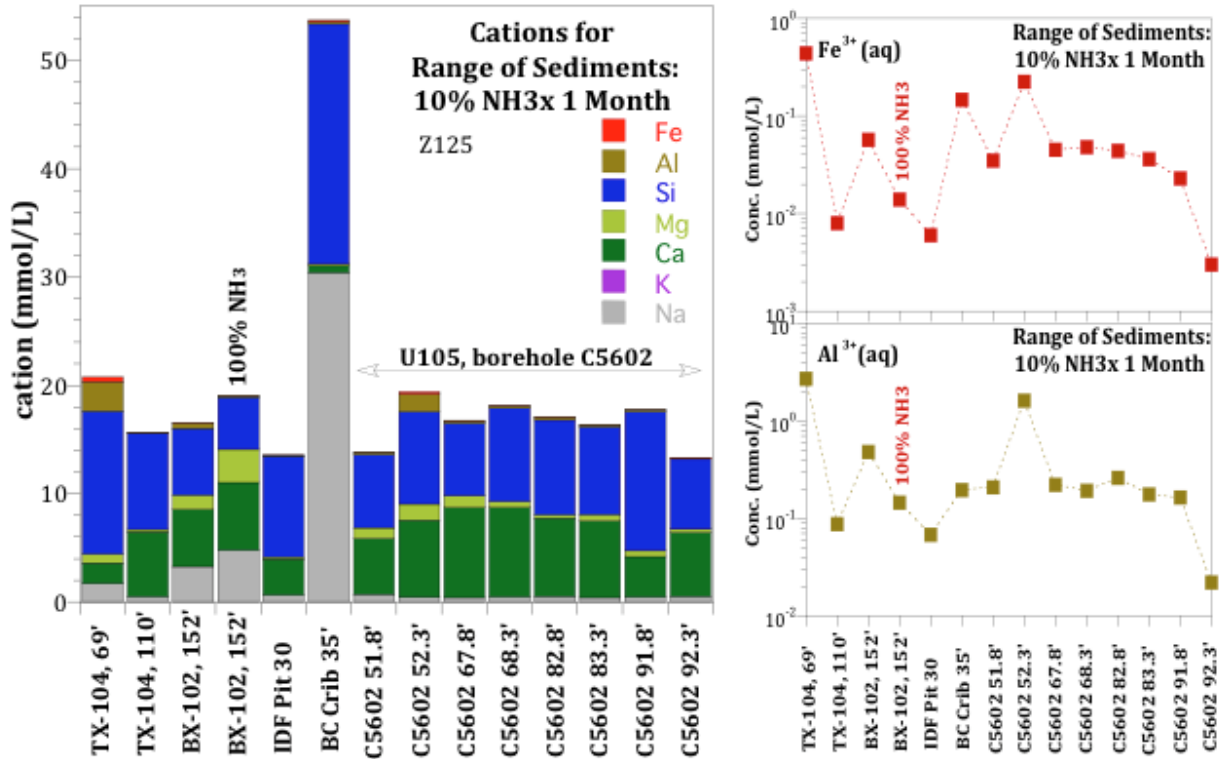
Figure E.27. Sediment pore water metals concentration for Hanford sediments after 10% NH₃ treatment after 1200 hours (Szecsody et al. 2010).

For the comparison of U-8 to TX104 sediment treatment with 5% NH_3, all four sediments showed a similar pH decreased from ~11 at 24 hours to 9-9.8 by 671 hours (Figure E.28b). The uranium concentration, however, did not decrease in most sediments (Figure E.28a) in spite of the significant Si and Al decrease (Figure E.28c and d). Although aqueous values of Al were similar between U-8 and TX104 sediments, the behavior of aqueous Si differed greatly. TX104 sediments showed a large (4x) decrease in aqueous silica, whereas U-8 sediments only showed a slight (10%) decrease. Clearly, aluminosilicate precipitation in U-8 sediments is slower than TX104 sediments. As expected, a metal that is generally not involved in precipitation (Na+) showed little change for all sediments (Figure E.28e). Concentrations of total carbon and total inorganic carbon were below detection limits (4 mg/L) in all samples. The concentrations of Cl, F, Br, PO_4, and NO_2 were below the detection limits in all samples. The concentrations of Mg, Mn, P, K, Sr, and Zo were also below detection limits.

U for 5% NH3 Treatment

pH for 5% NH3 Treatment

Si for 5% NH3 Treatment

Al for 5% NH3 Treatment
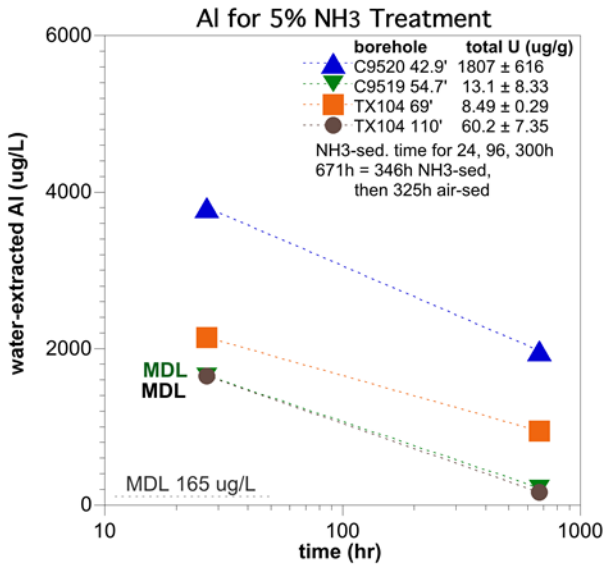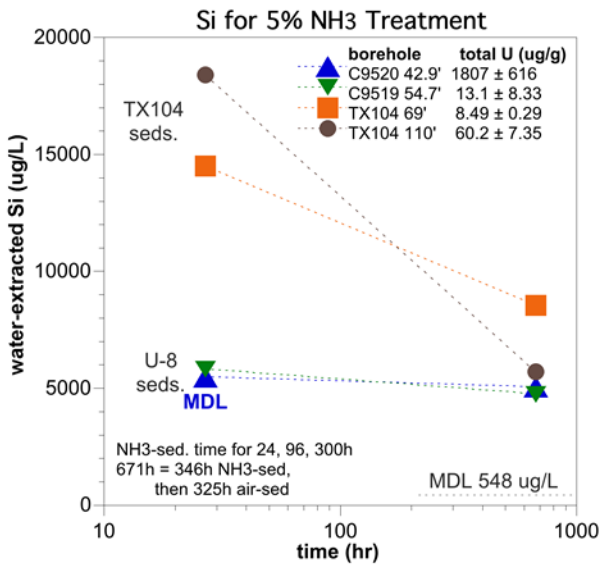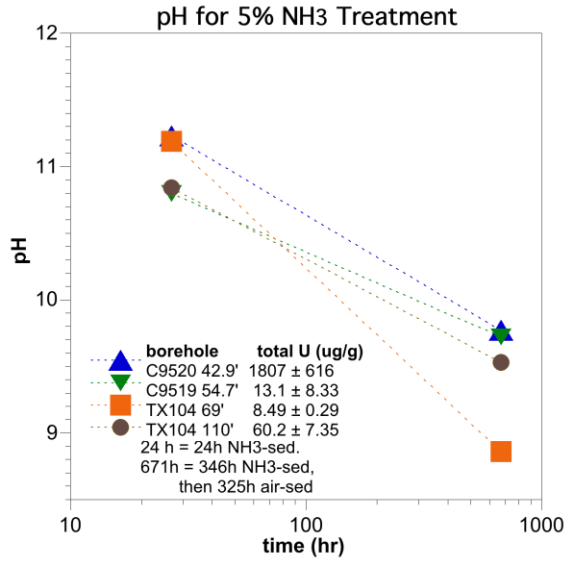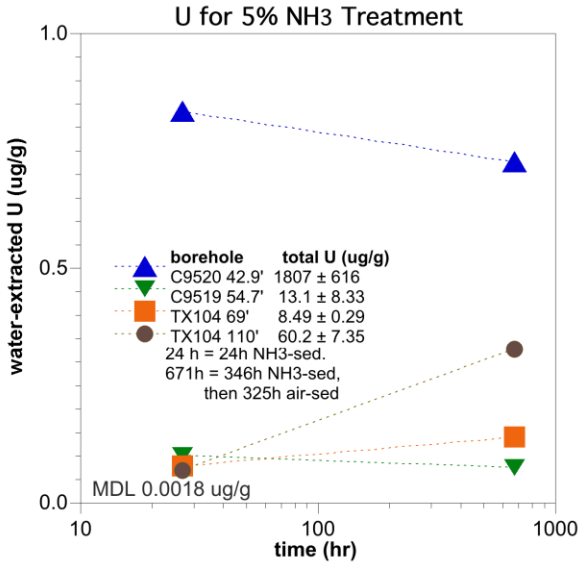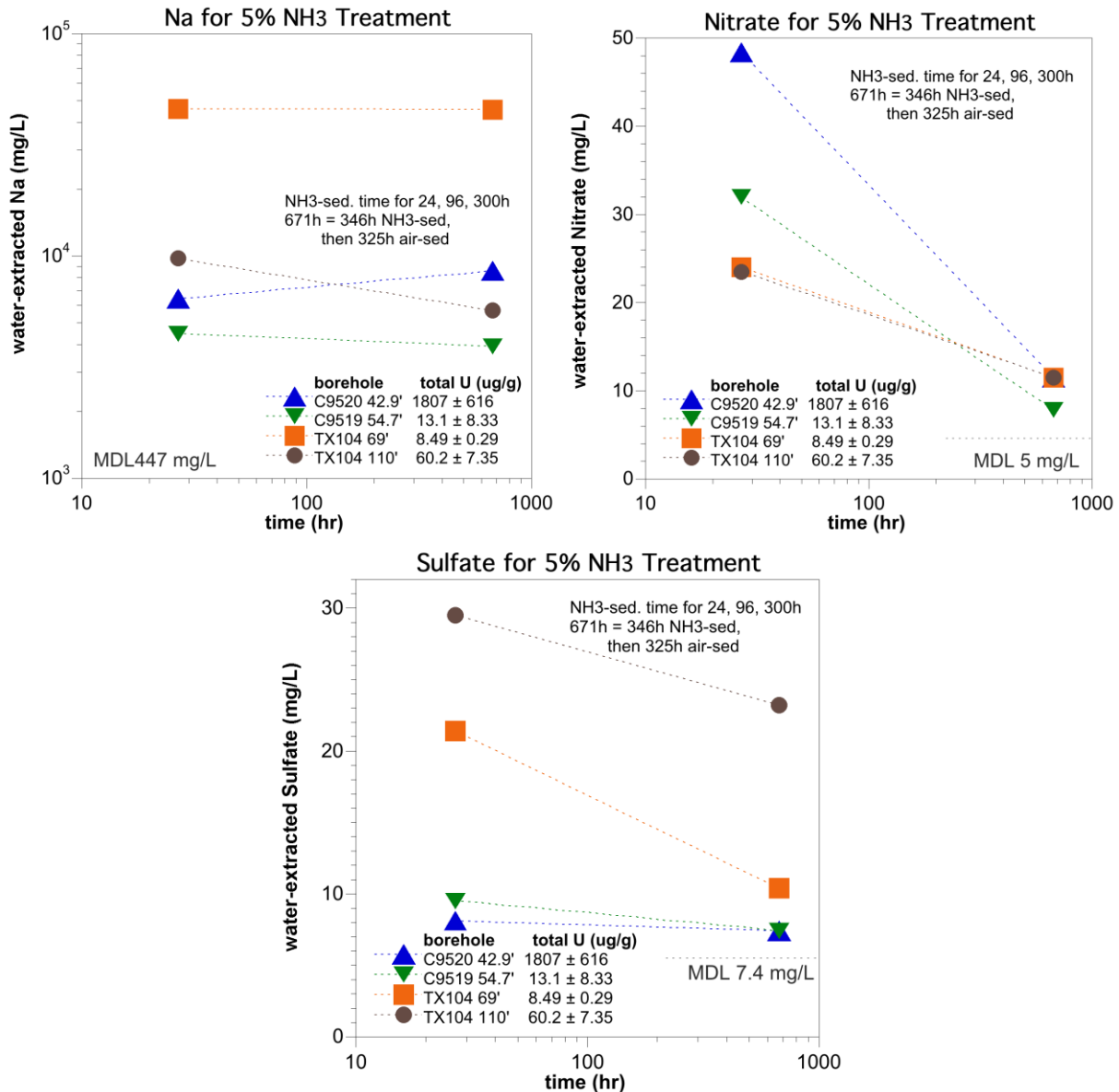
Figure E.28. 5% NH₃ treatment of U-8 and TX104 sediments showing change in aqueous extracted concentrations of: a) U, b) pH, c) Si, d) Al, e) Na, f) NO₃, and g) SO₄.

E.4 Hypothesis 3 - Uranium Immobilization by Higher NH₃ Concentration Treatment

Finally, it is hypothesized that dissolution of silicates at the pH induced by 5% NH₃ treatment (~pH 11.5) is not sufficient to create uranium-silicate precipitates or enough silicate precipitates to coat uranium surface phases in U-8 sediments; thus, a higher pH (~pH 12.2) may be needed to induce treatment. To test this hypothesis, 100% NH₃ gas treatment was conducted on a high-U sediment (C9520 42.9', total U = 1807 µg/g) and a low-U sediment (C9519 54.7', total U = 13.0 µg/g). At selected times (24, 100, 330, 670 hours), the eight 1-D columns were treated with 100% NH₃ for 500 pore volumes, and deionized water extracted samples were analyzed for U, pH, metals, anions, total carbon, and total inorganic carbon.

Results were compared to the 5% NH_3 treatment experiments (Figure E.28). All total carbon, total inorganic carbon, Br, Cl, F, NO_3, PO_4, and SO_4 concentrations were below detection limits.

Results show that 100% NH_3 treatment of sediment initially has a higher pH (~11.9) compared with 5% NH_3 treatment of sediment (pH ~11.2; Figure E.29a and b). The actual pore water pH is higher because the pH measured in the deionized water addition results in a 65x dilution factor (i.e., initial pH is ~12.5). A Si concentration of 7.1 mg/L (diluted, Figure E.29e) corresponds to pore water concentration of 17.2 mmol/L in the 4% pore water, which is similar to that previously reported (Figure E.26a). An initial Al concentration of 5.1 mg/L (diluted, Figure E.29g) corresponds to 12.8 mmol/L in the 4% pore water and is much higher than previously reported pore water Al concentrations (Figure E.26b). The corresponding uranium concentration is initially higher for the 100% NH_3 treatment compared to the 5% NH_3 treatment (Figure E.29c and d), and decreases to similar values by 670 hours; thus, it is unclear whether there is a difference in the immobilization of uranium (i.e., leach experiments would be needed to best evaluate the change in mobility between 5% and 100% NH_3 treatment of sediments). Concentrations of Si (Figure E.29e and f) and Al (Figure E.29g and h) are initially higher for the 100% NH_3 treatment compared with 5% NH_3 treatment and decrease more rapidly. Clearly, a higher NH_3 concentration treatment results in greater mineral dissolution and more rapid aluminosilicate precipitation. The change in mobile uranium in these 5% and 100% treatments over time did not parallel the regular decrease in aqueous pH, Si, and Al concentrations. Therefore, while both 5% and 100% NH_3 treatments are effective at dissolving (at short time) then precipitating aluminosilicates (at longer time), the lack of decreased uranium mobility may be due to the inability of aluminosilicates to precipitate on (i.e., coat) the uranium hot spots (predominantly uranophane) and/or precipitate as uranophane or Na-boltwoodite in the low carbonate water.

pH for C9520 42.9' NH3 Treatment

100% NH3
5% NH3

total U: 1807 ± 616 ug/g
NH3-sed. time for 24, 96, 300h
671h = 346h NH3-sed,
then 325h air-sed

pH for C9519 54.7' NH3 Treatment

100% NH3
5% NH3

total U: 13.03 ± 8.33 ug/g
NH3-sed. time for 24, 96, 300h
671h = 346h NH3-sed,
then 325h air-sed

U for C9520 42.9' NH3 Treatment

100% NH3
5% NH3

total U: 1807 ± 616 ug/g
NH3-sed. time for 24, 96, 300h
671h = 346h NH3-sed,
then 325h air-sed

MDL 0.0018 ug/g

U for C9519 54.7' NH3 Treatment

5% NH3
100% NH3

total U: 13.03 ± 8.33 ug/g
NH3-sed. time for 24, 96, 300h
671h = 346h NH3-sed,
then 325h air-sed

MDL 0.0018 ug/g

Si for C9520 42.9' NH3 Treatments

100% NH3
5% NH3
MDL

total U: 1807 ± 616 ug/g
NH3-sed. time for 24, 96, 300h
671h = 346h NH3-sed,
then 325h air-sed

MDL 548 ug/L

Si for C9519 54.7' NH3 Treatment

100% NH3
5% NH3

total U: 13.03 ± 8.33 ug/g
NH3-sed. time for 24, 96, 300h
671h = 346h NH3-sed,
then 325h air-sed

MDL 548 ug/L

E.39

Figure E.29. Comparison of 100% NH₃ and 5% NH₃ treatment of U-8 sediments shown by extraction water concentrations of (a and b) pH, (c and d) U, (e and f) Si, g, and (h) Al.

E.5   References

Emerson HP, S Di Pietro, Y Katsenovich, and J Szecsody. 2018. "Potential for U sequestration with select minerals and sediments via base treatment." *J Environmental Management* 223:108-114.

Szecsody JE, MJ Truex, L Zhong, TC Johnson, NP Qafoku, MD Williams, JW Greenwood, EL Wallin, JD Bargar, and DK Faurie. 2012. "Geochemical and Geophysical Changes During NH3 Gas Treatment of Vadose Zone Sediments for Uranium Remediation." *Vadose Zone J.* 11(4) doi:10.2136/vzj2011.0158

Szecsody JE, MJ Truex, L Zhong, MD Williams, and CT Resch. 2010. *Remediation of Uranium in the Hanford Vadose Zone Using Gas-Transported Reactants: Laboratory-Scale Experiments*. PNNL-18879, Pacific Northwest National Laboratory, Richland, Washington.

Wan J, Y Kim, TK Tokunaga, Z Wang, S Dixit, CI Steefel, E Saiz, M Kunz, and N Tamura. 2009. "Spatially Resolved U(Vi) Partitioning and Speciation: Implications for Plume Scale Behavior of Contaminant U in the Hanford Vadose Zone." *Environ. Sci. Technol.* 43:2247-2253.

Wang Z, JM Zachara, W Yantasee, PL Gassman, CX Liu, and AG Joly. 2004. "Cryogenic Laser Induced Fluorescence Characterization of U(Vi) in Hanford Vadose Zone Pore Waters." *Environ. Sci. Technol.* 38:5591-5597.

Wang Z, JM Zachara, PL Gassman, C Liu, O Qafoku, and JG Catalano. 2005. "Fluorescence Spectroscopy of U(Vi)-Silicate and U(Vi)-Contaminated Hanford Sediment." *Geochim. Cosmochim. Acta* 69:1391-1403.

Wang Z, JM Zachara, C Liu, PL Gassman, AR Felmy, and SB Clark. 2008. "A Cryogenic Fluorescence Spectroscopic Study of Uranyl Carbonate, Phosphate and Oxyhydroxide Minerals." *Radiochim. Acta* 96: 591-598.

Um W, Z Wang, RJ Serne, BD Williams, CF Brown, CJ Dodge, and AJ Francis. 2009. "Uranium Phases in Contaminated Sediments Below Hanford's U Tank Farm." *Environ. Sci. Technol.* 43:4280-4286.

Xie Y, C Murray, G Last, R Mackley. 2003. *Mineralogical and Bulk-Rock Geochemical Signatures of Ringold and Hanford Formation Sediments*. PNNL-14202, Pacific Northwest National Laboratory, Richland, WA.

Zachara JM, CF Brown, JN Christensen, JA Davis, PE Dresel, C Liu, SD Kelly, et al. 2007. *A Site Wide Perspective on Uranium Geochemistry at the Hanford Site*. PNNL-17031, Pacific Northwest National Laboratory, Richland, WA.

Distribution

No. of
Copies

No. of
Copies

  #   **Hanford Distribution**
      CHPRC
        Dave St. John (PDF)

  #   **Local Distribution**
      Pacific Northwest National Laboratory
        MJ Truex (PDF)